

NACA RM No. SA9004

CONFIDENTIAL

RM No. SA9004

Source of Acquisition
CASI Acquired**NACA**

CLASSIFICATION CANCELLED

RESEARCH MEMORANDUM

for the

Air Materiel Command, U.S. Air Force

TESTS OF A FULL-SCALE MODEL OF THE REPUBLIC

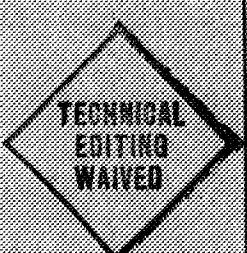
XF-91 AIRPLANE IN THE AGLS 40-- BY 80-FOOT WIND TUNNEL.--

FORCE AND MOMENT DATA

By Lynn W. Hutton and Joseph K. Dew

Ames Aeronautical Laboratory
Moffett Field, Calif.**CLASSIFIED DOCUMENT**

This document contains classified information affecting the National Defense of the United States within the meaning of the Espionage Act, USC 5031 and 32. Its transmission or the revelation of its contents in any manner to an unauthorized person is prohibited by law. Information so classified may be imparted only to persons in the military and naval Services of the United States, appropriate civilian officers and employees of the Federal Government who have a legitimate interest therein, and to United States citizens of known loyalty and discretion who of necessity must be informed thereof.


 TECHNICAL
EDITING
WAIVED

NATIONAL ADVISORY COMMITTEE COPY FOR AERONAUTICS

WASHINGTON

May 1, 1949

To be returned to
the files of the National
Advisory Committee

on file

N. A. C.

CLASSIFICATION CANCELLED

CONFIDENTIAL

Security Information

CONFIDENTIAL

NATIONAL ADVISORY COMMITTEE FOR AERONAUTICS

RESEARCH MEMORANDUM

for the

Air Materiel Command, U.S. Air Force

TESTS OF A FULL-SCALE MODEL OF THE REPUBLIC

XF-91 AIRPLANE IN THE AMES 40- BY 80-FOOT WIND TUNNEL.--

FORCE AND MOMENT DATA

By Lynn W. Hunton and Joseph K. Dew

SUMMARY

Wind-tunnel tests of a full-scale model of the Republic XF-91 airplane having swept-back wings and a vee tail were conducted to determine both the stability and control characteristics of the model longitudinally, laterally, and directionally. Configurations of the model were investigated involving such variables as external fuel tanks, a landing gear, trailing-edge flaps, leading-edge slats, and a range of wing incidences and tail incidences.

INTRODUCTION

The Republic XF-91 airplane is a jet- and rocket-powered interceptor fighter having a swept-back and inversely tapered wing and a vee tail. In view of the problems of stability and control likely to be encountered with such a unique design, the U.S. Air Force requested that an investigation be made of a full-scale model in the Ames 40- by 80-foot wind tunnel. The first part of the investigation, reported in reference 1, consisted of tests of the wing alone and of the wing-fuselage combination. For the second part of the full-scale investigation, consisting of the determination of the general stability and control characteristics of the complete model together with pressure measurements over the wing fuel tanks and vee tail, the model was modified slightly to make the configuration comparable to the current design of the airplane. This modification was comprised of (1) a change from a discontinuous to a continuous leading-edge slat, (2) a replacement of the split flaps with plain trailing-edge flaps, (3) the addition of a ventral fin, and (4) the reorientation of the rocket motors in the tail. Presented in this report are the results of only the stability and control tests. The results of the pressure-distribution measurements are to follow in a subsequent report.

CONFIDENTIAL

CLASSIFICATION CANCELLED

SYMBOLS

The results of the tests are presented as standard NACA coefficients of forces and moments. All force data are referred to the wind axes and all moment data are referred to the stability axes originating at a center-of-gravity position located on the wing chord plane and at 0.18 mean aerodynamic chord. The positive directions of the stability axes, of angular displacements of the airplane and control surfaces, and of forces and moments are shown in figure 1. The coefficients and symbols are defined as follows:

C_L lift coefficient $\left(\frac{\text{lift}}{qS} \right)$

C_D drag coefficient $\left(\frac{\text{drag}}{qS} \right)$

C_Y side-force coefficient $\left(\frac{\text{side force}}{qS} \right)$

C_m pitching-moment coefficient $\left(\frac{\text{pitching moment}}{qS\bar{c}} \right)$

C_n yawing-moment coefficient $\left(\frac{\text{yawing moment}}{qSb} \right)$

C_l rolling-moment coefficient $\left(\frac{\text{rolling moment}}{qSb} \right)$

C_h hinge-moment coefficient $\left(\frac{\text{hinge moment}}{2qM} \right)$

$\frac{dC_m}{dt}$ rate of change of pitching-moment coefficient with incidence of the tail, per degree

b wing span measured perpendicular to plane of symmetry, feet

c local wing chord, feet

\bar{c} wing mean aerodynamic chord $\left(\frac{\int_0^{b/2} c^2 dy}{\int_0^{b/2} c dy} \right)$, feet

i_w	incidence of the wing to the fuselage reference axis, degrees
i_t	incidence of the tail to the fuselage reference axis, degrees
M	first moment of control-surface area aft of hinge line about hinge line ($M_{eR} = M_{eL} = 5.06 \text{ ft}^3$; $M_{aR} = M_{aL} = 22.11 \text{ ft}^3$)
q	free-stream dynamic pressure, pounds per square foot
S	wing area, square feet
y	lateral coordinate, perpendicular to plane of symmetry, feet
α	angle of attack of fuselage reference axis, degrees
α_w	angle of attack of wing chord plane, degrees
β	angle of sideslip, degrees
δ	angular deflection measured perpendicular to hinge line, degrees

Subscripts

a	aileron
e	single elerudder surface, or both elerudder surfaces used for pure elevator action
r	both elerudder surfaces used for pure rudder action
f	plain trailing-edge flaps
L	left
R	right

MODEL AND EQUIPMENT

The full-scale model of the XF-91 airplane used in these tests was basically the same model used in the tests reported in reference 1 with the exception of the following modifications: (1) the lower two rockets, formerly grouped side by side just below the jet exhaust pipe, were rearranged with their axes in a vertical plane, (2) a ventral fin was installed, (3) a vee tail was installed, (4) the former split trailing-edge flaps were replaced by plain trailing-edge flaps, and (5) the full-span drooped-slat installation was modified to eliminate the former midspan discontinuity reported in reference 1. Detailed pertinent dimensions of the complete model are presented in table I, and in figure 2 is shown a three-view drawing of the model.

The wing had a sweepback of 37.5° of the one-quarter chord line and was inversely tapered. The incidence of the wing with respect to the fuselage axis was adjustable from 0° to 6° . A detailed description of the wing layout can be found in reference 1; a table of section ordinates is given in figure 3.

The wings were equipped with two auxiliary-lift devices: partial-span, trailing-edge, plain flaps and full-span, leading-edge, drooped slats. The plain flaps were constant-percent chord and could be deflected to 30° , 40° , or 50° . The drooped slats had a constant-percent chord and were extended forward and rotated downwardly as shown by the detailed sketch of the slat configuration given in figure 4. Because of this constant extension along the span, in conjunction with the constant-percent chord of the surface, the slat trailing edge at the inboard part of the wing was ahead of the leading edge of the fixed part of the wing; to evaluate this effect, a temporary modification of the slat trailing edge was made to obtain a constant overlap. (See fig. 4.)

The ailerons on the model had a constant-percent chord and were internally balanced and sealed as shown in figure 4. The balance area, including one-half of the seal area and allowing for cutouts, was equal to 30 percent of the aileron area aft of the hinge line.

The vee-tail surfaces on the model had 38° of dihedral, were untapered, and had 40° of sweepback in the plan view. The incidence of the vee tail was adjustable to fixed settings of -2.2° , 0° , or 1.8° in a vertical plane through the axis of symmetry. The section ordinates are presented in table II. The elerudders were internally sealed and balanced, and had a chord aft of the hinge line of 30 percent of the

tail surface chord. (The balance area including one-half of the seal area was about 29 percent of the elerudder area aft of the hinge line). A trim tab was located on the right elerudder. A cross section of the tab is shown in figure 4 and detail dimensions are given in table I.

The right aileron and both elerudders were each equipped with an electric actuator, a selsyn-type indicator, and an electrical resistance-type strain gage for remote control, indication of deflection angle, and indication of hinge moment, respectively.

Additional equipment on the model included two jettisonable external fuel tanks and a tricycle landing gear. The external tanks were mounted on fairing struts beneath the wing and at an incidence of -4° to the wing as shown in figure 2. The landing gear, with dual main-gear wheels in tandem, retracted outwardly into the tip of the wing.

Shown in figures 5(a) through 5(c) are photographs of the installation of the model in the tunnel test section. The conventional three-strut support system was used, but the direction of the supports were reversed in the air stream in order to gain additional angle-of-attack and angle-of-sideslip ranges.

TESTS

All the tests were performed at an average dynamic pressure of approximately 40 pounds per square foot, which for sea-level conditions corresponds to a velocity of about 125 miles per hour and a Reynolds number of 11.5×10^6 based on the wing mean aerodynamic chord of 10.59 feet.

Stability tests, for the various configurations of the model, were conducted (1) through an angle-of-attack range from -2° to the wing stalling angle at constant angles of sideslip and (2) through an angle-of-sideslip range from 4° to -12° at constant angles of attack.

Control studies of the aileron and elerudder, for various configurations of the model, included (1) tests through an angle-of-attack range with fixed angles of control-surface deflection and (2) tests through a range of control-surface deflections at constant angles of both attack and sideslip. Only the right aileron was tested.

CONFIDENTIAL

CORRECTIONS

All the test data have been corrected for jet-boundary effects and inclination of the air stream. The wall corrections added to the angle of attack, drag coefficients, and pitching-moment coefficients were as follows:

$$\Delta\alpha = 0.706 C_L$$

$$\Delta C_D = 0.012 C_L^2$$

$$\Delta C_m = 0.016 C_L$$

(The correction to the pitching-moment coefficient is based on an assumed value of $dC_m/di_t = -0.03$. Since the actual tail-incidence data subsequently obtained and shown herein indicate a lower value, the longitudinal-stability results thus presented are slightly in error equivalent to a forward shift of the neutral point of 0.9 percent mean aerodynamic chord.)

No tares of the support struts were applied to the data reported herein. With the exception of the drag tare, the tares are known to be relatively small. In reference 1, the drag tare was reported to be of the order of 0.0030 at zero lift. However, for the present tests as a result of the presence of large bundles of tubing taped around the support-strut tips, the drag-coefficient tare increased to approximately 0.0120 at zero lift for all the test configurations except those involving the wing tanks. Since the tanks shrouded the struts a significant reduction in the drag tare would be anticipated, although the order of magnitude of the reduction is not known owing to the questionable extent of interference effects between the tank and the support-strut fairing.

RESULTS AND DISCUSSION

An outline of the model configurations tested, the results presented, and the figures in which the results may be found is given in table III. Throughout the results presented herein, unless noted otherwise, the following notation: gear, drooped slats, or flaps will denote the complete landing gear fully extended; the full-span, leading-edge drooped slats deflected as shown in figure 4; and the trailing-edge plain flaps deflected 40° , respectively.

Stability Characteristics

The results of the investigation of the general stability characteristics of the various model configurations involving combinations of the tanks, gear, drooped slats, and flaps are presented in figures 6 to 26. Since the original design of the airplane called for a variable incidence of the wing (6° for take-off, landing, and high-altitude cruise; 0° for climb and high-speed at low altitude), data were obtained, throughout this investigation, at either or both 0° and 6° incidence of the wing, depending on the configuration under test. In figures 17 and 18 is shown the effect of the partially extended right landing gear on the airplane (simulating a malfunctioning gear). A sketch is included in the figures detailing the gear position relative to the wing. In figure 21 are presented the results of tests of the drooped-slat modification (fig. 4) consisting of an extension of the slat trailing edge. As is evident in the data, the addition of the extension strip did not alter the efficiency of the drooped slat as an auxiliary-lift device.

With the addition of the complete gear to the model there occurred an unstable break in the pitching-moment curve at a lift coefficient of about 0.7. In figure 10, only slight indications of this break appear in the data; whereas in figure 12, which shows data obtained with the drooped slat deflected, the abrupt change in stability is clearly evident. Because of this stability change, a few additional tests were initiated in an attempt to isolate the particular part of the gear responsible for the trouble. The results of these additional tests are presented in figures 27 to 31. By systematically removing various parts of the gear it was found that the break in stability was attributable mainly to the large main-gear doors, as may be seen in figure 27. Tests of the main-gear doors alone, shown in figures 29 and 30, indicated an unstable shift in the neutral point of approximately 4 percent at a lift coefficient of about 0.75, either with tail on or tail off. Thus, the likelihood of a change in downwash at the tail due to the doors may be excluded from the problem. Instead, therefore, the problem would appear to be associated with a shift in location of the aerodynamic center of the wing caused by a redistribution in wing loading. Owing to the angular position of the gear doors (giving a drooped-tip effect), it is believed that separation occurred at the leading edge of the door when the wing was at an attitude of about 6° ($C_L \approx 0.75$) which would then spoil the flow over the relatively large tip of the wing. Such a flow condition, although not extensive enough to be evident in the over-all lift- and drag-force results, could nevertheless

CONFIDENTIAL

shift the center of pressure inboard, resulting in a destabilizing pitching moment.

The tail-off stability of the model, both in the clean condition and with gear, drooped slats, and flaps, is indicated by the data presented in figures 32 to 35. The basic model for these tail-off tests differs from that reported in reference 1 by the addition of a ventral fin and the relocation of the rocket motors as described previously in this report.

Control Characteristics

The effectiveness of the right aileron for several different configurations of the model is indicated in the results presented in figures 36 to 53. Included in the investigation were tests to determine the effect of a partially extended gear on the aileron effectiveness and hinge-moment characteristics. These results are shown in figures 42 to 44.

The characteristics of the vee tail are given in figures 54 to 72. For the majority of this investigation, tests were conducted on only the right elerudder. Through such a test procedure both the longitudinal- and directional-control characteristics are obtained simultaneously. Furthermore, the data in this form are believed to be of greater value for purposes of a detailed analysis of the vee-tail control problem than would be the case if the results were in the form of a composite of two differentially deflected surfaces. However, since the results of such a test procedure would be open to question as regards the effects of interaction, a few additional tests were conducted on the effectiveness of the complete tail (both right and left elerudder surfaces) operated for pure elevator action (fig. 71) and for pure rudder action (fig. 72). By a comparison of these results with those of the single elerudder surface, it was found that the effects of interaction were virtually nonexistent.

The effectiveness of either a variable wing incidence or a variable tail incidence as a longitudinal-control device is shown in figures 73 to 75 and 76 to 77, respectively, for several configurations of the airplane.

Ames Aeronautical Laboratory,
National Advisory Committee for Aeronautics,
Moffett Field, Calif.

CONFIDENTIAL

REFERENCE

1. Hunton, Lynn W. and Dew, Joseph K.: An Investigation of the Wing and the Wing-Fuselage Combination of a Full-Scale Model of the Republic XP-91 Airplane in the Ames 40- by 80-Foot Wind Tunnel. NACA ~~MF~~ No. SA8F09, 1948.

Rm

CONFIDENTIAL

TABLE I

MODEL DIMENSIONS

Wing

Area, sq ft (true)	320
Span ² , ft	31.33
Sweep of 0.25-chord line deg.	37.5
M. A. C., ft	10.59
Aspect ratio	3.07
Taper ratio (inverse)	1.63
Root chord ³ , ft	7.92
Tip chord, ft	12.88
Dihedral, deg.	0
Twist, deg.	0

Drooped Slat (retracted -- one side)

Span, ft.	12.60
Chord, percent wing chord	15.3

Aileron (one surface)

Area, aft of hinge line, sq ft	19.14
Span, ft.	6.13
Chord, aft of hinge line at inboard edge, ft.	2.86
Chord, aft of hinge line at outboard edge, ft	3.39
Area of structural balance plus one half seal area, sq ft	5.77
Deflection range, deg	±18

Plain flap (one surface)

Chord, percent wing	27
Span, percent wing	41
Deflection, deg	30, 40, and 50

²All spans are measured perpendicular to the plane of symmetry unless otherwise noted.

³All chords are measured parallel to the plane of symmetry.

CONFIDENTIAL

TABLE I.- CONCLUDED

MODEL DIMENSIONS

Empennage (total)

Area, sq ft

True	80.00
Horizontal projection	63.04
Vertical projection	49.25
Span, ft	16.30
Sweep, (plan view) deg	40
M. A. C., ft	3.93
Taper ratio	1
Dihedral, deg	38
M. A. C. distance above fuselage reference line, ft . . .	1.33
M. A. C. distance measured perpendicular to plane of symmetry, ft	4.07
Distance from 0.25 M. A. C. of wing to 0.25 M. A. C. of tail, ft	16.71

Elerudder (one surface-- measured in plane of surface)

Area, aft of hinge line, sq ft	10.23
Span, perpendicular to fuselage reference line, ft	8.67
Chord, aft of hinge line, ft	1.18
Deflection range, deg	-35 to 25
Area of structural balance plus one-half seal area, sq ft .	2.99
Inboard edge location from fuselage reference line, ft . .	1.00

Elerudder trim tab (right surface-- measured in plane of surface)

Area, sq ft	1.31
Span, perpendicular to fuselage reference line, ft	2.64
Chord, aft of hinge line, ft	0.49
Deflection range, deg	±20
Inboard edge location from fuselage reference line, ft . .	1.00

CONFIDENTIAL

CONFIDENTIAL

TABLE II

VEE TAIL ORDINATES

VEE TAIL	
STATION PERCENT CHORD	ORDINATE PERCENT CHORD
0.5	0.788
.75	.964
1.25	1.240
2.5	1.740
5.0	2.421
7.5	2.915
10.	3.307
15.	3.903
20.	4.330
25.	4.635
30.	4.841
35.	4.961
40.	5.000
45.	4.960
50.	4.839
55.	4.635
60.	4.347
65.	3.979
70.	3.536
75.	3.078
80.	2.583
85.	2.007
90.	1.369
95.	.605
96.	.558
98.	.280
100.	0
L.E. radius: 0.625 percent chord T.E. angle: 16.11°	

CONFIDENTIAL

TABLE III

INDEX TO THE BASIC DATA FIGURES

General Configuration	Wing Incidence (deg)	Data Presented	Variable	Fig. No.
Stability				
Clean	0	$C_D \alpha C_m C_Y C_n C_l$ vs C_L	β	6
	6	do	β	6
	0	$C_Y C_l C_n C_L C_m$ vs β	α	7
	6	do	α	7
Tanks	0	$C_D \alpha C_m C_Y C_n C_l$ vs C_L	β	8
	0	$C_Y C_l C_n C_L C_m$ vs β	α	9
Tanks + gear	0	$C_D \alpha C_m C_Y C_n C_l$ vs C_L	β	10
	0	$C_Y C_l C_n C_L C_m$ vs β	α	11
Tanks + gear + drooped slats	0	$C_D \alpha C_m C_Y C_n C_l$ vs C_L	β	12
	6	do	β	12
	0	$C_Y C_l C_n C_L C_m$ vs β	α	13
	6	do	α	13
Gear + drooped slats	6	$C_D \alpha C_m$ vs C_L	δ_F	14
Gear + drooped slats + flaps	6	$C_D \alpha C_m C_Y C_n C_l$ vs C_L	β	15
	6	$C_Y C_l C_n C_L C_m$ vs β	α	16
Partial gear + drooped slats + flaps	6	$C_D \alpha C_m C_Y C_n C_l$ vs C_L	β	17
	6	$C_Y C_l C_n C_L C_m$ vs β	α	18

CONFIDENTIAL

CONFIDENTIAL

TABLE III.- CONTINUED

General Configuration	Wing Incidence (deg)	Data Presented	Variable	Fig. No.
Stability				
Drooped slats + flaps	0	$C_D \alpha C_m C_Y C_n C_l$ vs C_L	β	19
	6	do	β	19
	0	$C_Y C_l C_n C_L C_m$ vs β	α	20
	6	do	α	20
	6	$C_D \alpha C_m$ vs C_L	slat modification	21
Drooped slats	0	$C_D \alpha C_m C_Y C_n C_l$ vs C_L	β	22
	0	$C_Y C_l C_n C_L C_m$ vs β	α	23
Clean	0	$C_D \alpha C_m$ vs C_L	δ_f	24
Flaps	0	$C_D \alpha C_m C_Y C_n C_l$ vs C_L	β	25
	0	$C_Y C_l C_n C_L C_m$ vs β	α	26
Stability (Gear breakdown)				
Drooped slats + flaps	6	$C_D \alpha C_m$ vs C_L	gear parts	27
Drooped slats + flaps + gear - main gear doors	6	$C_Y C_l C_n C_L C_m$ vs β	α	28
Drooped slats + flaps	6	$C_D \alpha C_m$ vs C_L	main gear doors	29
Drooped slats + flaps - tail	6	do	do	30
Drooped slats + flaps - tail + gear	6	do	oleo strut doors	31

CONFIDENTIAL

CONFIDENTIAL

TABLE III.- CONTINUED

General Configuration	Wing Incidence (deg)	Data Presented	Variable	Fig. No.
Stability (Tail off)				
Clean	0	$C_D \alpha C_m C_Y C_n C_l$ vs C_L	β	32
	0	$C_Y C_l C_n C_L C_m$ vs β	α	33
Gear + drooped slats + flaps	6	$C_D \alpha C_m C_Y C_n C_l$ vs C_L	β	34
	6	$C_Y C_l C_n C_L C_m$ vs β	α	35
Control (Aileron)				
Clean	0	$\alpha C_m C_n C_l C_{h_a}$ vs C_L	δ_a	36
	0	$C_n C_m C_l C_{h_a}$ vs δ_a	α	37
	0	do	α, β	38
Gear + drooped slats + flaps	6	$\alpha C_m C_n C_l C_{h_a}$ vs C_L	δ_a	39
	6	$C_n C_m C_l C_{h_a}$ vs δ_a	α	40
	6	do	α, β	41
Partial gear + drooped slats + flaps	6	$\alpha C_m C_n C_l C_{h_a}$ vs C_L	δ_a	42
	6	$C_n C_m C_l C_{h_a}$ vs δ_a	α	43
	6	do	α, β	44
Drooped slats + flaps	6	$\alpha C_m C_n C_l C_{h_a}$ vs C_L	δ_a	45
	6	$C_n C_m C_l C_{h_a}$ vs δ_a	α	46
	6	do	α, β	47

CONFIDENTIAL

CONFIDENTIAL

TABLE III.- CONTINUED

General Configuration	Wing Incidence (deg)	Data Presented	Variable	Fig. No.
Control (Aileron)				
Drooped slats	0	$\alpha C_m C_n C_l C_{h_a}$ vs C_L	δ_a	48
	0	$C_n C_m C_l C_{h_a}$ vs δ_a	α	49
	0	do	α, β	50
Flaps	0	$\alpha C_m C_n C_l C_{h_a}$ vs C_L	δ_a	51
	0	$C_n C_m C_l C_{h_a}$ vs δ_a	α	52
	0	do	α, β	53
Control (Elerudder)				
Clean	0	$\alpha C_l C_Y C_m C_n C_{h_e}$ vs C_L	δ_e	54
	0	$C_n C_m C_{h_e} C_L C_Y C_l$ vs δ_e	α	55
	0	do	α, β	56
	0	$C_n C_m C_{h_e} C_Y C_l$ vs β	δ_e, α	57
	0	$\alpha C_m C_n C_{h_e}$ vs C_L	δ_{tab}, δ_e	58
	0	$C_n C_m C_{h_e}$ vs δ_e	δ_{tab}	59
Tanks	0	$\alpha C_l C_Y C_m C_n C_{h_e}$ vs C_L	δ_e	60
	0	$C_n C_m C_{h_e} C_L C_Y C_l$ vs δ_e	α	61
	0	$C_n C_m C_{h_e} C_Y C_l$ vs δ_e	α, β	62

CONFIDENTIAL

CONFIDENTIAL

TABLE III.- CONTINUED

General Configuration	Wing Incidence (deg)	Data Presented	Variable	Fig. No.
Control (Elerudder)				
Tanks + gear + drooped slats	6	$\alpha C_l C_Y C_m C_n C_{h_e}$ vs C_L	δ_e	63
	6	$C_n C_m C_{h_e} C_L C_Y C_l$ vs δ_e	α	64
	6	do	α, β	65
	6	$C_n C_m C_{h_e} C_Y C_l$ vs β	δ_e, α	66
Gear + drooped slats + flaps	6	$\alpha C_l C_Y C_m C_n C_{h_e}$ vs C_L	δ_e	67
	6	$C_n C_m C_{h_e} C_l C_Y C_l$ vs δ_e	α	68
	6	do	α, β	69
	6	$C_n C_m C_{h_e} C_Y C_l$ vs β	δ_e, α	70
Control (Pure elevator action)				
Tank	0	$C_n C_m C_{h_e} C_L C_Y C_l$ vs δ_e	α	71
Control (Pure rudder action)				
Tank	0	$C_n C_m C_{h_r} C_L C_Y C_l$ vs δ_r	α, β	72
Control (Wing incidence)				
Clean	—	$C_D \alpha C_m C_{h_e}$ vs C_L	i_w	73
Tanks + gear + drooped slats	—	do	i_w	74
Gear + drooped slats + flaps	—	do	i_w	75

CONFIDENTIAL

CONFIDENTIAL

TABLE III.- CONCLUDED

General Configuration	Wing Incidence (deg)	Data Presented	Variable	Fig. No.
Control (Tail incidence)				
Clean	0	$C_D \propto C_m C_{h_e}$ vs C_L	i_t	76
Gear + drooped slats + flaps	6	do	i_t	77

CONFIDENTIAL

CONFIDENTIAL

FIGURE LEGENDS

Figure 1.-- Sign convention for the standard NACA coefficients. All forces, moments, angles, and control-surface deflections are shown as positive.

Figure 2.-- Three-view drawing of the Republic XF-91 full-scale model.

Figure 3.-- Details of the Republic XF-91 inverse-taper wing.

Figure 4.-- Drooped slat, aileron, and elerudder cross sections.

Figure 5.-- Views of the test installation of the full-scale model of Republic XF-91 in the Ames 40- by 80-foot wind tunnel. (a) Three-quarter front view of the clean model.

Figure 5.-- Continued. (b) Front view of the model with tanks at a negative angle of sideslip.

Figure 5.-- Concluded. (c) Three-quarter rear view of model with the gear, flaps, and drooped slats extended.

Figure 6.-- Aerodynamic characteristics in pitch of the model at various angles of sideslip. Plain wing. (a) i_w , 0° ; C_D , α , C_m vs C_L .

Figure 6.-- Continued. (b) i_w , 0° ; C_Y , C_n , C_l vs C_L .

Figure 6.-- Continued. (c) i_w , 6° ; C_D , α , C_m vs C_L .

Figure 6.-- Concluded. (d) i_w , 6° ; C_Y , C_n , C_l vs C_L .

Figure 7.-- Aerodynamic characteristics in sideslip of the model at various angles of attack. Plain wing. (a) i_w , 0° ; C_Y , C_l , C_n vs β .

Figure 7.-- Continued. (b) i_w , 0° ; C_L , C_m vs β .

Figure 7.-- Continued. (c) i_w , 6° ; C_Y , C_l , C_n vs β .

Figure 7.-- Concluded. (d) i_w , 6° ; C_L , C_m vs β .

Figure 8.-- Aerodynamic characteristics in pitch of the model at various angles of sideslip. External tanks; i_w , 0° . (a) C_D , α , C_m vs C_L .

Figure 8.-- Concluded. (b) C_Y , C_n , C_l vs C_L .

Figure 9.-- Aerodynamic characteristics in sideslip of the model at various angles of attack. External tanks; i_w , 0° . (a) C_Y , C_l , C_m vs β .

Figure 9.-- Concluded. (b) C_L , C_m vs β .

Figure 10.- Aerodynamic characteristics in pitch of the model at various angles of sideslip. External tanks; gear; $i_w, 0^\circ$.
(a) C_D, α, C_m vs C_L .

Figure 10.- Concluded. (b) C_Y, C_n, C_l vs C_L .

Figure 11.- Aerodynamic characteristics in sideslip of the model at various angles of attack. External tanks; gear; $i_w, 0^\circ$.
(a) C_Y, C_l, C_n vs β .

Figure 11.- Concluded. (b) C_L, C_m vs β .

Figure 12.- Aerodynamic characteristics in pitch of the model at various angles of sideslip. External tanks; gear; drooped slats.
(a) $i_w, 0^\circ; C_D, \alpha, C_m$ vs C_L .

Figure 12.- Continued. (b) $i_w, 0^\circ; C_Y, C_n, C_l$ vs C_L .

Figure 12.- Continued. (c) $i_w, 6^\circ; C_D, \alpha, C_m$ vs C_L .

Figure 12.- Concluded. (d) $i_w, 6^\circ; C_Y, C_n, C_l$ vs C_L .

Figure 13.- Aerodynamic characteristics in sideslip of the model at various angles of attack. External tanks; gear; drooped slats.
(a) $i_w, 0^\circ; C_Y, C_l, C_n$ vs β .

Figure 13.- Continued. (b) $i_w, 0^\circ; C_L, C_m$ vs β .

Figure 13.- Continued. (c) $i_w, 6^\circ; C_Y, C_l, C_n$ vs β .

Figure 13.- Concluded. (d) $i_w, 6^\circ; C_L, C_m$ vs β .

Figure 14.- Effect of plain flap angle on the aerodynamic characteristics of the model in pitch. Gear; drooped slats; $i_w, 6^\circ$.

Figure 15.- Aerodynamic characteristics in pitch of the model at various angles of sideslip. Gear; drooped slats; plain flaps. $40^\circ; i_w, 6^\circ$. (a) C_D, α, C_m vs C_L .

Figure 15.- Concluded. (b) C_Y, C_n, C_l vs C_L .

Figure 16.- Aerodynamic characteristics in sideslip of the model at various angles of attack. Gear; drooped slats; plain flaps, $40^\circ; i_w, 6^\circ$. (a) C_Y, C_l, C_n vs β .

Figure 16.- Concluded. (b) C_L , C_m vs β .

Figure 17.- Aerodynamic characteristics in pitch of the model at various angles of sideslip. Right gear partially extended; drooped slats; plain flaps, 40° ; i_w , 6° . (a) C_D , α , C_m vs C_L .

Figure 17.- Concluded. (b) C_Y , C_n , C_l vs C_L .

Figure 18.- Aerodynamic characteristics in sideslip of the model at various angles of attack. Right gear partially extended; drooped slats; plain flaps, 40° ; i_w , 6° . (a) C_Y , C_l , C_n vs β .

Figure 18.- Concluded. (b) C_L , C_m vs β .

Figure 19.- Aerodynamic characteristics in pitch of the model at various angles of sideslip. Drooped slats; plain flaps, 40° . (a) i_w , 0° ; C_D , α , C_m vs C_L .

Figure 19.- Continued. (b) i_w , 0° ; C_Y , C_n , C_l vs C_L .

Figure 19.- Continued. (c) i_w , 6° ; C_D , α , C_m vs C_L .

Figure 19.- Concluded. (d) i_w , 6° ; C_Y , C_n , C_l vs C_L .

Figure 20.- Aerodynamic characteristics in sideslip of the model at various angles of attack. Drooped slats; plain flaps, 40° . (a) i_w , 0° ; C_Y , C_l , C_n vs β .

Figure 20.- Continued. (b) i_w , 0° ; C_L , C_m vs β .

Figure 20.- Continued. (c) i_w , 6° ; C_Y , C_l , C_n vs β .

Figure 20.- Concluded. (d) i_w , 6° ; C_L , C_n vs β .

Figure 21.- Effect of the drooped slat modification on the aerodynamic characteristics of model in pitch. Plain flaps, 40° ; i_w , 6° .

Figure 22.- Aerodynamic characteristics in pitch of the model at various angles of sideslip. Drooped slats; i_w , 0° . (a) C_D , α , C_m vs C_L .

Figure 22.- Concluded. (b) C_Y , C_n , C_l vs C_L .

Figure 23.- Aerodynamic characteristics in sideslip of the model at various angles of attack. Drooped slats; i_w , 0° . (a) C_Y , C_l , C_n vs β .

Figure 23.- Concluded. (b) C_L , C_m vs β .

Figure 24.- Effect of plain flap angle on the aerodynamic characteristics of the model in pitch. i_w , 0° .

Figure 25.- Aerodynamic characteristics in pitch of the model at various angles of sideslip. Plain flaps, 40° ; i_w , 0° .
(a) C_D , α , C_m vs C_L .

Figure 25.- Concluded. (b) C_Y , C_n , C_l vs C_L .

Figure 26.- Aerodynamic characteristics in sideslip of the model at various angles of attack. Plain flaps, 40° ; i_w , 0° . (a) C_Y , C_l , C_n vs β .

Figure 26.- Concluded. (b) C_L , C_m vs β .

Figure 27.- Effect of different parts of the gear on the aerodynamic characteristics of the model in pitch. Drooped slats; plain flaps, 40° ; i_w , 6° .

Figure 28.- Effect of the gear with main gear doors removed on the aerodynamic characteristics of the model in sideslip. Drooped slats; plain flaps, 40° ; i_w , 6° . (a) C_Y , C_l , C_n vs β .

Figure 28.- Concluded. (b) C_L , C_m vs β .

Figure 29.- Effect of the main gear doors on the aerodynamic characteristics of the model in pitch. Drooped slats; plain flaps, 40° ; i_w , 6° .

Figure 30.- Effect of the main gear doors on the aerodynamic characteristics of the model in pitch with tail removed. Drooped slats; plain flaps; 40° ; i_w , 6° .

Figure 31.- Effect of the main gear oleo-strut doors on the aerodynamic characteristics of the model in pitch with the tail removed. Gear; drooped slats; plain flaps, 40° ; i_w , 6° .

Figure 32.- Aerodynamic characteristics in pitch of the model with tail removed at various angles of sideslip. Plain wing; i_w , 0° .
(a) C_D , α , C_m vs C_L .

Figure 32.- Concluded. (b) C_Y , C_n , C_l vs C_L .

Figure 33.-- Aerodynamic characteristics in sideslip of the model with tail removed at various angles of attack. Plain wing; $i_w, 0^\circ$.

(a) C_Y, C_L, C_n vs β .

Figure 33.-- Concluded. (b) C_L, C_m vs β .

Figure 34.-- Aerodynamic characteristics in pitch of the model with tail removed at various angles of sideslip. Gear; drooped slats; plain flaps, 40° ; $i_w, 6^\circ$. (a) C_D, α, C_m vs C_L .

Figure 34.-- Concluded. (b) C_Y, C_n, C_l vs C_L .

Figure 35.-- Aerodynamic characteristics in sideslip of the model with tail removed at various angles of attack. Gear; drooped slats; plain flaps, 40° ; $i_w, 6^\circ$. (a) C_Y, C_l, C_n vs β .

Figure 35.-- Concluded. (b) C_L, C_m vs β .

Figure 36.-- Effect of fixed deflections of the right aileron on the aerodynamic characteristics of the model in pitch. Plain wing; $i_w, 0^\circ$. (a) α, C_m, C_n vs C_L .

Figure 36.-- Concluded. (b) C_l, C_{h_a} vs C_L .

Figure 37.-- Variation with right aileron deflection of the aerodynamic characteristics of the model at several angles of attack. Plain wing; $i_w, 0^\circ$. (a) C_n, C_m vs δ_a .

Figure 37.-- Concluded. (b) C_l, C_{h_a} vs δ_a .

Figure 38.-- Variation with right aileron deflection of the aerodynamic characteristics of the model in sideslip at several angles of attack. Plain wing; $i_w, 0^\circ$. (a) C_n, C_m vs δ_a .

Figure 38.-- Concluded. (b) C_l, C_{h_a} vs δ_a .

Figure 39.-- Effect of fixed deflections of the right aileron on the aerodynamic characteristics of the model in pitch. Gear; drooped slats; plain flaps, 40° ; $i_w, 6^\circ$. (a) α, C_m, C_n vs C_L .

Figure 39.-- Concluded. (b) C_l, C_{h_a} vs C_L .

Figure 40.-- Variation with right aileron deflection of the aerodynamic characteristics of the model at several angles of attack. Gear; drooped slats; plain flaps, 40° ; $i_w, 6^\circ$. (a) C_n, C_m vs δ_a .

Figure 40.- Concluded. (b) C_L , C_{h_a} vs δ_a .

Figure 41.- Variation with right aileron deflection of the aerodynamic characteristics of the model in sideslip at several angles of attack. Gear; drooped slats; plain flaps, 40° ; i_w , 6° . (a) C_n , C_m vs δ_a .

Figure 41.- Concluded. (b) C_L , C_{h_a} vs δ_a .

Figure 42.- Effect of fixed deflections of the right aileron on the aerodynamic characteristics of the model in pitch. Right gear partially extended; drooped slats; plain flaps, 40° ; i_w , 6° . (a) α , C_m , C_n vs C_L .

Figure 42.- Concluded. (b) C_L , C_{h_a} vs C_L .

Figure 43.- Variation with right aileron deflection of the aerodynamic characteristics of the model at several angles of attack. Right gear partially extended; drooped slats; plain flaps, 40° ; i_w , 6° . (a) C_n , C_m vs δ_a .

Figure 43.- Concluded. (b) C_L , C_{h_a} vs δ_a .

Figure 44.- Variation with right aileron deflection of the aerodynamic characteristics of the model in sideslip at several angles of attack. Right gear partially extended; drooped slats; plain flaps, 40° ; i_w , 6° . (a) C_n , C_m vs δ_a .

Figure 44.- Concluded. (b) C_L , C_{h_a} vs δ_a .

Figure 45.- Effect of fixed deflections of the right aileron on the aerodynamic characteristics of the model in pitch. Drooped slats; plain flaps, 40° ; i_w , 6° . (a) α , C_m , C_n vs C_L .

Figure 45.- Concluded. (b) C_L , C_{h_a} vs C_L .

Figure 46.- Variation with right aileron deflection of the aerodynamic characteristics of the model at several angles of attack. Drooped slats; plain flaps, 40° ; i_w , 6° . (a) C_n , C_m vs δ_a .

Figure 46.- Concluded. (b) C_L , C_{h_a} vs δ_a .

Figure 47.- Variation with right aileron deflection of the aerodynamic characteristics of the model in sideslip at several angles of attack. Drooped slats; plain flaps, 40° ; i_w , 6° . (a) C_n , C_m vs δ_a .

Figure 47.- Concluded. (b) C_L , C_{h_a} vs δ_a .

Figure 48.- Effect of fixed deflections of the right aileron on the aerodynamic characteristics of the model in pitch. Drooped slats; $i_w, 0^\circ$. (a) α, C_m, C_n vs C_L .

Figure 48.- Concluded. (b) C_l, C_{h_a} vs C_L .

Figure 49.- Variation with right aileron deflection of the aerodynamic characteristics of the model at several angles of attack. Drooped slats; $i_w, 0^\circ$. (a) C_n, C_m vs δ_a .

Figure 49.- Concluded. (b) C_l, C_{h_a} vs δ_a .

Figure 50.- Variation with right aileron deflection of the aerodynamic characteristics of the model in sideslip at several angles of attack. Drooped slats; $i_w, 0^\circ$. (a) C_n, C_m vs δ_a .

Figure 50.- Concluded. (b) C_l, C_{h_a} vs δ_a .

Figure 51.- Effect of fixed deflections of the right aileron on the aerodynamic characteristics of the model in pitch. Plain flaps, 40° ; $i_w, 0^\circ$. (a) α, C_m, C_n vs C_L .

Figure 51.- Concluded. (b) C_l, C_{h_a} vs C_L .

Figure 52.- Variation with right aileron deflection of the aerodynamic characteristics of the model at several angles of attack. Plain flaps, 40° ; $i_w, 0^\circ$. (a) C_n, C_m vs δ_a .

Figure 52.- Concluded. (b) C_l, C_{h_a} vs δ_a .

Figure 53.- Variation with right aileron deflection of the aerodynamic characteristics of the model in sideslip at several angles of attack. Plain flaps, 40° , $i_w, 0^\circ$. (a) C_n, C_m vs δ_a .

Figure 53.- Concluded. (b) C_l, C_{h_a} vs δ_a .

Figure 54.- Effect of fixed deflections of the elerudder on the aerodynamic characteristics of the model in pitch. Plain wing; $i_w, 0^\circ$. (a) α, C_l, C_y vs C_L .

Figure 54.- Concluded. (b) $C_m, C_n, C_{h_{e_R}}$ vs C_L .

Figure 55.- Variation with elerudder deflection of the aerodynamic characteristics of the model at several angles of attack. Plain wing; $i_w, 0^\circ$.

Figure 56.- Variation with elerudder deflection of the aerodynamic characteristics of the model in sideslip at several angles of attack. Plain wing; $i_w, 0^\circ$.

Figure 57.- Effect of fixed deflections of the elerudder on the aerodynamic characteristics of the model in sideslip. Plain wing; $i_w, 0^\circ$. (a) $\alpha_w, 0.1^\circ$; C_n, C_m, C_{he_R} vs β .

Figure 57.- Continued. (b) $\alpha_w, 0.1^\circ$; C_Y, C_L, C_n vs β .

Figure 57.- Continued. (c) $\alpha_w, 12.6^\circ$; C_n, C_m, C_{he_R} vs β .

Figure 57.- Concluded. (d) $\alpha_w, 12.6^\circ$; C_Y, C_L vs β .

Figure 58.- Effect of fixed elerudder trim tab deflection on the aerodynamic characteristics of the model in pitch at several elerudder angles. Plain wing; $i_w, 0^\circ$. (a) $\delta_{e_R}, 8^\circ$; $\alpha, C_m, C_n, C_{he_R}$ vs C_L .

Figure 58.- Continued. (b) $\delta_{e_R}, 0^\circ$; $\alpha, C_m, C_n, C_{he_R}$ vs C_L .

Figure 58.- Concluded. (c) $\delta_{e_R}, -16^\circ$; $\alpha, C_m, C_n, C_{he_R}$ vs C_L .

Figure 59.- Variation with elerudder deflection of the aerodynamic characteristics of the model for several trim tab angles. Plain wing; $i_w, 0^\circ$.

Figure 60.- Effect of fixed deflections of the elerudder on the aerodynamic characteristics of the model in pitch. External tanks; $i_w, 0^\circ$. (a) α, C_L, C_Y vs C_L .

Figure 60.- Concluded. (b) C_m, C_n, C_{he} vs C_L .

Figure 61.- Variation with elerudder deflection of the aerodynamic characteristics of the model at several angles of attack. External tanks; $i_w, 0^\circ$.

Figure 62.- Variation with elerudder deflection of the aerodynamic characteristics of the model in sideslip at several angles of attack. External tanks; $i_w, 0^\circ$.

Figure 63.- Effect of fixed deflections of the elerudder on the aerodynamic characteristics of the model in pitch. External tanks; gear; drooped slats; i_w , 6° . (a) α , C_l , C_Y vs C_L .

Figure 63.- Concluded. (b) C_m , C_n , C_{he_R} vs C_L .

Figure 64.- Variation with elerudder deflection of the aerodynamic characteristics of the model at several angles of attack. External tanks; drooped slats; gear; i_w , 6° .

Figure 65.- Variation with elerudder deflection of the aerodynamic characteristics of the model in sideslip at several angles of attack. Gear; external tanks; drooped slats; i_w , 6° .

Figure 66.- Effect of fixed deflections of the elerudder on the aerodynamic characteristics of the model in sideslip. External tanks; gear; drooped slats; i_w , 6° . (a) α_w , 0° ; C_n , C_m , C_{he} vs β .

Figure 66.- Continued. (b) α_w , 0° ; C_Y , C_l vs β .

Figure 66.- Continued. (c) α_w , 18.8° ; C_n , C_m , C_{he} vs β .

Figure 66.- Concluded. (d) α_w , 18.8° ; C_Y , C_l vs β .

Figure 67.- Effect of fixed deflections of the elerudder on the aerodynamic characteristics of the model in pitch. Gear; drooped slats; plain flaps, 40° ; i_w , 6° . (a) α , C_l , C_Y vs C_L .

Figure 67.- Concluded. (b) C_m , C_n , C_{he_R} vs C_L .

Figure 68.- Variation with elerudder deflection of the aerodynamic characteristics of the model at several angles of attack. Gear; drooped slats; plain flaps, 40° ; i_w , 6° .

Figure 69.- Variation with elerudder deflection of the aerodynamic characteristics of the model in sideslip at several angles of attack. Gear; drooped slats, plain flaps, 40° ; i_w , 6° .

Figure 70.- Effect of fixed deflections of the elerudder on the aerodynamic characteristics of the model in sideslip. Gear; drooped slats; plain flaps, 40° ; i_w , 6° . (a) α_w , 0.3° ; C_n , C_m , C_{he} vs β .

Figure 70.- Continued. (b) α_w , 0.3° ; C_Y , C_L vs β .

Figure 70.- Continued. (c) α_w , 18.8° ; C_n , C_m , C_{he} vs β .

Figure 70.- Concluded. (d) α_w , 18.8° C_Y , C_L vs β .

Figure 71.- Effectiveness of the complete elerudder system operated for pure elevator action with the model at several angles of attack. External tanks; i_w , 0° ; β , 0° .

Figure 72.- Effectiveness of the complete elerudder system operated for pure rudder action with the model at several angles of attack. External tanks; i_w , 0° .

Figure 72.- Concluded. (b) β , -8° .

Figure 73.- Effect of fixed angles of wing incidence on the aerodynamic characteristics of the model in pitch. Plain wing; δ_e , 0° .
(a) C_D , α , vs C_L .

Figure 73.- Concluded. (b) C_m , C_{heR} vs C_L .

Figure 74.- Effect of fixed angles of wing incidence on the aerodynamic characteristics of the model in pitch. External tanks; gear; drooped slats; δ_e , 0° . (a) C_D , α , vs C_L .

Figure 74.- Concluded. (b) C_m , C_{heR} vs C_L .

Figure 75.- Effect of fixed angles of wing incidence on the aerodynamic characteristics of the model in pitch. Gear; drooped slats; plain flaps, 40° ; δ_e , 0° . (a) C_D , α , vs C_L .

Figure 75.- Concluded. (b) C_m , C_{heR} vs C_L .

Figure 76.- Effect of fixed angles of tail incidence on the aerodynamic characteristics of the model in pitch. Plain wings; i_w , 0° , δ_e , 0° .
(a) C_D , α , vs C_L .

Figure 76.- Concluded. (b) C_m , C_{heR} vs C_L .

Figure 77.- Effect of fixed angles of tail incidence on the aerodynamic characteristics of the model in pitch. Gear; drooped slats; plain flaps, 40° ; i_w , 6° ; δ_e , 0° . (a) C_D , α vs C_L .

Figure 77.- Concluded. (b) C_m , C_{heR} vs C_L .

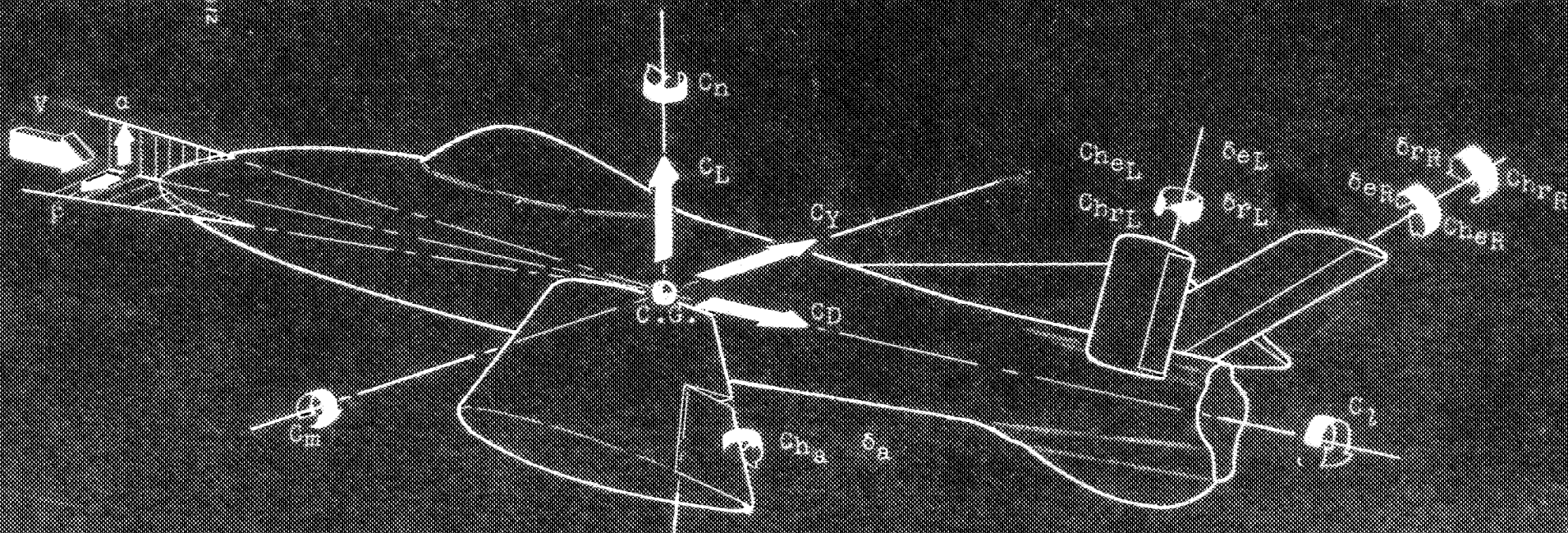


FIGURE 1.- SIGN CONVENTION FOR THE STANDARD NACA COEFFICIENTS.

ALL FORCES, MOMENTS, ANGLES, AND CONTROL SURFACE DEFLECTIONS
ARE SHOWN AS POSITIVE.

CONFIDENTIAL

NATIONAL ADVISORY COMMITTEE FOR AERONAUTICS

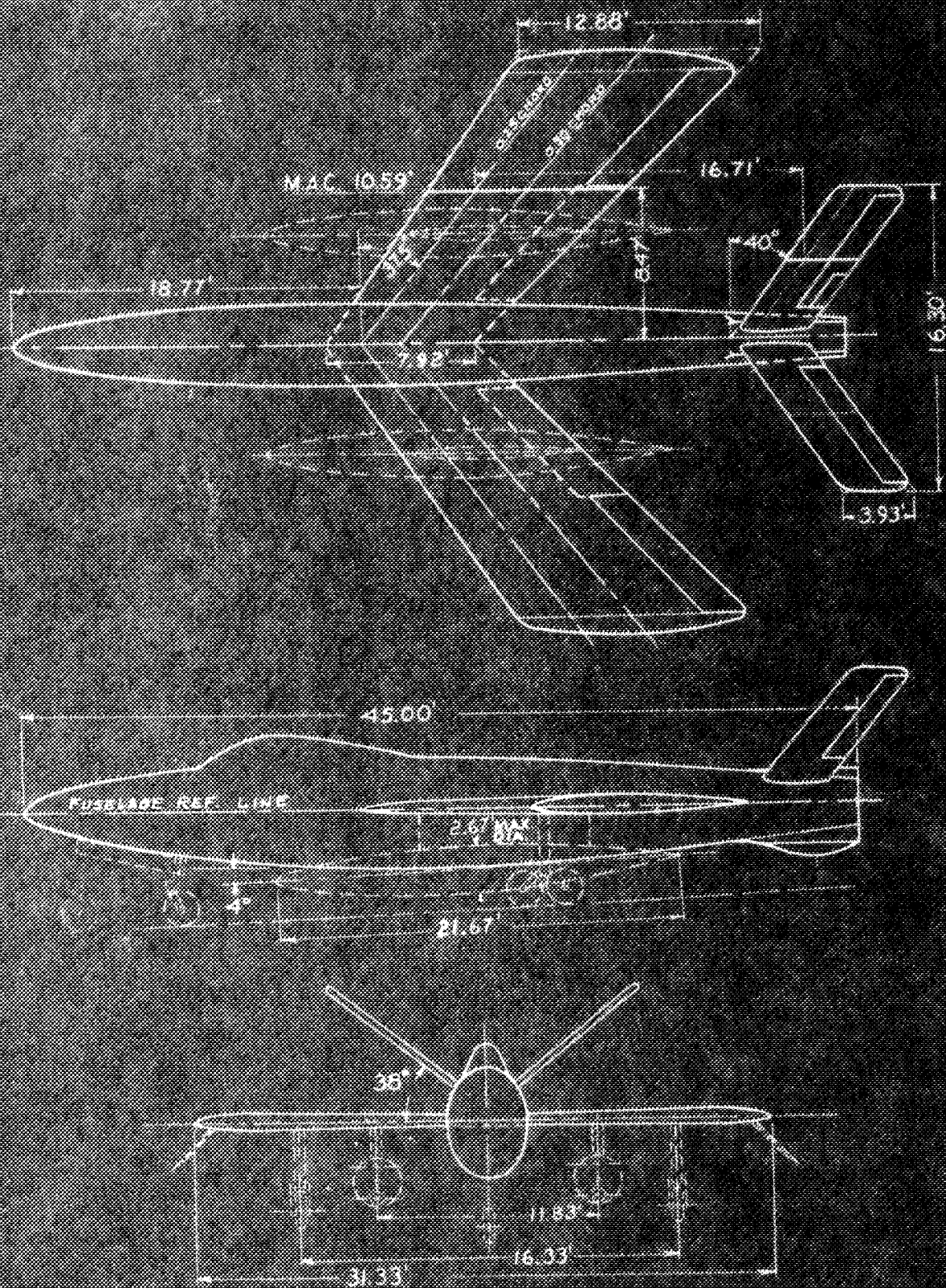


FIGURE 2.- THREE-VIEW DRAWING OF THE REPUBLIC XP-91 FULL-SCALE MODEL.

CONFIDENTIAL

NATIONAL ADVISORY COMMITTEE FOR AERONAUTICS

WING-AIRFOIL			ORDINATES	
CHORDS 1 to 0.50 - CHORD LINE				
x %c	y (UPPER) % CHORD		y (LOWER) % CHORD	
	Sta. 27"	Sta. 188"	Sta. 27"	Sta. 188"
.5	.839	.876	.683	.715
.75	1.024	1.061	.844	.881
1.25	1.331	1.378	1.090	1.132
2.5	1.896	1.943	1.520	1.562
5	2.680	2.721	2.104	2.141
7.5	3.270	3.294	2.520	2.545
10	3.747	3.756	2.844	2.863
15	4.485		3.325	
20	5.015		3.650	
25	5.405		3.875	
30	5.670		4.010	
35	5.835		4.090	
40	5.910		4.090	
45	5.895		4.035	
50	5.775		3.905	
55	5.570		3.705	
60	5.255		3.440	
65	4.855		3.105	
70	4.365		2.710	
75	3.795		2.265	
80	3.145		1.785	
85	2.435		1.290	
90	1.680		.790	
95	.880		.335	
100	----		----	
L.E.R. (STA. 27) = 0.569%c				
L.E.R. (STA. 188) = 0.615%c				
L.E.R. HEIGHT = 0.042%c				
T.E.R. = 0.032"				

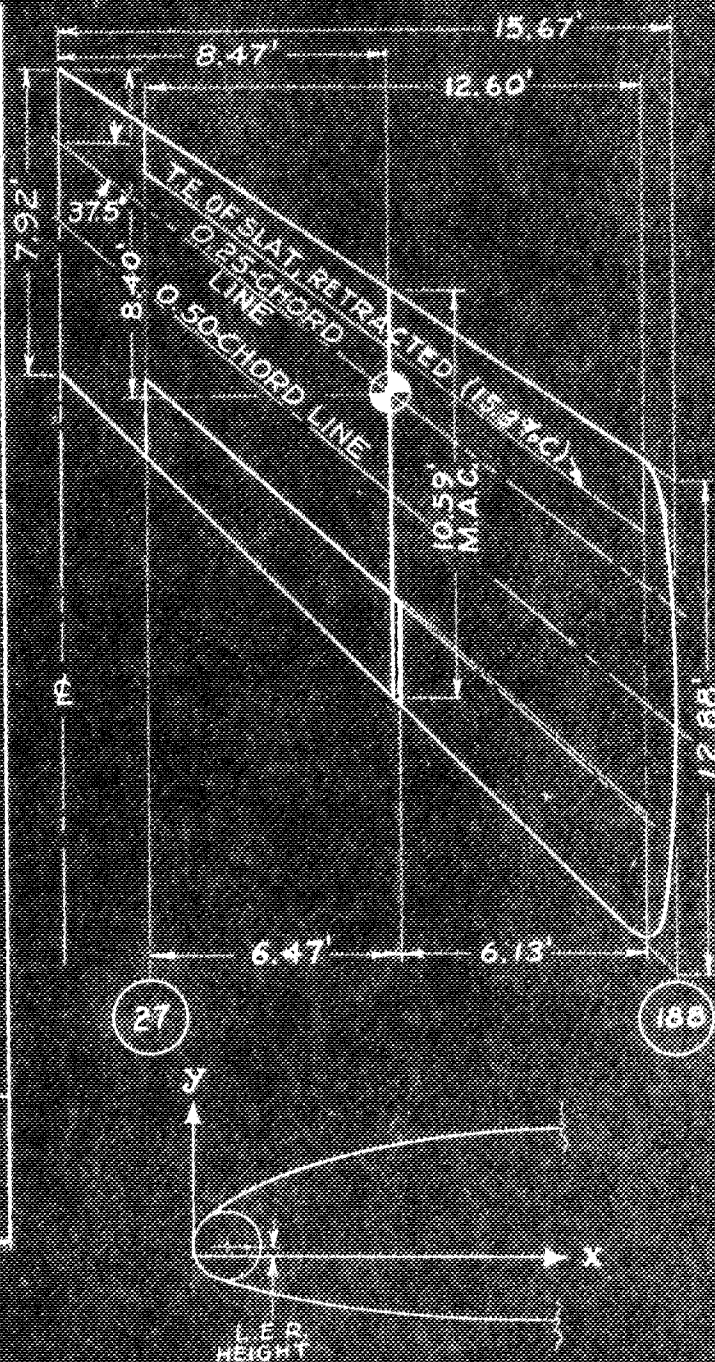
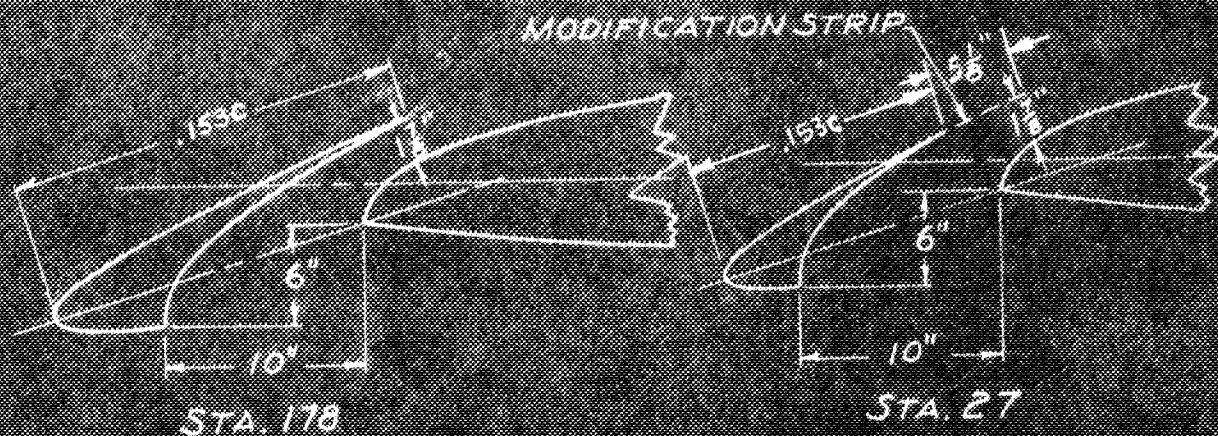


FIGURE 3.- DETAILS OF THE REPUBLIC XF-91 INVERSE-TAPER WING.

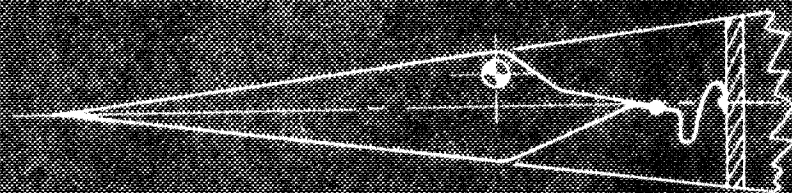
CONFIDENTIAL

NATIONAL ADVISORY COMMITTEE FOR AERONAUTICS

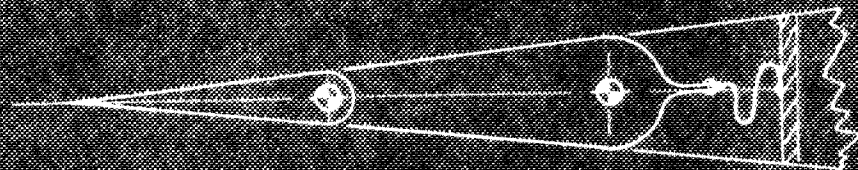


DROOPED - SLAT DETAILS

NOTE: ALL DIMENSIONS ARE PARALLEL TO THE PLANE OF SYMMETRY.
STRIP EXTENDS FROM STA. 27 TO 178 AND IS TAPERED UNIFORMLY IN WIDTH.



AILERON CROSS SECTION

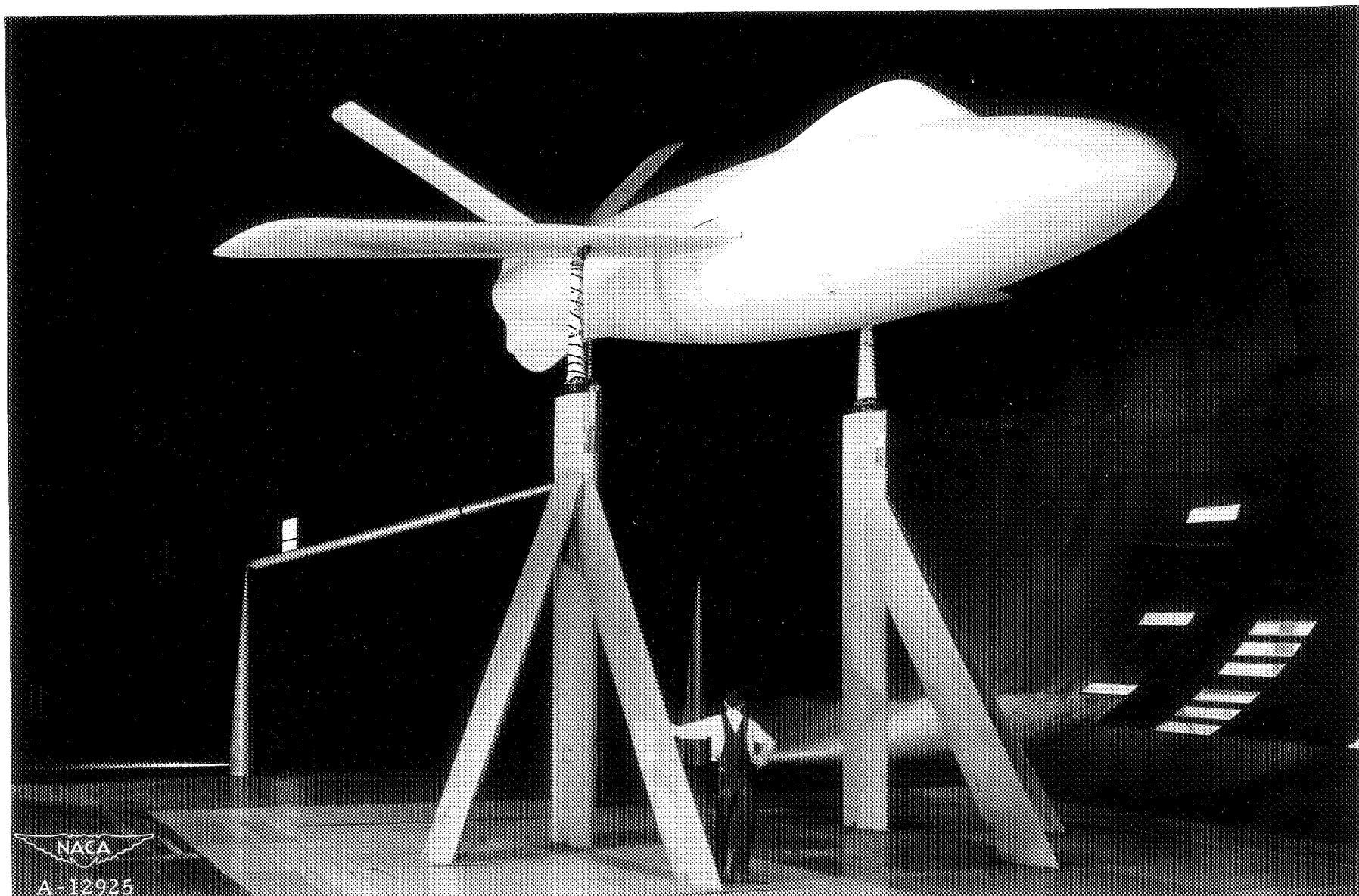


ELERUDDER AND TRIM-TAB
CROSS SECTION

FIGURE 1. - DROOPED SLAT, AILERON, AND ELERUDDER CROSS SECTIONS.

CONFIDENTIAL

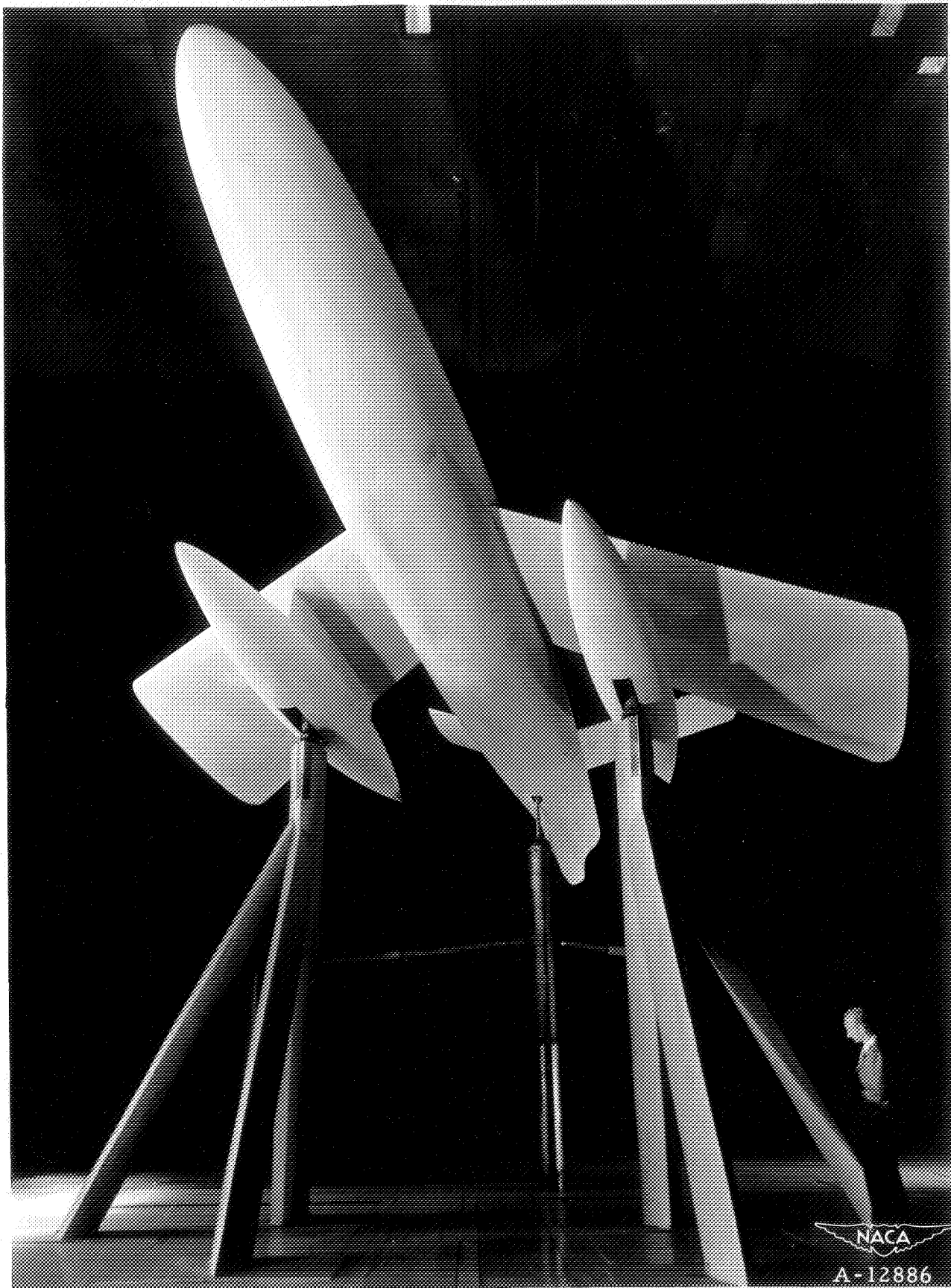
EXCLUDED FROM AUTOMATIC DOWNGRADING AND DECLASSIFICATION



(a) Three-quarter front view of the clean model.

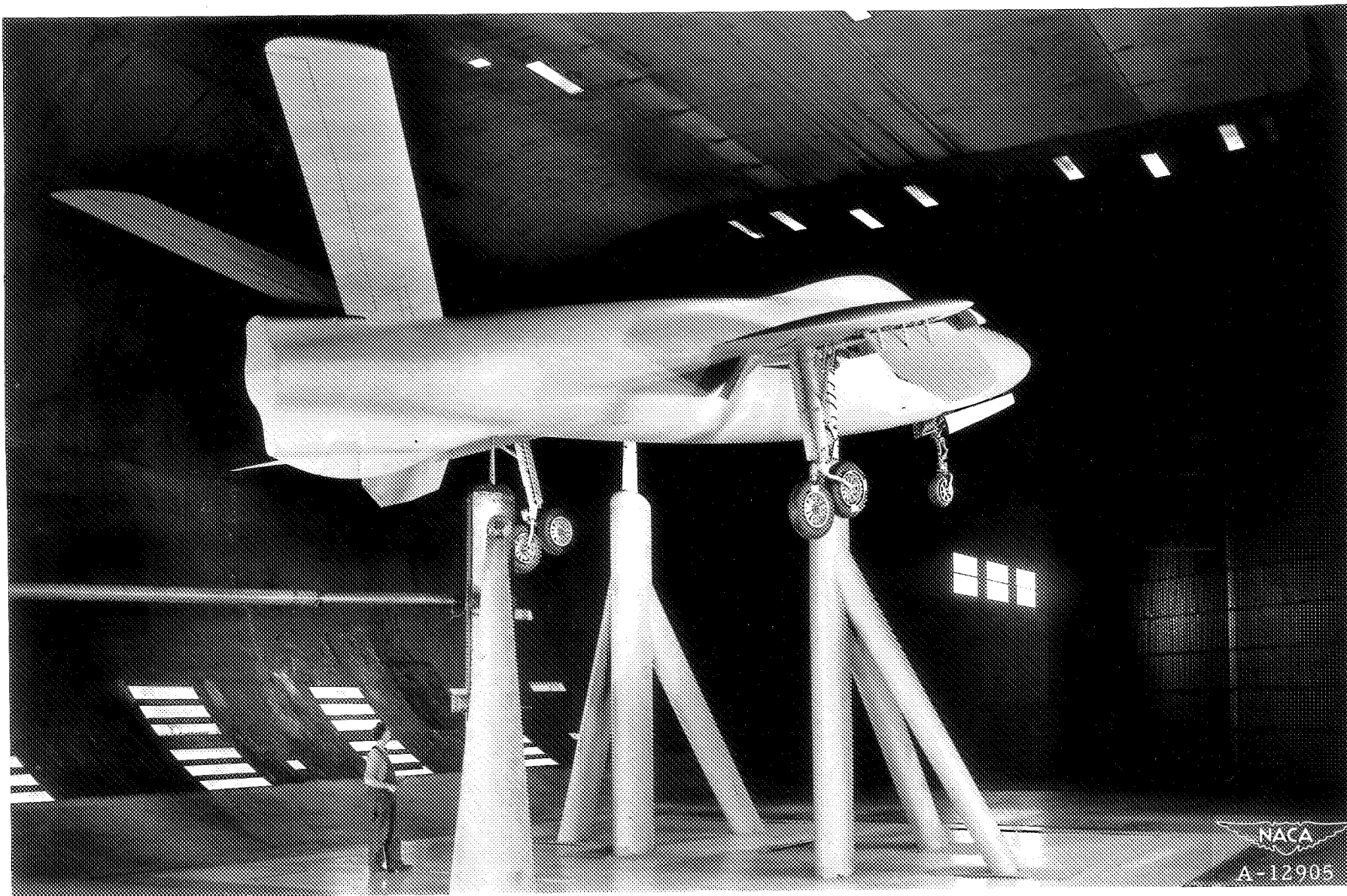
Figure 5.— Views of the test installation of the full-scale model of Republic XF-91 in the Ames 40- by 80-foot wind tunnel.

CONFIDENTIAL
NATIONAL ADVISORY COMMITTEE FOR AERONAUTICS
AMES AERONAUTICAL LABORATORY, MOFFETT FIELD, CALIF.



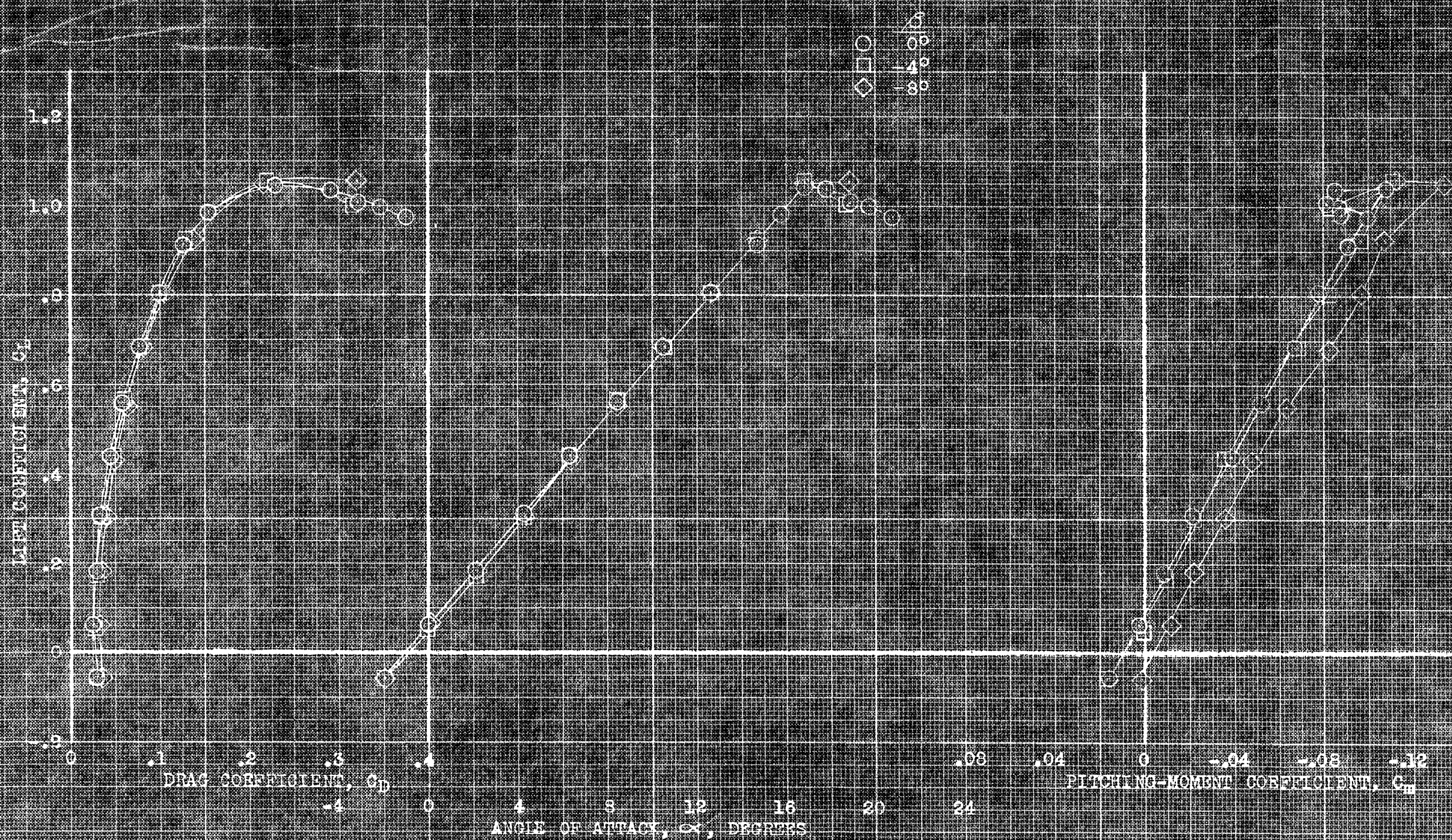
(b) Front view of the model with tanks at a negative angle of sideslip.

Figure 5.- Continued.



(c) Three-quarter rear view of model with the gear, flaps, and drooped slats extended.

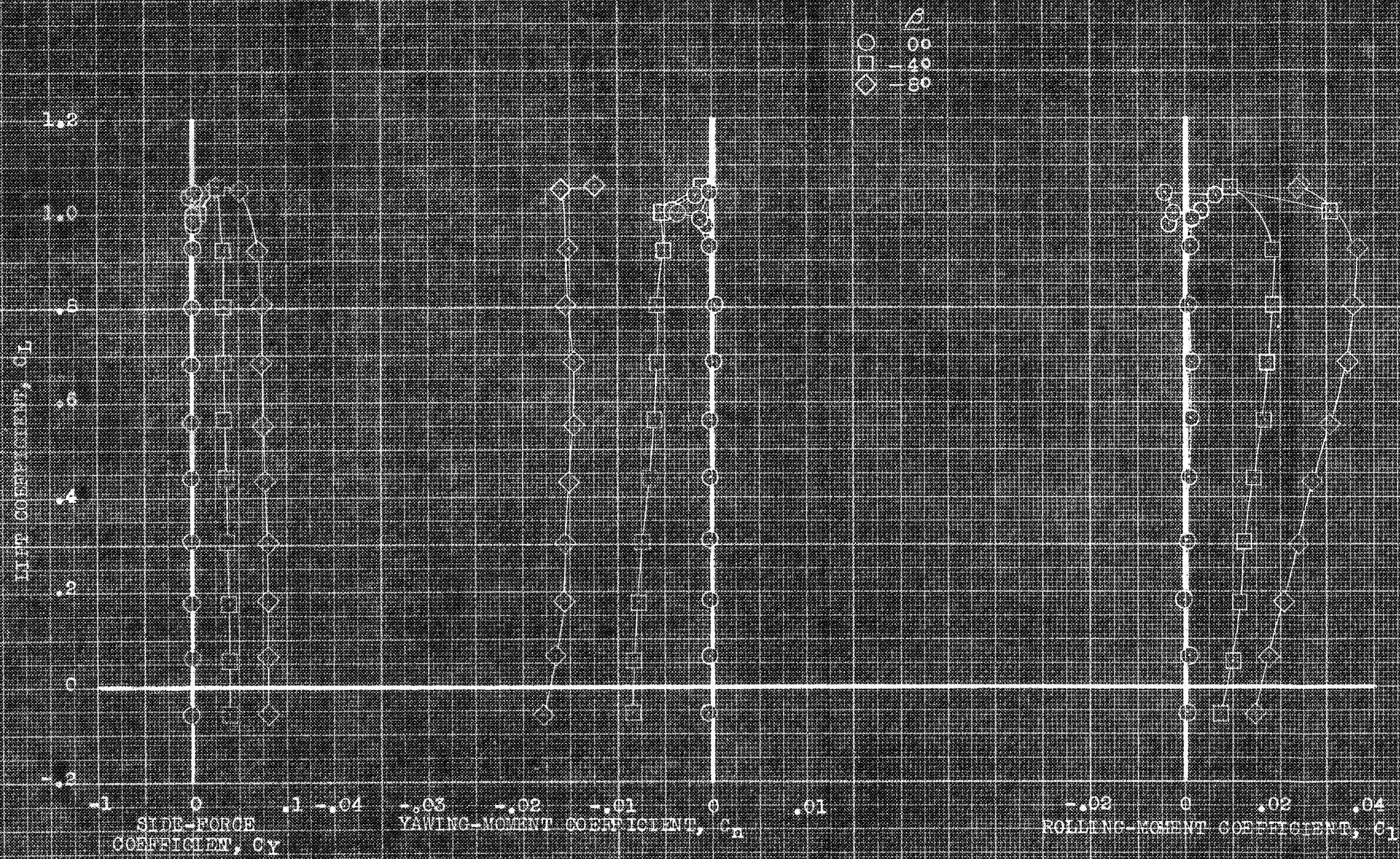
Figure 5.- Concluded.



(a) C_L , C_D , C_m vs. α

FIGURE 6. AERODYNAMIC CHARACTERISTICS IN PITCH OF THE MODEL AT VARIOUS ANGLES OF ATTACK, PLAIN AIRFOIL.

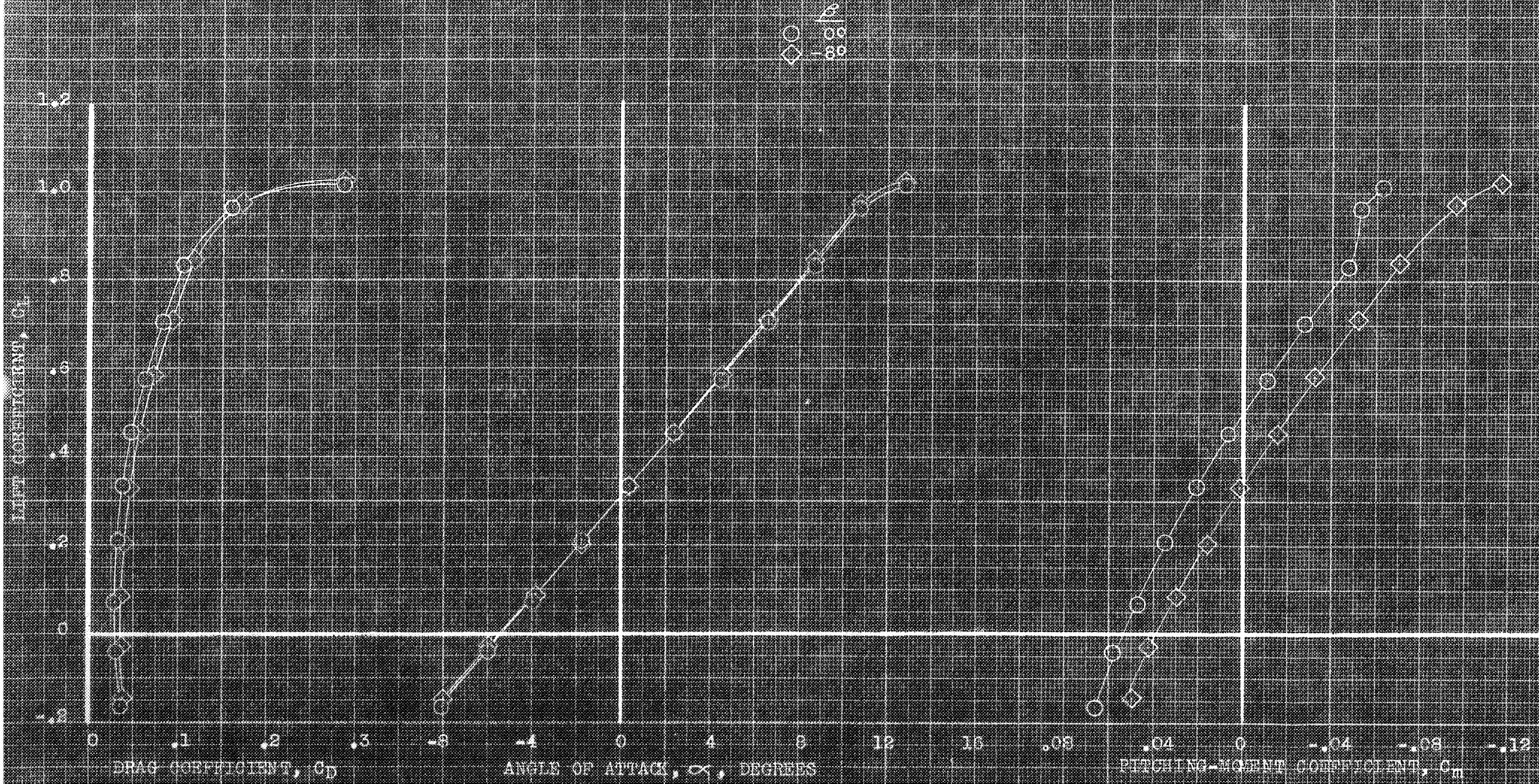
CONFIDENTIAL
 AIR FORCE RESEARCH AND DEVELOPMENT COMMAND
 WRIGHT-PATTERSON AIR FORCE BASE, OHIO



(b) C_Y , C_N , C_L , C_L vs C_L .

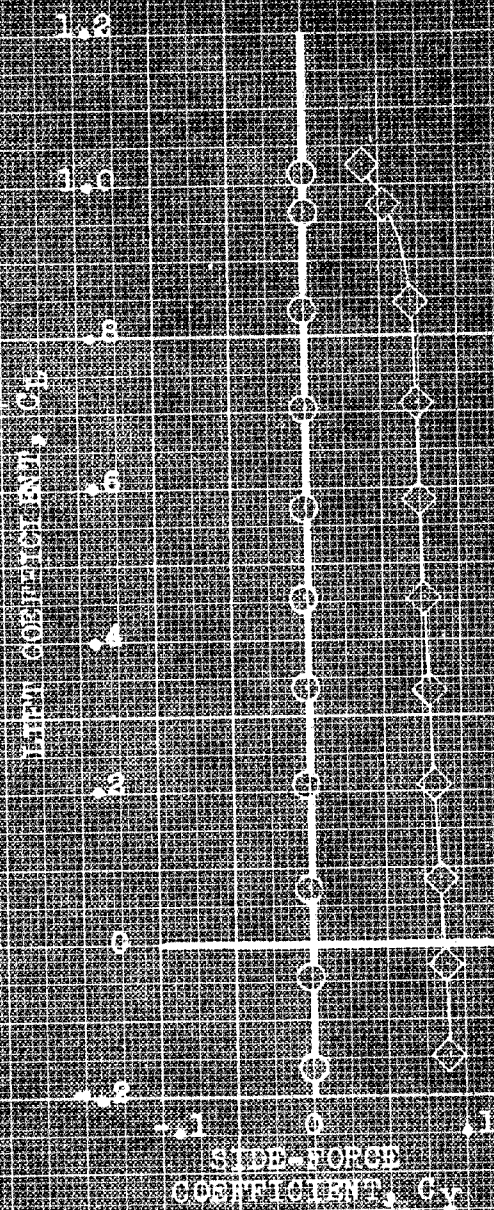
FIGURE 6.- CONTINUED.

CONFIDENTIAL
UNCLASSIFIED FOR SOURCE CONTAINING FOR AERONAUTICS



(c) 1.4, 6°, C_L , C_D , α , C_m vs C_L .

FIGURE 6.- CONTINUED.



YAWING-MOMENT COEFFICIENT, C_{N1}

YAWING-MOMENT COEFFICIENT, C_{N1}

ROLLING-MOMENT COEFFICIENT, C_{L1}

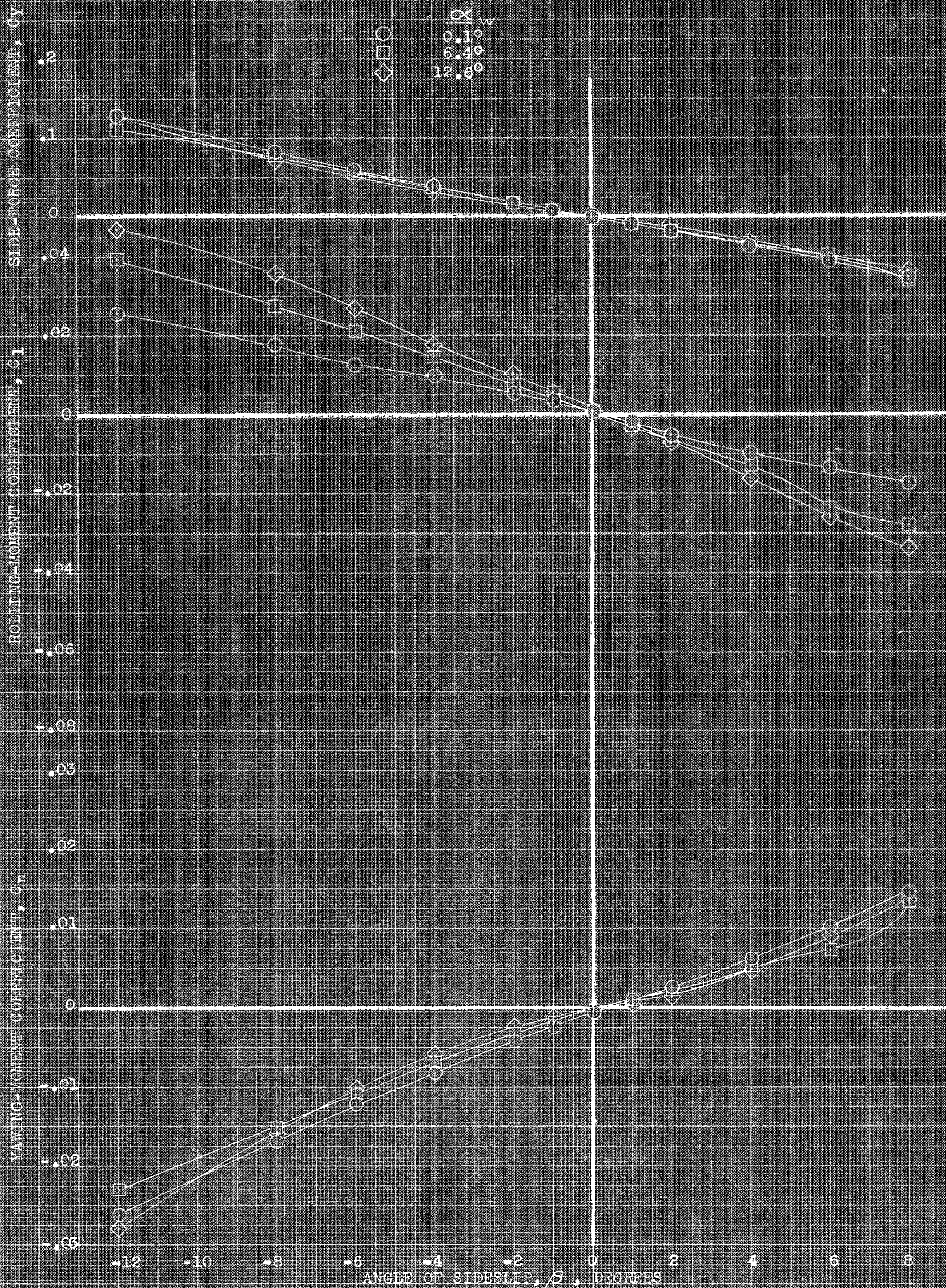
ROLLING-MOMENT COEFFICIENT, C_{L1}

(a) $1^\circ, 5^\circ, 9^\circ$; $C_{Y1} = 0$; $C_{L1} = 0$ vs C_{Y1}

FIGURE 6. - CONCLUDED.

CONFIDENTIAL

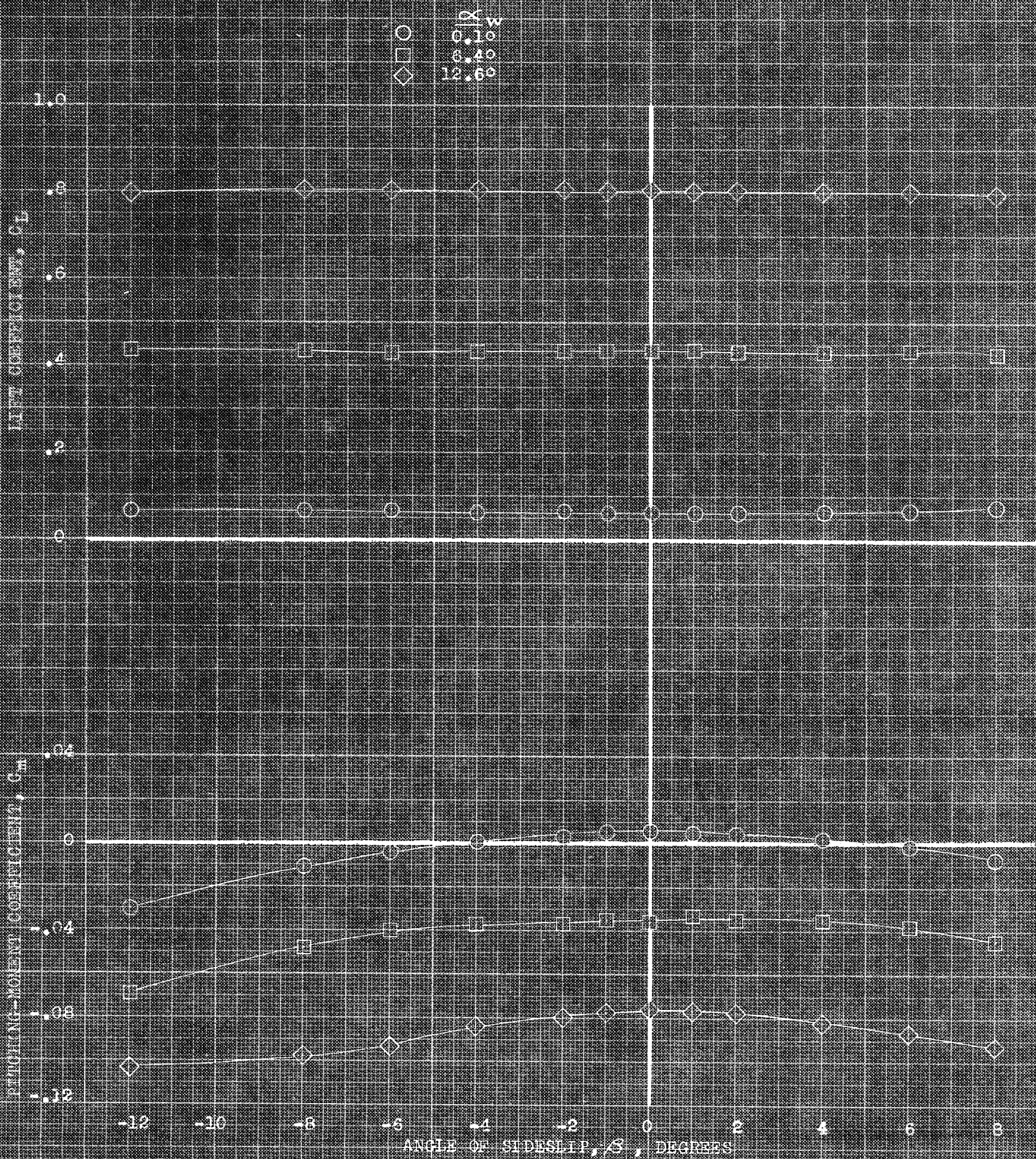
NATIONAL AERONAUTICS AND SPACE ADMINISTRATION



(a) i_w , 0° ; C_v , C_1 , C_n vs β .

FIGURE 7.—AERODYNAMIC CHARACTERISTICS IN SIDESLIP OF THE MODEL AT VARIOUS ANGLES OF ATTACK, PLAIN WING.

CONFIDENTIAL
NATIONAL ADVISORY COMMITTEE FOR AERONAUTICS

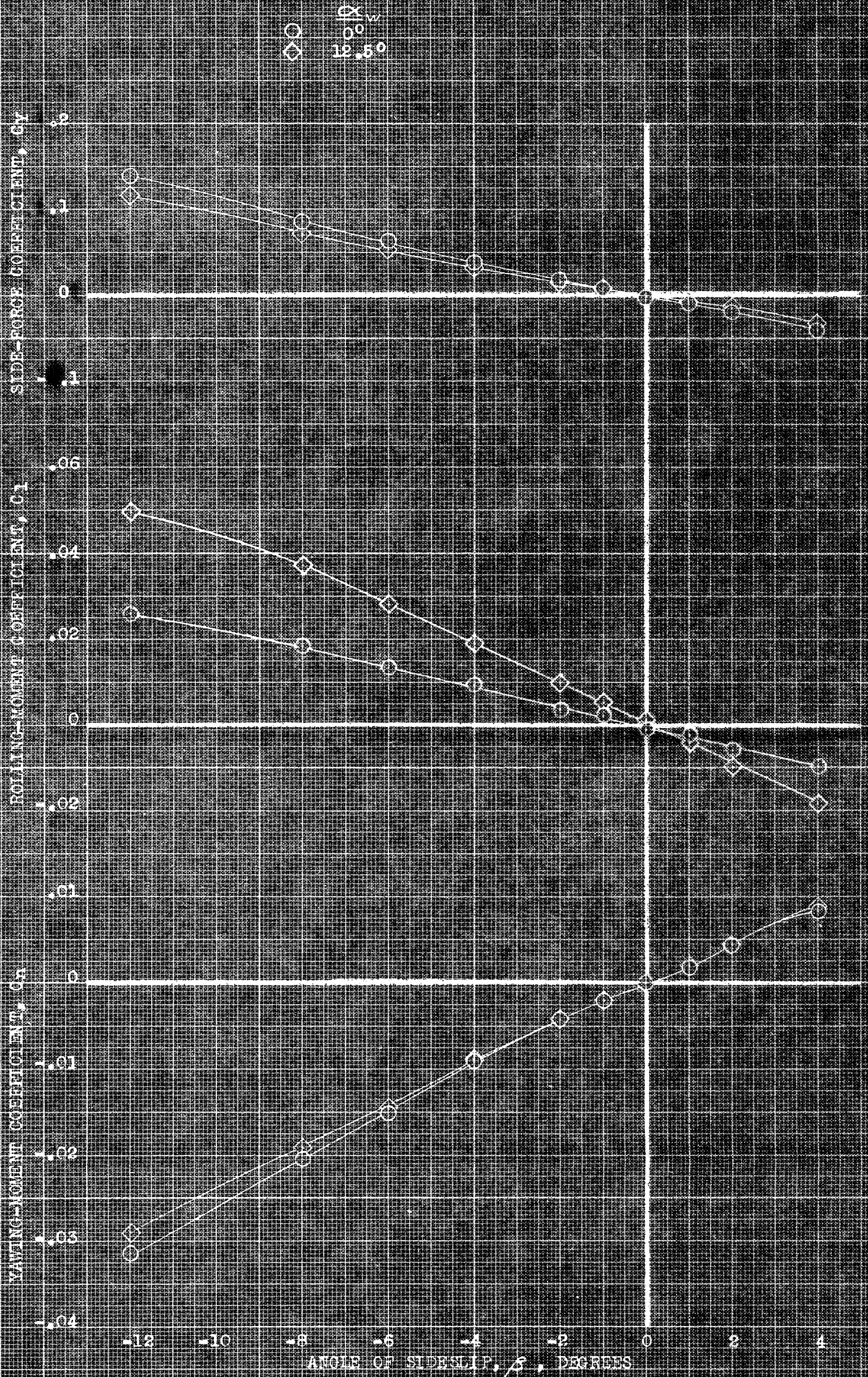


(b) $i_w, 0^\circ$; C_L, C_m vs. β

FIGURE 7.- CONTINUED.

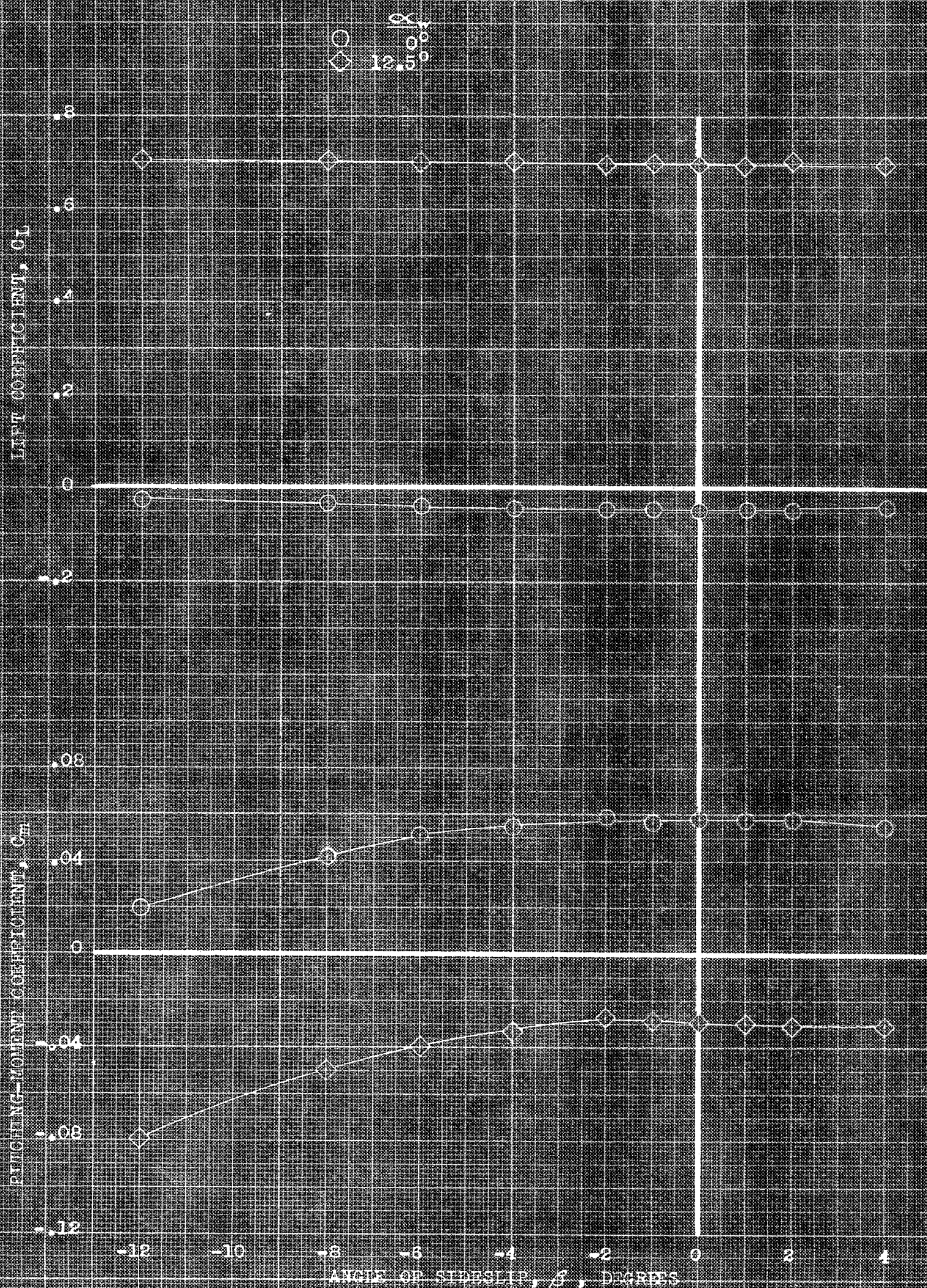
CONFIDENTIAL

NAVY AND AIR FORCE COMMITTEE FOR ASSIGNMENT



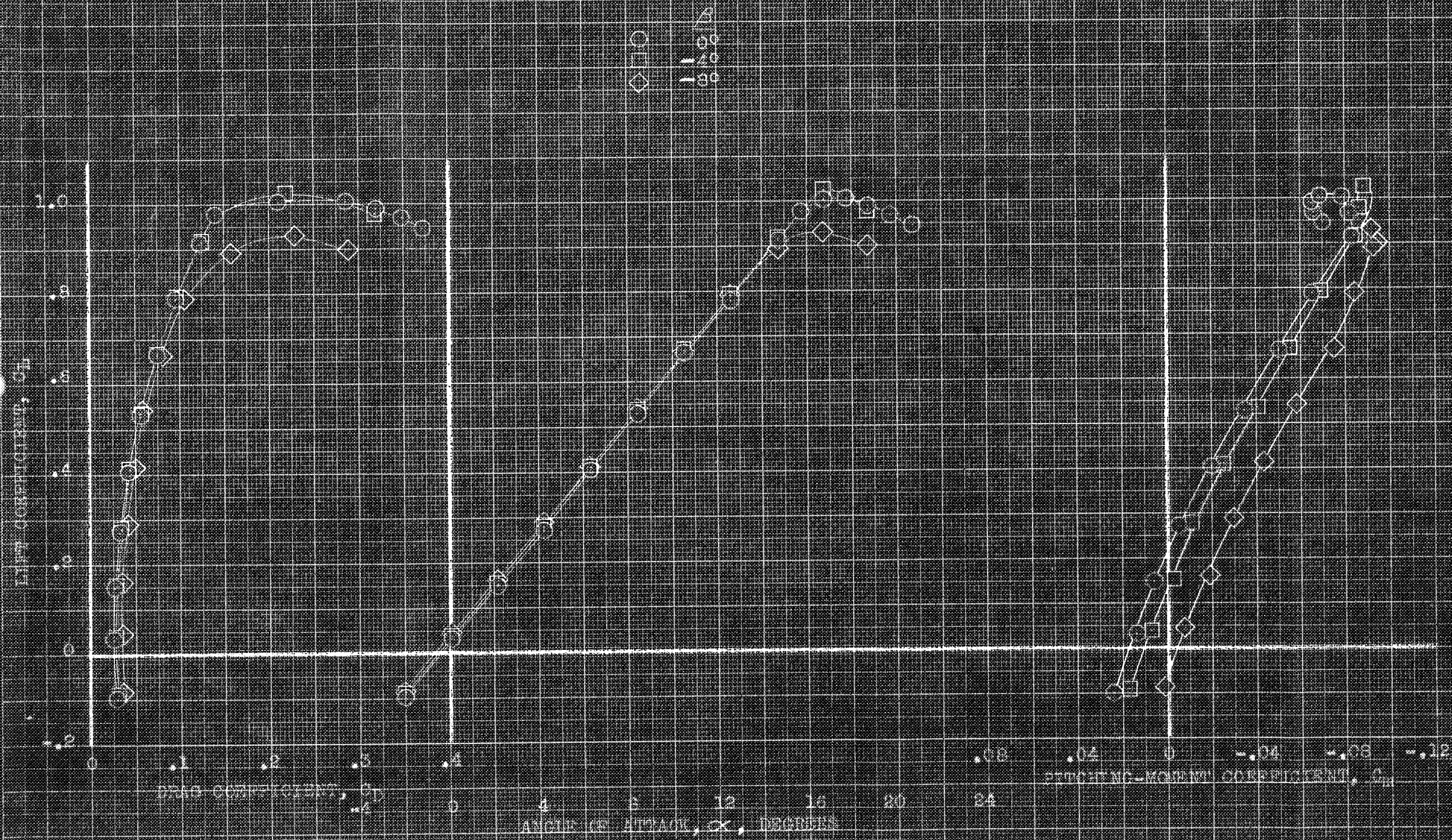
(c) C_{LW} , C_{Y} , C_{L} , C_{N} vs β .

FIGURE 7. CONTINUED.



(a) 1, 6°; C_L , C_M vs β

FIGURE 7.- CONCLUDED.

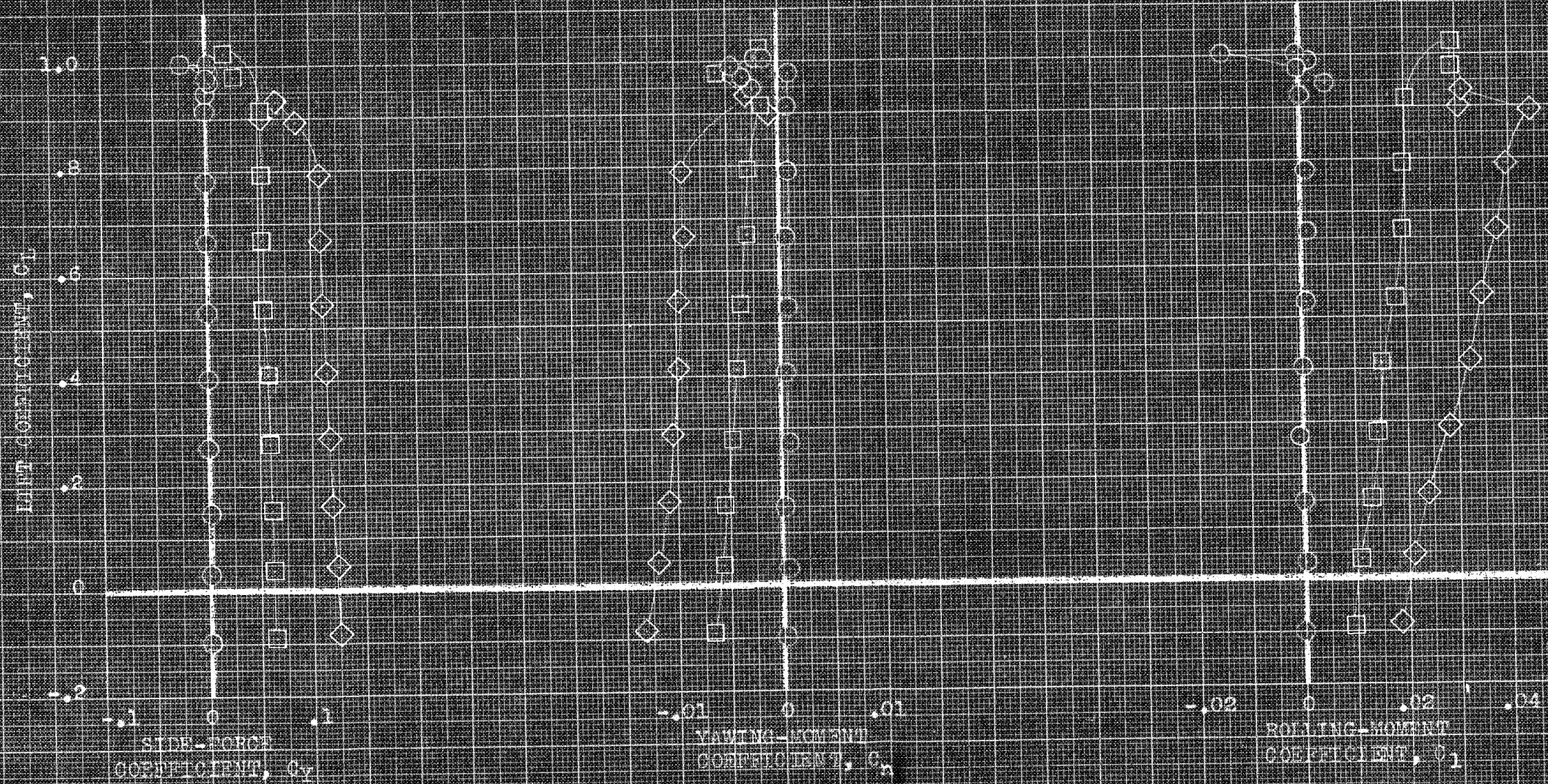


(a) C_D , α , C_M vs C_L .

FIGURE 1. - AERODYNAMIC CHARACTERISTICS IN FLIGHT OF THE BUDEL AT VARIOUS ANGLES OF ATTACK. EXTERNAL PRESSURE, P_w , 0°.

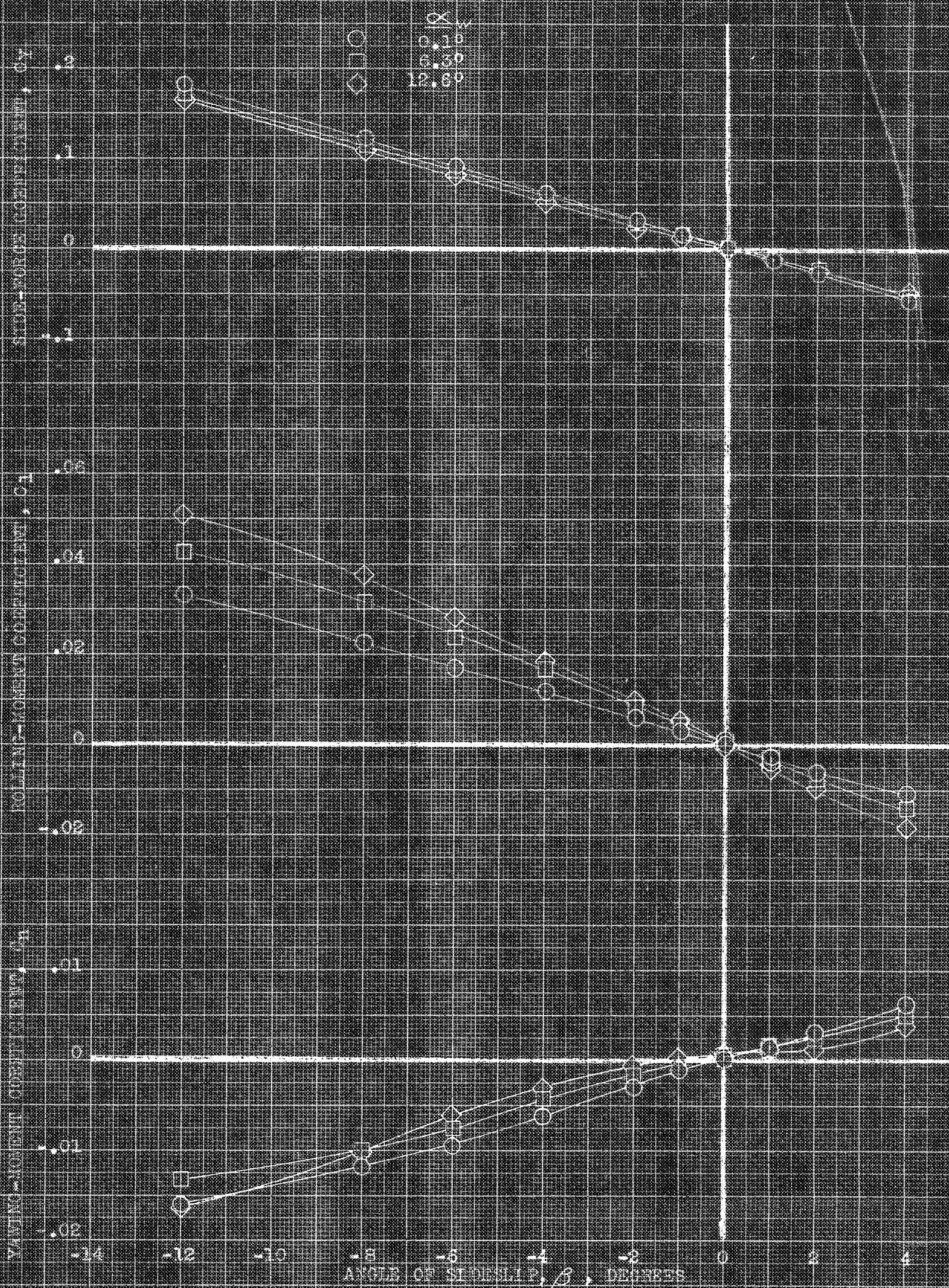
CONFIDENTIAL

NATIONAL ADVISORY COMMITTEE FOR AERONAUTICS



(b) C_y , C_n , C_{l1} vs C_{l1} .

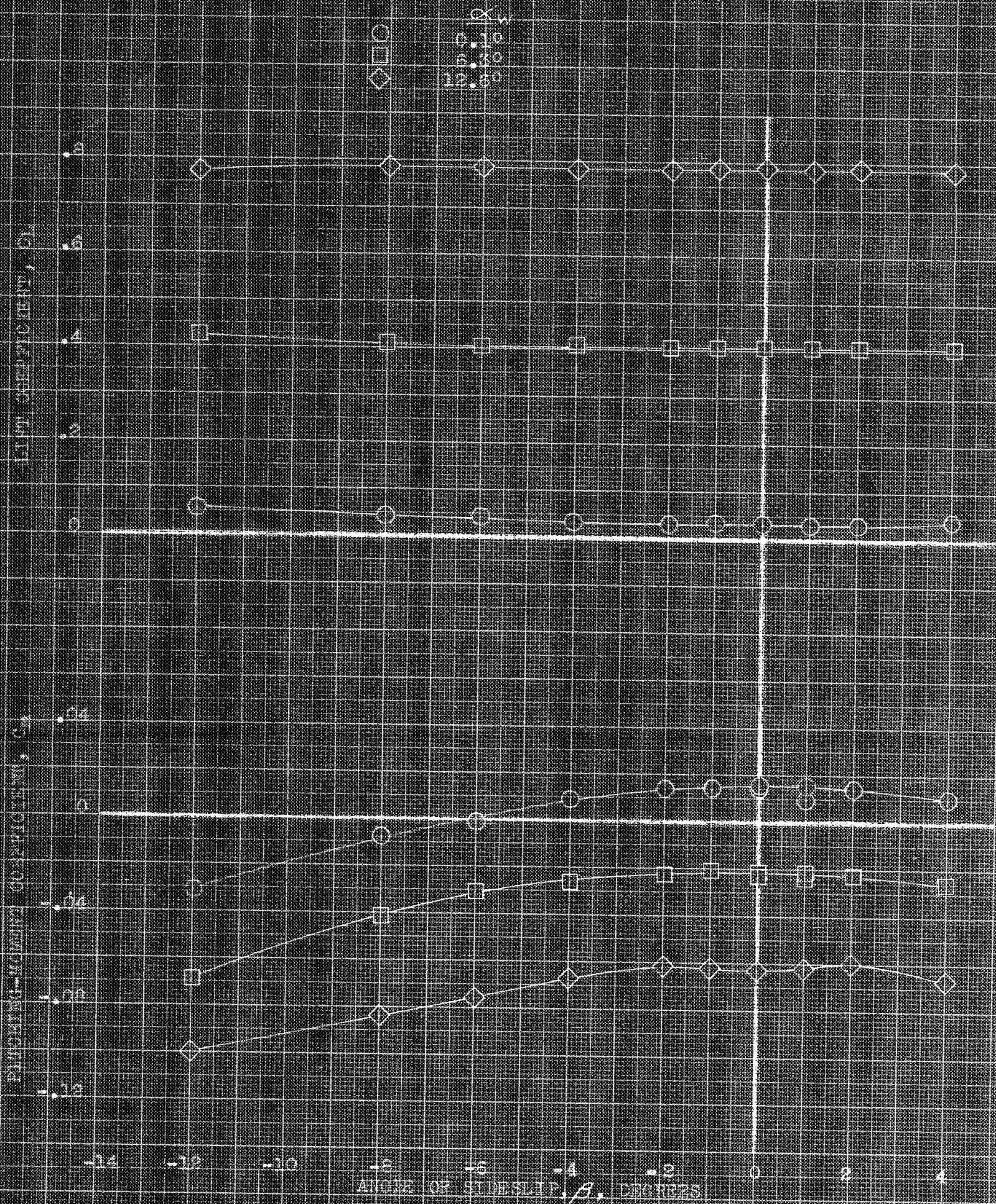
FIGURE 1. - CONCLUDED.



(a) C_Y, C_L, C_M vs. β .

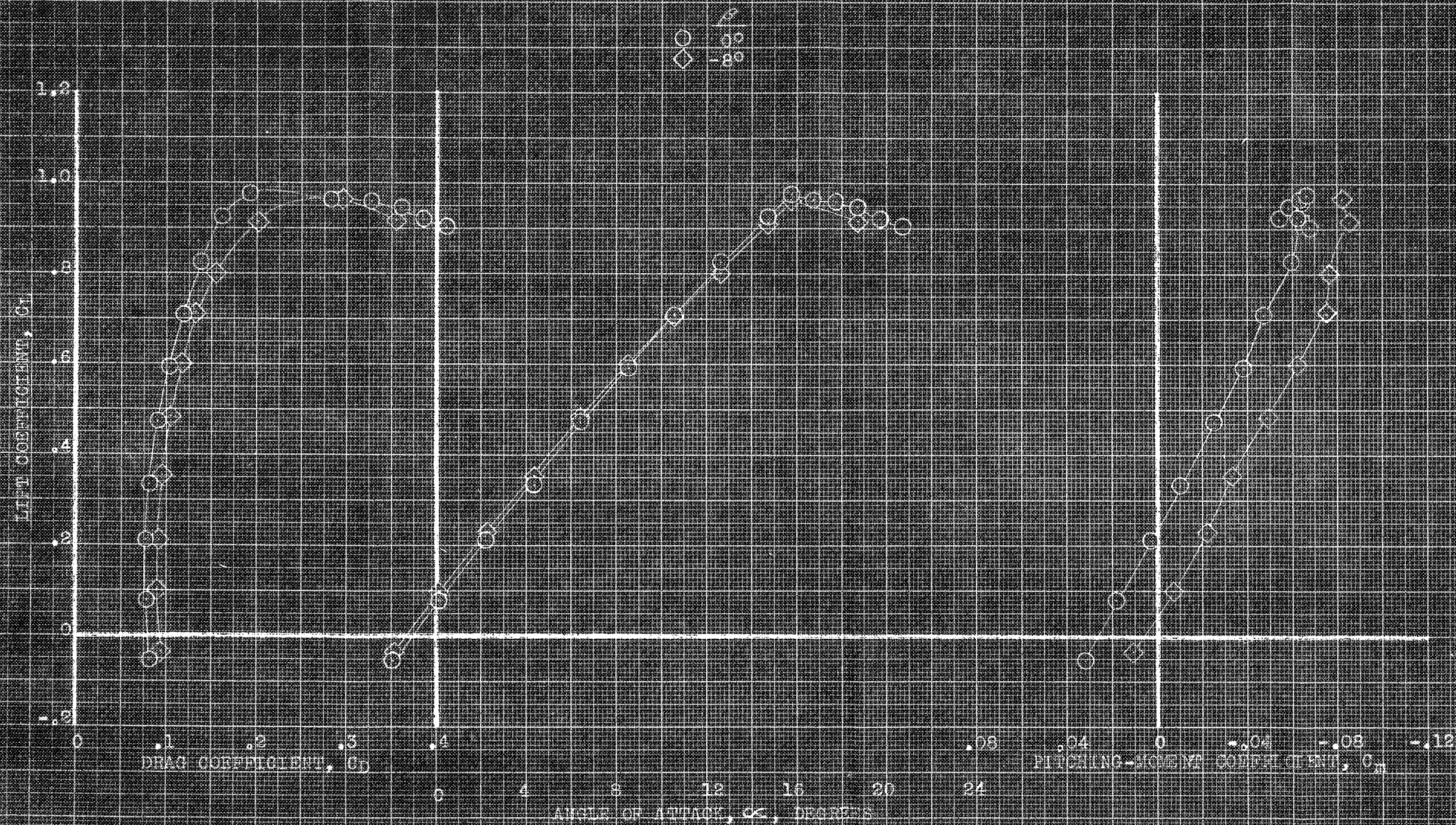
FIGURE 1. - AERODYNAMIC CHARACTERISTICS IN SIDESLIP OF THE MODEL AT VARIOUS ANGLES OF ATTACK. EXTERNAL DUMPS; 1, 0°.

CONFIDENTIAL
 NATIONAL ADVISORY COMMITTEE FOR AERONAUTICS



(b) C_L, C_m vs. β .

FIGURE 2.- CONCLUDED.

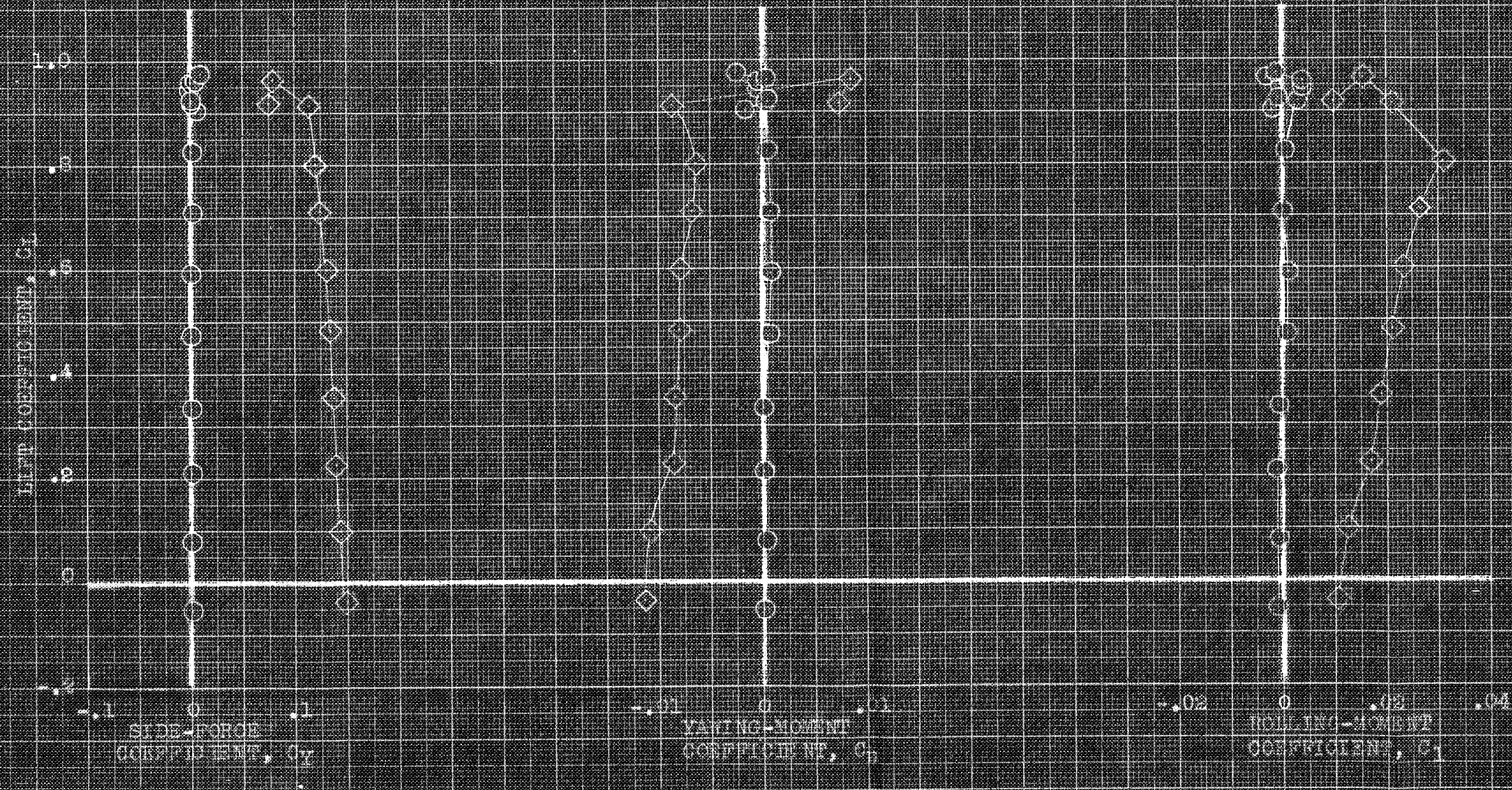


(a) C_L , C_D , C_m vs. α .

FIGURE 10. - AERODYNAMIC CHARACTERISTICS IN FLIGHT OF THE MODEL AT VARIOUS ANGLES OF SIDESLIP. EXTERNAL TANKS; CLEAR, $1_w, 0^\circ$.

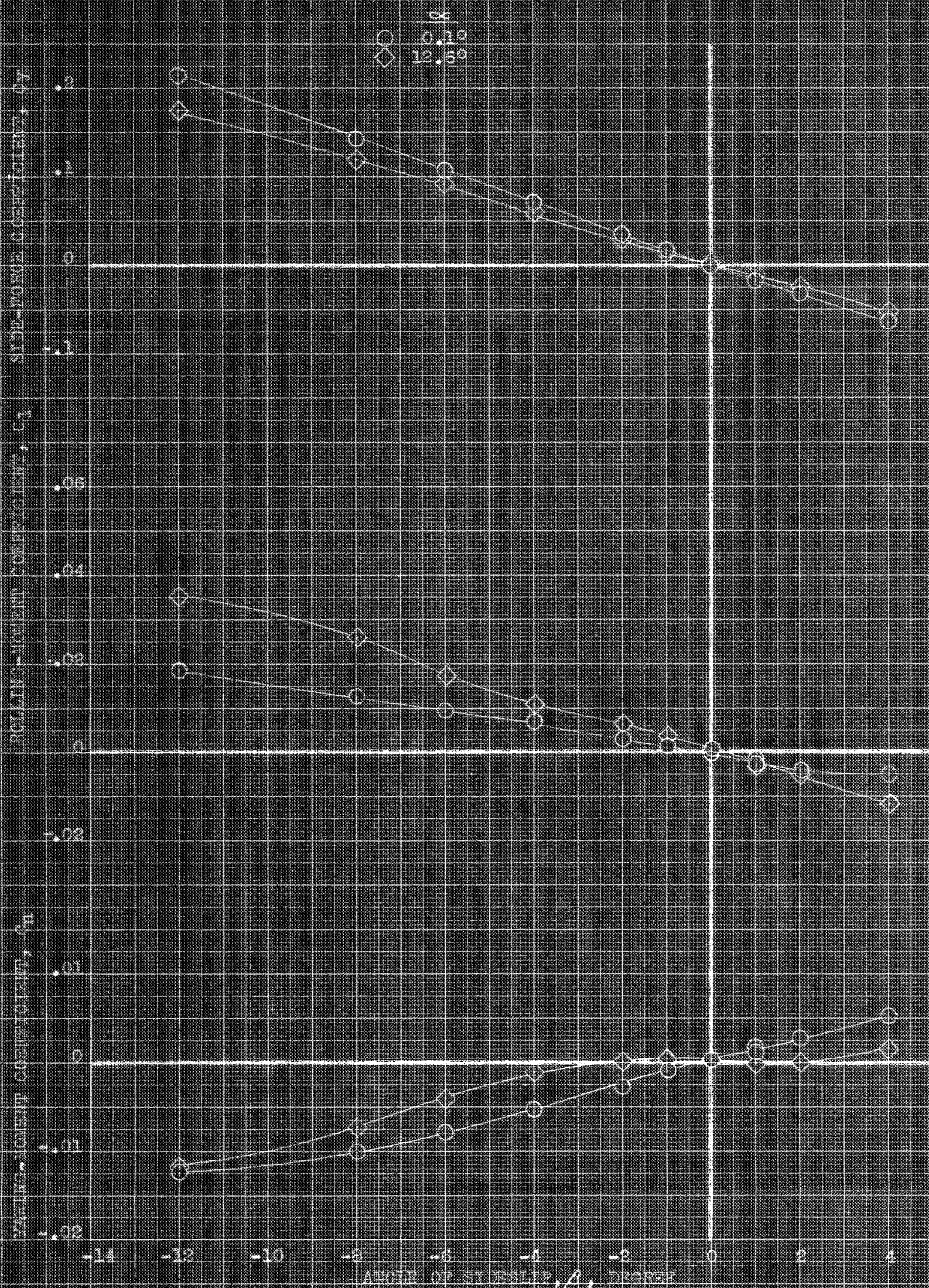
CONFIDENTIAL

NATIONAL ADVISORY COMMITTEE FOR AERONAUTICS



(b) C_L , C_Y , C_l vs. C_n .

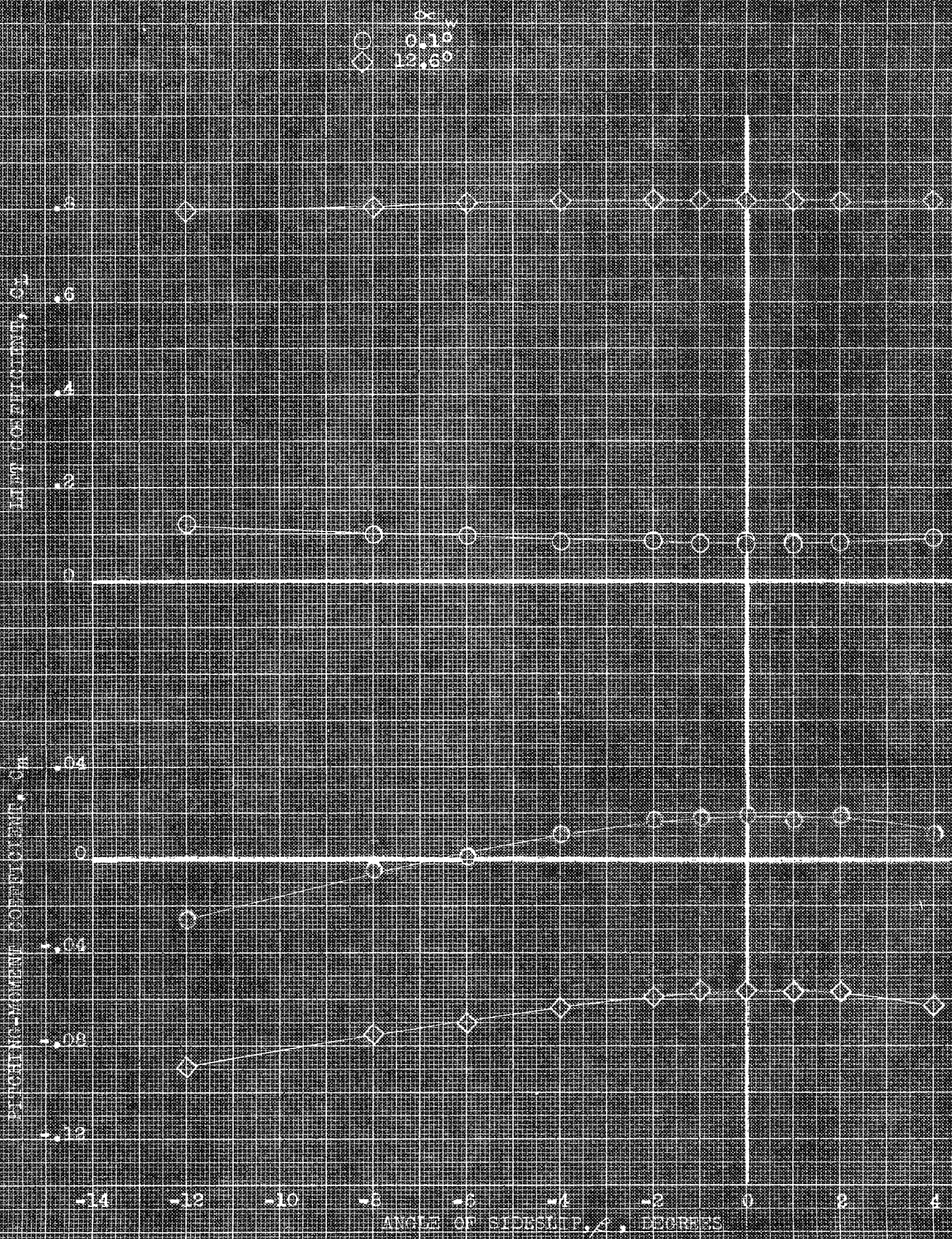
FIGURE 10. - CONTINUED.



(a) C_y , C_l , C_n vs β .

FIGURE 11.- AERODYNAMIC CHARACTERISTICS IN SIDESLIP OF THE MODEL AT VARIOUS ANGLES OF ATTACK. EXTERNAL TANKS; GEAR; i_w , 0° .

CONFIDENTIAL
NATIONAL ADVISORY COMMITTEE FOR AERONAUTICS

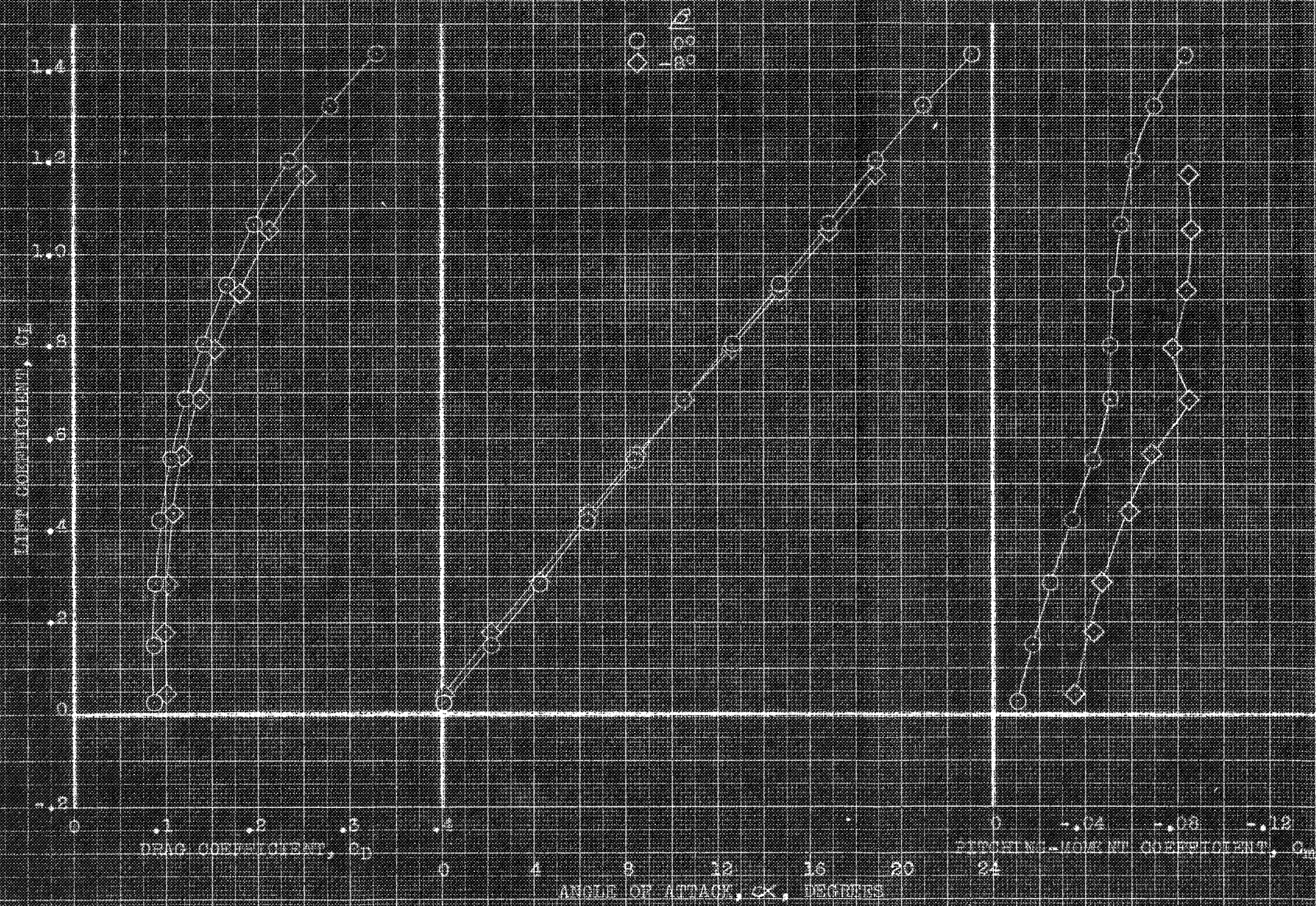


(b) C_L, C_M vs β .

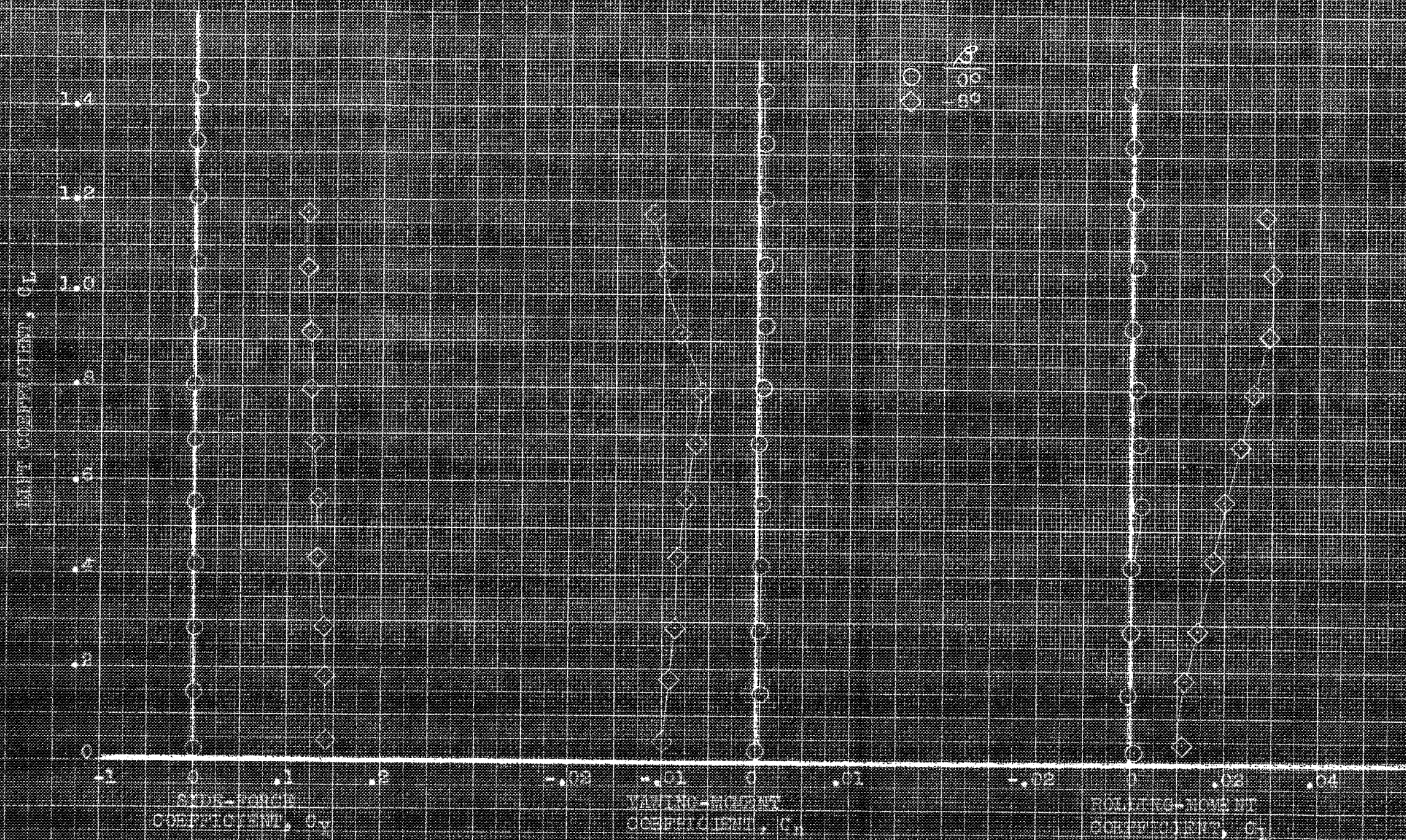
FIGURE 11.- CONCLUDED.

CONFIDENTIAL

NATIONAL ADVISORY COMMITTEE FOR AERONAUTICS



(a) C_L , C_D , α , C_M vs α .
 FIGURE 12. AERODYNAMIC CHARACTERISTICS IN FITTE OF THE MODEL AT VARIOUS ANGLES OF SLIP. EXTERNAL FIELDS; EAR, BROOKLYN SLIP.

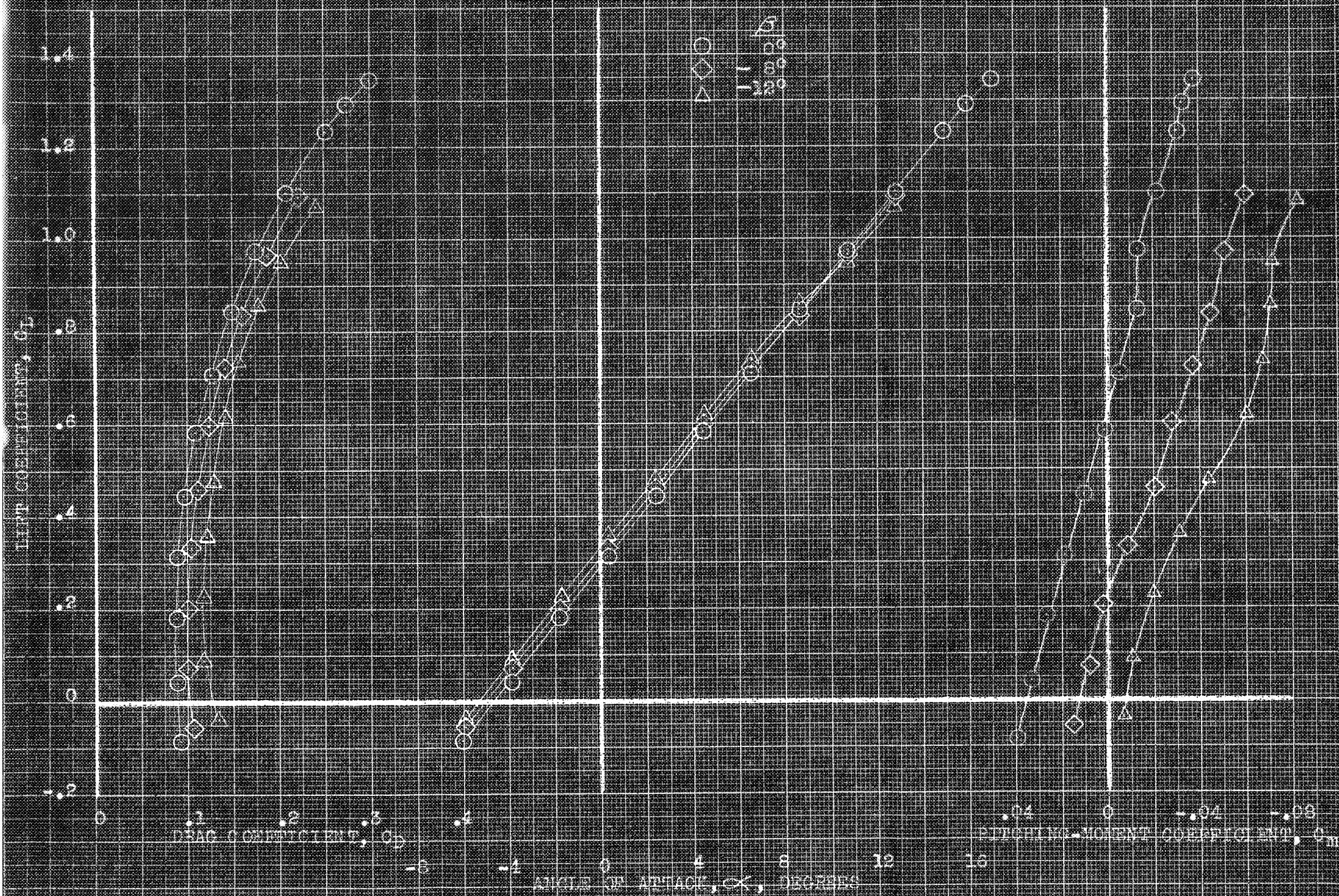


(a) C_L , C_y , C_n , C_r vs. C_L .

FIGURE 2. - CONTINUED.

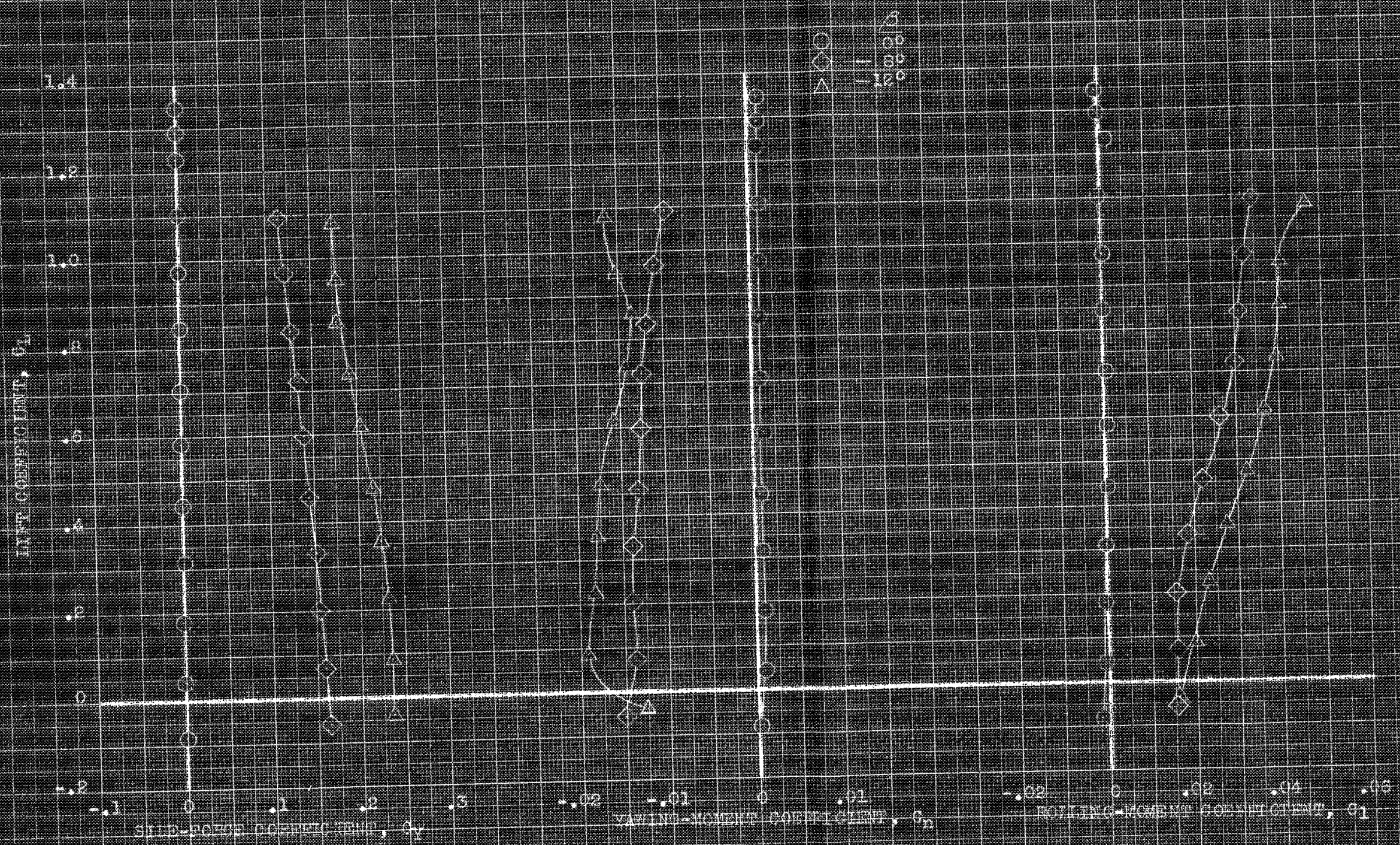
CONFIDENTIAL

NATIONAL ADVISORY COMMITTEE FOR AERONAUTICS



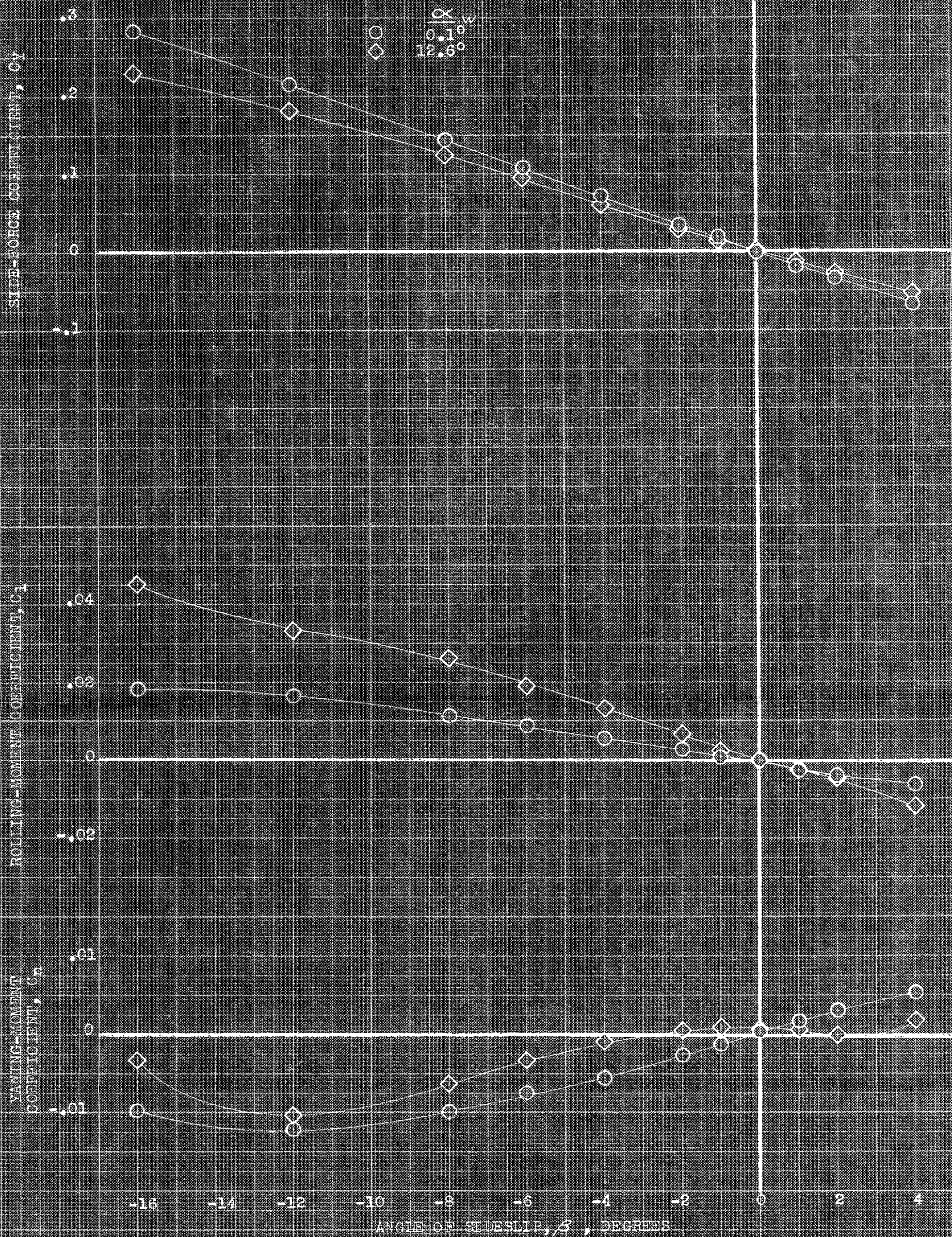
(c) C_L, C_D, C_m vs. α

FIGURE 1. - CONTINUED.



(1) Law of C_L , C_n , C_l vs C_v .

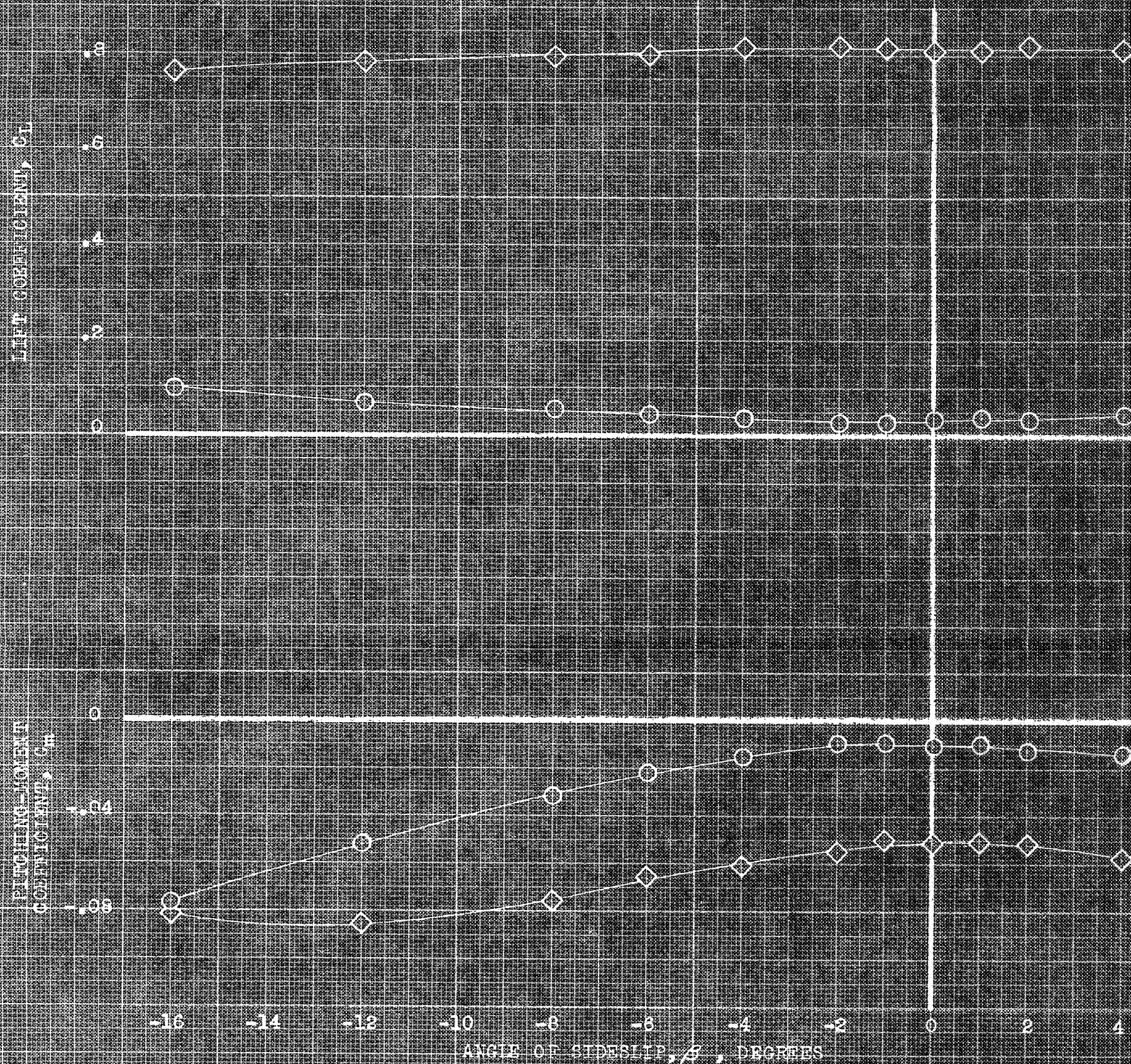
FIGURE 1. CONCLUDED.



(a) $i_w, 0^\circ$; C_Y, C_L, C_n vs β .

FIGURE 12.- AERODYNAMIC CHARACTERISTICS IN SIDESLIP OF THE MODEL AT VARIOUS ANGLES OF ATTACK. EXTERNAL TANKS; GEAR; DROOPED SLATS.

α_w
 0.10°
 12.60°



(o) C_w , 0° ; C_L , C_m vs β .
 FIGURE 15.- CONTINUED.

Side-Surge Coefficient, C_{Y_s}

Rolling Moment Coefficient, C_{l_r}

Yawing Moment Coefficient, C_{n_y}

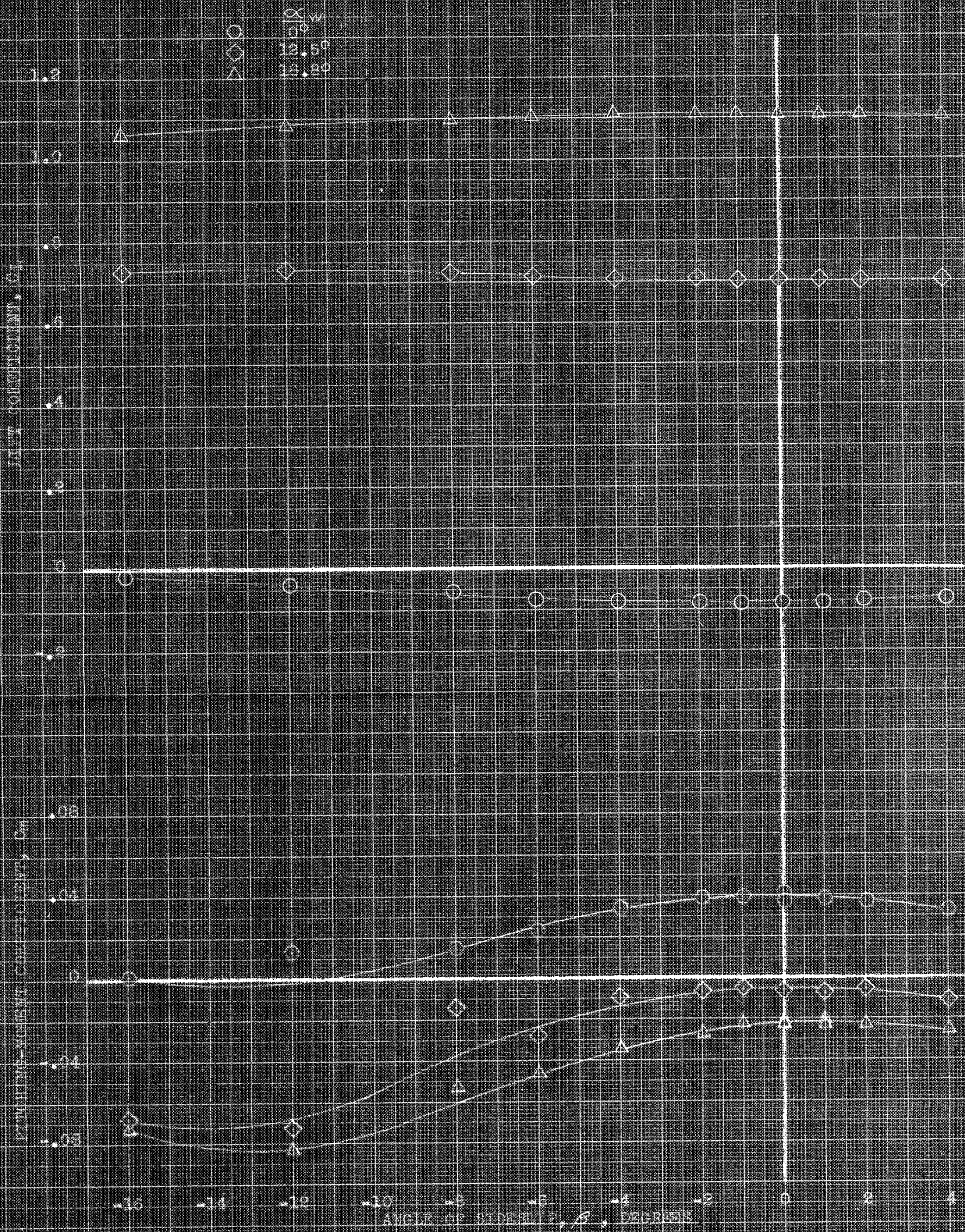
α_w
 \circ 0°
 \diamond 12.5°
 \triangle 13.3°

Angle of Sideslip, β , degrees

(a) 1_M , 6°; C_{Y_s} , C_{l_r} , C_{n_y} vs β

FIGURE 13. - CONTINUED.

CONFIDENTIAL
 NATIONAL ADVISORY COMMITTEE FOR AERONAUTICS



(a) $\alpha_w = 0^\circ$; C_L , C_M vs α
 FIGURE 12.- CONCLUDED.

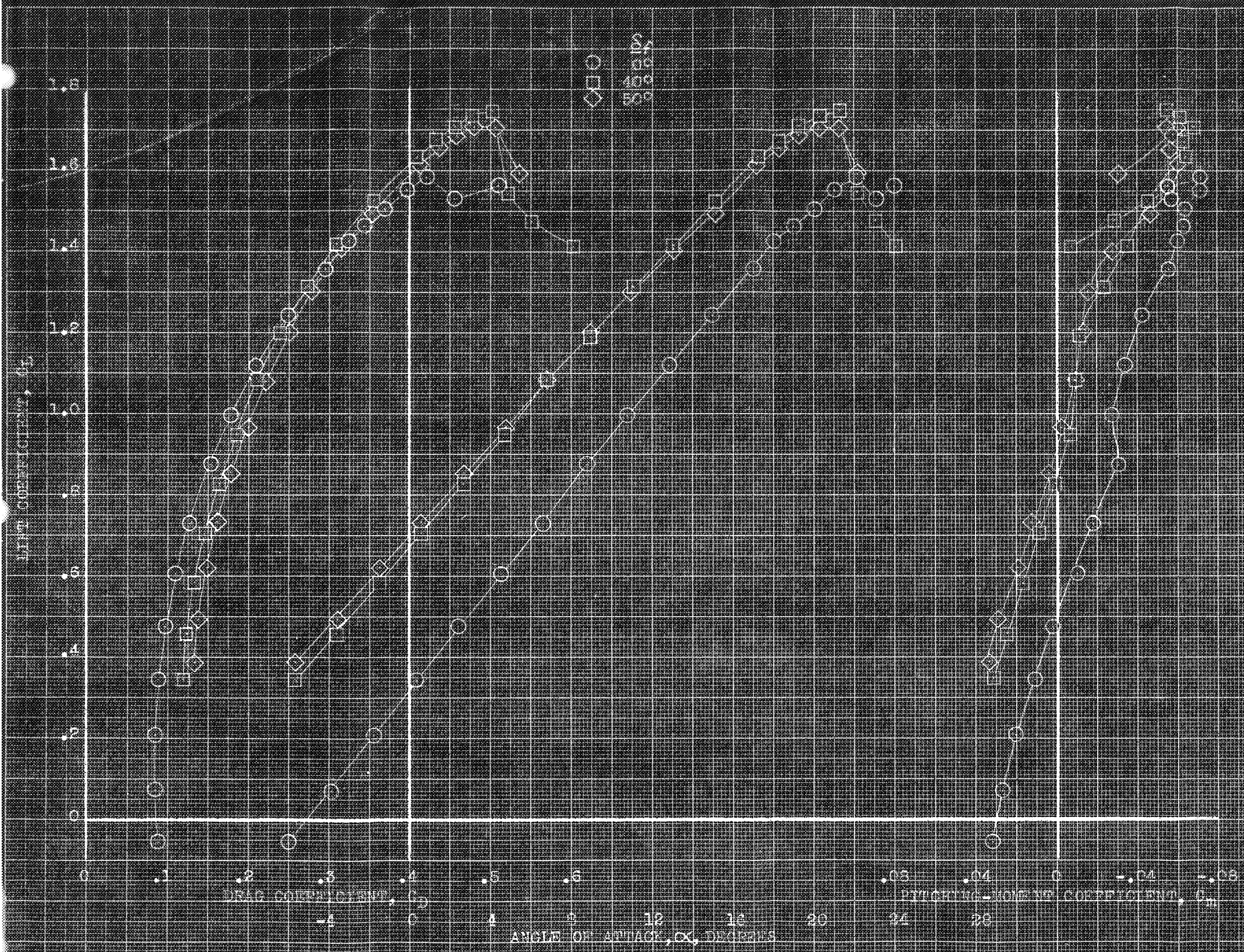
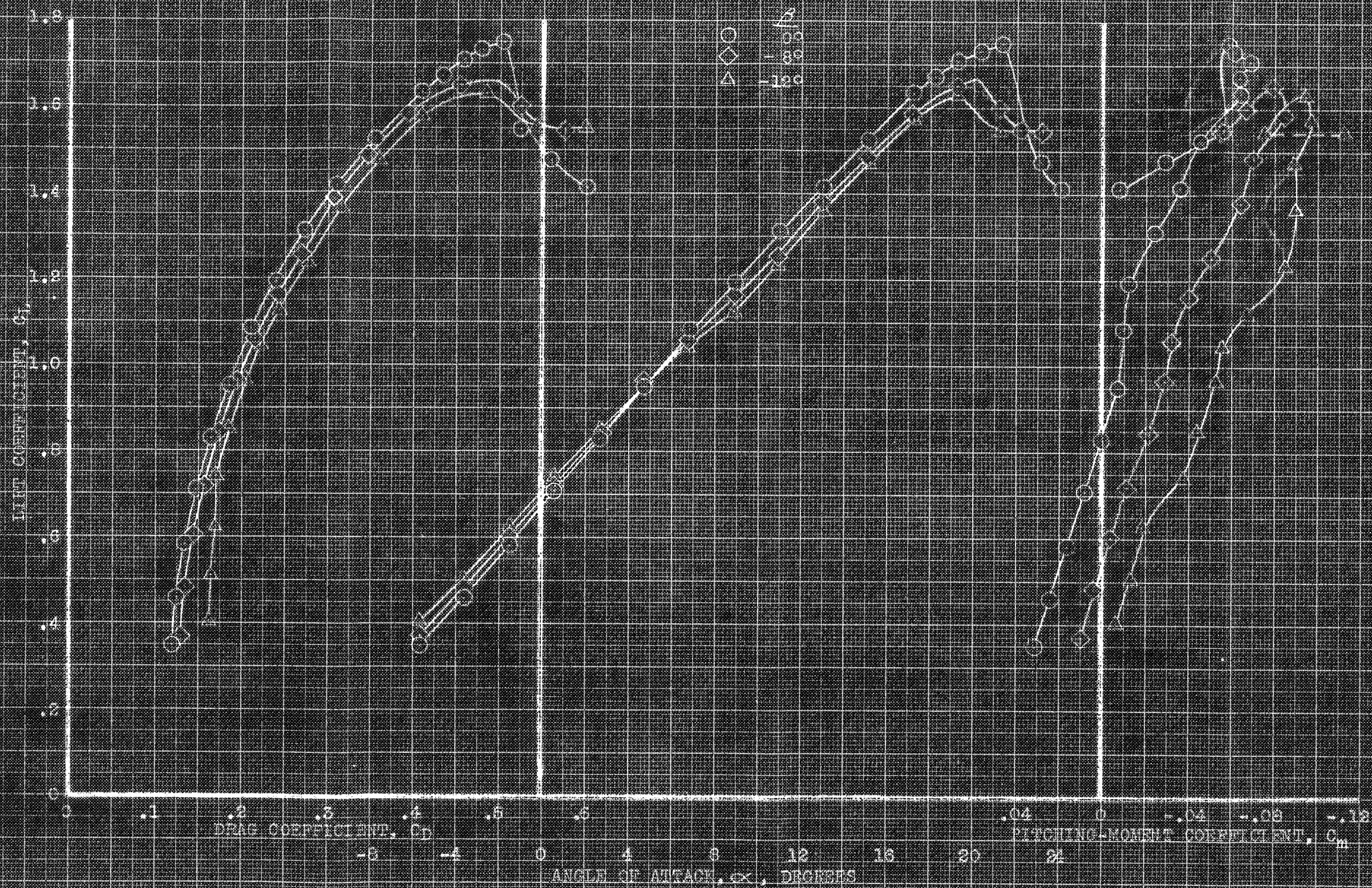


Figure 1. — Graph of Lift, Drag, and Pitching Moment Coefficients of a Thin Airfoil in Pitch, Yaw, and Roll; C_d and C_m are zero at $\alpha = 0$.

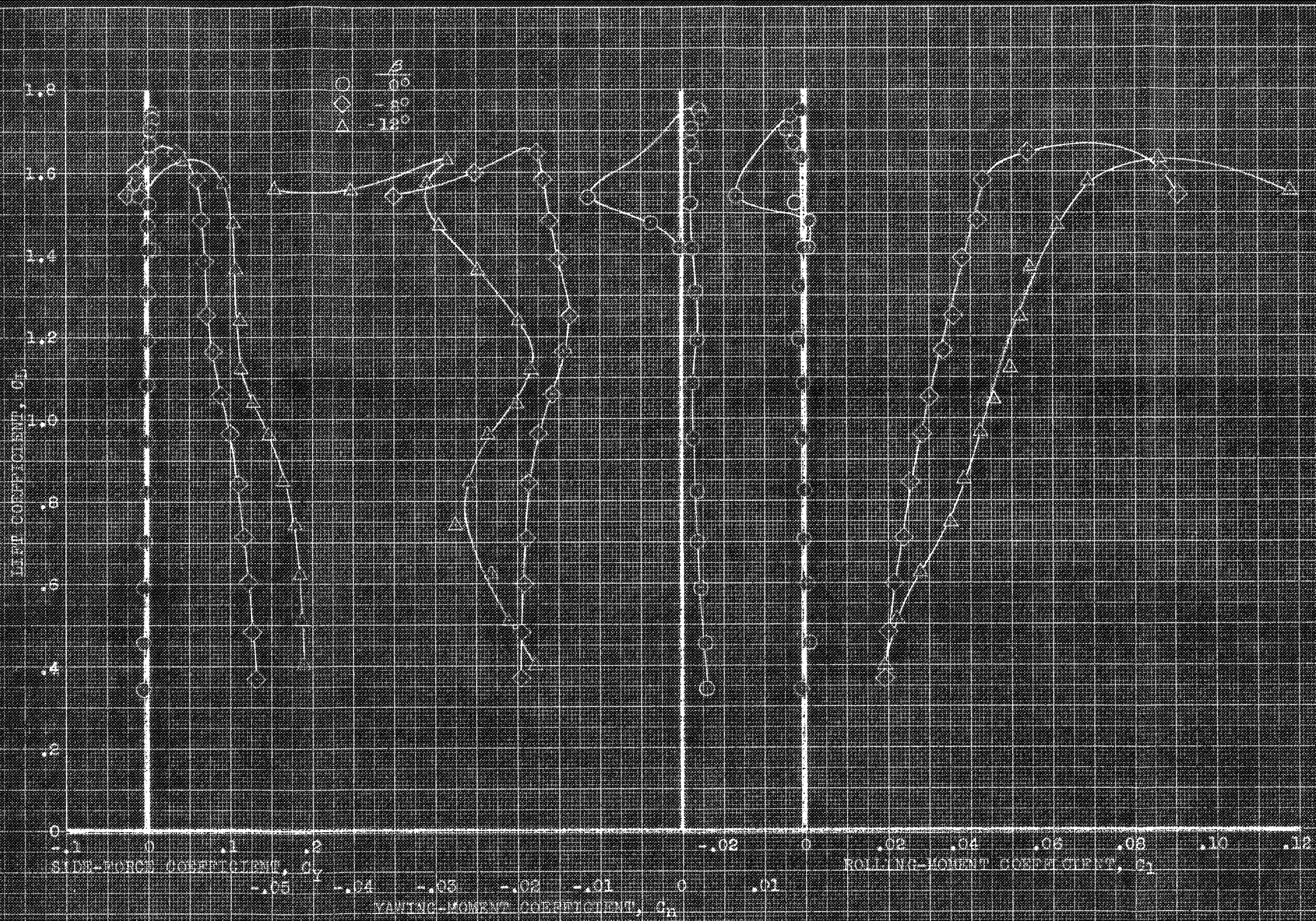


(a) C_D , α , C_m vs C_L

FIGURE 10. AERODYNAMIC CHARACTERISTICS IN PITCH OF THE MODEL AT VARIOUS ANGLES OF SIDESLIP. GEAR; DROPPED BLADES; FLAT PLATE, 45° ; $1/4$, 6° .

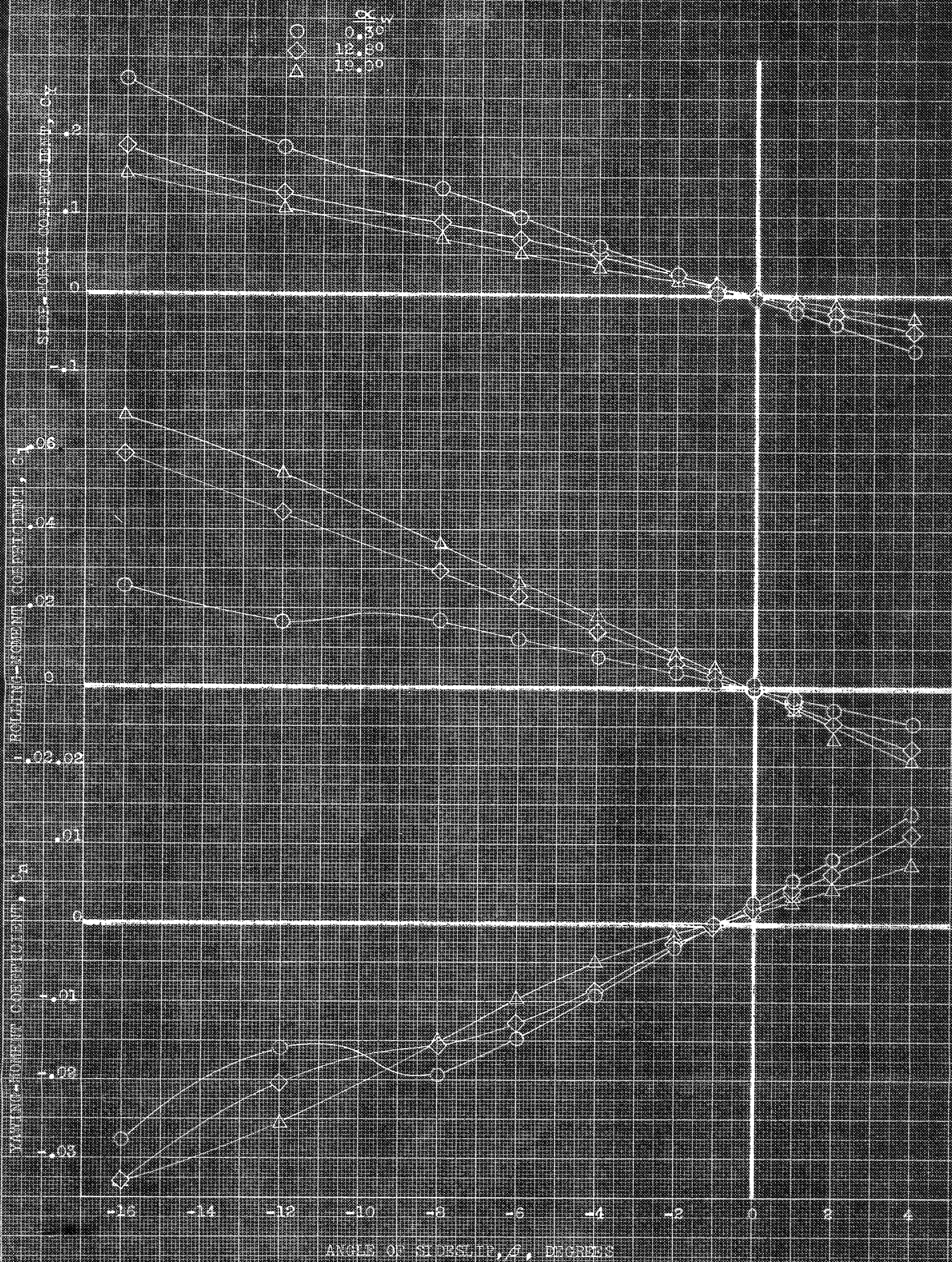
CONFIDENTIAL

NATIONAL ADVISORY COMMITTEE FOR AERONAUTICS



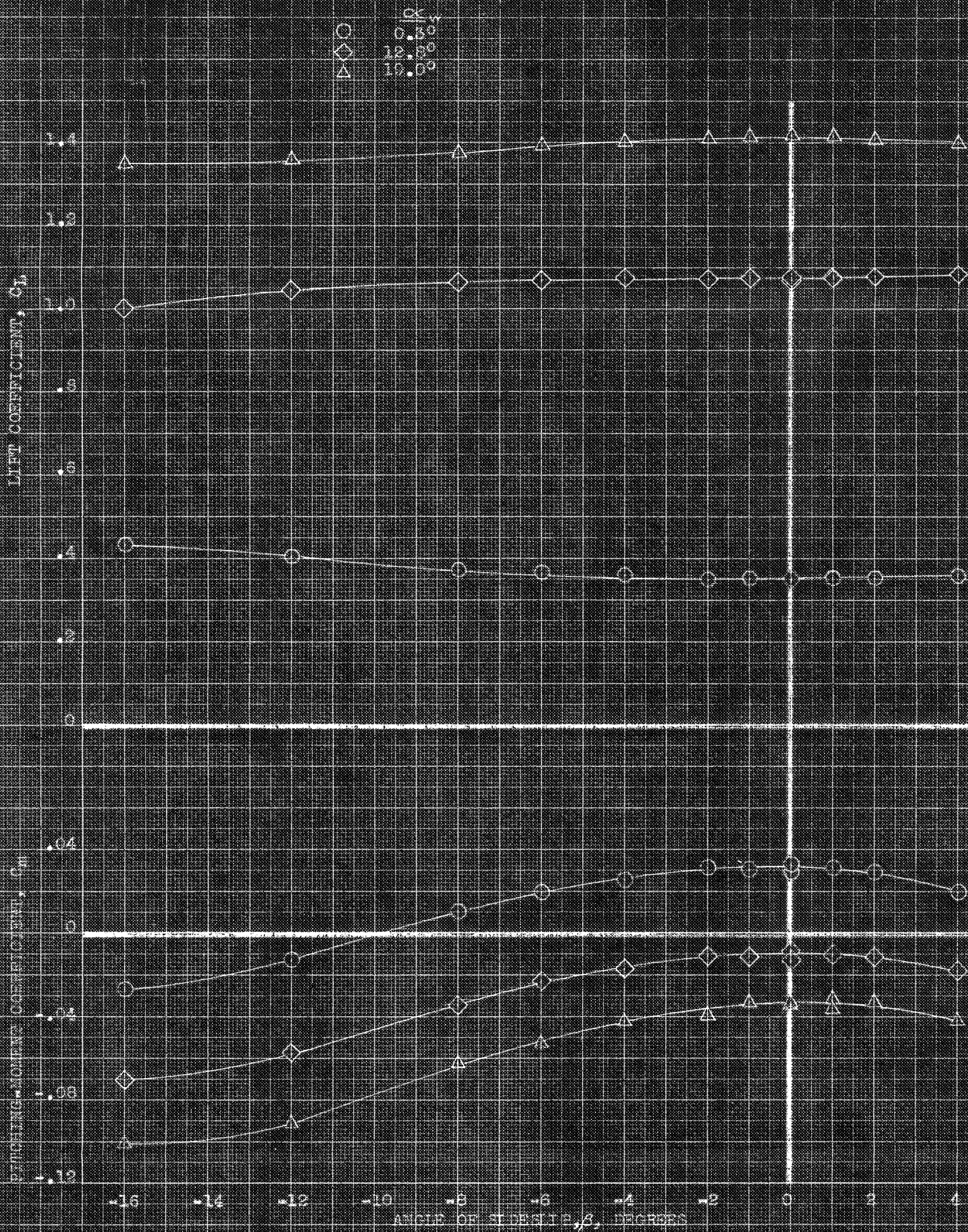
(b) C_L , C_Y , C_R vs. β

FIGURE 1 - CONTINUED.



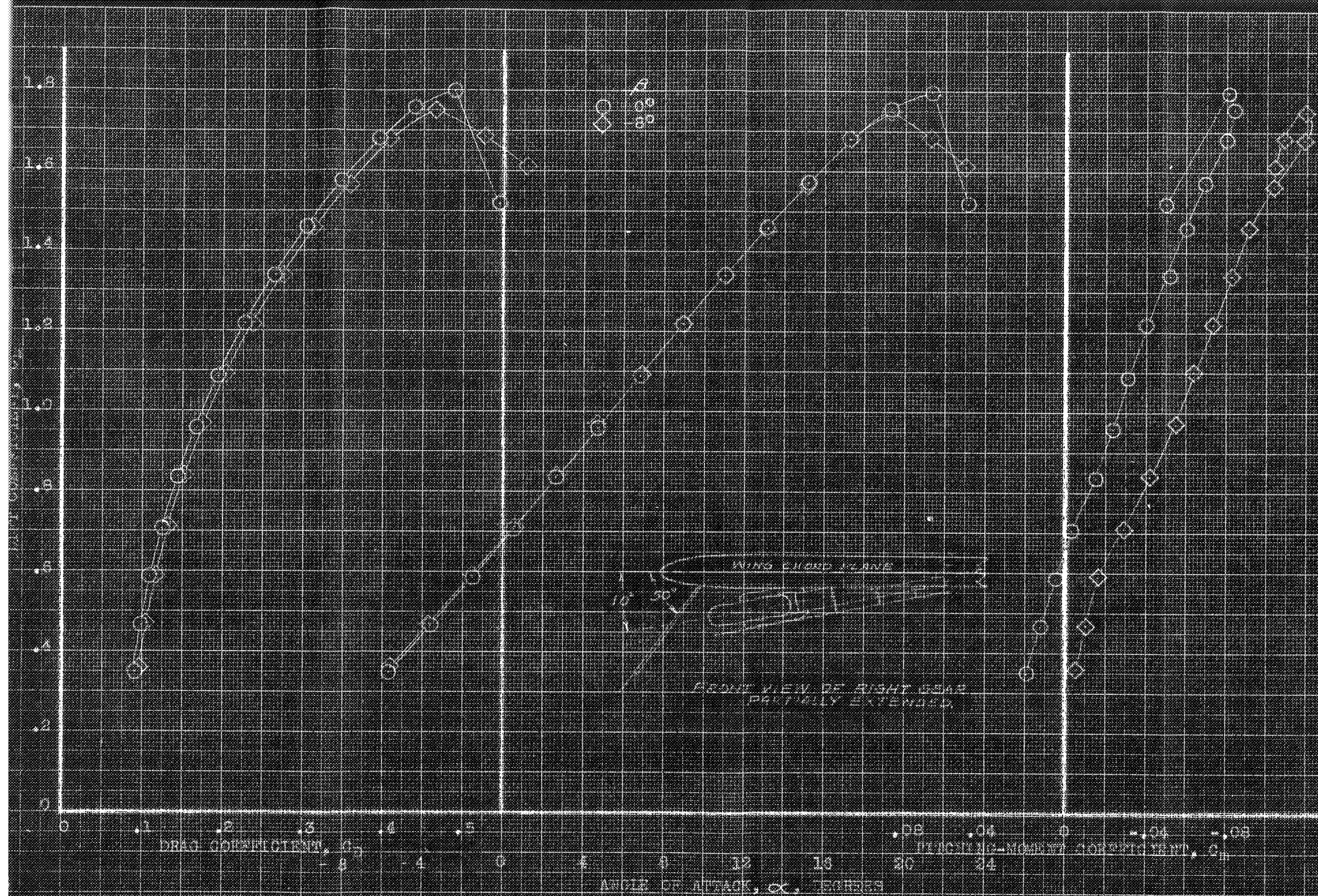
(a) C_Y, C_L, C_N vs β

FIGURE 15.- AERODYNAMIC CHARACTERISTICS IN SIDESLIP OF THE MODEL AT VARIOUS ANGLES OF ATTACK. GEAR; BROOKED SLATS; PLAIN FLATS, 40° ; 1° , 5° .



(b) C_L, C_m vs. β .

FIGURE 12. - CONCLUDED.



(a) C_D , α , C_m vs α .

FIGURE 17. - AERODYNAMIC CHARACTERISTICS IN FLIGHT OF THE MODEL AT VARIOUS ANGLES OF SIDESLIP. RIGHT GEAR PARTIALLY EXTENDED; DROUGD SLATS; FLARE PLATE, 40°; λ_w , 0°.

CONFIDENTIAL

NATIONAL ADVISORY COMMITTEE FOR AERONAUTICS

LIFT COEFFICIENT, C_L

SIDE-FORCE
COEFFICIENT, C_Y

YAWING-MOMENT COEFFICIENT, C_n

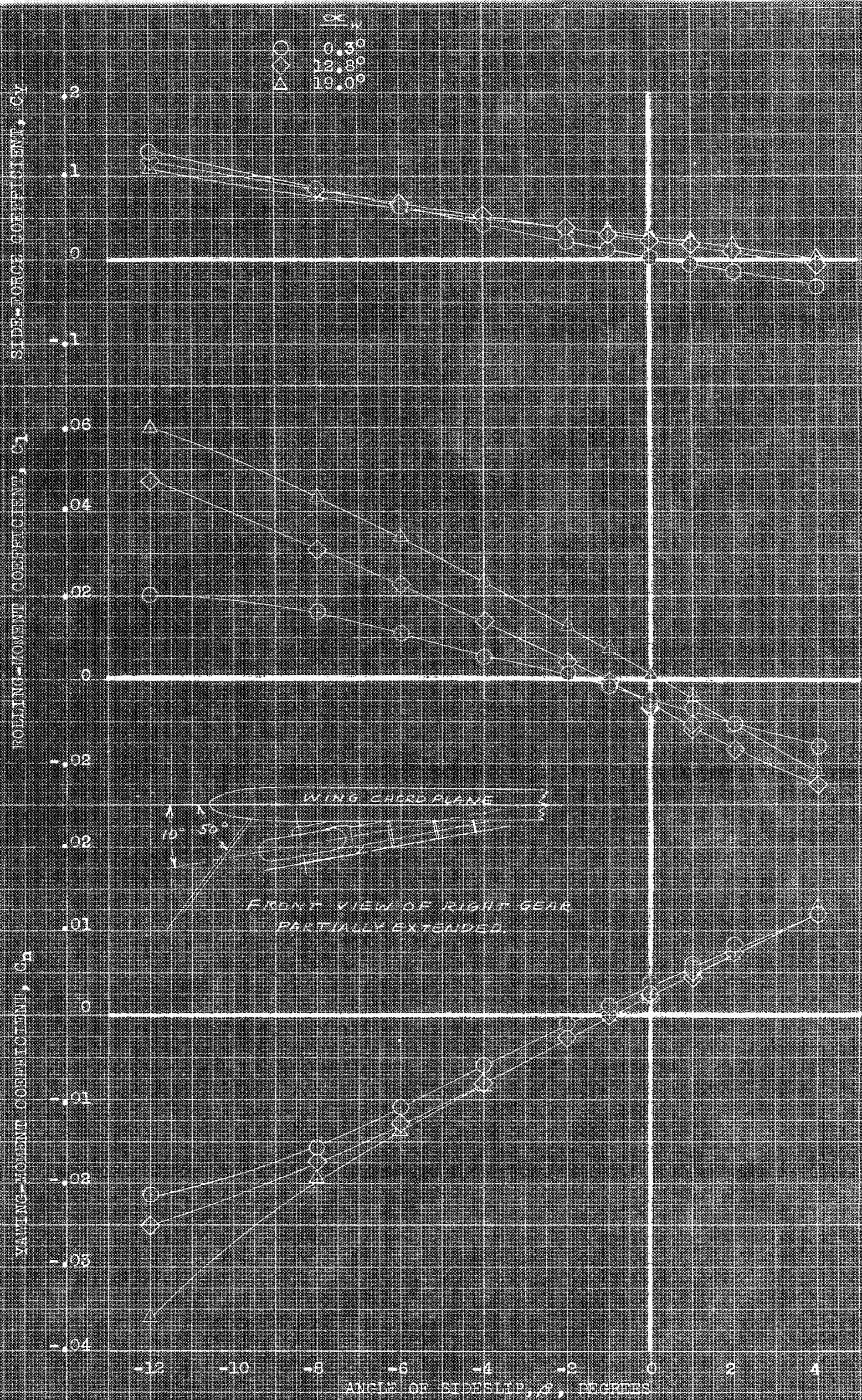
ROLLING-MOMENT COEFFICIENT, C_l

(b) C_Y , C_n , C_l vs C_L

FIGURE 11. - HANDBOOK.

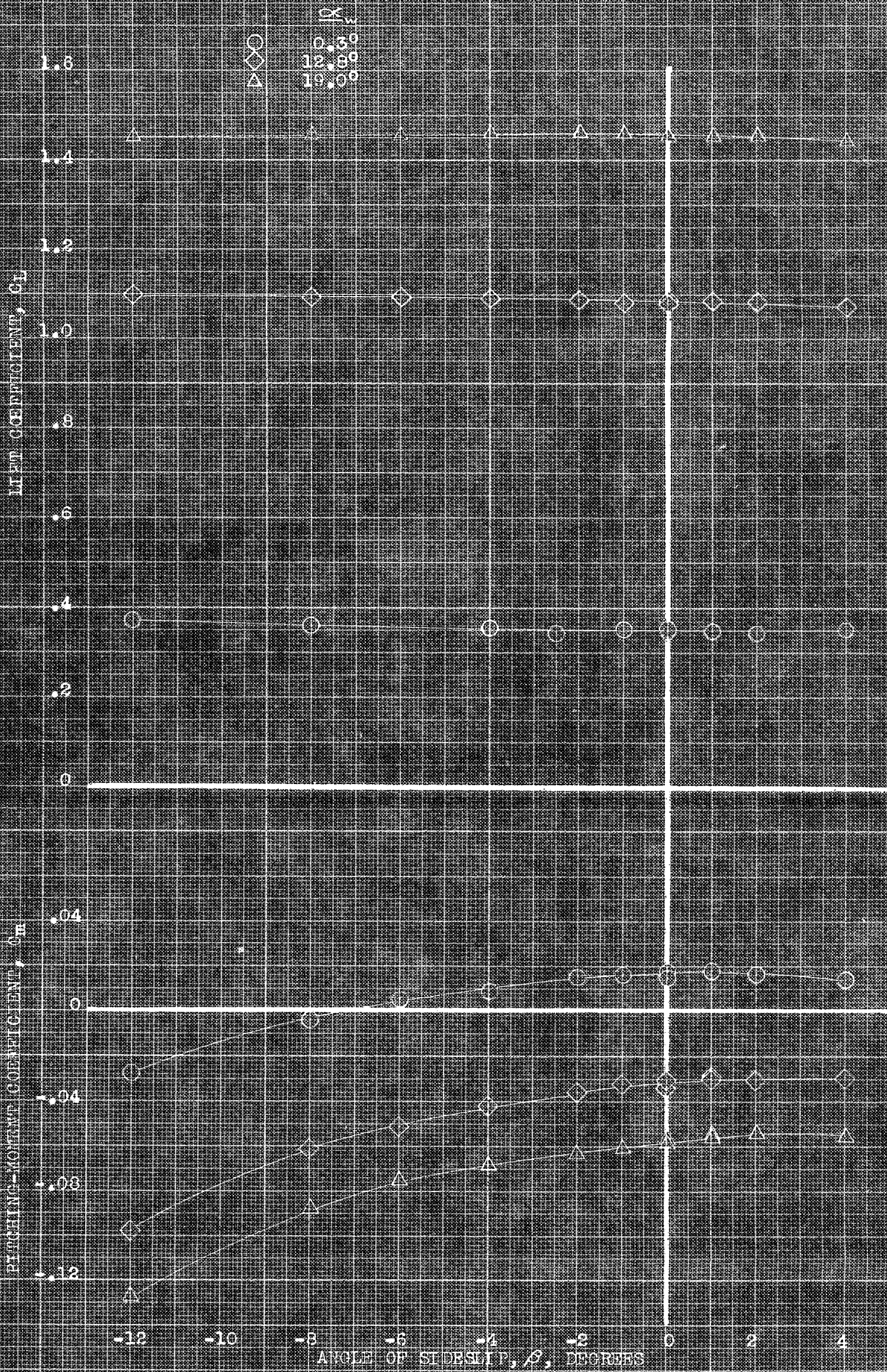
CONFIDENTIAL

NATIONAL ADVISORY COMMITTEE FOR AERONAUTICS



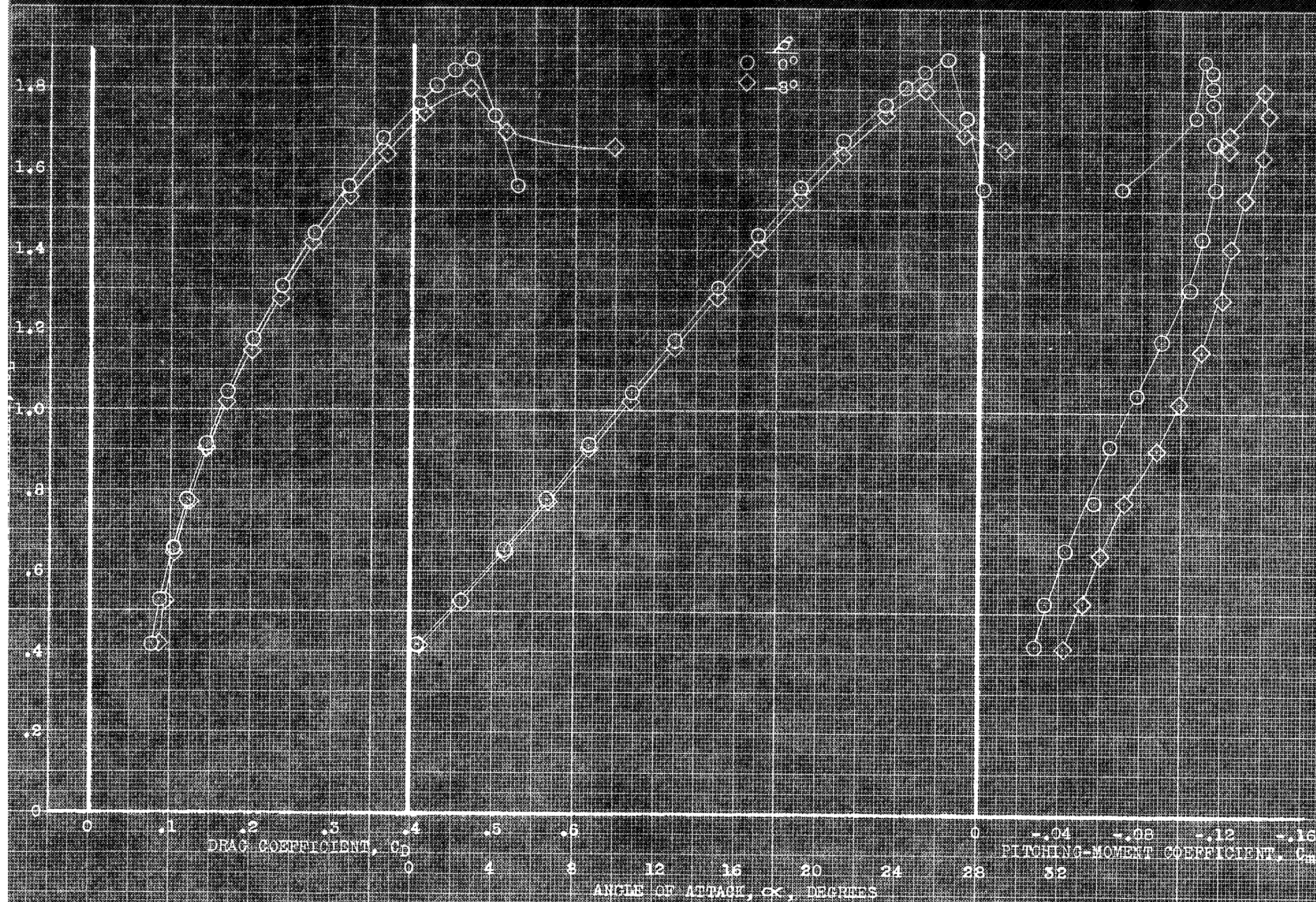
(4) C_Y, C_L, C_N vs β

FIGURE 13. -- AERODYNAMIC CHARACTERISTICS IN SIDESLIP OF THE MODEL AT VARIOUS
 ANGLES OF ATTACK. RIGHT GEAR PARTIALLY EXTENDED; DROOPED SLATS; PLAIN
 FLAPS, 40°; i_w , 6°.



(b) C_L , C_m vs β .

FIGURE 13. - CONCLUDED.

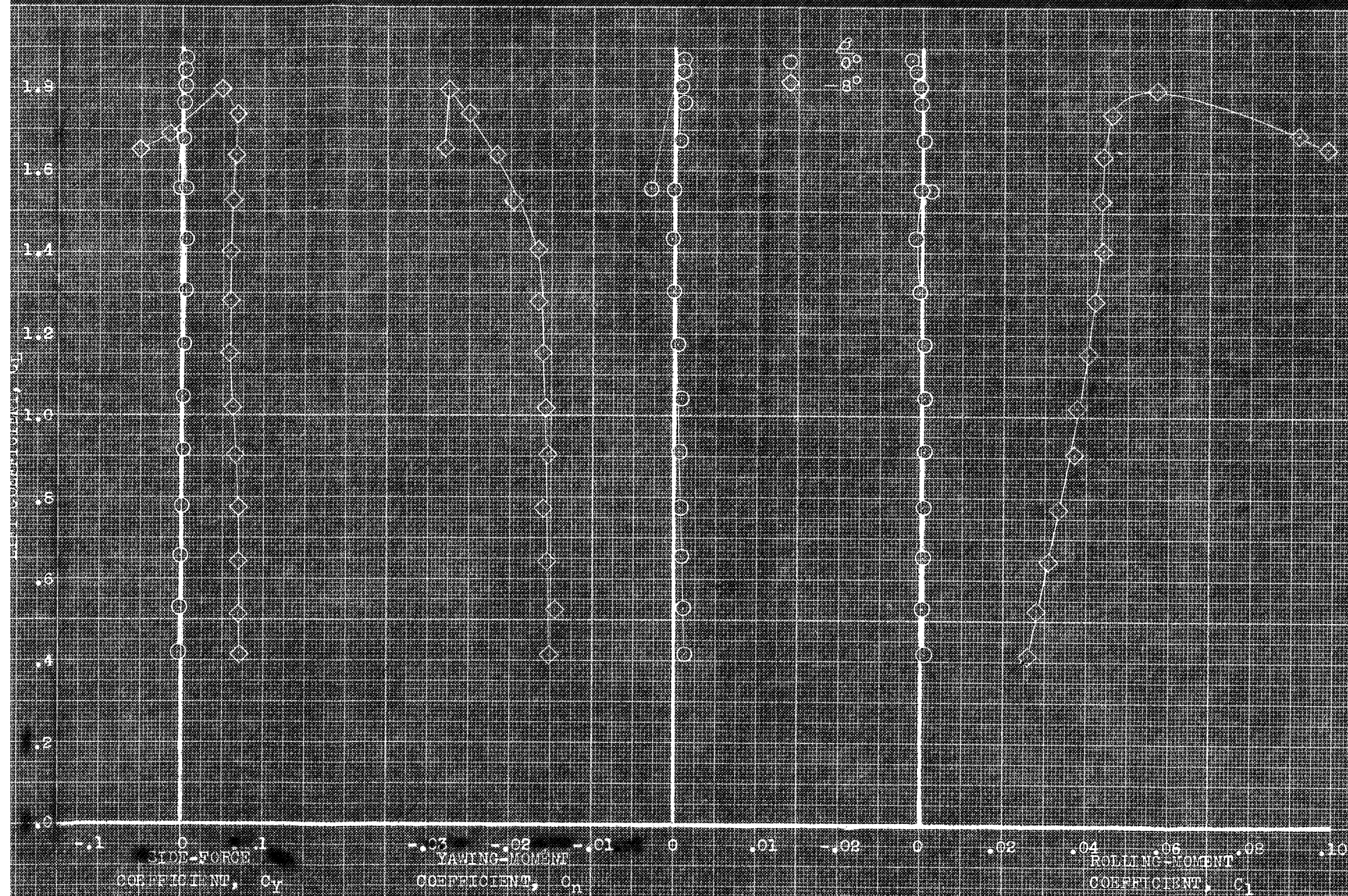


(a) $1/4$, 0° , 0° , C_D vs α , C_m vs α

FIGURE 19. AERODYNAMIC CHARACTERISTICS IN PLANE OF THE MODEL AT VARIOUS ANGLES OF SIDESLIP. DROOPED FLAPS, PLAIN FLAPS, 40° .

CONFIDENTIAL

NATIONAL ADVISORY COMMITTEE FOR AERONAUTICS

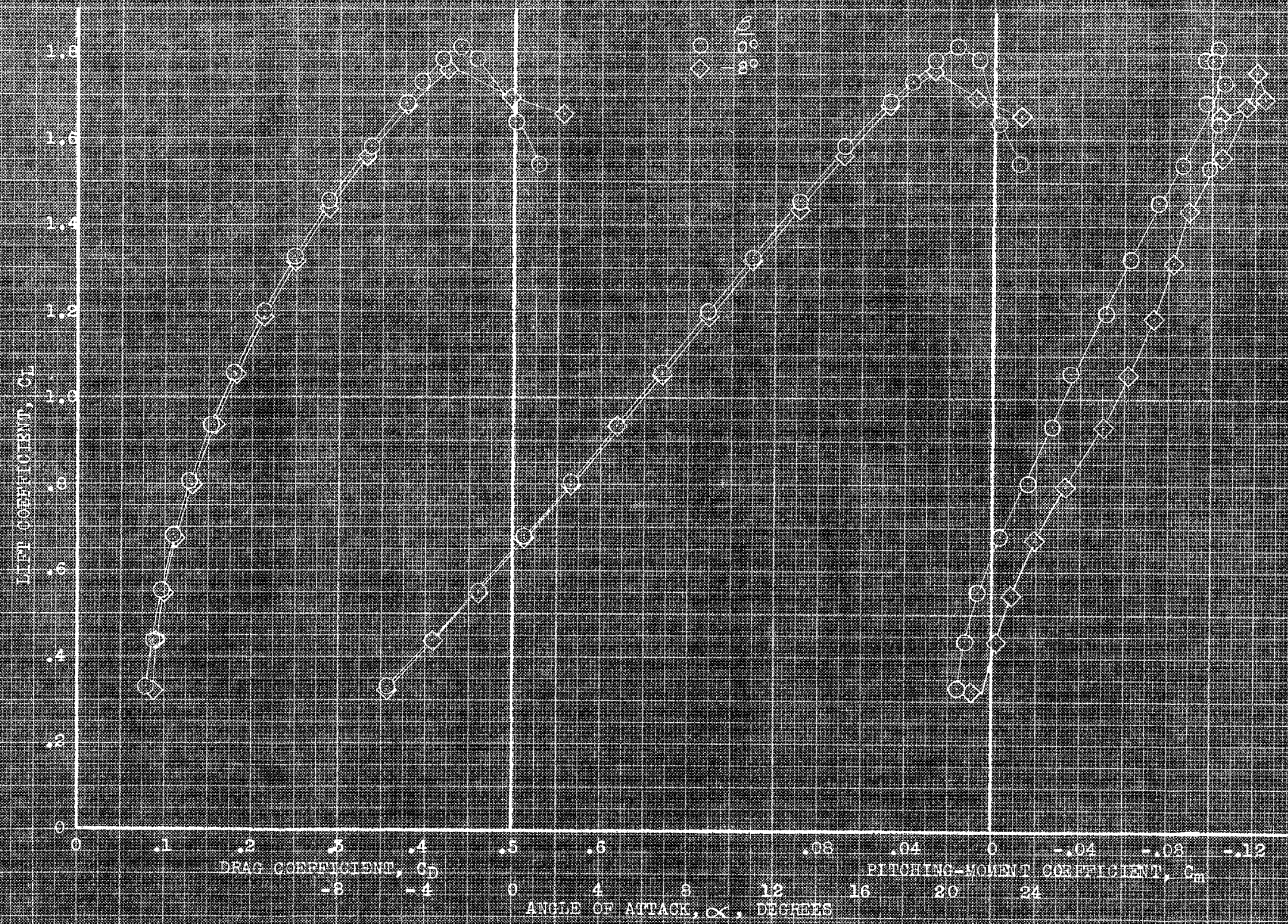


(b) $i_w, 0^\circ; 0^\circ, 0^\circ, 0^\circ, 0^\circ$ vs α .

FIGURE 19.- CONTINUED.

CONFIDENTIAL

National Advisory Committee for Aeronautics



(c) $Re = 6 \times 10^6$; C_D , α , C_m vs C_L .

FIGURE 19b. - CONTINUED.

LIFT COEFFICIENT, C_L

SIDE-FORCE
COEFFICIENT, C_Y

YAWING-MOMENT COEFFICIENT, C_n

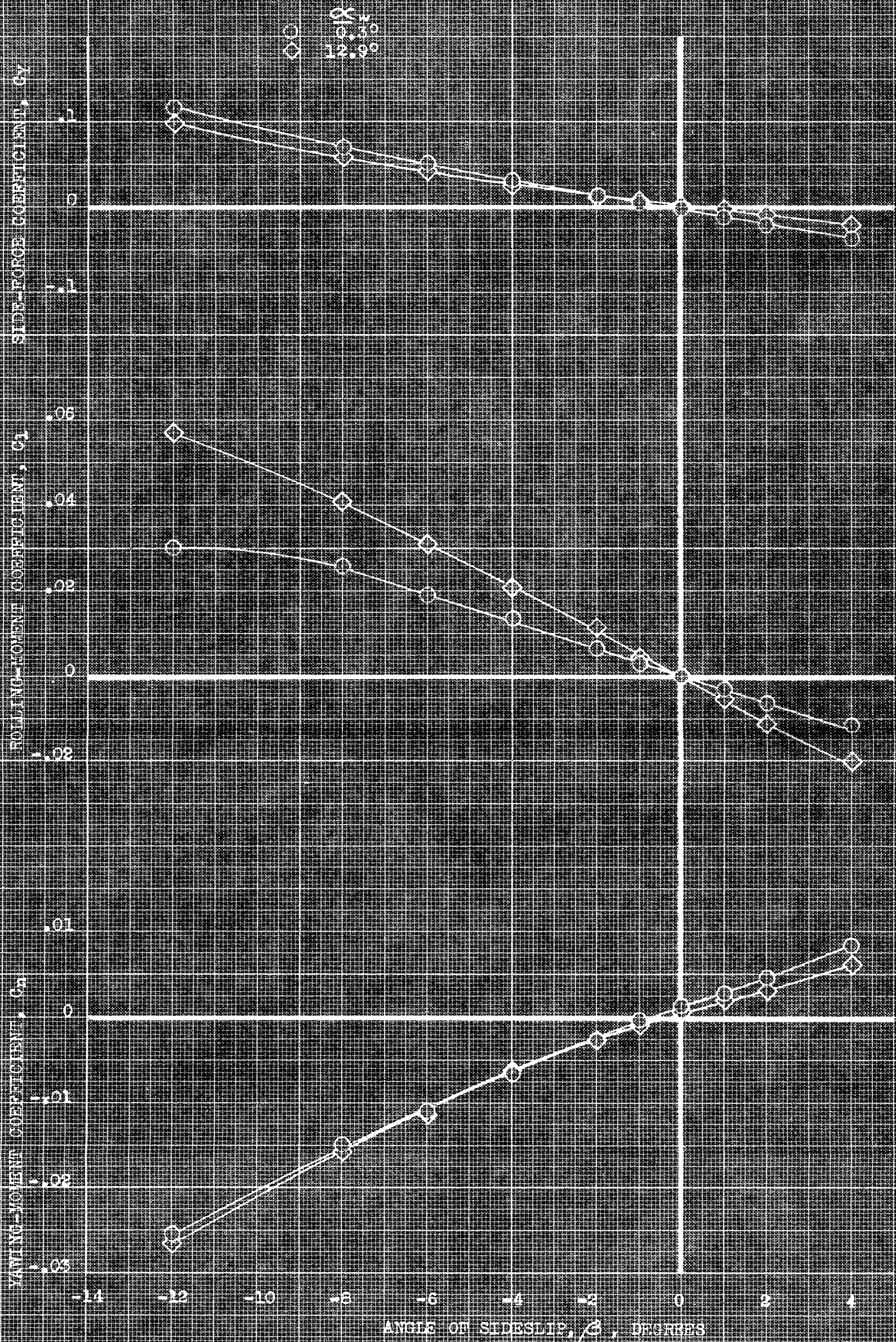
ROLLING-MOMENT COEFFICIENT, C_l

(a) 14° , 6° ; C_Y , C_n , C_l vs C_L

FIGURE 19. CONCLUDED.

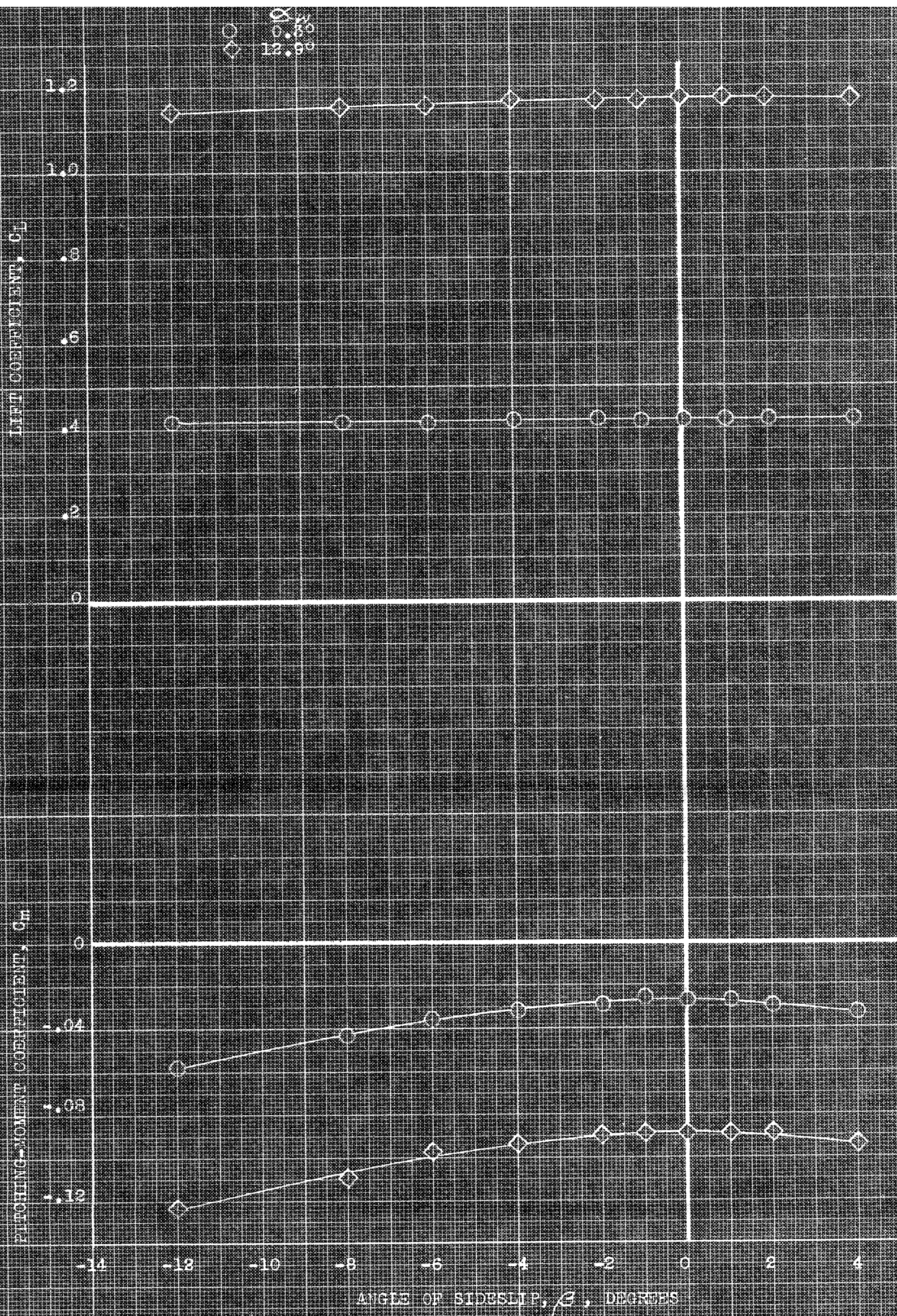
CONFIDENTIAL

Approved for public release; distribution is unlimited.



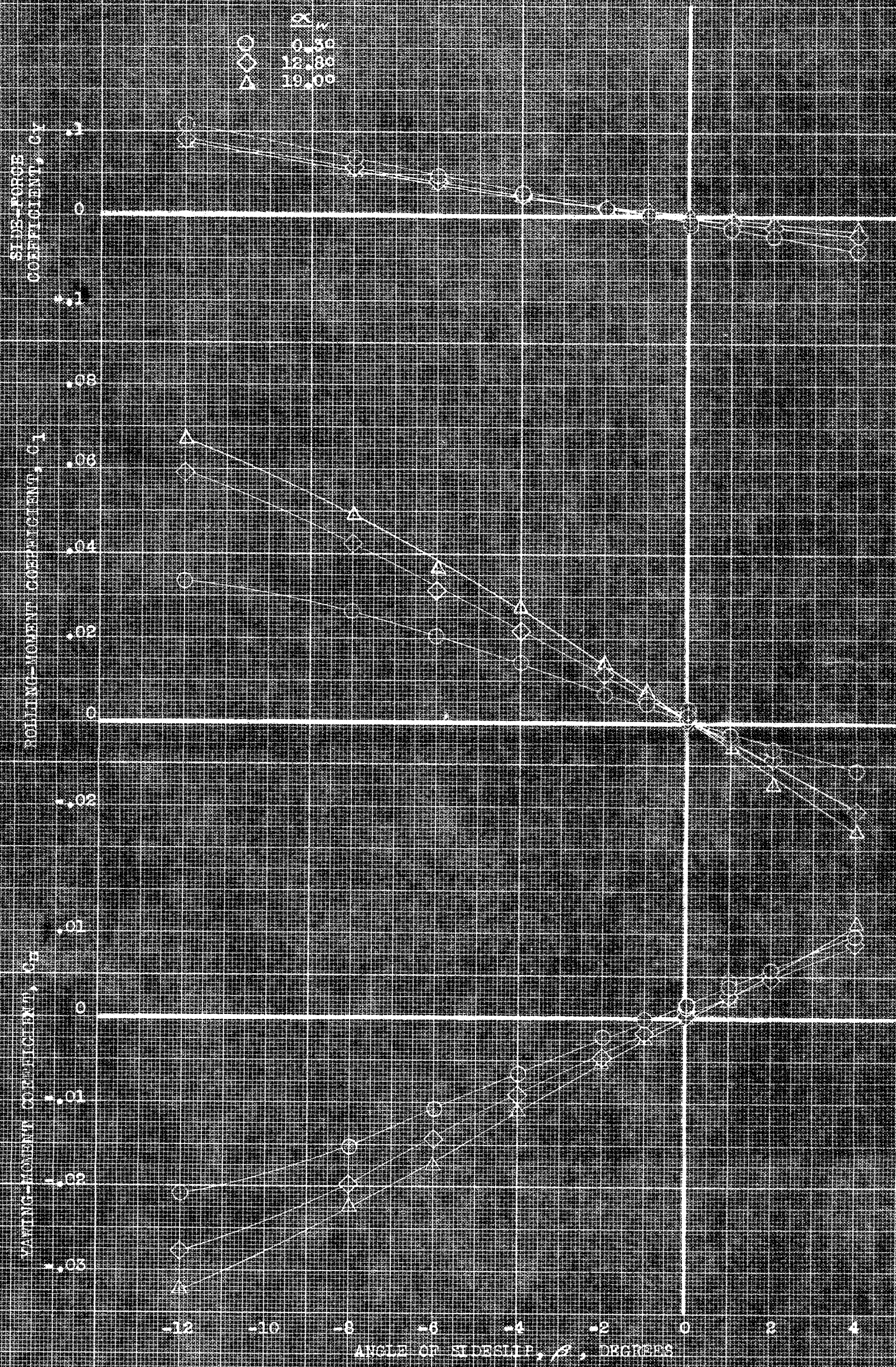
(a) $1_w, 0^\circ; C_y, C_l, C_n$ vs β .

FIGURE 20.- AERODYNAMIC CHARACTERISTICS IN SIDESLIP OF THE MODEL AT VARIOUS ANGLES OF ATTACK. DROOPED SEATS; MAIN FLAPS, 40° .



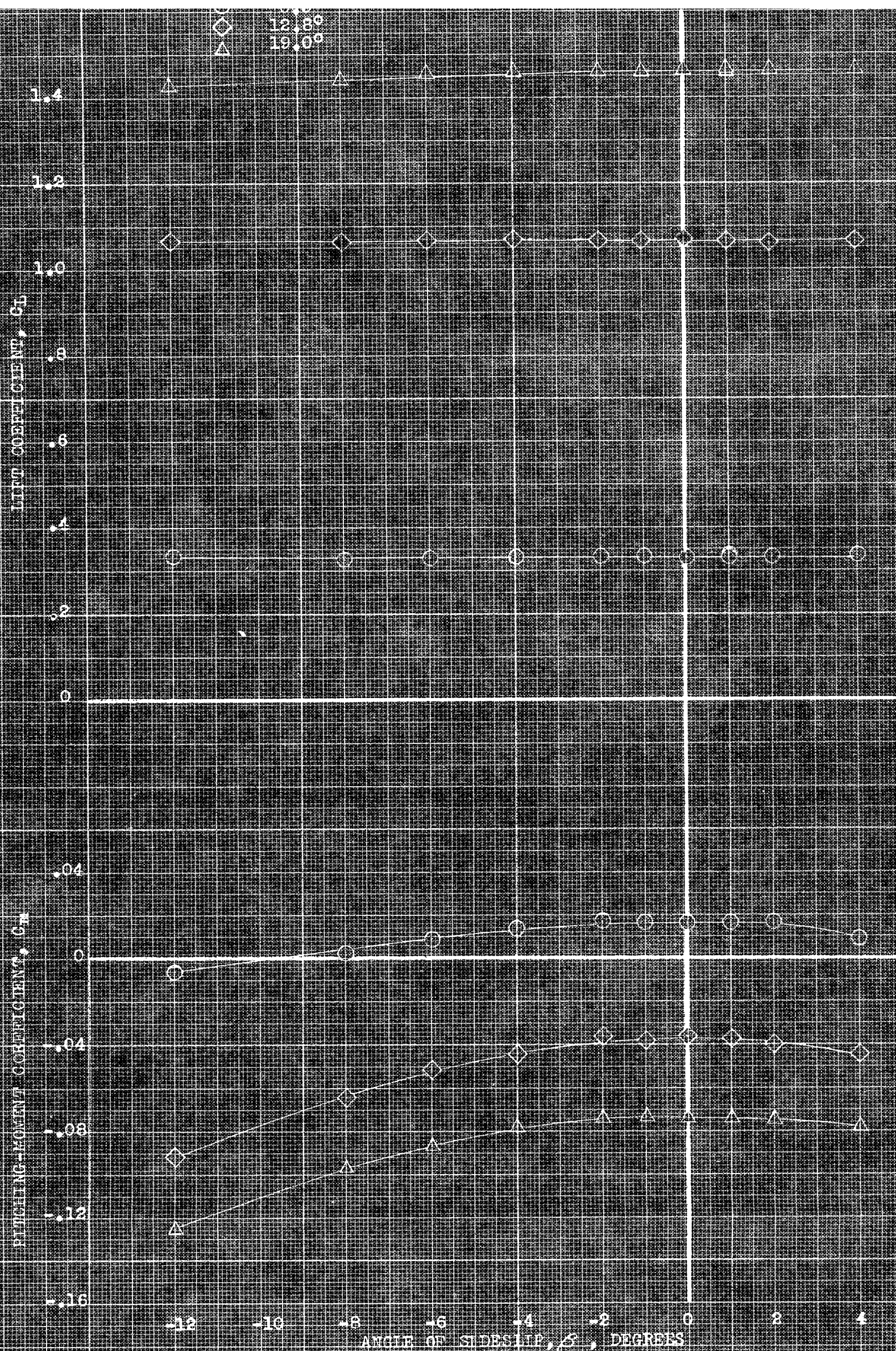
(b) $1_w, 0^\circ$; C_L, C_M vs β .

FIGURE 20. - CONTINUED.



(e) $1.75, 6^\circ$; C_y, C_l, C_n vs β .

FIGURE 20. - CONTINUED.



(d) $1w, 60.1^\circ, C_L, C_M$ vs β

FIGURE 20. CONCLUDED.

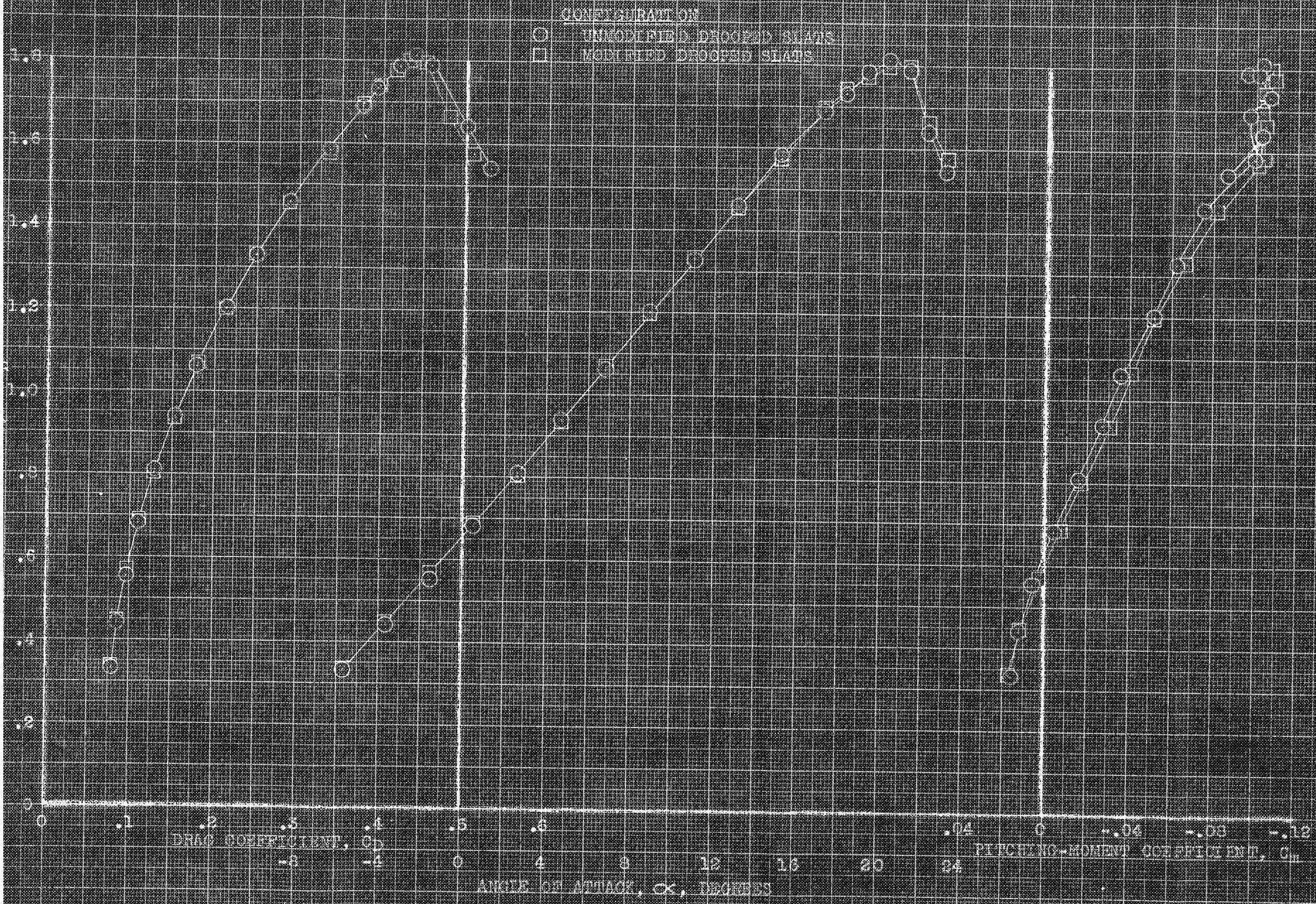
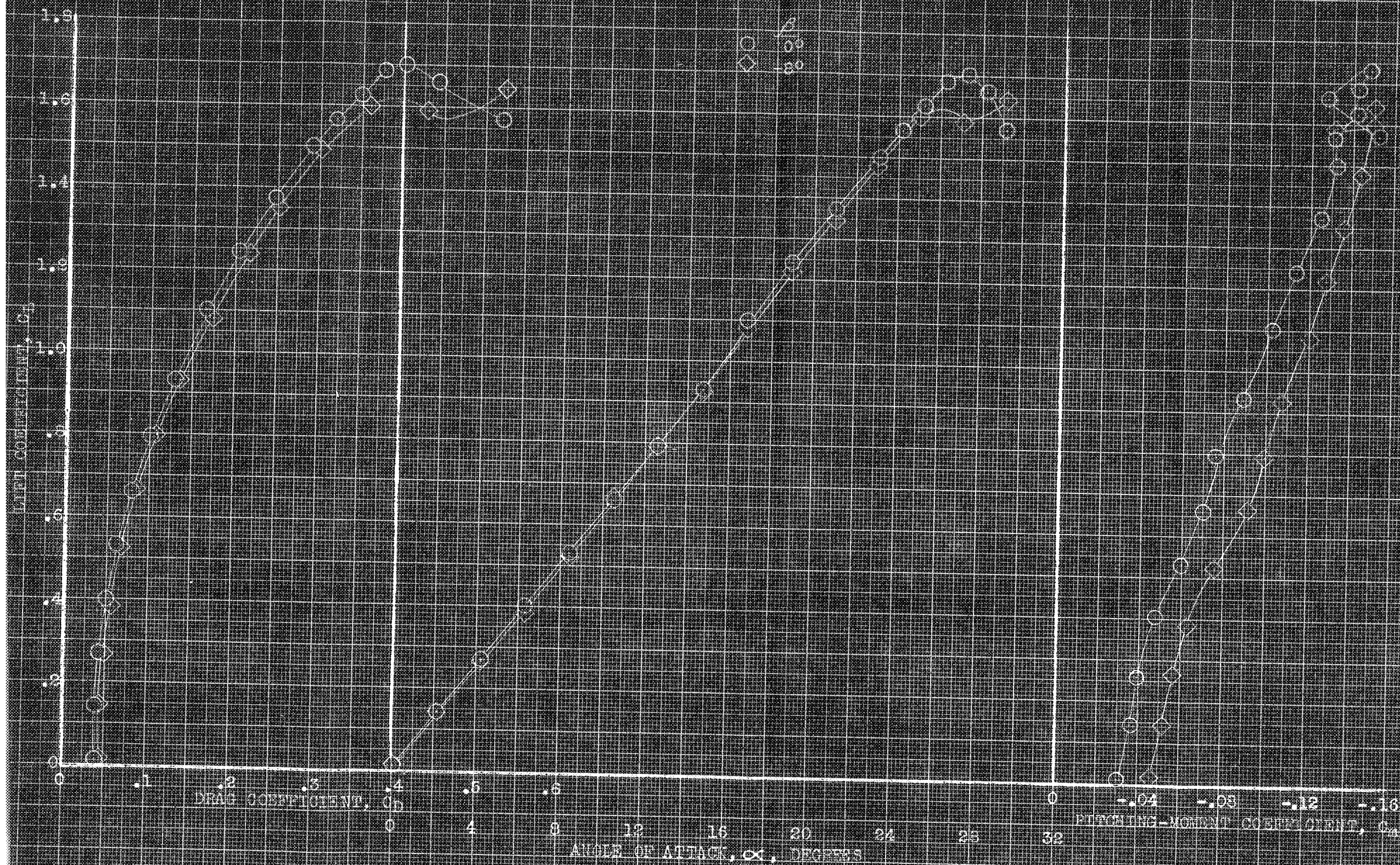
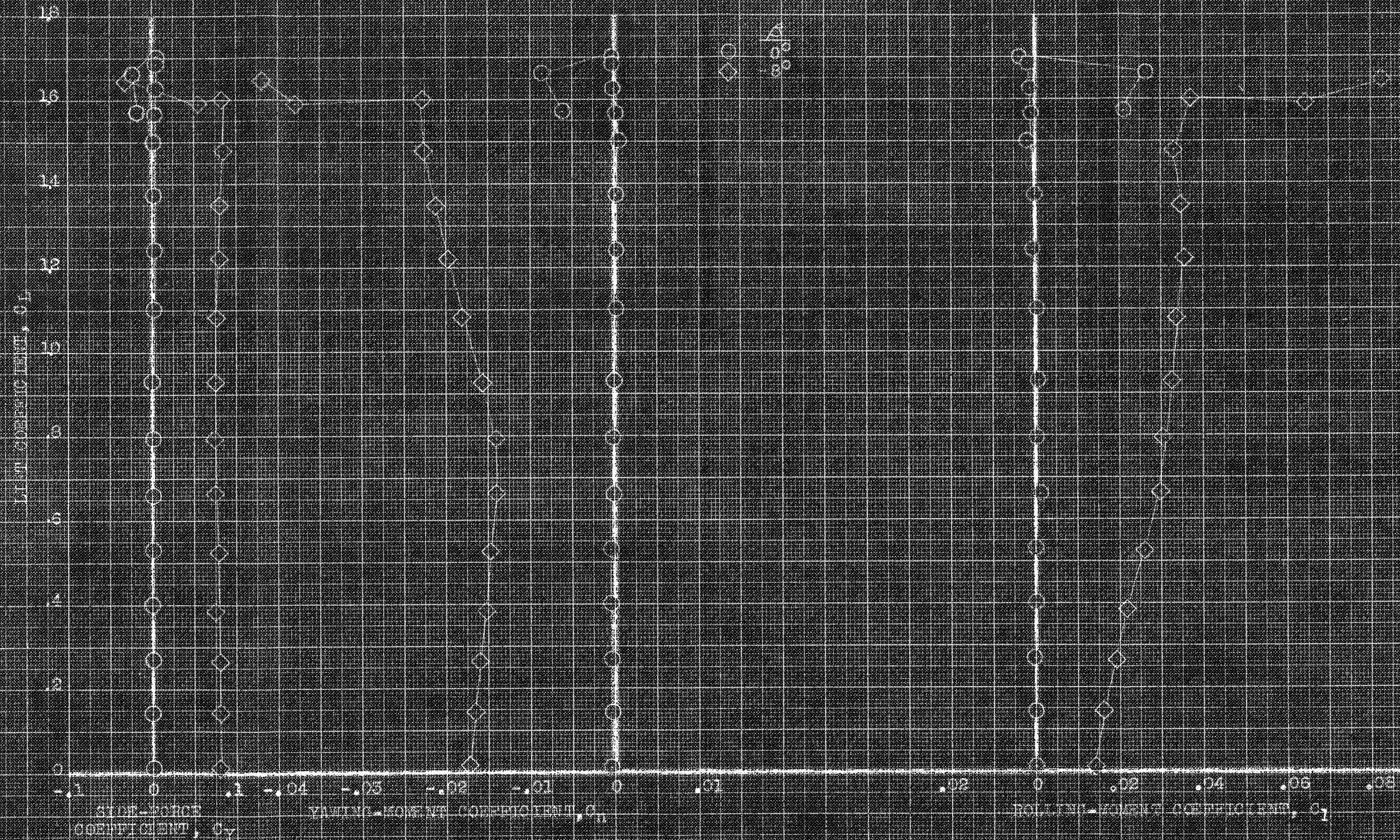


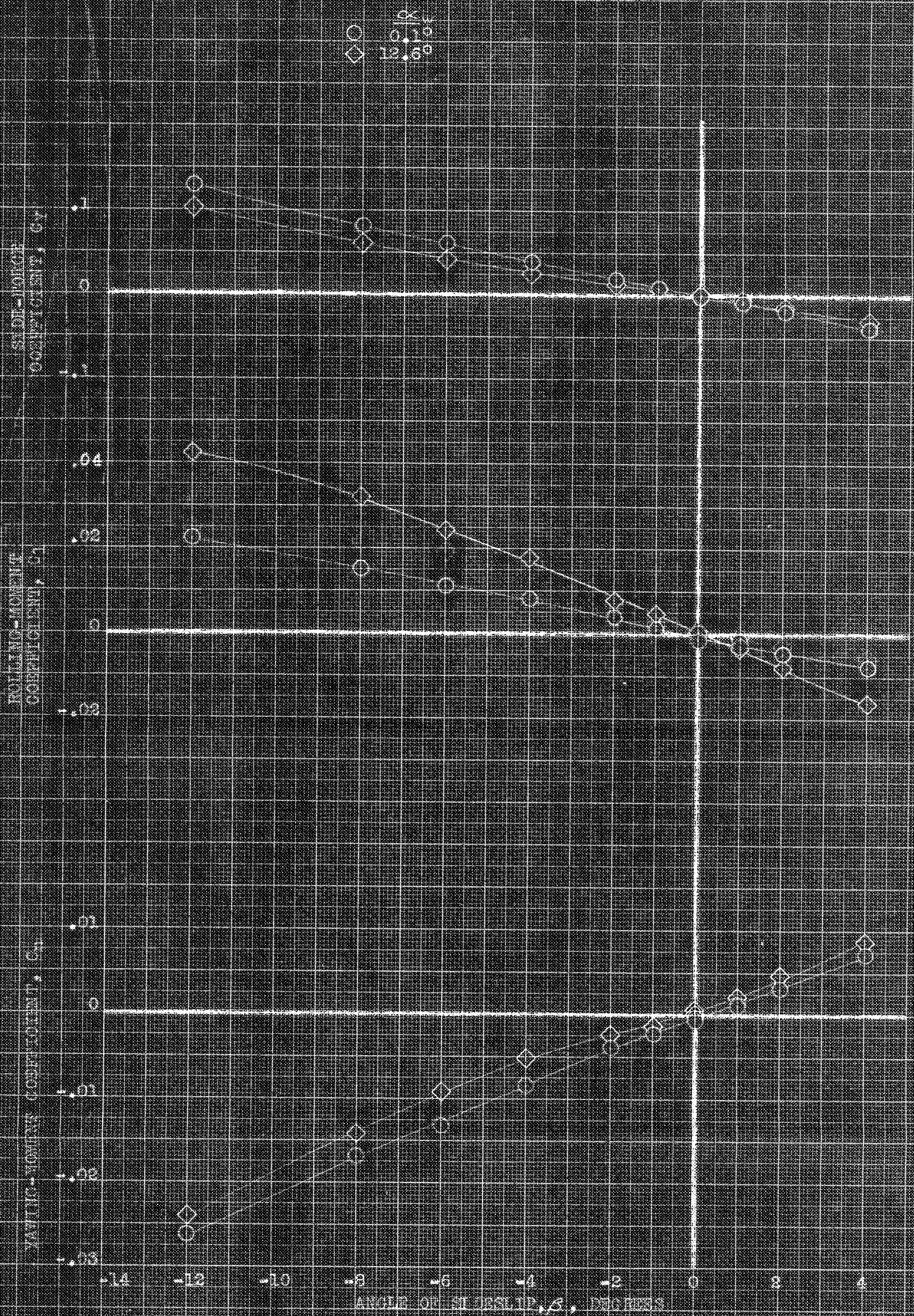
FIGURE 21. EFFECT OF THE DROOPED SEAT CONFIGURATION ON THE AERODYNAMIC CHARACTERISTICS OF MODEL IN FIGURE 1. MAIN PLANE, 100° ; 1.5° .



(a) C_D , C_L , C_M vs α .

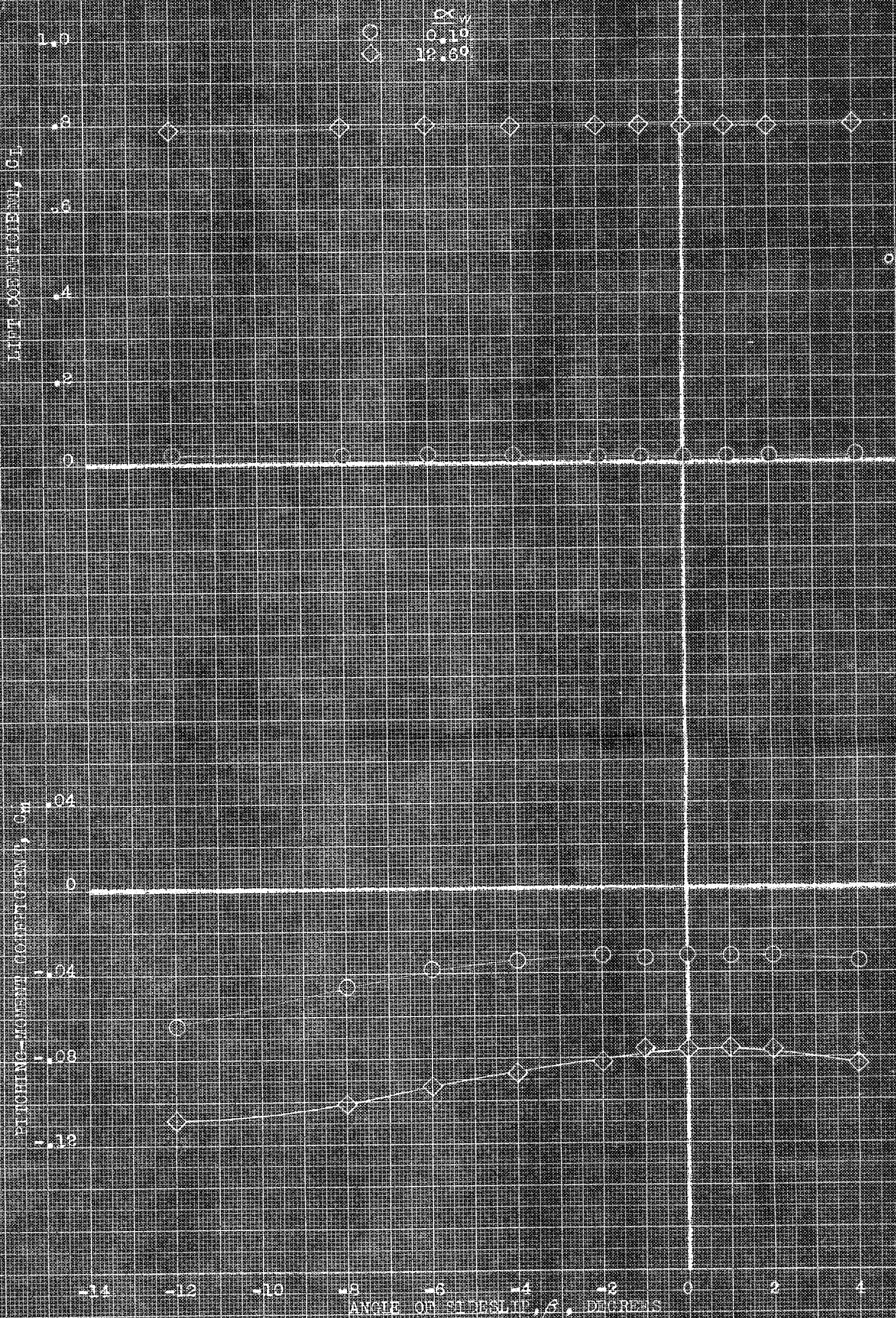
FIGURE 2. - APPROXIMATE CHARACTERISTICS IN WIND OF THE MODEL AT VARIOUS ANGLES OF ATTACK. (Modeling, 1, 2, 3, 4, 5, 6, 7, 8, 9, 10, 11, 12, 13, 14, 15, 16, 17, 18, 19, 20, 21, 22, 23, 24, 25, 26, 27, 28, 29, 30, 31, 32, 33, 34, 35, 36, 37, 38, 39, 40, 41, 42, 43, 44, 45, 46, 47, 48, 49, 50, 51, 52, 53, 54, 55, 56, 57, 58, 59, 60, 61, 62, 63, 64, 65, 66, 67, 68, 69, 70, 71, 72, 73, 74, 75, 76, 77, 78, 79, 80, 81, 82, 83, 84, 85, 86, 87, 88, 89, 90, 91, 92, 93, 94, 95, 96, 97, 98, 99, 100, 101, 102, 103, 104, 105, 106, 107, 108, 109, 110, 111, 112, 113, 114, 115, 116, 117, 118, 119, 120, 121, 122, 123, 124, 125, 126, 127, 128, 129, 130, 131, 132, 133, 134, 135, 136, 137, 138, 139, 140, 141, 142, 143, 144, 145, 146, 147, 148, 149, 150, 151, 152, 153, 154, 155, 156, 157, 158, 159, 160, 161, 162, 163, 164, 165, 166, 167, 168, 169, 170, 171, 172, 173, 174, 175, 176, 177, 178, 179, 180, 181, 182, 183, 184, 185, 186, 187, 188, 189, 190, 191, 192, 193, 194, 195, 196, 197, 198, 199, 200, 201, 202, 203, 204, 205, 206, 207, 208, 209, 210, 211, 212, 213, 214, 215, 216, 217, 218, 219, 220, 221, 222, 223, 224, 225, 226, 227, 228, 229, 230, 231, 232, 233, 234, 235, 236, 237, 238, 239, 240, 241, 242, 243, 244, 245, 246, 247, 248, 249, 250, 251, 252, 253, 254, 255, 256, 257, 258, 259, 260, 261, 262, 263, 264, 265, 266, 267, 268, 269, 270, 271, 272, 273, 274, 275, 276, 277, 278, 279, 280, 281, 282, 283, 284, 285, 286, 287, 288, 289, 290, 291, 292, 293, 294, 295, 296, 297, 298, 299, 300, 301, 302, 303, 304, 305, 306, 307, 308, 309, 310, 311, 312, 313, 314, 315, 316, 317, 318, 319, 320, 321, 322, 323, 324, 325, 326, 327, 328, 329, 330, 331, 332, 333, 334, 335, 336, 337, 338, 339, 340, 341, 342, 343, 344, 345, 346, 347, 348, 349, 350, 351, 352, 353, 354, 355, 356, 357, 358, 359, 360, 361, 362, 363, 364, 365, 366, 367, 368, 369, 370, 371, 372, 373, 374, 375, 376, 377, 378, 379, 380, 381, 382, 383, 384, 385, 386, 387, 388, 389, 390, 391, 392, 393, 394, 395, 396, 397, 398, 399, 400, 401, 402, 403, 404, 405, 406, 407, 408, 409, 410, 411, 412, 413, 414, 415, 416, 417, 418, 419, 420, 421, 422, 423, 424, 425, 426, 427, 428, 429, 430, 431, 432, 433, 434, 435, 436, 437, 438, 439, 440, 441, 442, 443, 444, 445, 446, 447, 448, 449, 450, 451, 452, 453, 454, 455, 456, 457, 458, 459, 460, 461, 462, 463, 464, 465, 466, 467, 468, 469, 470, 471, 472, 473, 474, 475, 476, 477, 478, 479, 480, 481, 482, 483, 484, 485, 486, 487, 488, 489, 490, 491, 492, 493, 494, 495, 496, 497, 498, 499, 500, 501, 502, 503, 504, 505, 506, 507, 508, 509, 510, 511, 512, 513, 514, 515, 516, 517, 518, 519, 520, 521, 522, 523, 524, 525, 526, 527, 528, 529, 530, 531, 532, 533, 534, 535, 536, 537, 538, 539, 540, 541, 542, 543, 544, 545, 546, 547, 548, 549, 550, 551, 552, 553, 554, 555, 556, 557, 558, 559, 560, 561, 562, 563, 564, 565, 566, 567, 568, 569, 570, 571, 572, 573, 574, 575, 576, 577, 578, 579, 580, 581, 582, 583, 584, 585, 586, 587, 588, 589, 590, 591, 592, 593, 594, 595, 596, 597, 598, 599, 600, 601, 602, 603, 604, 605, 606, 607, 608, 609, 610, 611, 612, 613, 614, 615, 616, 617, 618, 619, 620, 621, 622, 623, 624, 625, 626, 627, 628, 629, 630, 631, 632, 633, 634, 635, 636, 637, 638, 639, 640, 641, 642, 643, 644, 645, 646, 647, 648, 649, 650, 651, 652, 653, 654, 655, 656, 657, 658, 659, 660, 661, 662, 663, 664, 665, 666, 667, 668, 669, 670, 671, 672, 673, 674, 675, 676, 677, 678, 679, 680, 681, 682, 683, 684, 685, 686, 687, 688, 689, 690, 691, 692, 693, 694, 695, 696, 697, 698, 699, 700, 701, 702, 703, 704, 705, 706, 707, 708, 709, 710, 711, 712, 713, 714, 715, 716, 717, 718, 719, 720, 721, 722, 723, 724, 725, 726, 727, 728, 729, 730, 731, 732, 733, 734, 735, 736, 737, 738, 739, 740, 741, 742, 743, 744, 745, 746, 747, 748, 749, 750, 751, 752, 753, 754, 755, 756, 757, 758, 759, 760, 761, 762, 763, 764, 765, 766, 767, 768, 769, 770, 771, 772, 773, 774, 775, 776, 777, 778, 779, 780, 781, 782, 783, 784, 785, 786, 787, 788, 789, 790, 791, 792, 793, 794, 795, 796, 797, 798, 799, 800, 801, 802, 803, 804, 805, 806, 807, 808, 809, 810, 811, 812, 813, 814, 815, 816, 817, 818, 819, 820, 821, 822, 823, 824, 825, 826, 827, 828, 829, 830, 831, 832, 833, 834, 835, 836, 837, 838, 839, 840, 841, 842, 843, 844, 845, 846, 847, 848, 849, 850, 851, 852, 853, 854, 855, 856, 857, 858, 859, 860, 861, 862, 863, 864, 865, 866, 867, 868, 869, 870, 871, 872, 873, 874, 875, 876, 877, 878, 879, 880, 881, 882, 883, 884, 885, 886, 887, 888, 889, 890, 891, 892, 893, 894, 895, 896, 897, 898, 899, 900, 901, 902, 903, 904, 905, 906, 907, 908, 909, 910, 911, 912, 913, 914, 915, 916, 917, 918, 919, 920, 921, 922, 923, 924, 925, 926, 927, 928, 929, 930, 931, 932, 933, 934, 935, 936, 937, 938, 939, 940, 941, 942, 943, 944, 945, 946, 947, 948, 949, 950, 951, 952, 953, 954, 955, 956, 957, 958, 959, 960, 961, 962, 963, 964, 965, 966, 967, 968, 969, 970, 971, 972, 973, 974, 975, 976, 977, 978, 979, 980, 981, 982, 983, 984, 985, 986, 987, 988, 989, 990, 991, 992, 993, 994, 995, 996, 997, 998, 999, 1000).





(a) C_y, C_l, C_n vs. β .

FIGURE 24. AERODYNAMIC CHARACTERISTICS IN SIDESLIP OF THE MODEL AT VARIOUS ANGLES OF ATTACK. DEFORMED FLATS; $\alpha = 0^\circ$.



(b) C_L, C_m vs α

FIGURE 24. - CONTINUED.

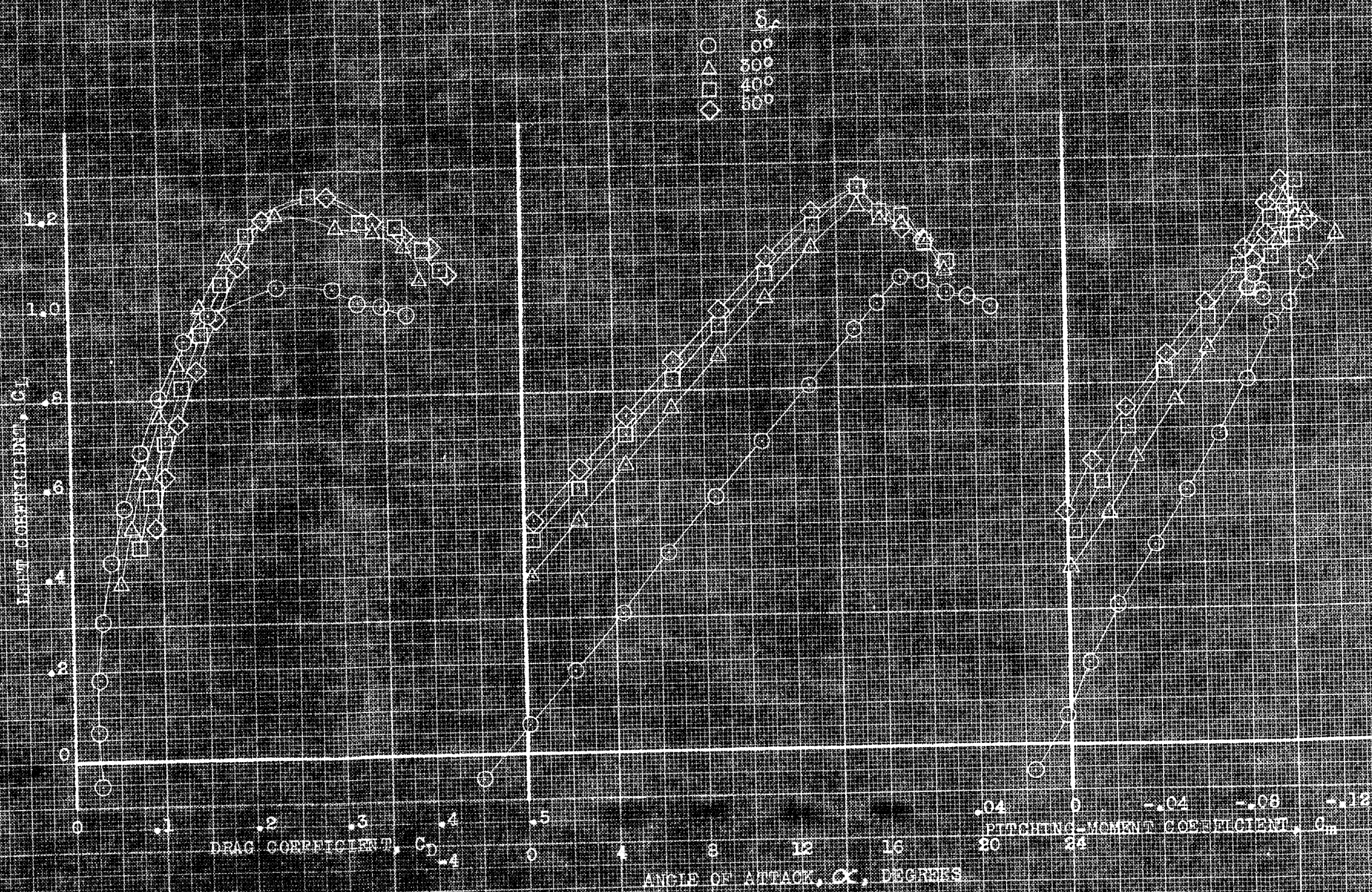
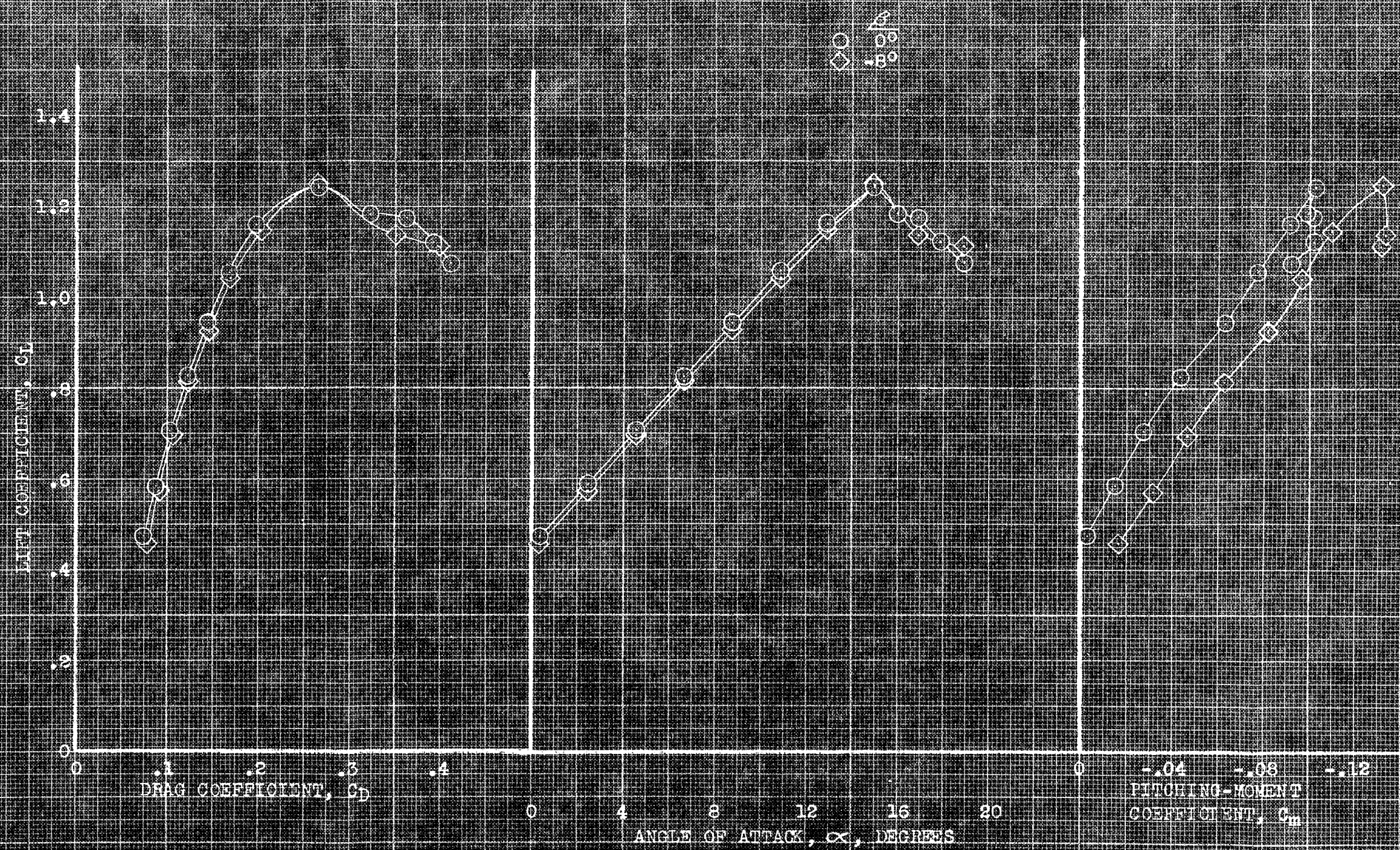
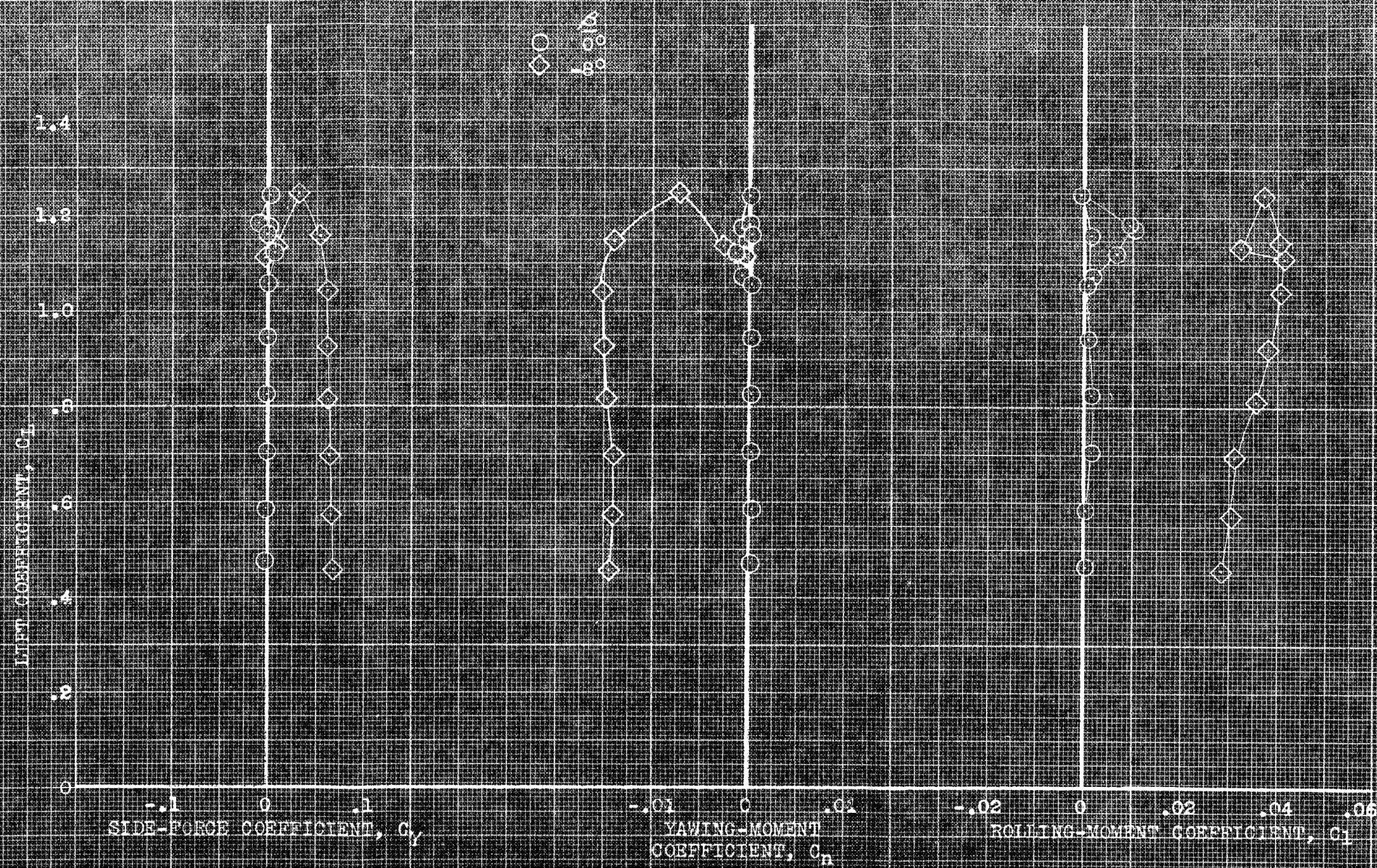


FIGURE 21. EFFECT OF PLAIN PLATE ANGLE ON THE AERODYNAMIC CHARACTERISTICS OF THE MODEL IN PITCH, α , C_D .



(a) C_L , α , C_m vs C_D .

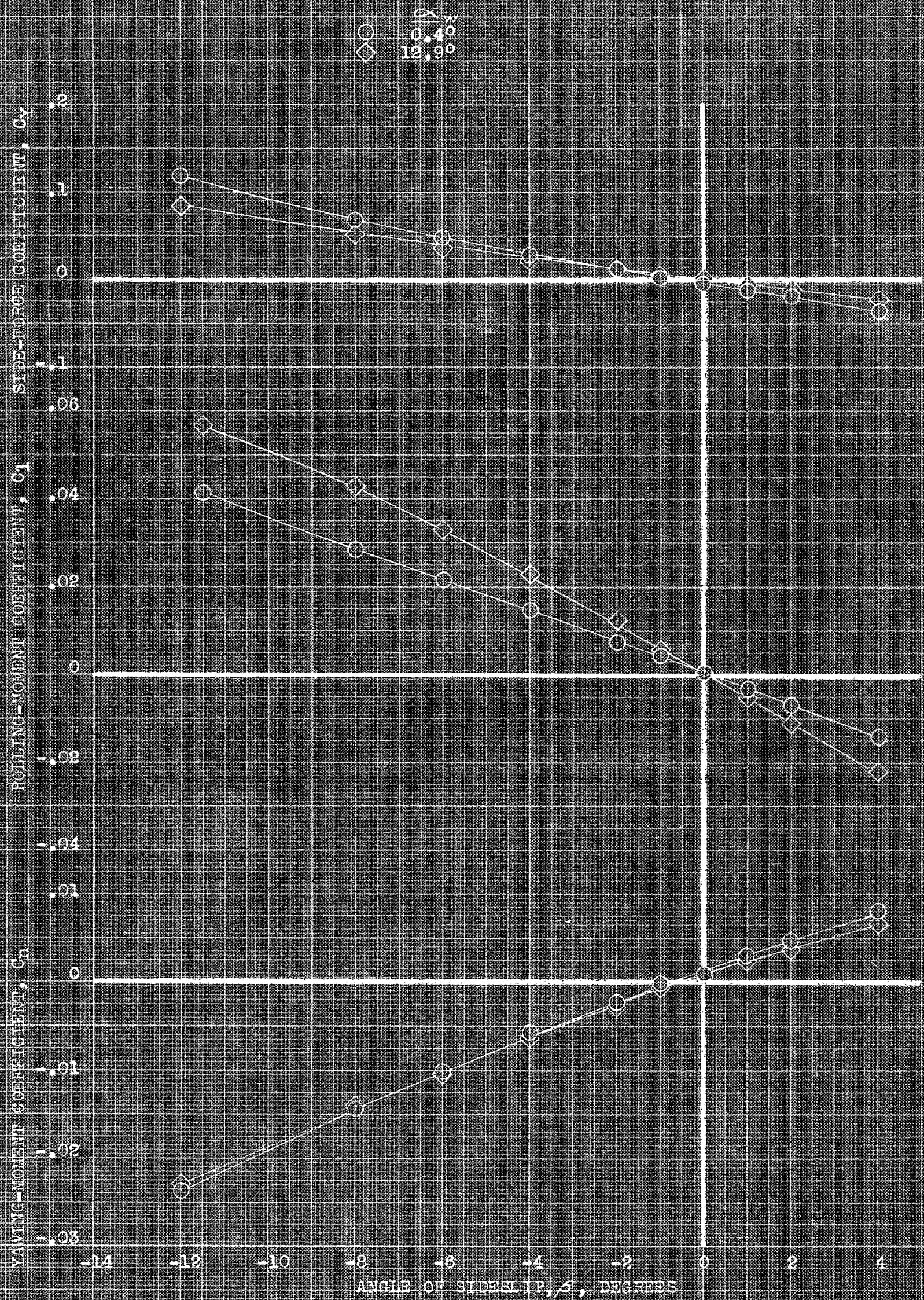
FIGURE 21. AERODYNAMIC CHARACTERISTICS IN FLIGHT OF THE MODEL AT VARIOUS ANGLES OF SIDESLIP. PLAIN FLAPS, 400; M_∞ , 0.8.



(b) C_Y , C_N , C_L vs C_L .

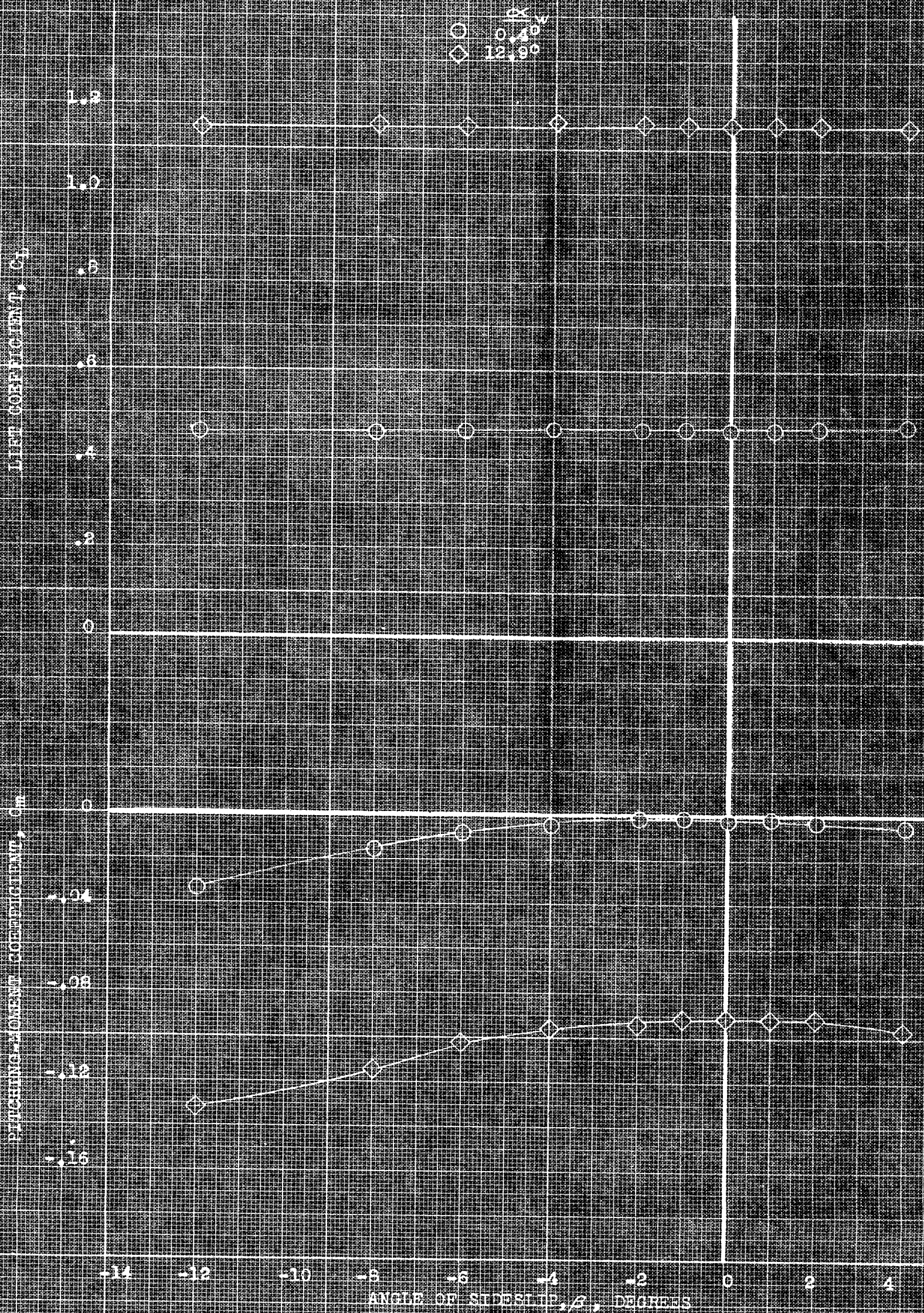
FIGURE 21. - CONCLUDED.

Downloaded from ascelibrary.org by University of California, San Diego on 06/16/15. Copyright ASCE. For personal use only; all rights reserved.



(c) C_Y, C_l, C_m vs β

FIGURE 25. — AERODYNAMIC CHARACTERISTICS IN SIDESLIP OF THE MODEL AT VARIOUS ANGLES OF ATTACK: FLAT FLAPS, 40° ; i_w , 0° .



(b) C_L , C_m vs β

FIGURE 26. CONCLUDED.

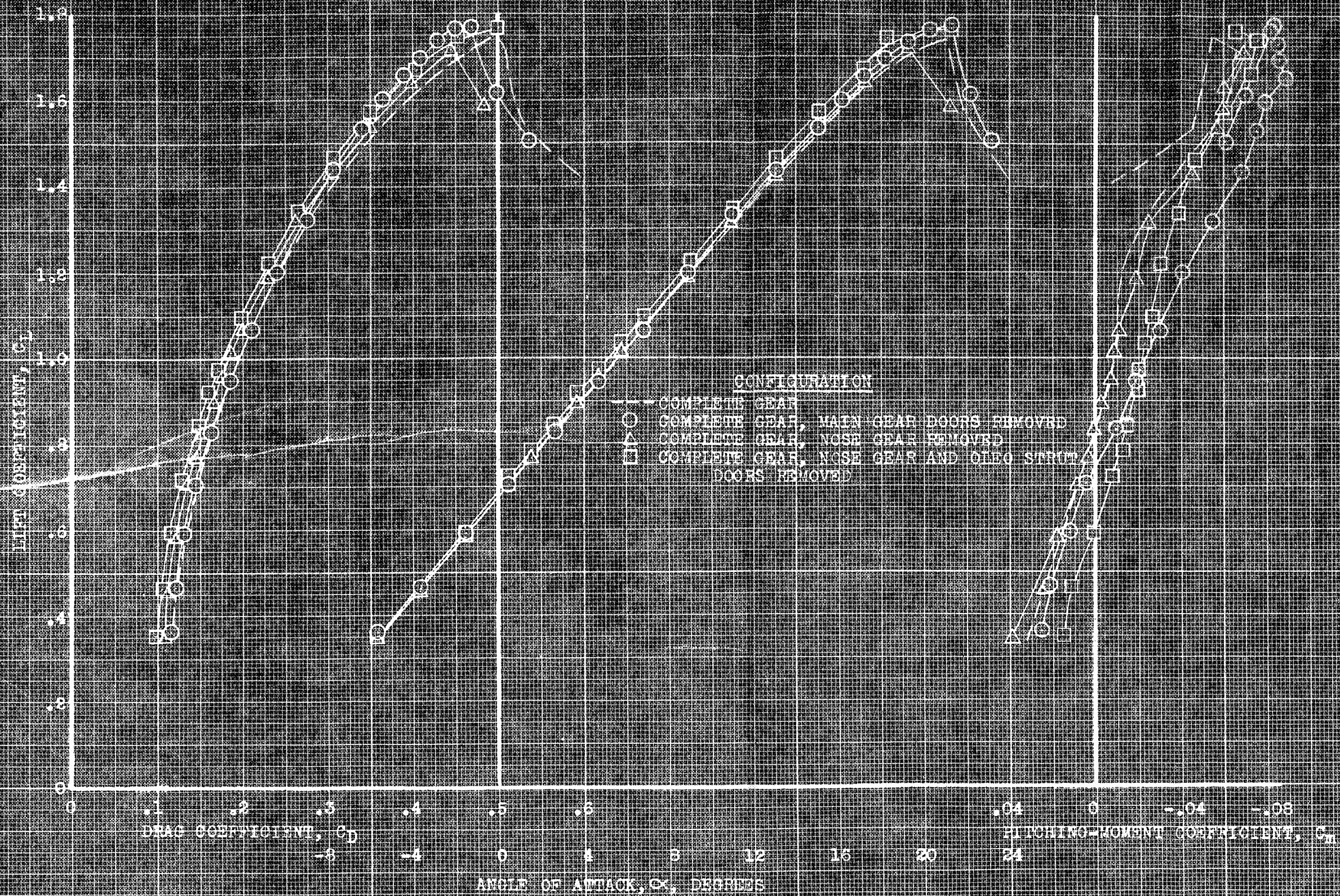
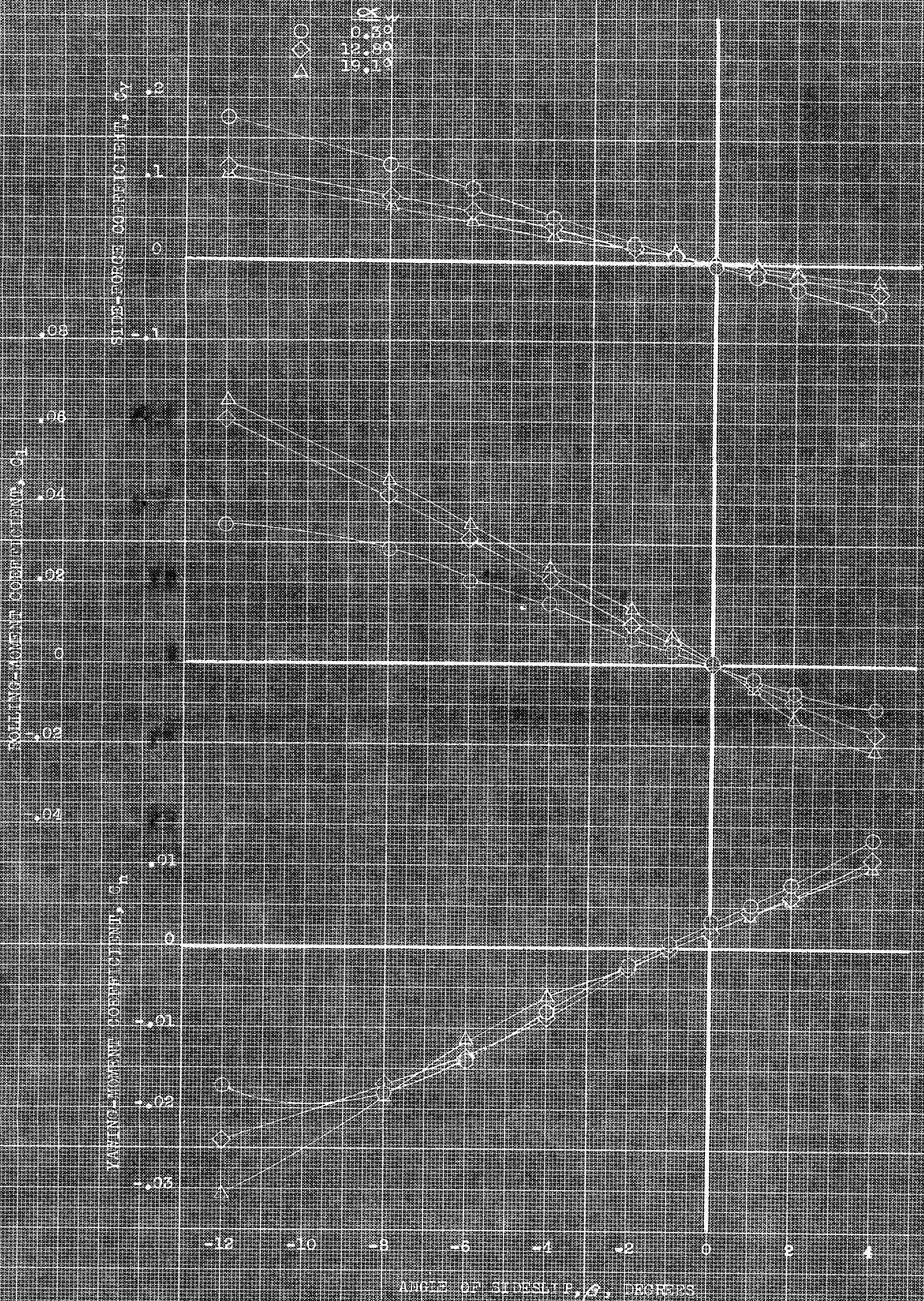


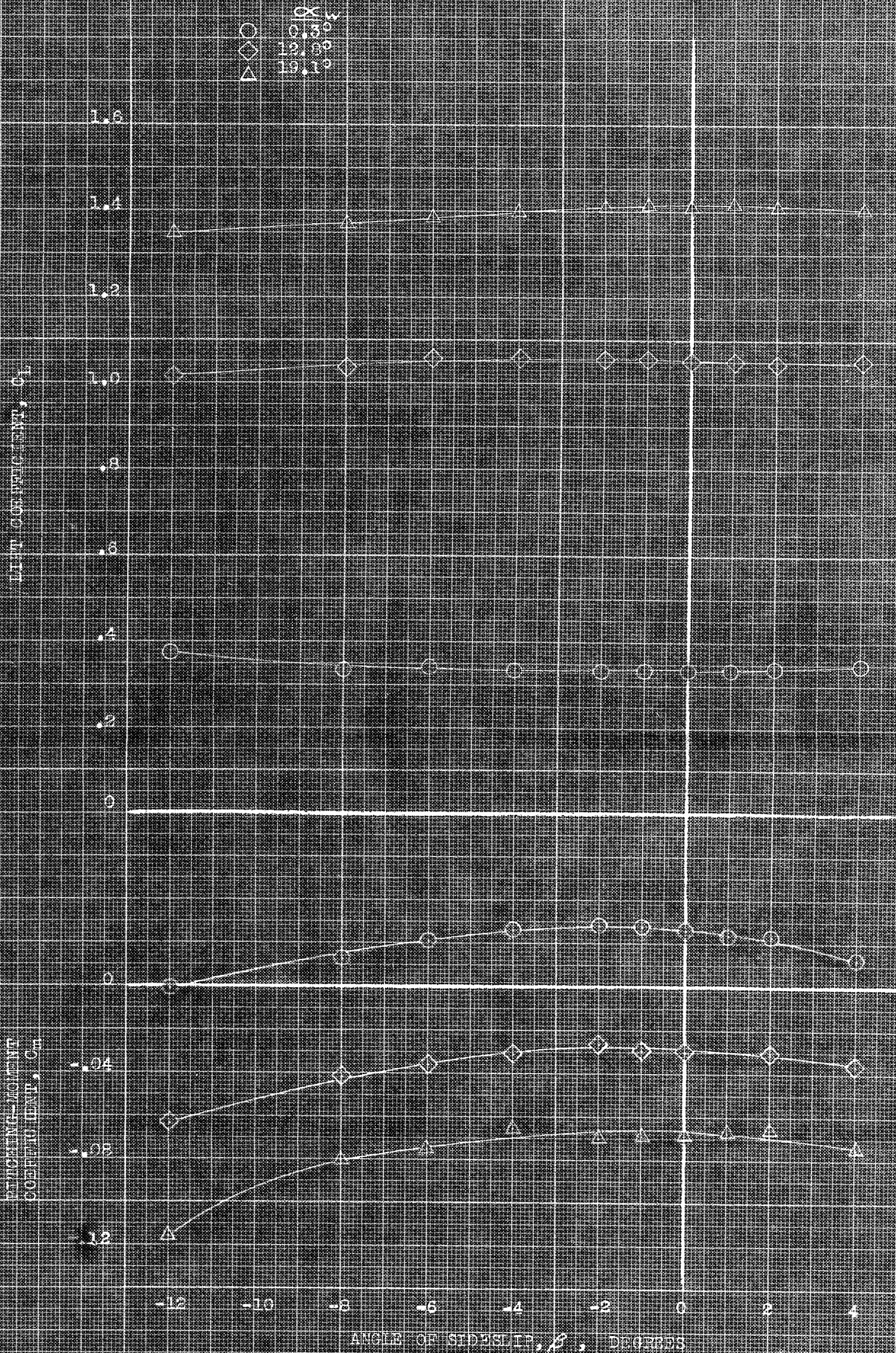
FIGURE 27. EFFECT OF DIFFERENT PARTS OF THE GEAR ON THE AERODYNAMIC CHARACTERISTICS OF THE MODEL IN HIGH, DROOPED SLATS, 40°.

14100



(a) C_y , C_l , C_h vs β .

FIGURE 28. - EFFECT OF THE GEAR WITH MAIN GEAR DOORS REMOVED ON THE AERODYNAMIC CHARACTERISTICS OF THE MODEL IN SIDESLIP. DROPPED SLATS. PLAIN FLAPS, 40°; 1°, 6°.



(b) C_L, C_m vs. β

FIGURE 28.- CONCLUDED.

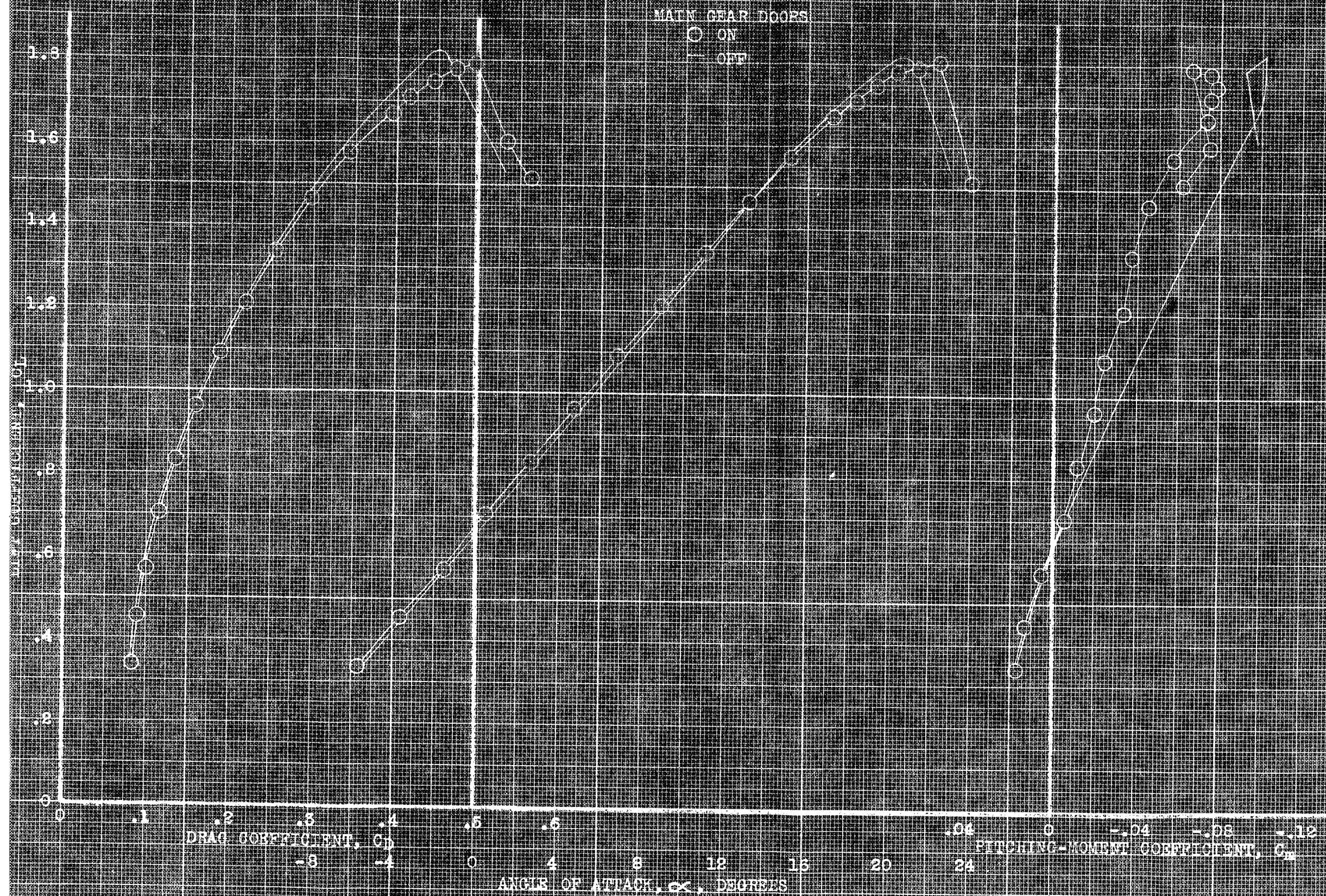


FIGURE 29.— EFFECT OF THE MAIN GEAR DOORS ON THE AERODYNAMIC CHARACTERISTICS OF THE MODEL IN PITCH, DROOED SLATS, PLAIN FLAPS, 400, 1-W, 6°.

CONFIDENTIAL

NO COPY TO BE MADE OR REPRODUCED WITHOUT AUTHORIZATION

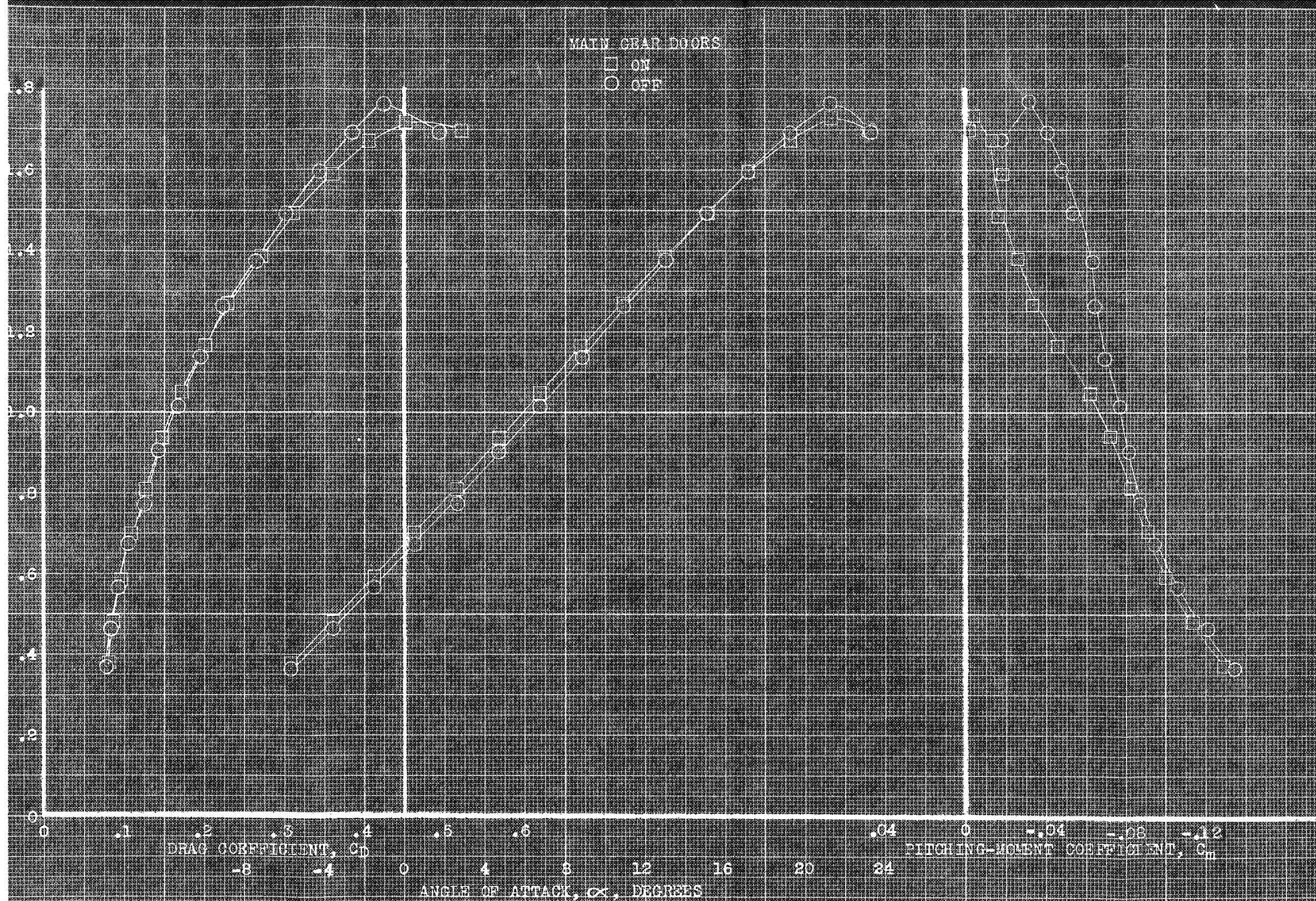


FIGURE 30. EFFECT OF THE MAIN GEAR DOORS ON THE AERODYNAMIC CHARACTERISTICS OF THE MODEL IN PITCH WITH TAIL REMOVED. DROOPED SLATS, MAIN PLAT, 40°, 1W, 6°.

RESEARCH
AERONAUTICAL ENGINEERING

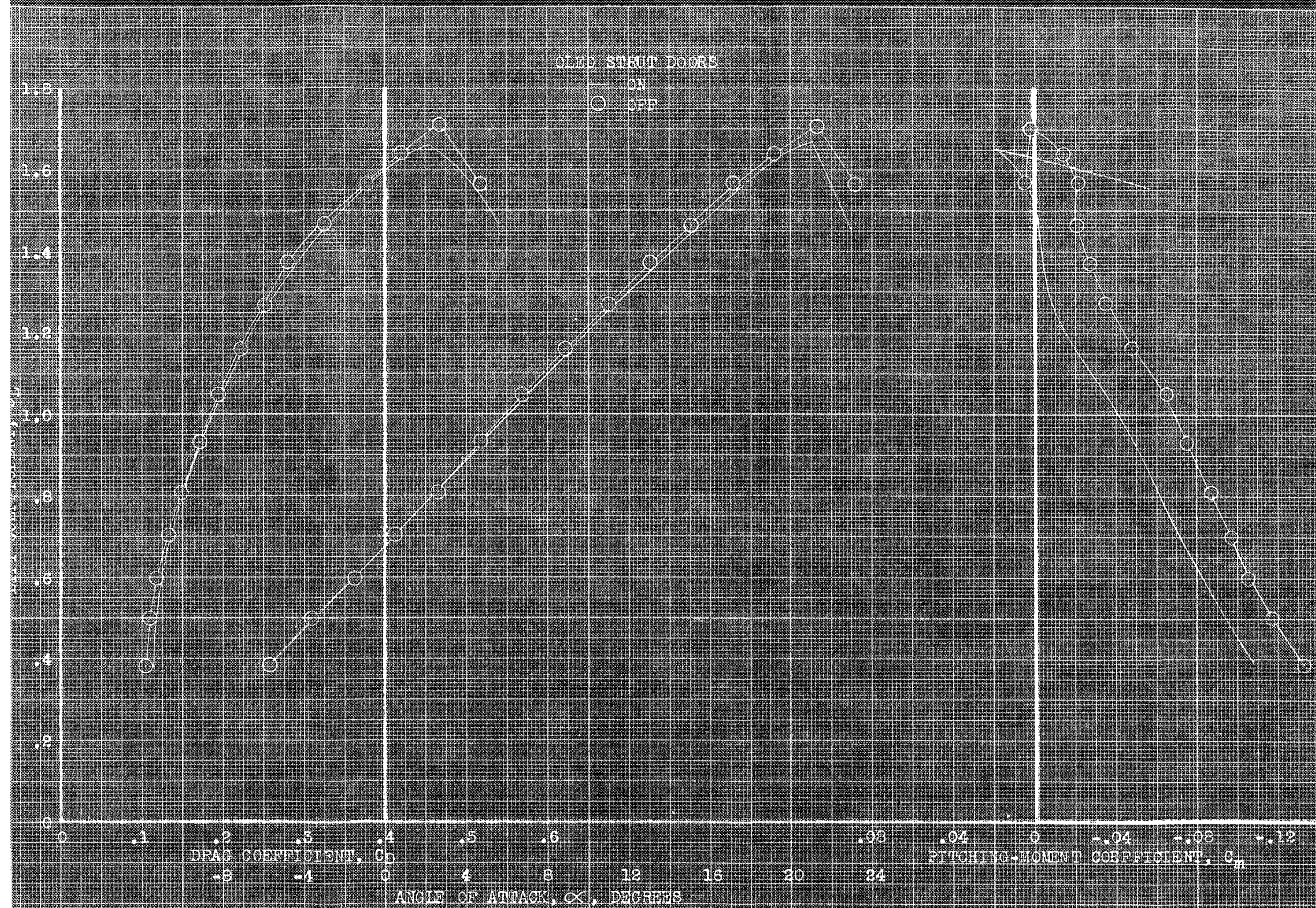
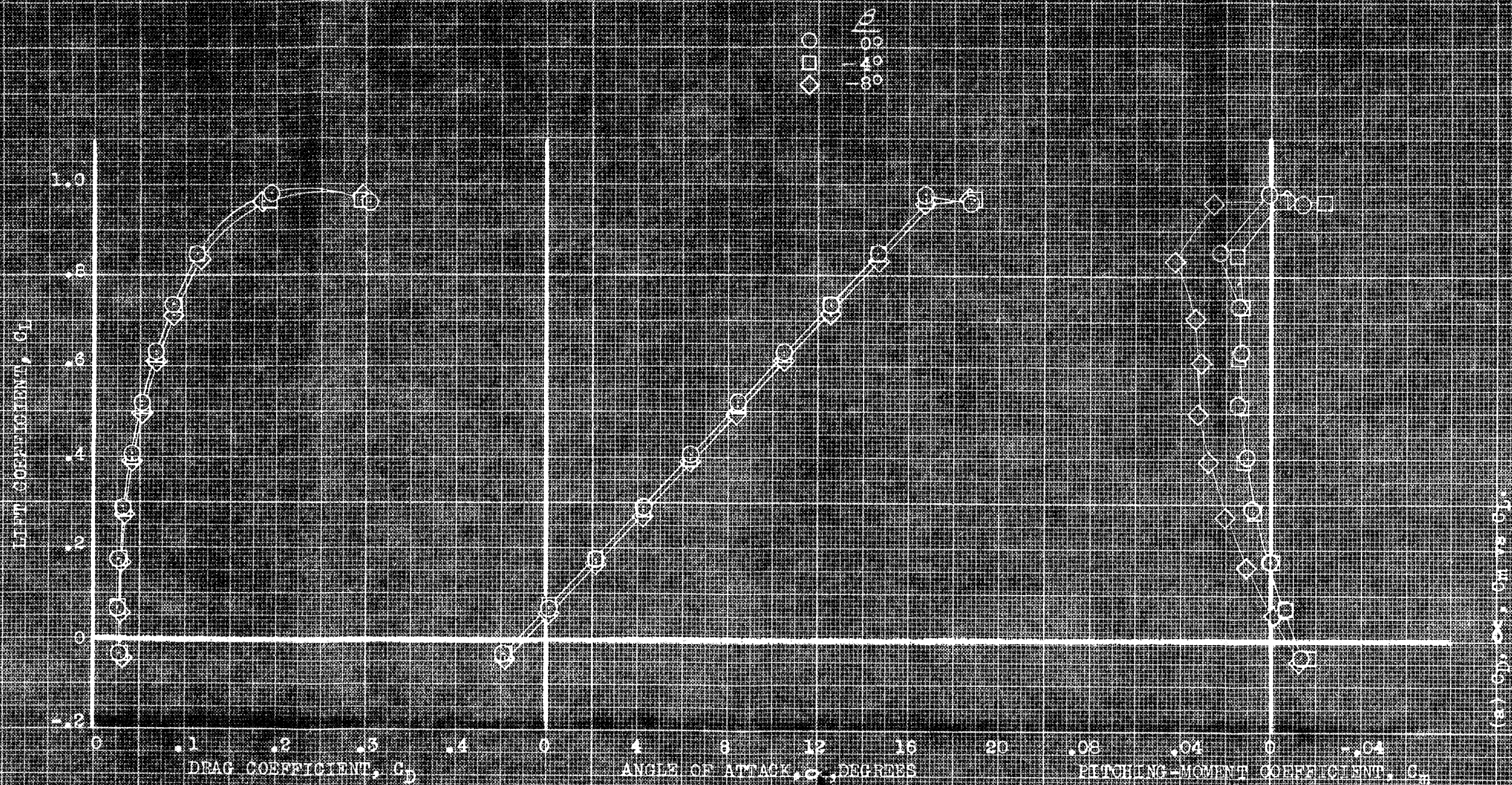
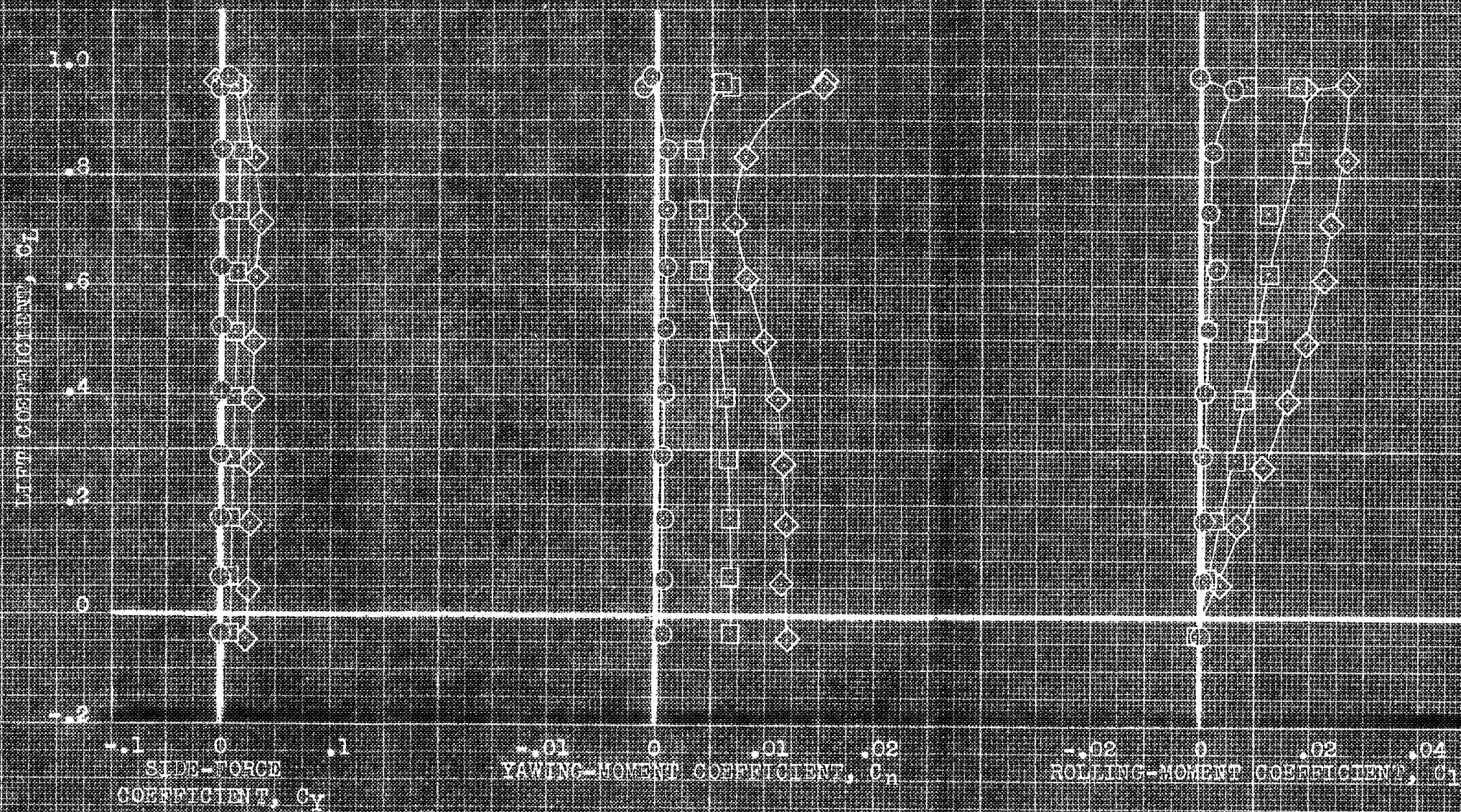


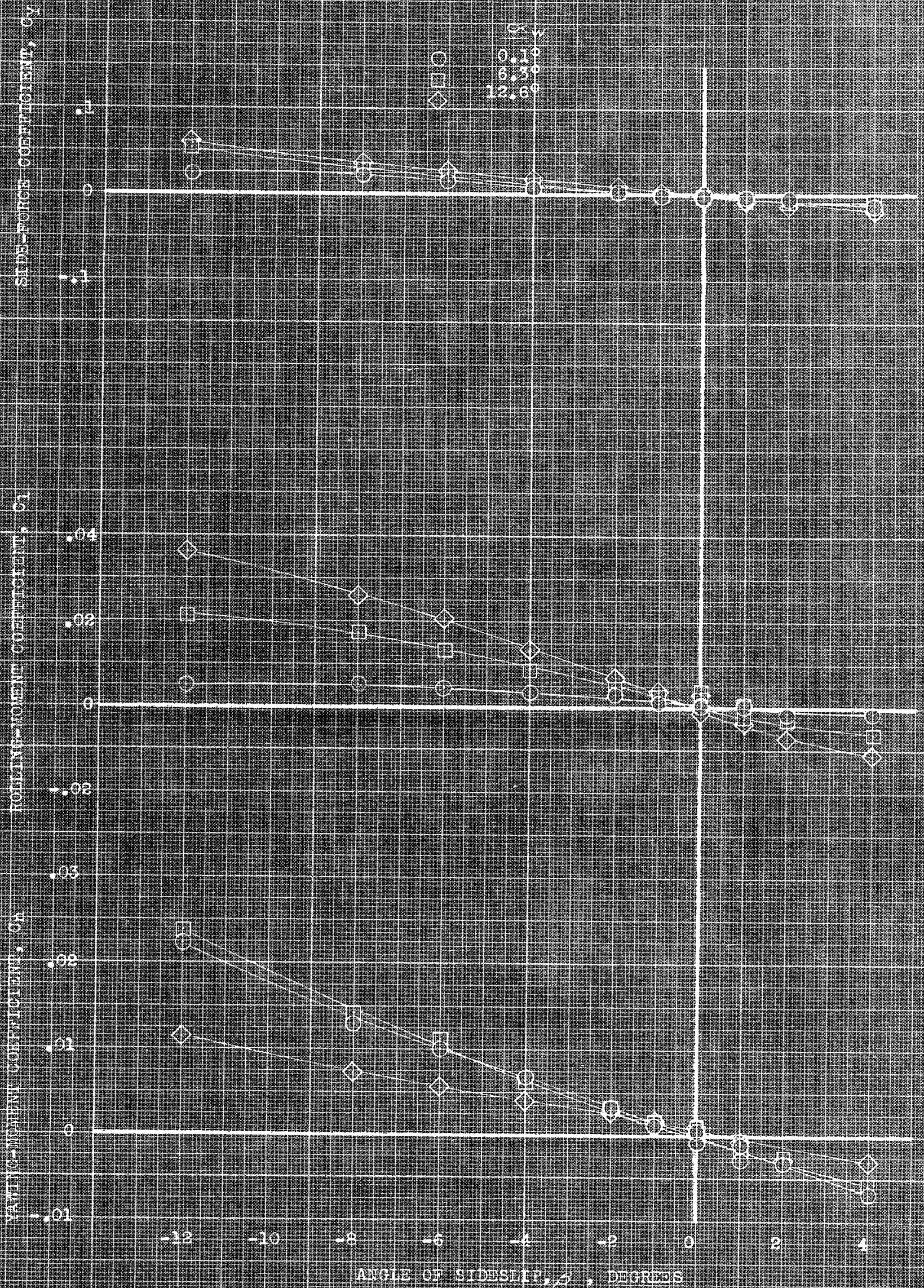
FIGURE 11. EFFECT OF THE MAIN OLEO-STRUT DOORS ON THE AERODYNAMIC CHARACTERISTICS OF THE MODEL IN FLIGHT WITH THE TAIL REMOVED. SEAR, DROOPED SLATS; MAIN FLAPS, 40°, l_w , 6°.





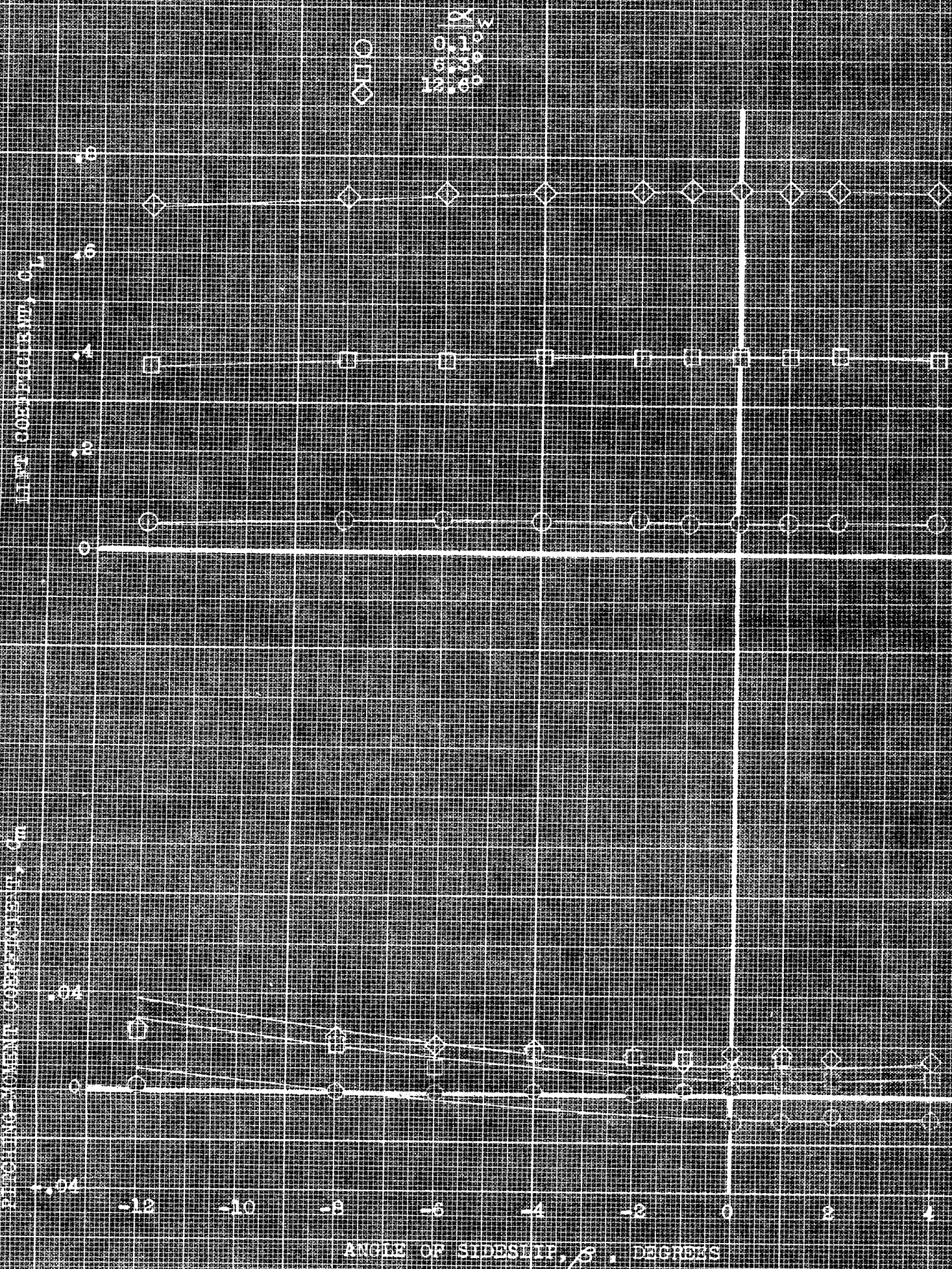
(b) C_Y , C_N , C_L vs C_L .

FIGURE 52. CONTINUED.



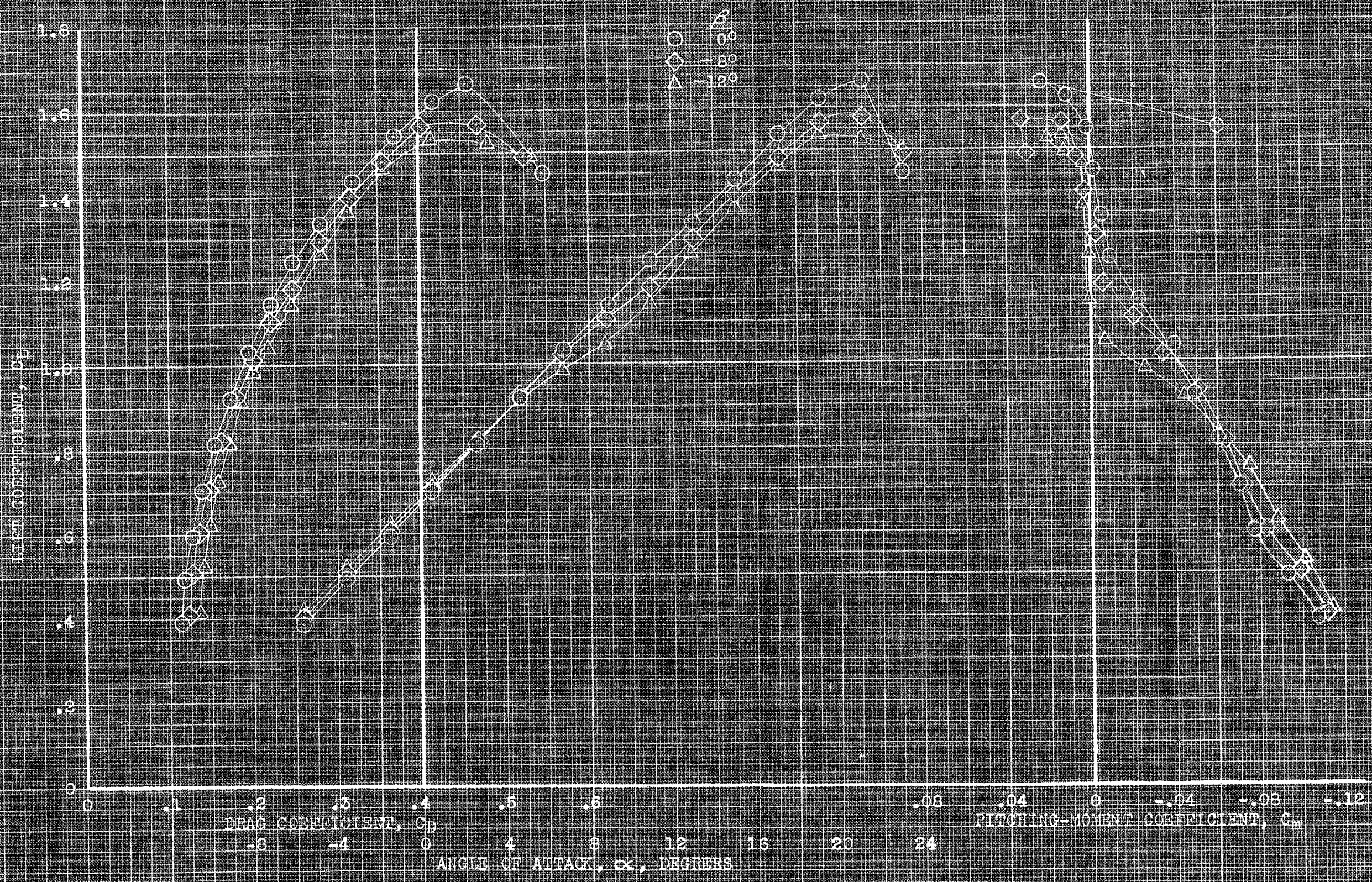
(a) C_y, C_1, C_n vs β

FIGURE 32.- AERODYNAMIC CHARACTERISTICS IN SIDESLIP OF THE MODEL WITH TAIL REMOVED AT VARIOUS ANGLES OF ATTACK. PLAIN WING; $\alpha_0, 0^\circ$.



(b) C_L , C_m vs. δ

FIGURE 27. - CONCLUDED

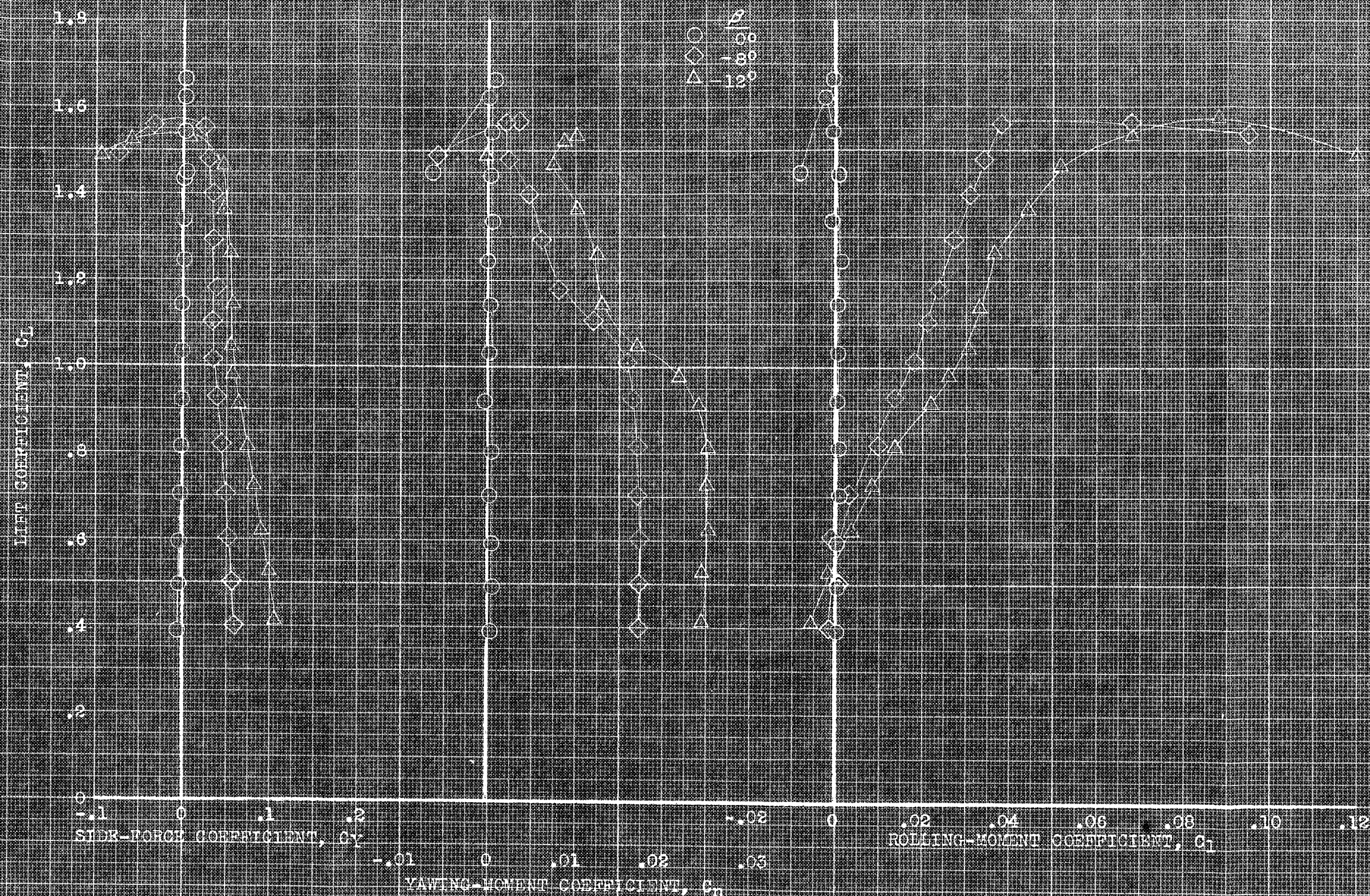


(a) C_L , C_D , C_m vs. α

FIGURE 5. - AERODYNAMIC CHARACTERISTICS IN PITCH OF THE MODEL WITH TAIL REMOVED AT VARIOUS ANGLES OF SIDESLIP. GEAR; PROPOSED SLATS; FLAT PLATE, 40° ; 1.0 , 6.0 .

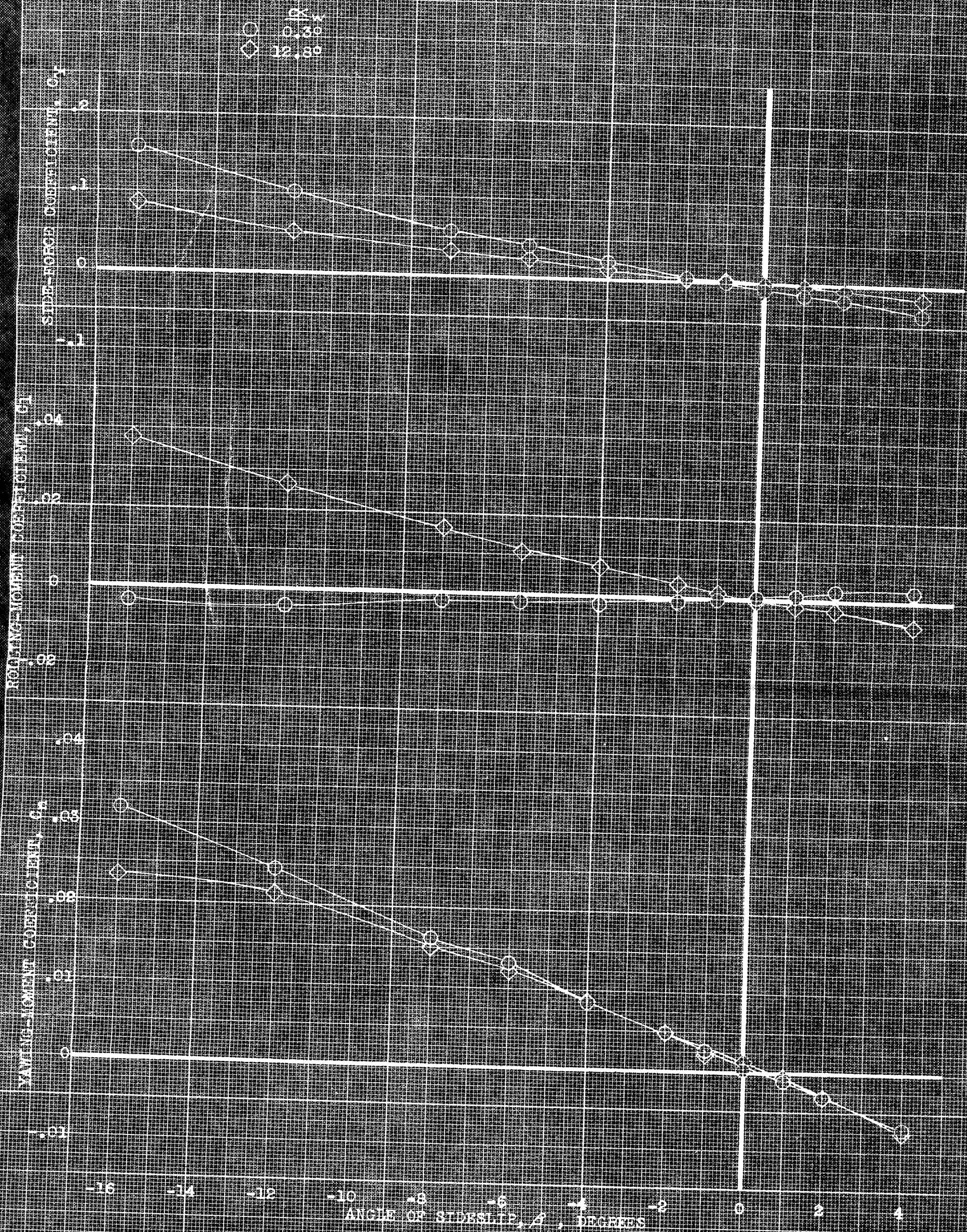
IDENTICAL

UNCLASSIFIED DOCUMENT FOR AIRCRAFT



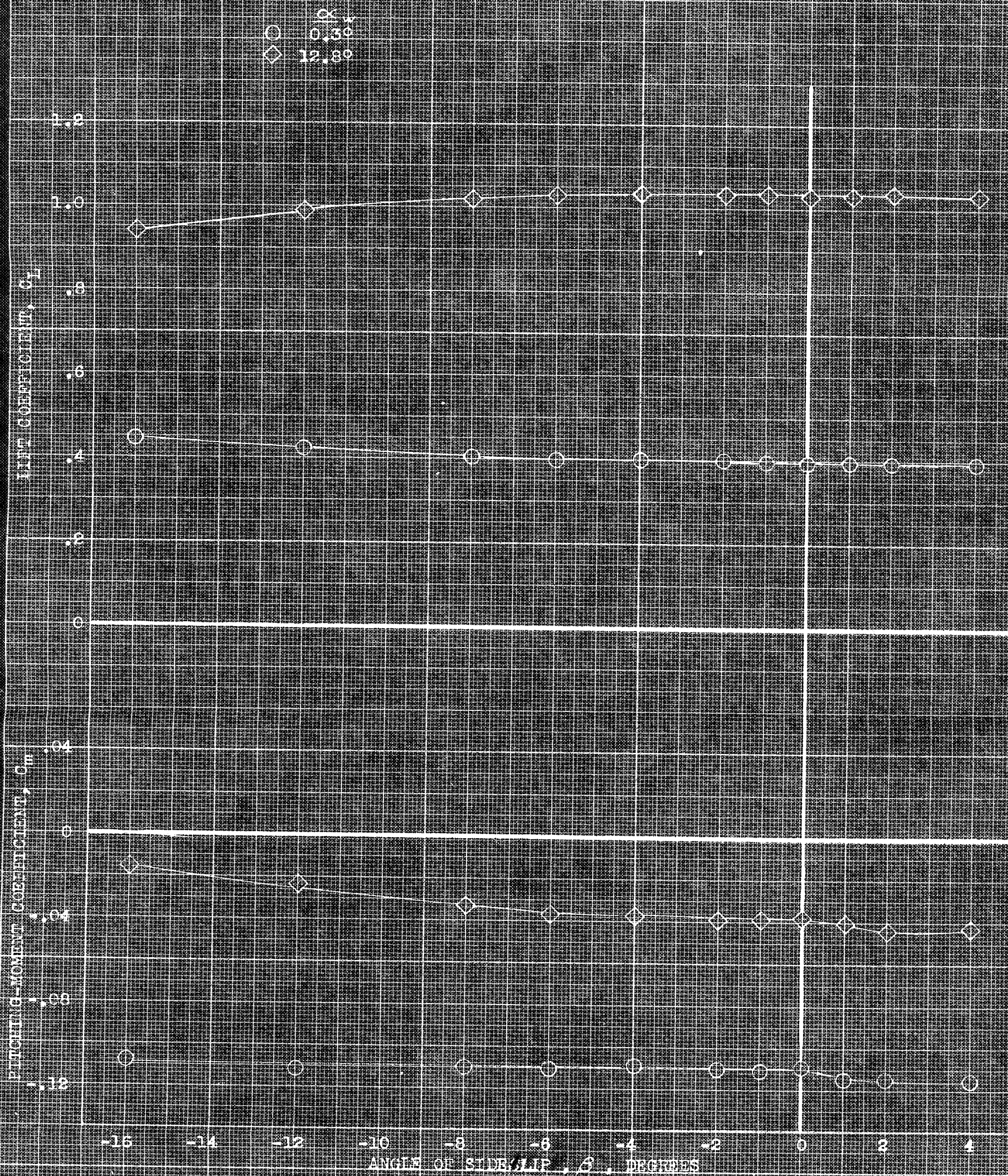
(b) C_Y , C_n , C_l vs C_L .

FIGURE 31. - CONCLUDED.



(a) C_Y, C_{lr}, C_n vs β

FIGURE 35.- AERODYNAMIC CHARACTERISTICS IN SIDESLIP OF THE MODEL WITH TAIL REMOVED AT VARIOUS ANGLES OF ATTACK. GEAR; DROOPED SLATS; PLAIN FLAPS, 40° ; $1.0, 60^\circ$.



(b) C_L , C_m vs. α

FIGURE 35.- CONCLUDED.

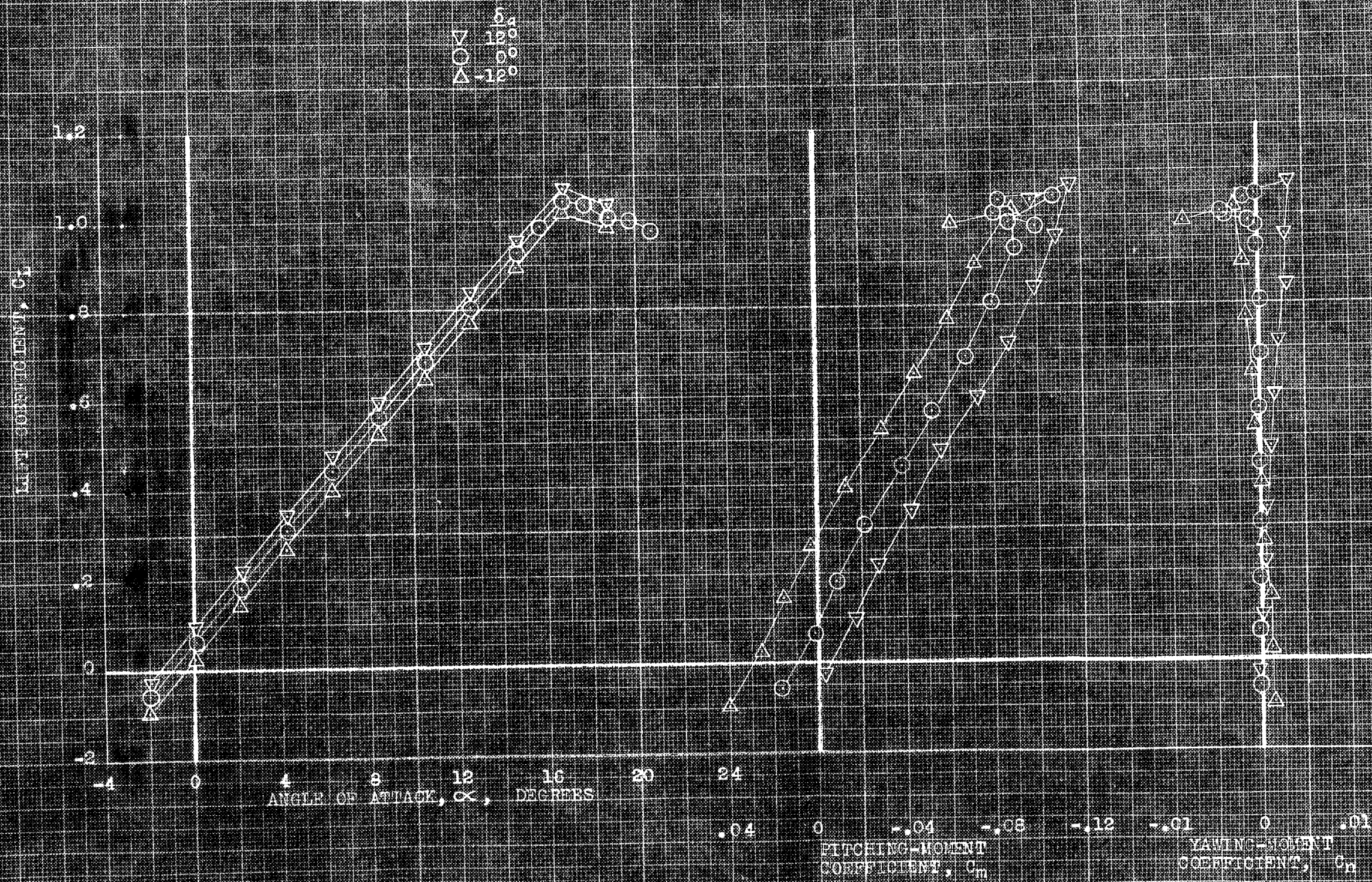
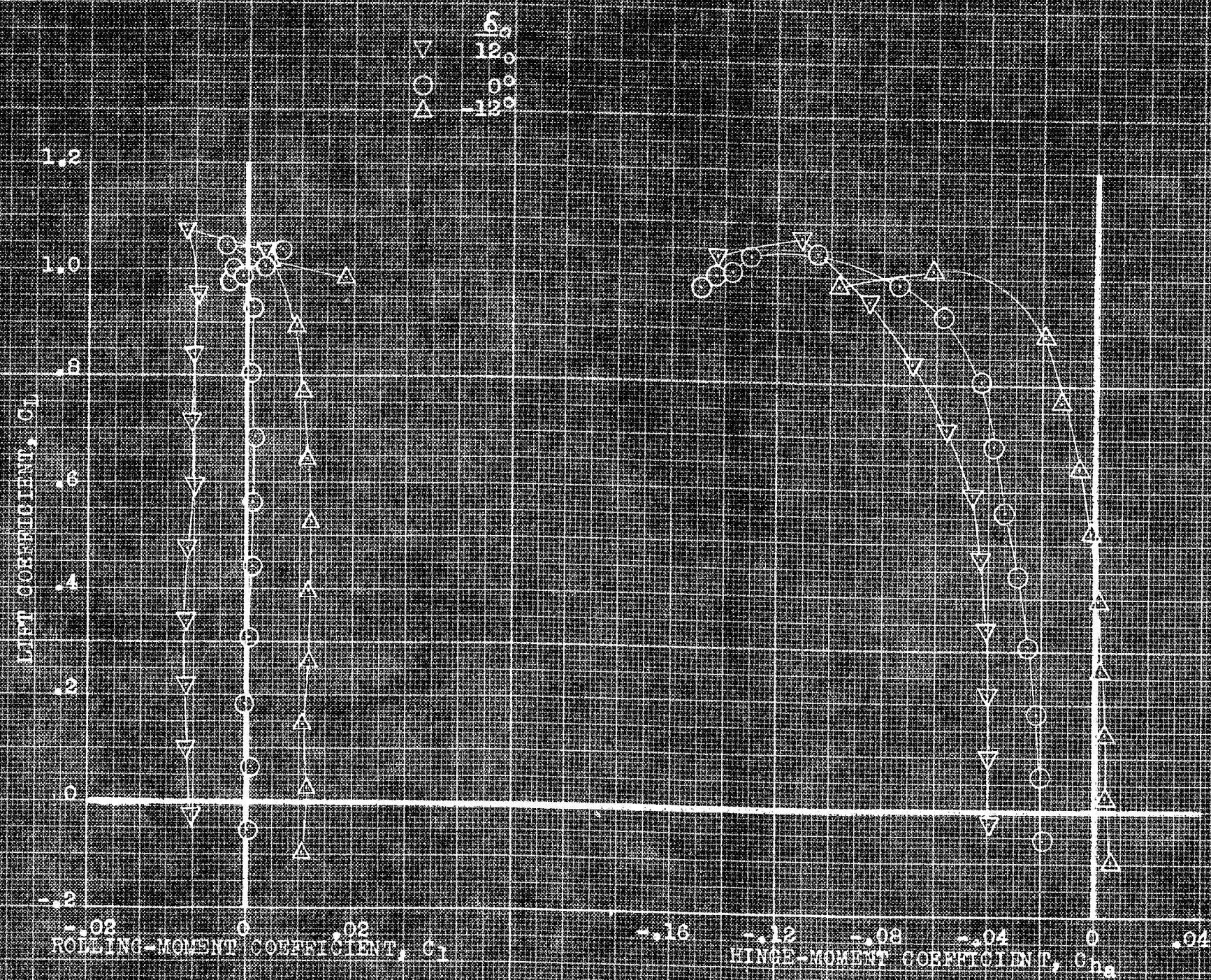


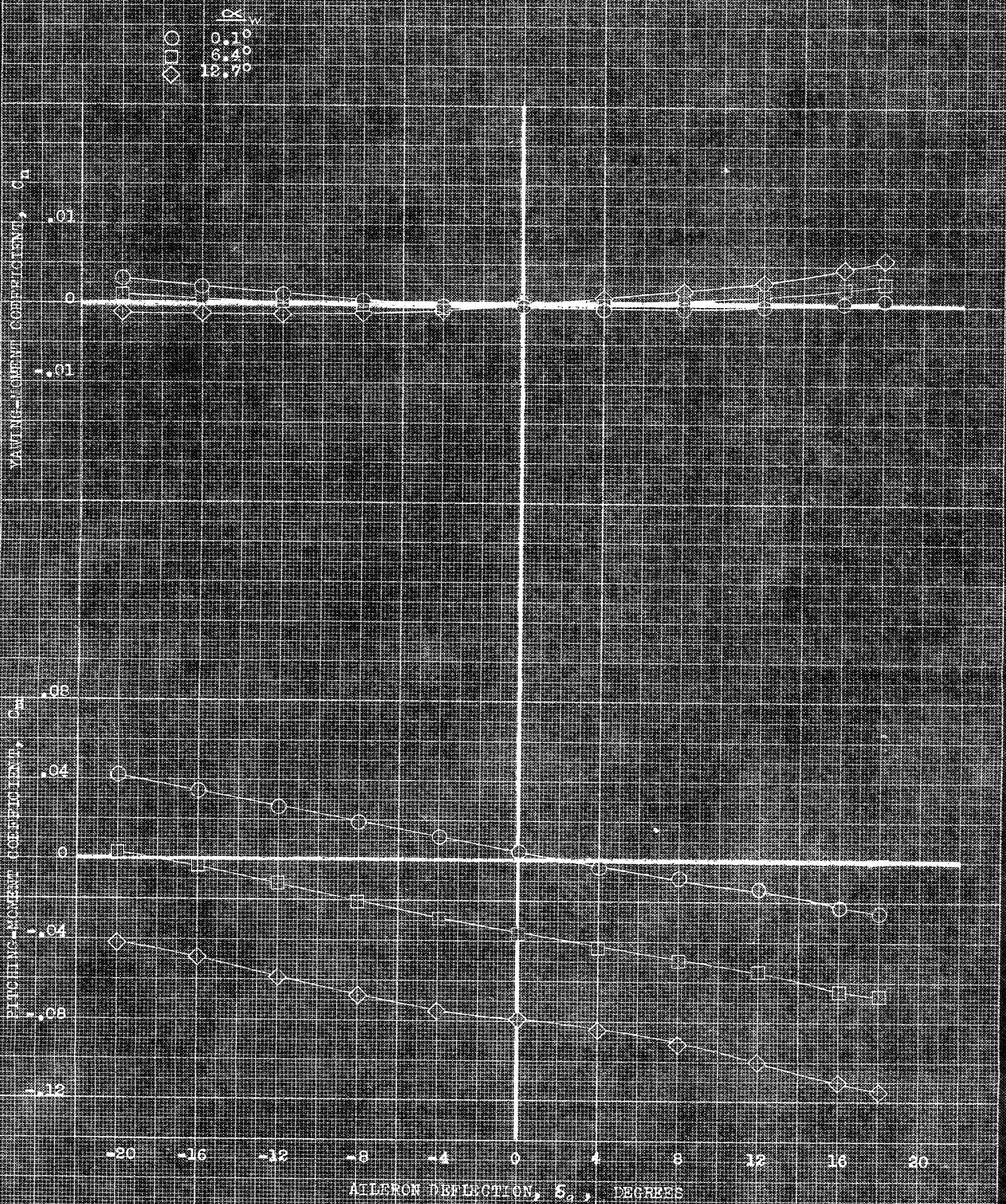
FIGURE 35. EFFECT OF FIXED DIRECTIONS OF THE RIGHT ALLERON ON THE AERODYNAMIC CHARACTERISTICS OF THE MODEL IN PITCH. PLAIN WING, $\delta = 0^\circ$.



(b) C_L , C_{hg} vs C_L

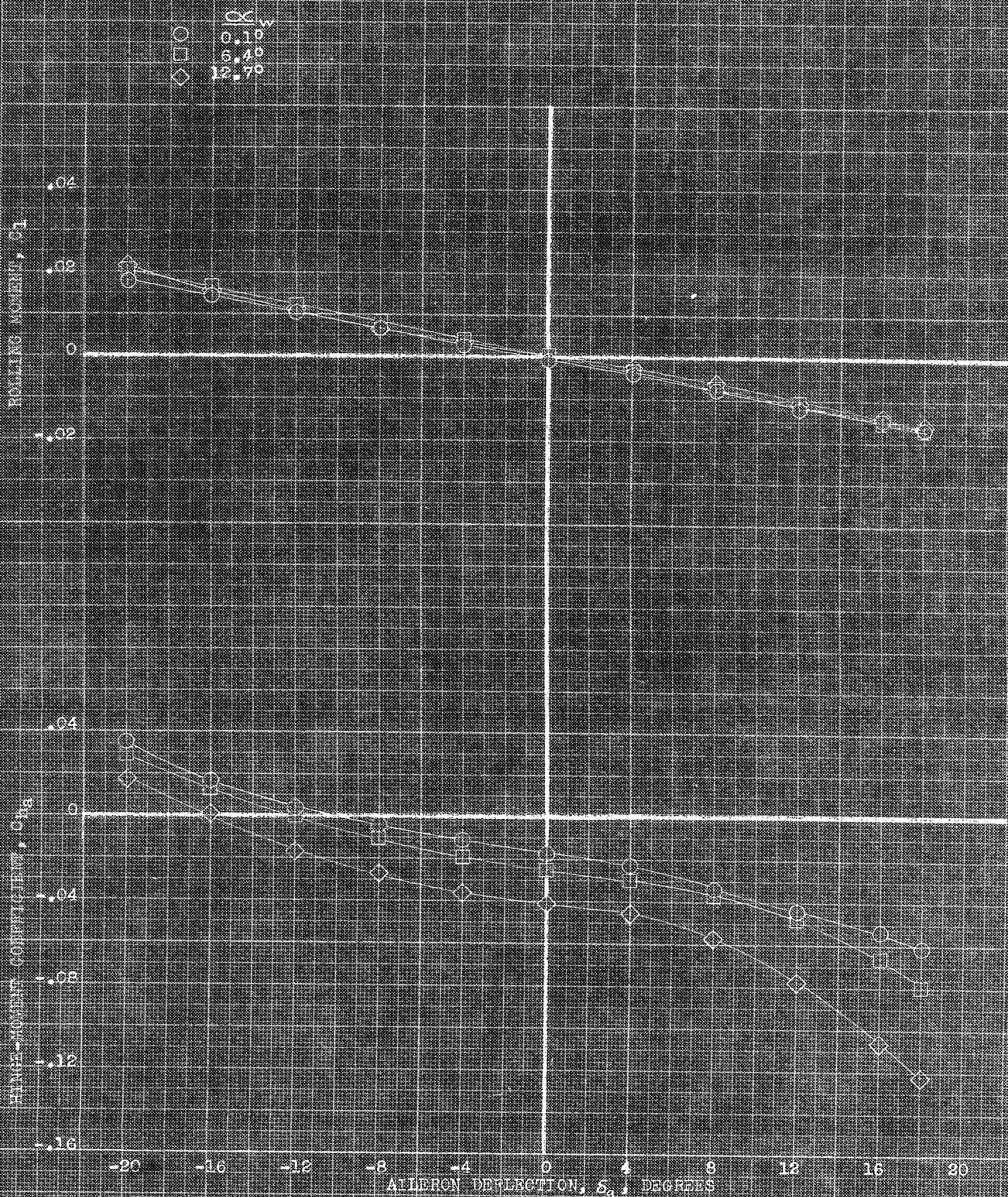
FIGURE 36.- CONCLUDED.

Copyright 1964 by the American Institute of Aeronautics and Astronautics, Inc.



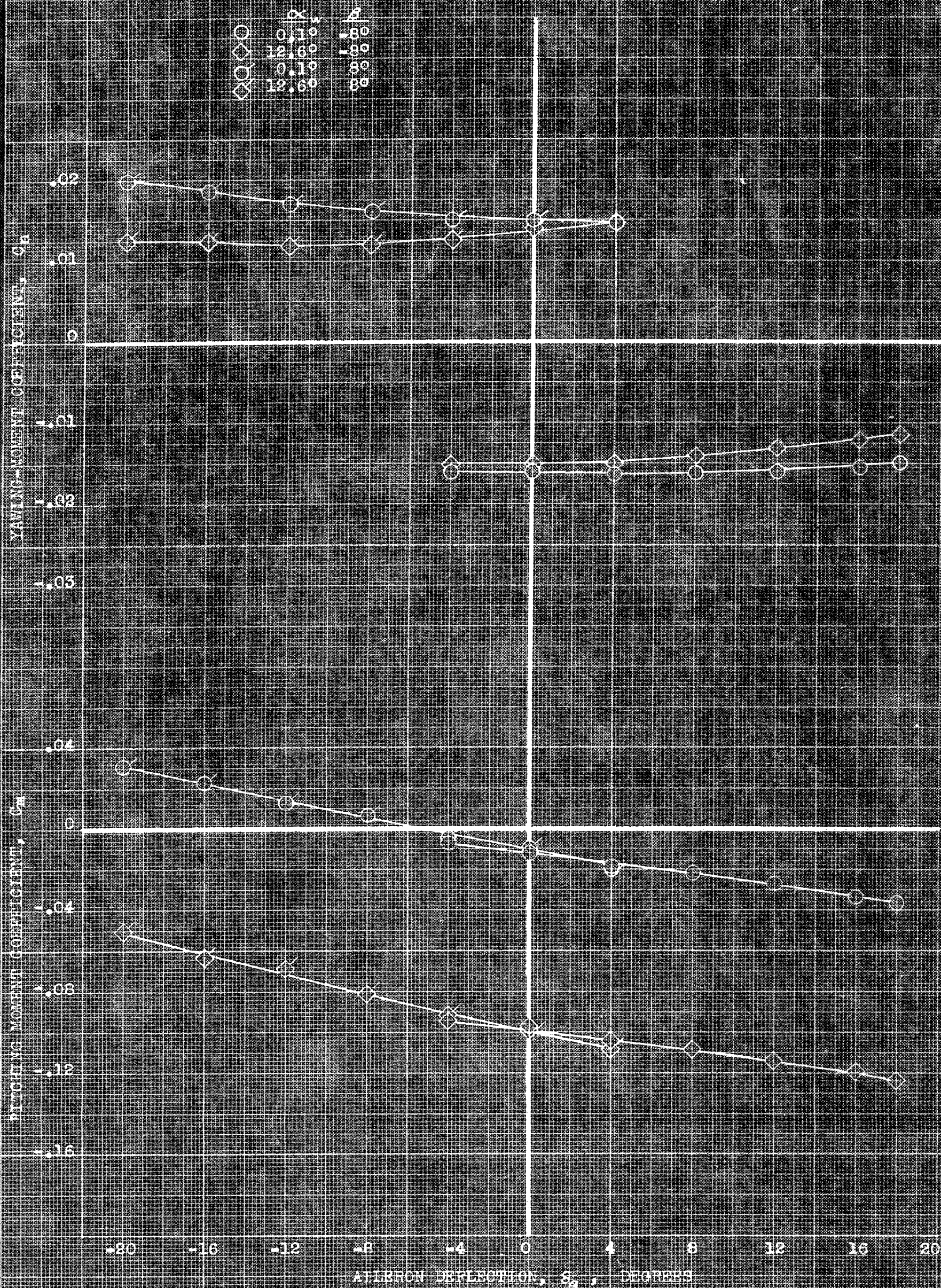
(a) C_n , C_m vs δ_a .

FIGURE 47.- VARIATION WITH RIGHT AILERON DEFLECTION OF THE AERODYNAMIC CHARACTERISTICS OF THE MODEL AT SEVERAL ANGLES OF ATTACK. PLAIN WINGS; $1_w, 0^\circ$.



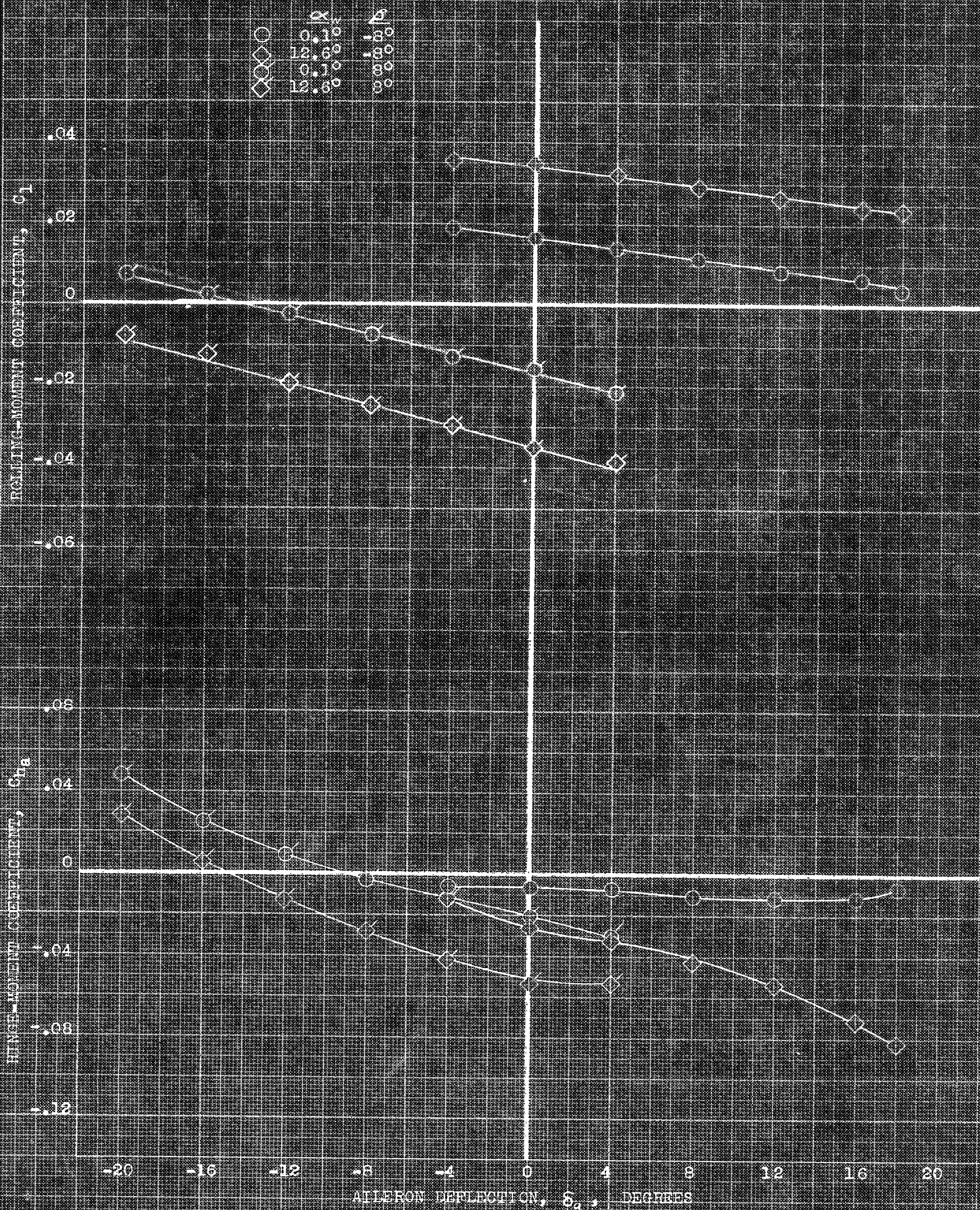
(b) C_l , $C_{h\alpha}$ vs δ_a .

FIGURE 27.- CONCLUDED.



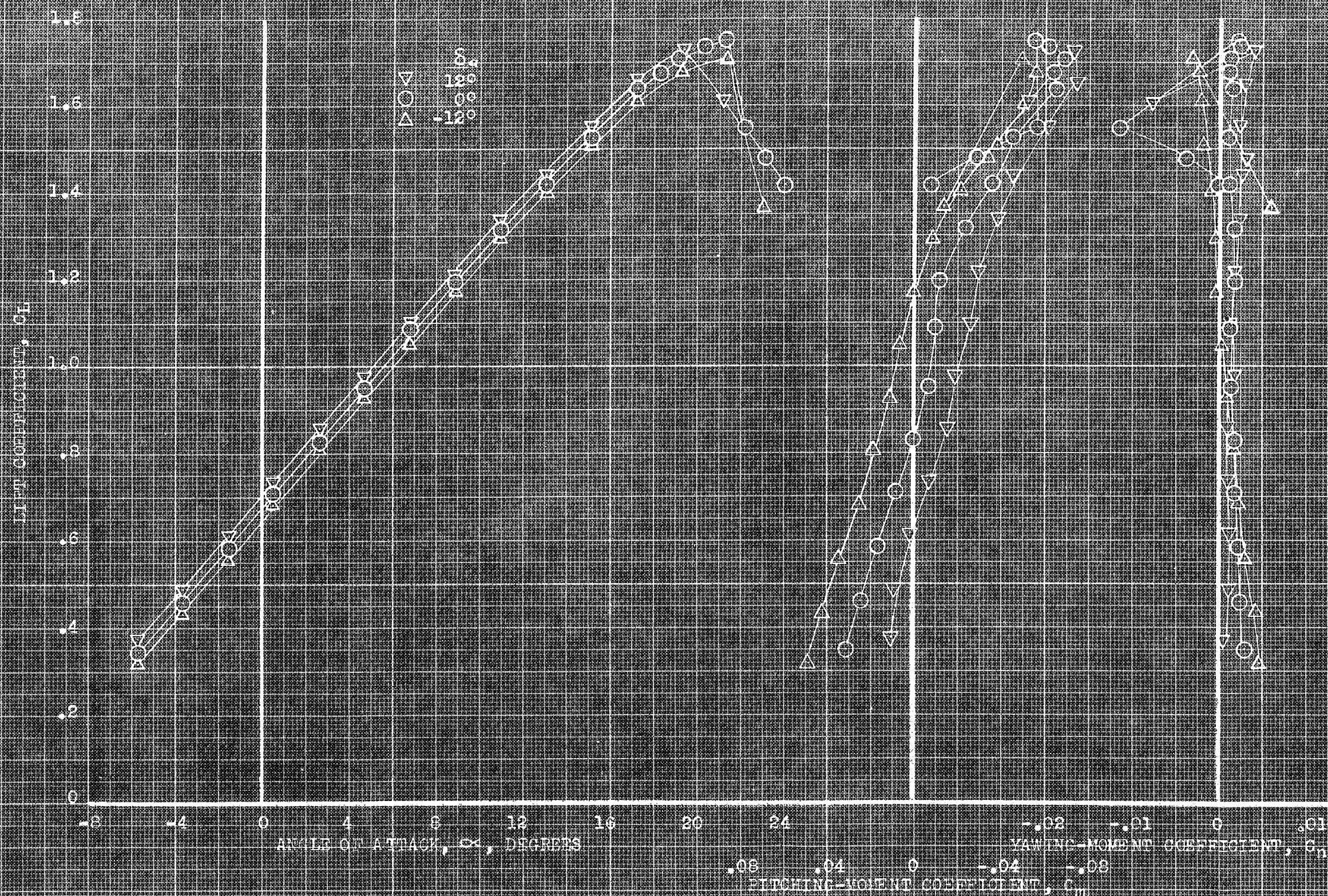
(a) C_L , C_m vs δ_a .

FIGURE 33. VARIATION WITH RIGHT AILERON DEFLECTION OF THE AERODYNAMIC CHARACTERISTICS OF THE MODEL IN SIDESLIP AT SEVERAL ANGLES OF ATTACK, PLAIN WING; α_w , 0°.



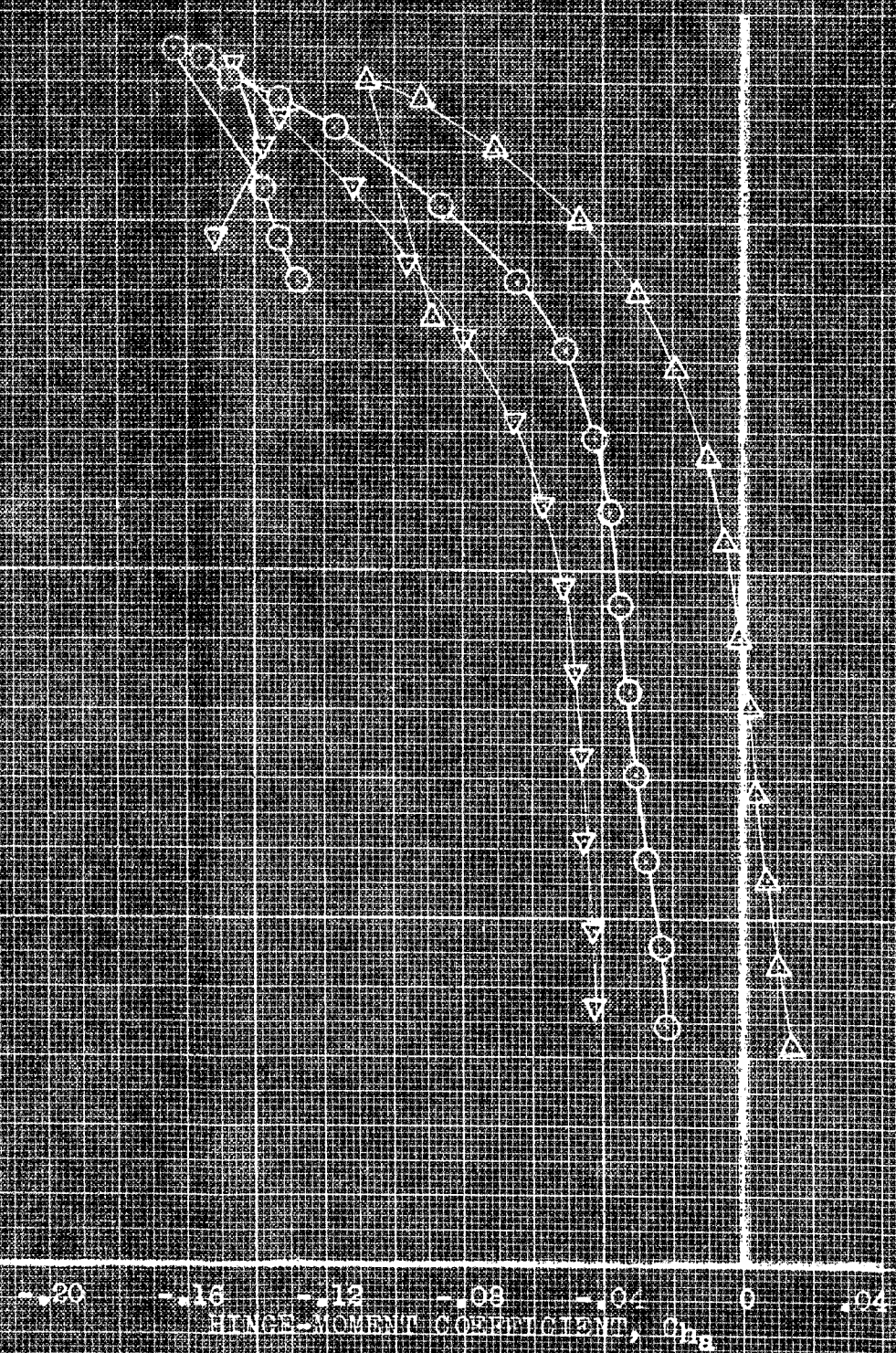
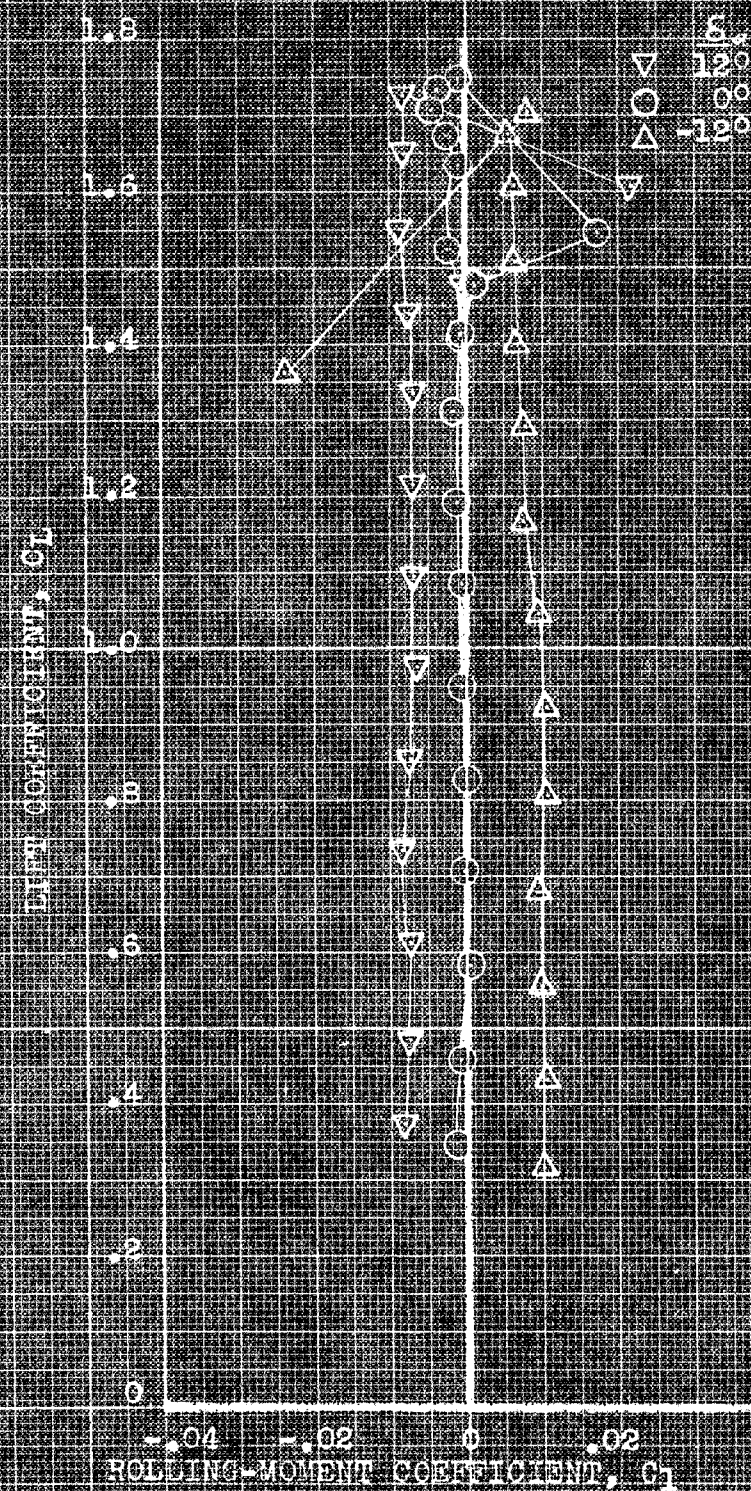
(b) C_l, C_{ha} vs δ_a .

FIGURE 38 - continued.

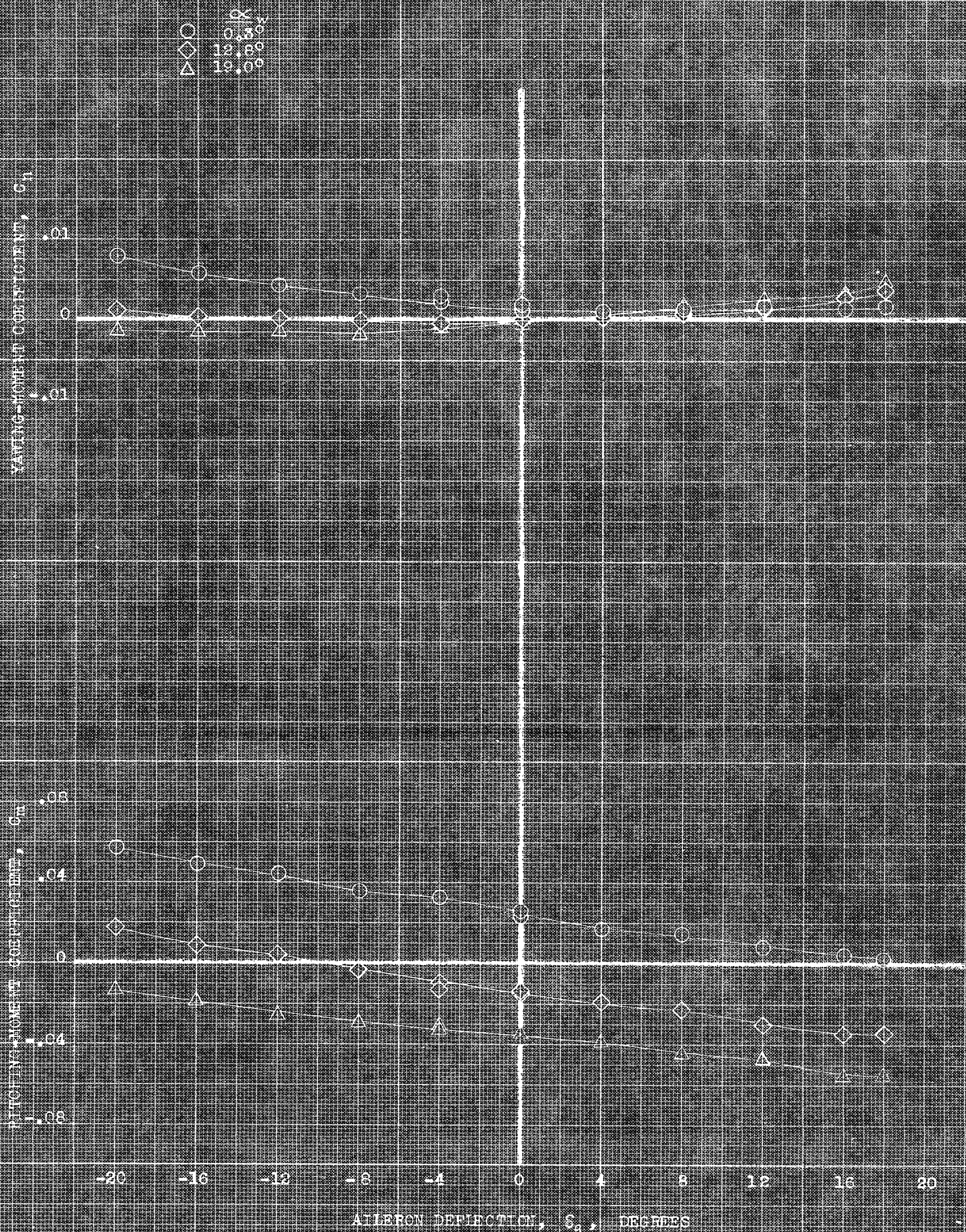


(a) α , C_m , C_n vs C_L .

FIGURE 2. EFFECT OF RECES CHARACTERISTICS ON THE PITCHING-MOMENT COEFFICIENT OF THE AIRCRAFT. CHARACTERISTICS OF THE MODEL IN PITCH: GEAR, DROOPED SLATS, PLAIN FLAPS, 40% CAMBER.

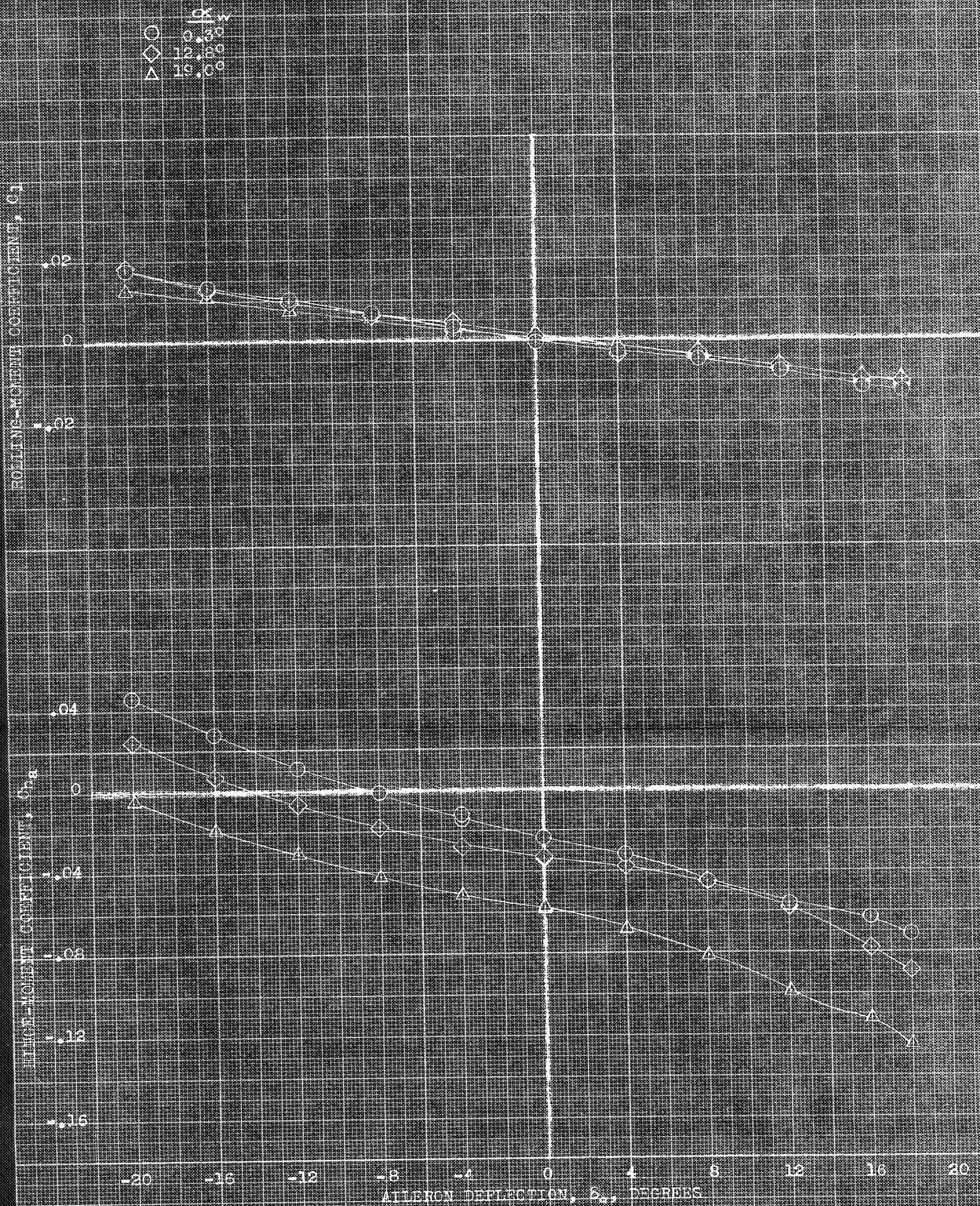


(b) C_L , C_{RL} vs C_L ,
Hinge-Moment Coefficient, C_{HB}



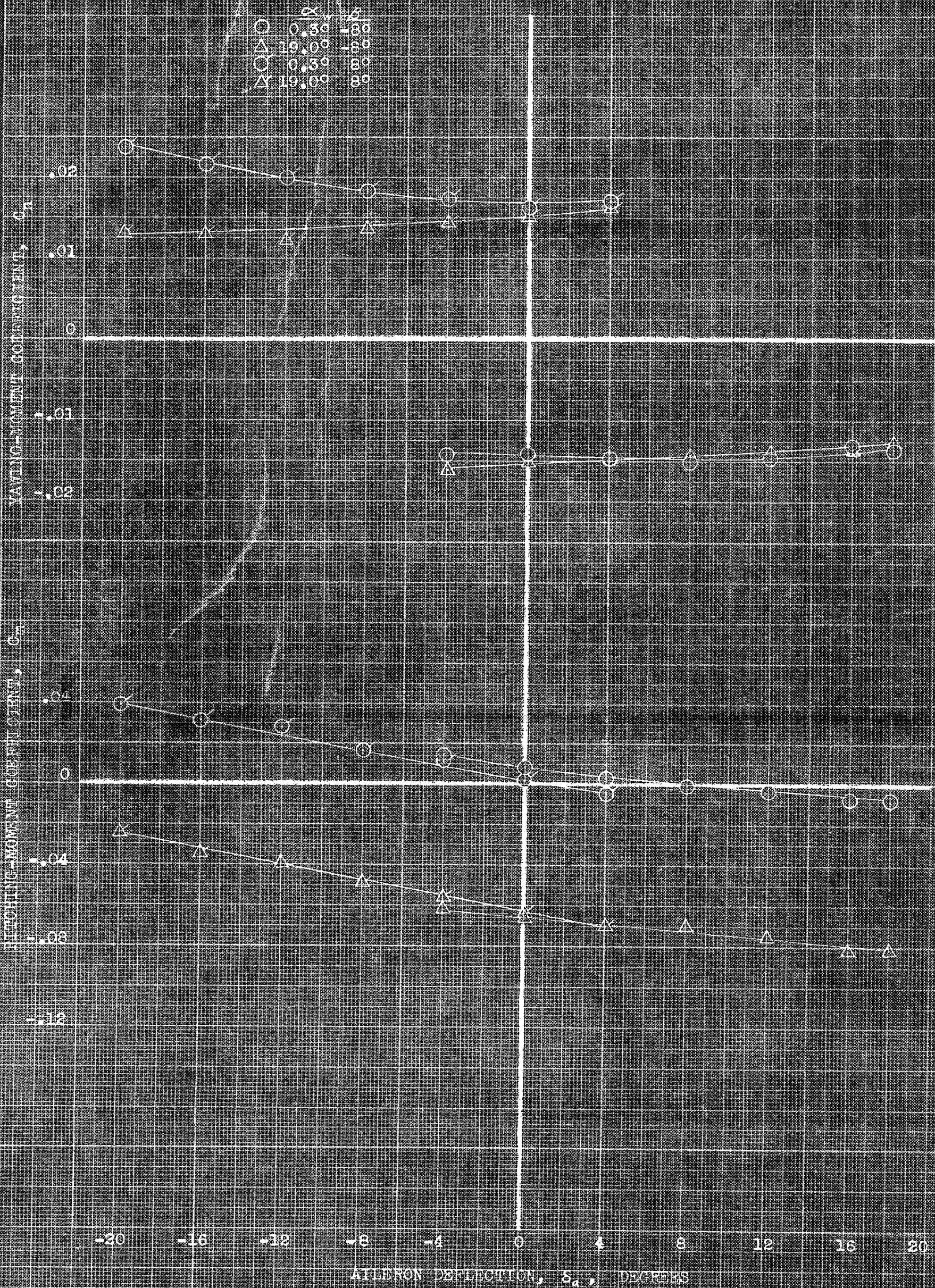
(a) C_n , C_m vs δ_a .

FIGURE 10.- VARIATION WITH RIGHT AILERON DEFLECTION OF THE AERODYNAMIC CHARACTERISTICS OF THE MODEL AT SEVERAL ANGLES OF ATTACK. GEAR; DROOPED SLATS; PLAIN FLAPS, 40°; α_w , 6°.



(b) C_L , C_{H_A} vs δ_a .

FIGURE 13. - CONCLUDED.



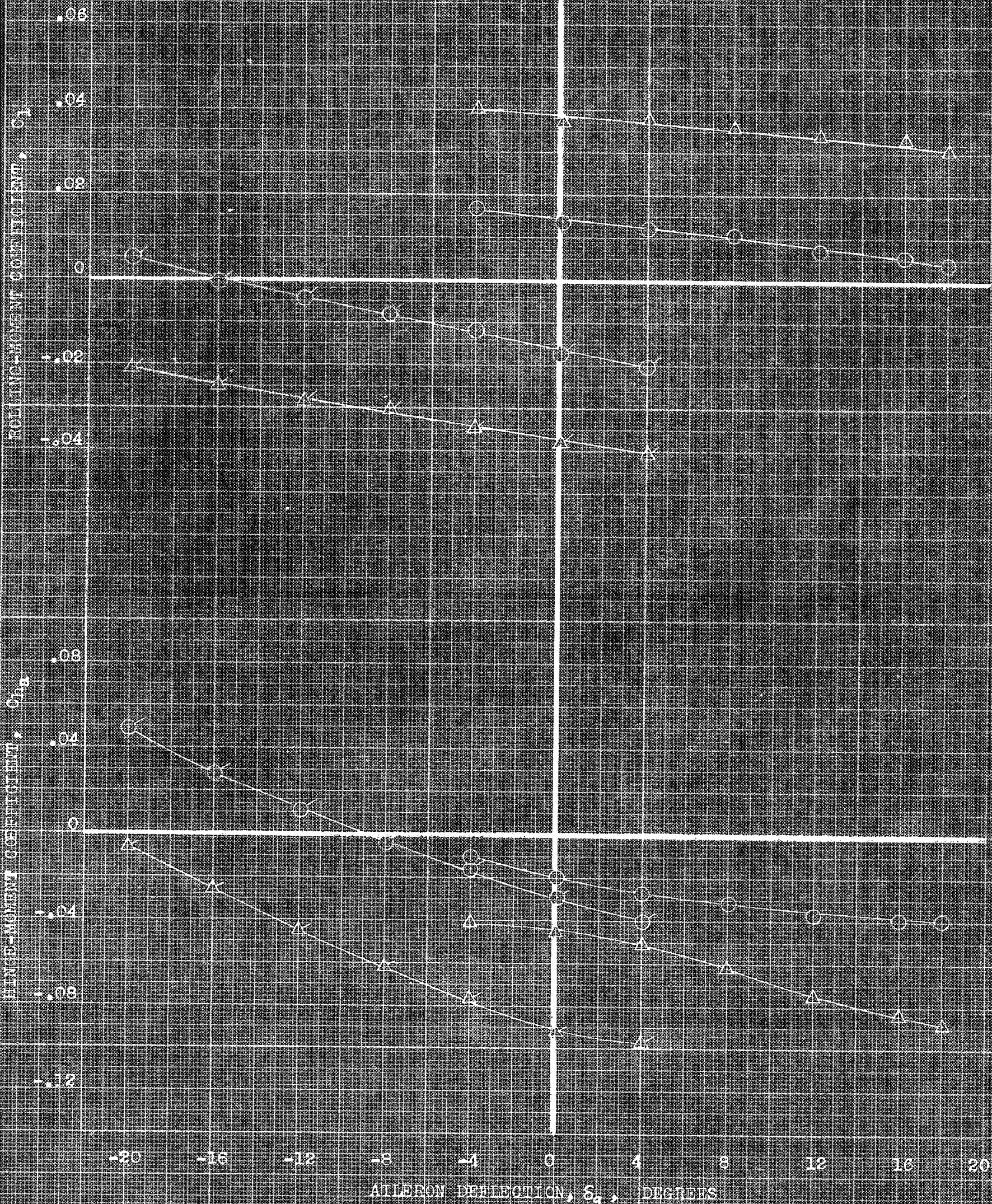
(a) C_n, C_m vs δ_a .

FIGURE 1. VARIATION WITH RIGHT AILERON DEFLECTION OF THE AERODYNAMIC CHARACTERISTICS OF THE MODEL IN SIDESLIP AT SEVERAL ANGLES OF ATTACK. GEAR; DROOPED SLATS; PLAIN FLAPS, 40°; i_w , 6°.

CONFIDENTIAL

NATIONAL ADVISORY COMMITTEE FOR AERONAUTICS

	α_{sw}	β
○	0.50	-80
△	19.00	-80
○	0.50	80
△	19.00	80



(b) C_{h1}, C_{h2} vs δ_a

FIGURE 11.- CONCLUDED.

CONFIDENTIAL
NATIONAL ADVISORY COMMITTEE FOR AERONAUTICS

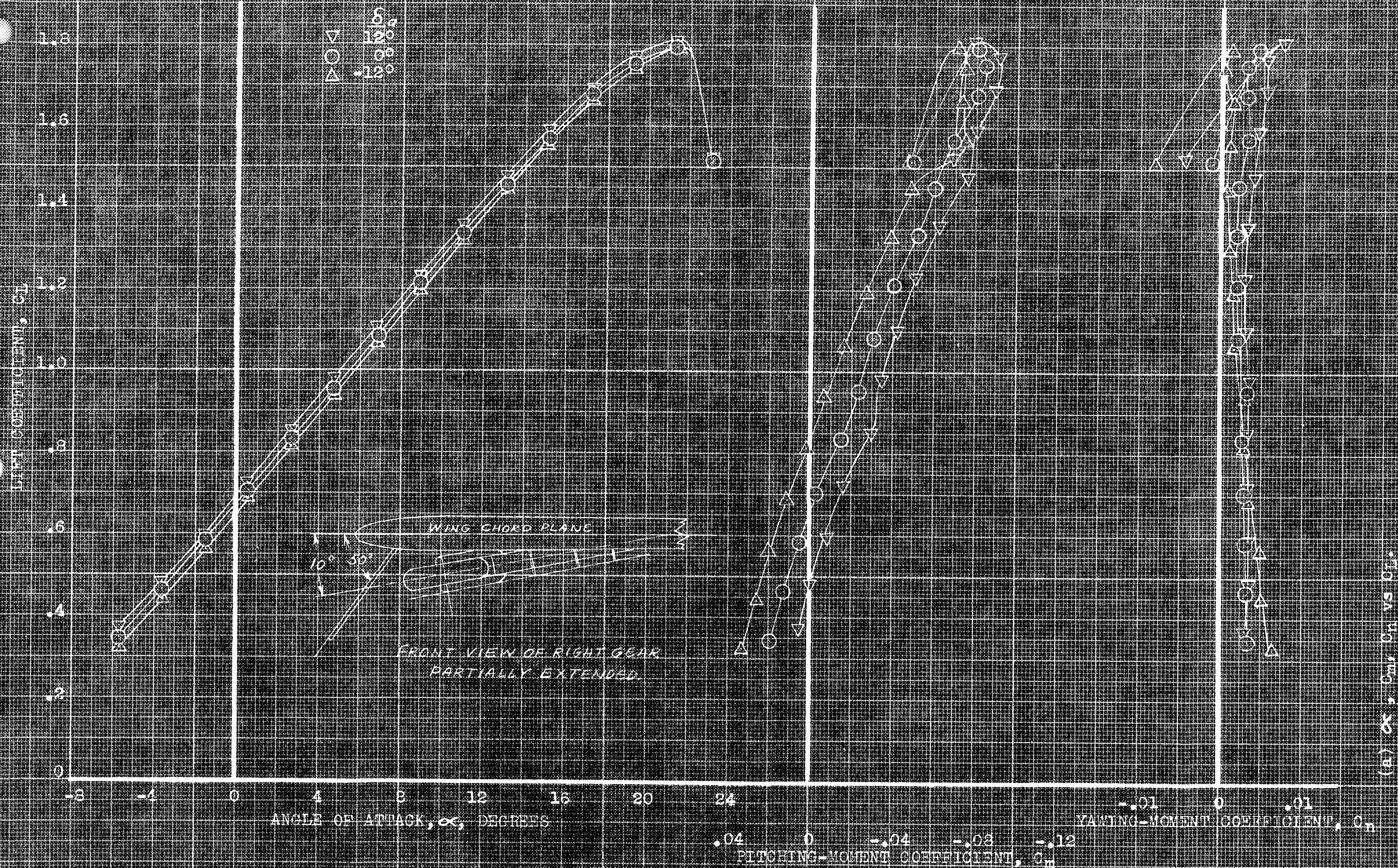
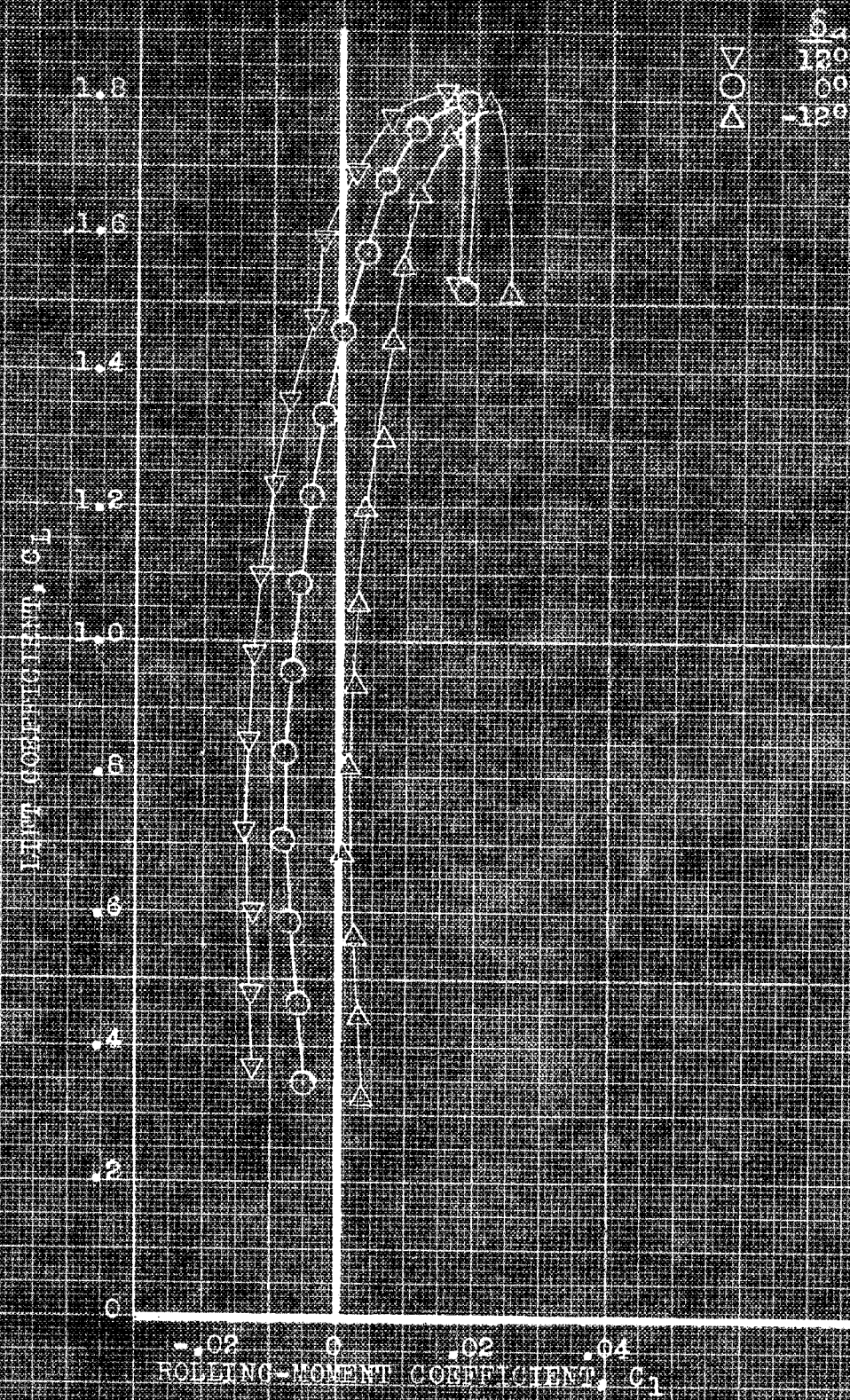


FIGURE 12. EFFECT OF FIXED DEFLECTIONS OF THE RIGHT AIRFOIL ON THE AERODYNAMIC CHARACTERISTICS OF THE MODEL IN PITCH. RIGHT GEAR PARTIALLY EXTENDED; BROOKLYN STARS; PLAIN FLAPS; 400; 1.5.

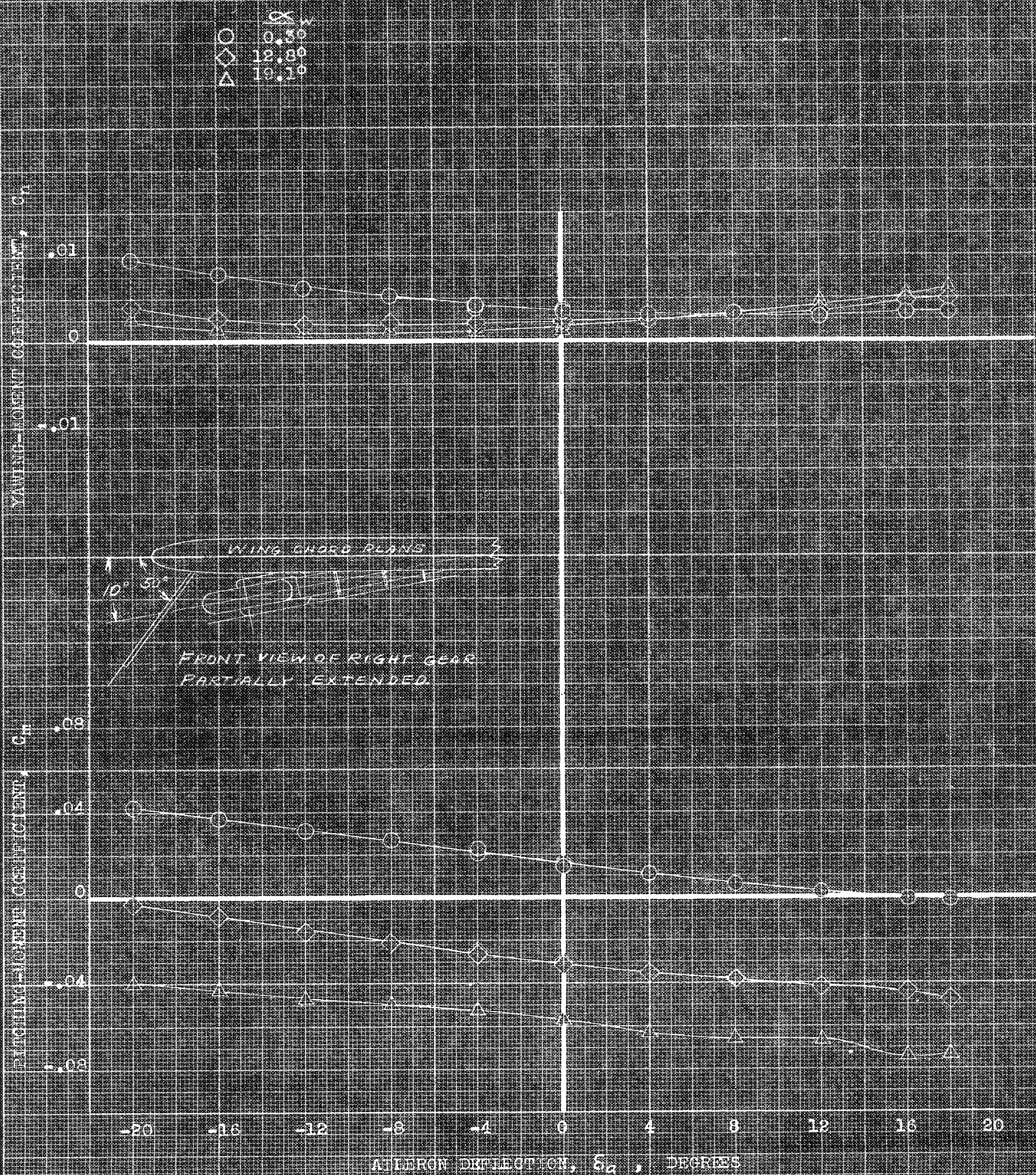
CONFIDENTIAL

NATIONAL AERONAUTICS COMMITTEE FOR AERONAUTICS



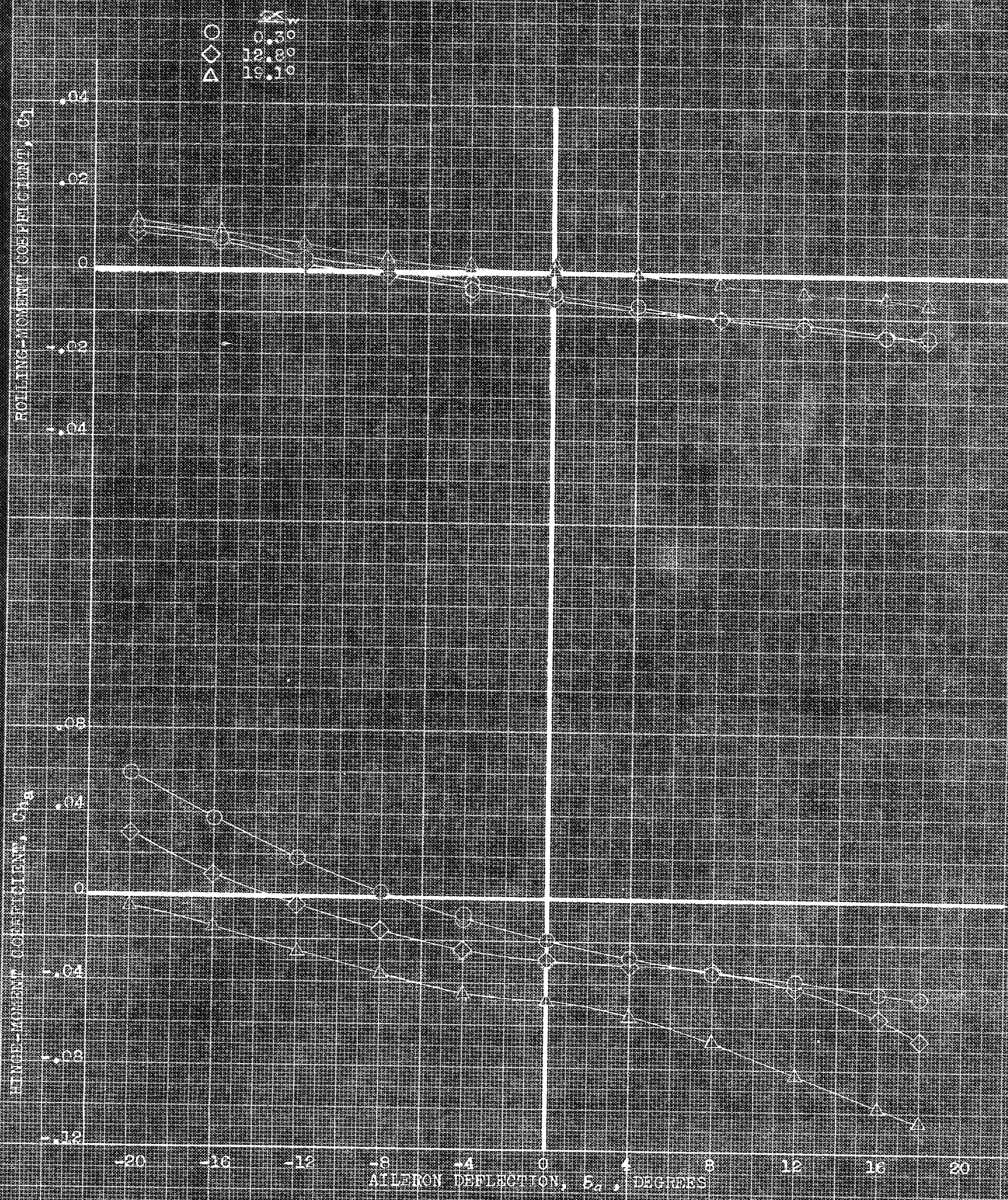
(b) C_L , C_H vs C_L .

FIGURE 10.7. CONTINUED.



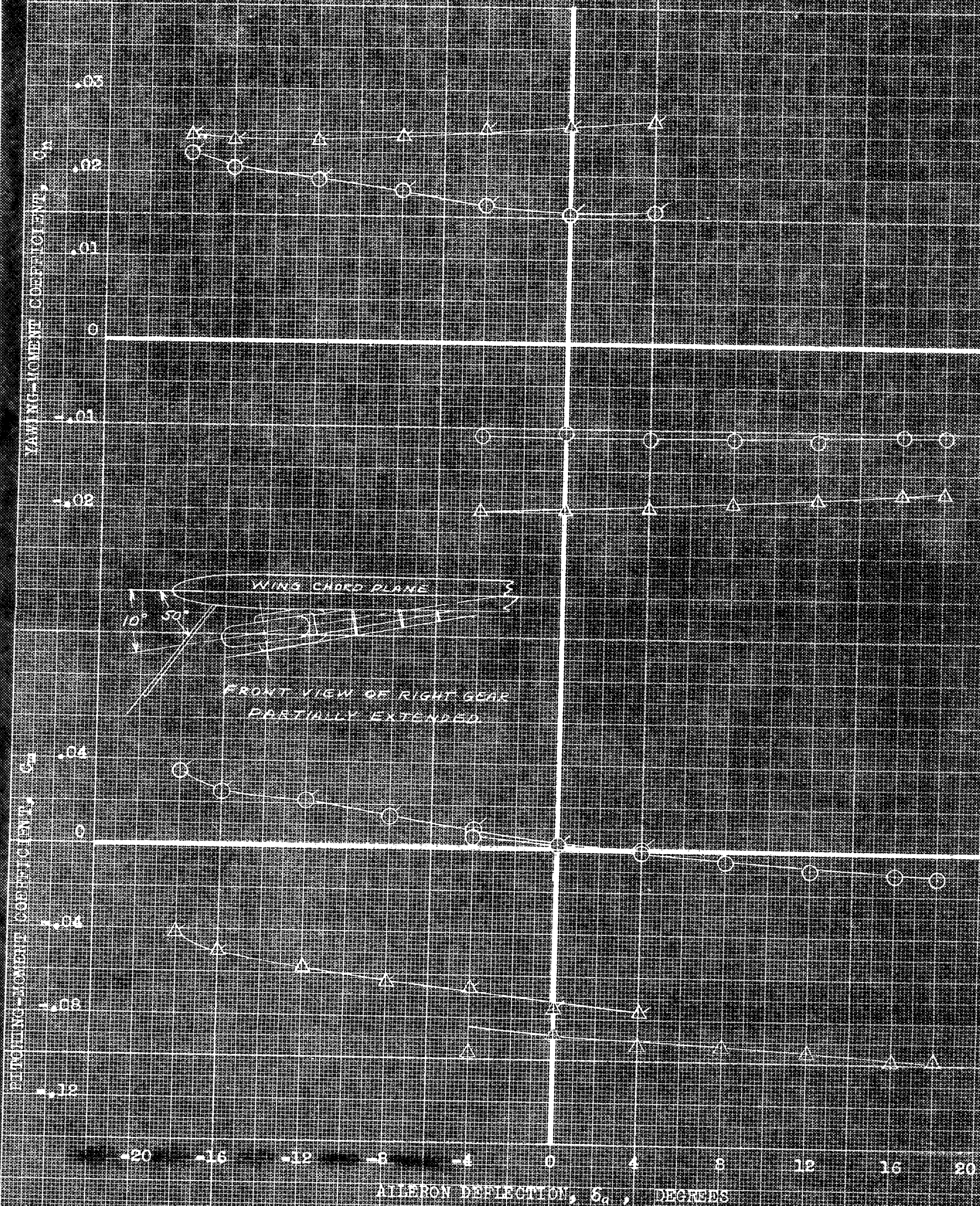
(a) C_y, C_r vs δ_a

FIGURE 12. VARIATION WITH RIGHT AILERON DEFLECTION OF THE AERODYNAMIC CHARACTERISTICS OF THE MODEL AT SEVERAL ANGLES OF ATTACK, RIGHT GEAR PARTIALLY EXTENDED; DROOPED SLATS; FLAP FLAPS, 40° ; $i_w, 6^\circ$.



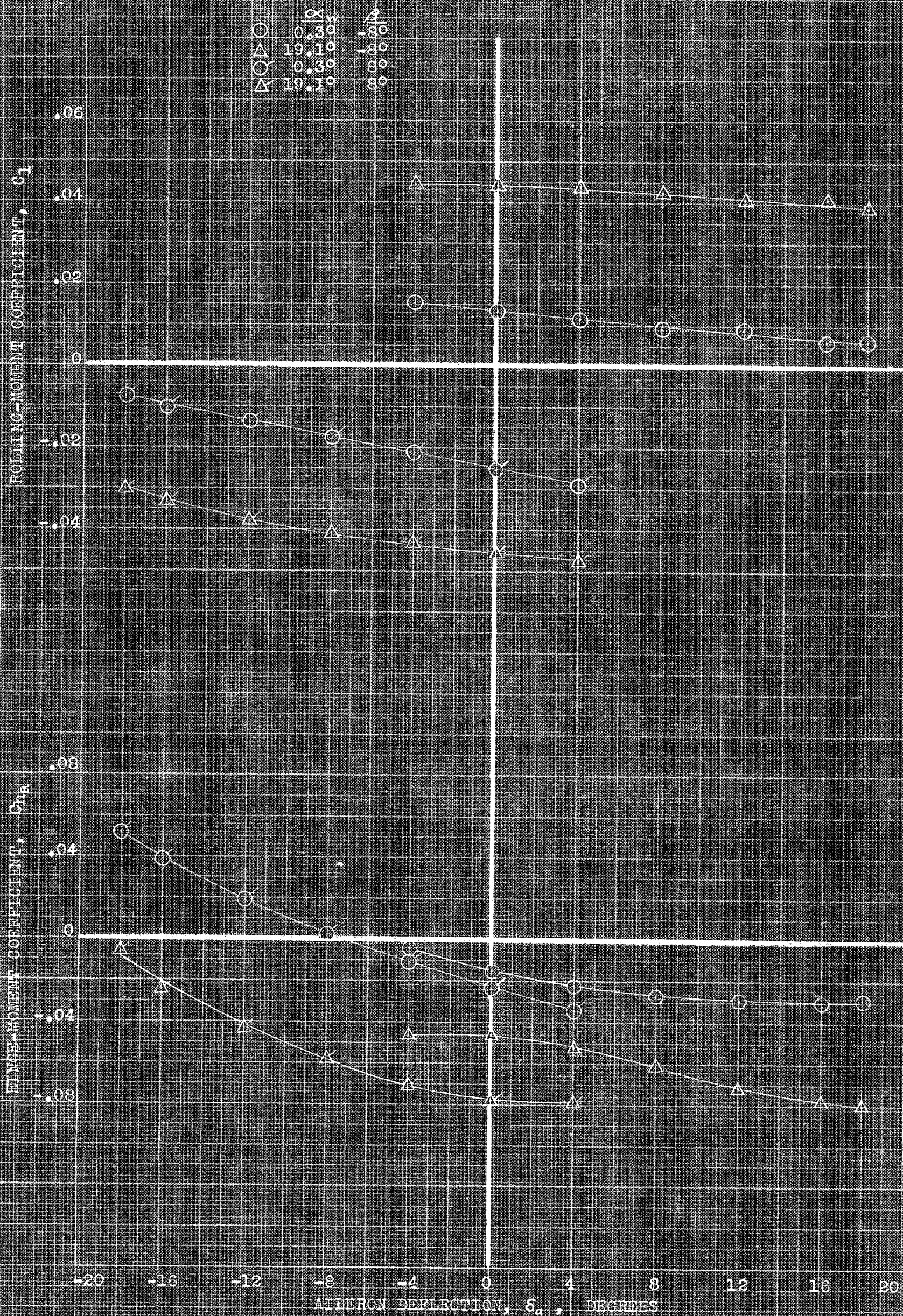
(b) C_l , C_{h_a} vs δ_a .
 FIGURE 16. - CONCLUDED.

	α_w	β
○	0.30°	-80
△	19.10°	-80
○	0.30°	80
△	19.10°	80



(a) C_y, C_m vs δ_a .

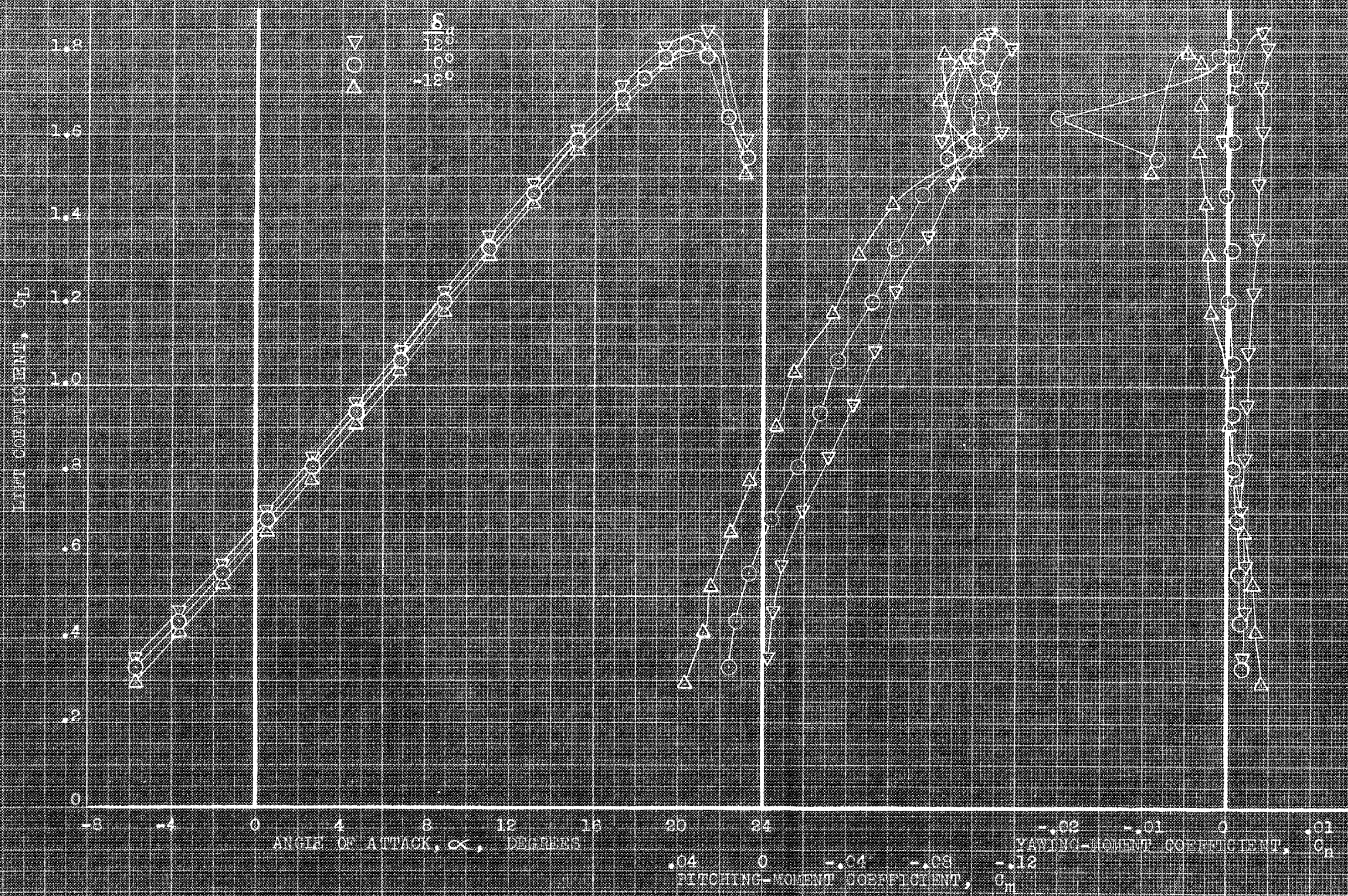
FIGURE 1. VARIATION WITH RIGHT AILERON DEFLECTION OF THE AERODYNAMIC CHARACTERISTICS OF THE MODEL IN SIDESLIP AT SEVERAL ANGLES OF ATTACK, RIGHT GEAR PARTIALLY EXTENDED; DROOPED STATS; PLAIN FLAPS, 40°; 1, 6°.



(b) C_l, C_{ha} vs δ_a .

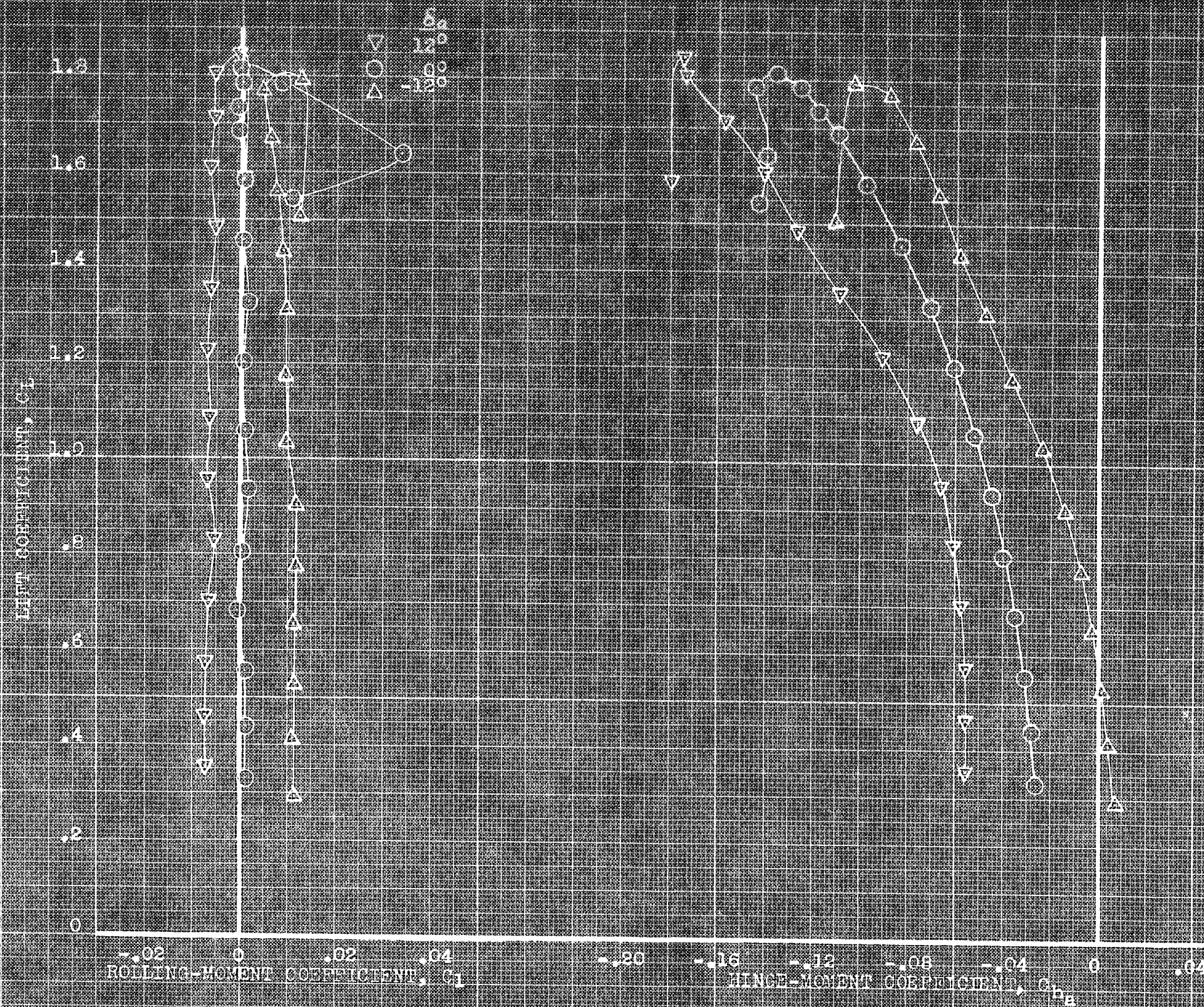
FIGURE 1. - CONCLUDED.

CONFIDENTIAL
NATIONAL ADVISORY COMMITTEE FOR AERONAUTICS

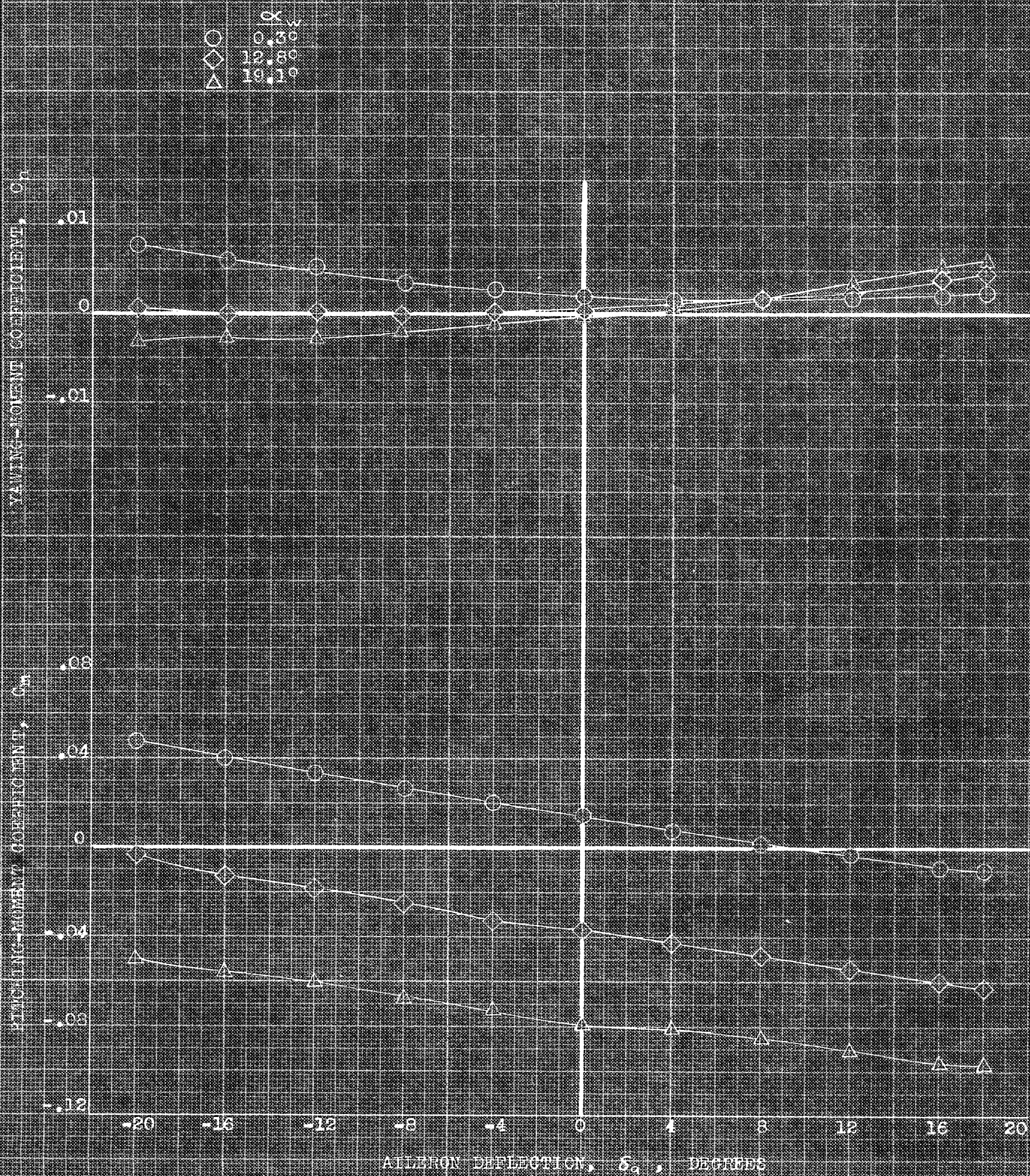


(a) α , C_m , C_n vs C_L .

FIGURE 1. - EFFECT OF FIXED DEFLECTIONS OF THE RIGHT ALLECON ON THE AERODYNAMIC CHARACTERISTICS OF THE MODEL IN PITCH. DROOPED FLAPS, 40°, 60°.

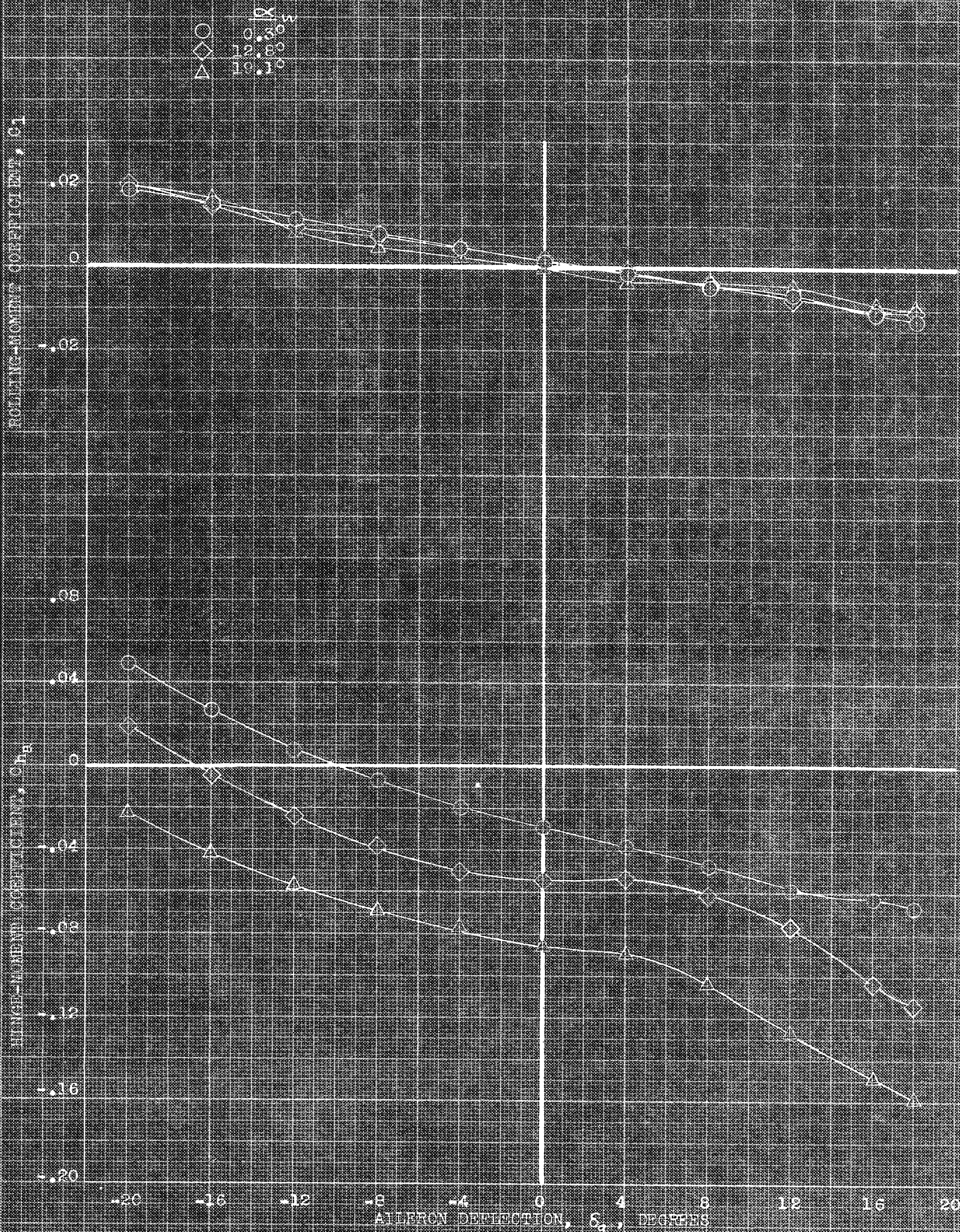


(b) C_L , C_{hB} vs. C_l .
FIGURE 15. - CONCLUDED.



(a) C_n, C_m vs δ_a .

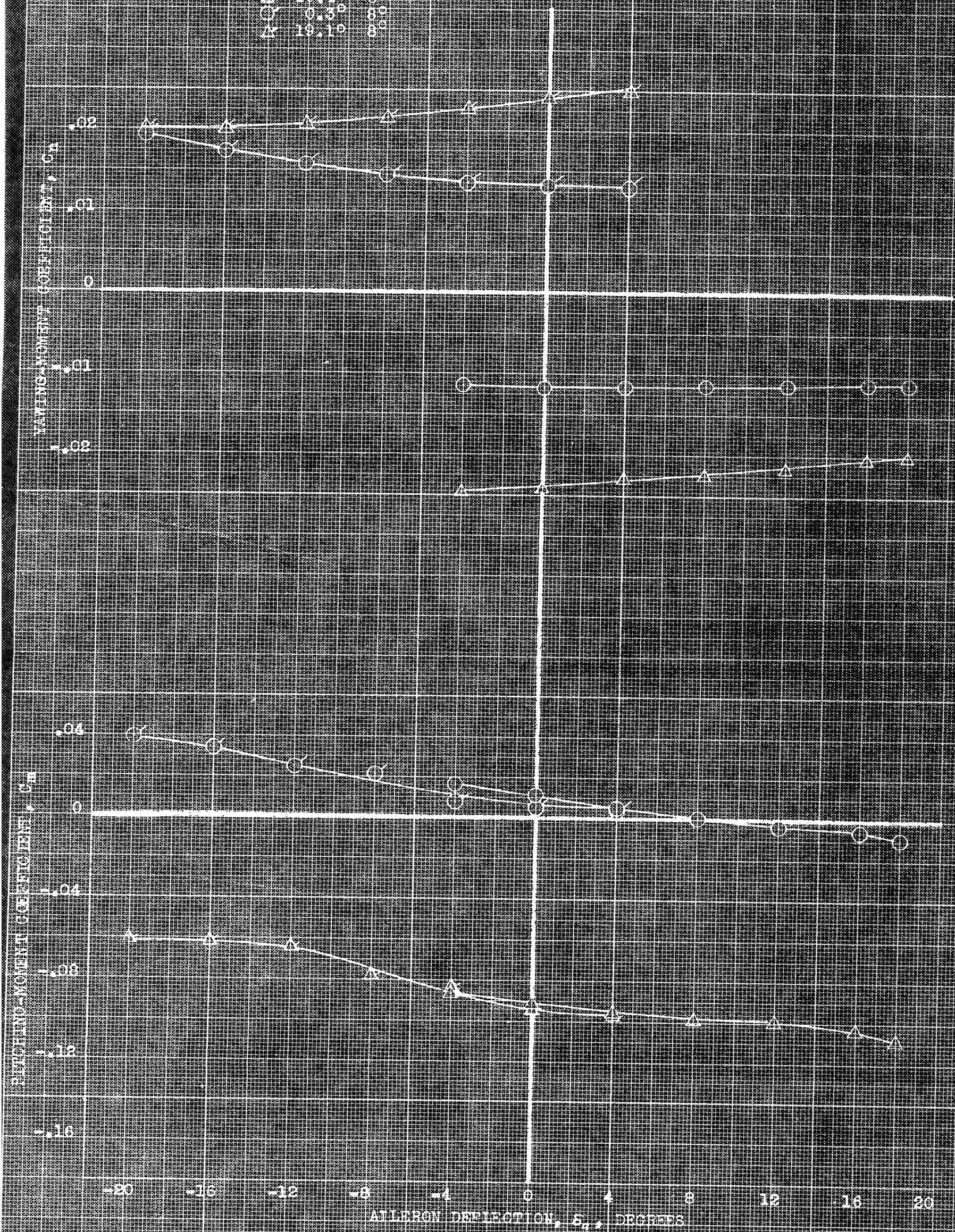
FIGURE 1K.- VARIATION WITH RIGHT AILERON DEFLECTION OF THE AERODYNAMIC CHARACTERISTICS OF THE MODEL AT SEVERAL ANGLES OF ATTACK, DROOPED SLATS; PLAIN FLAPS, 40°, 1°, 3°.



(b) C_l , C_{h_a} vs δ_a .

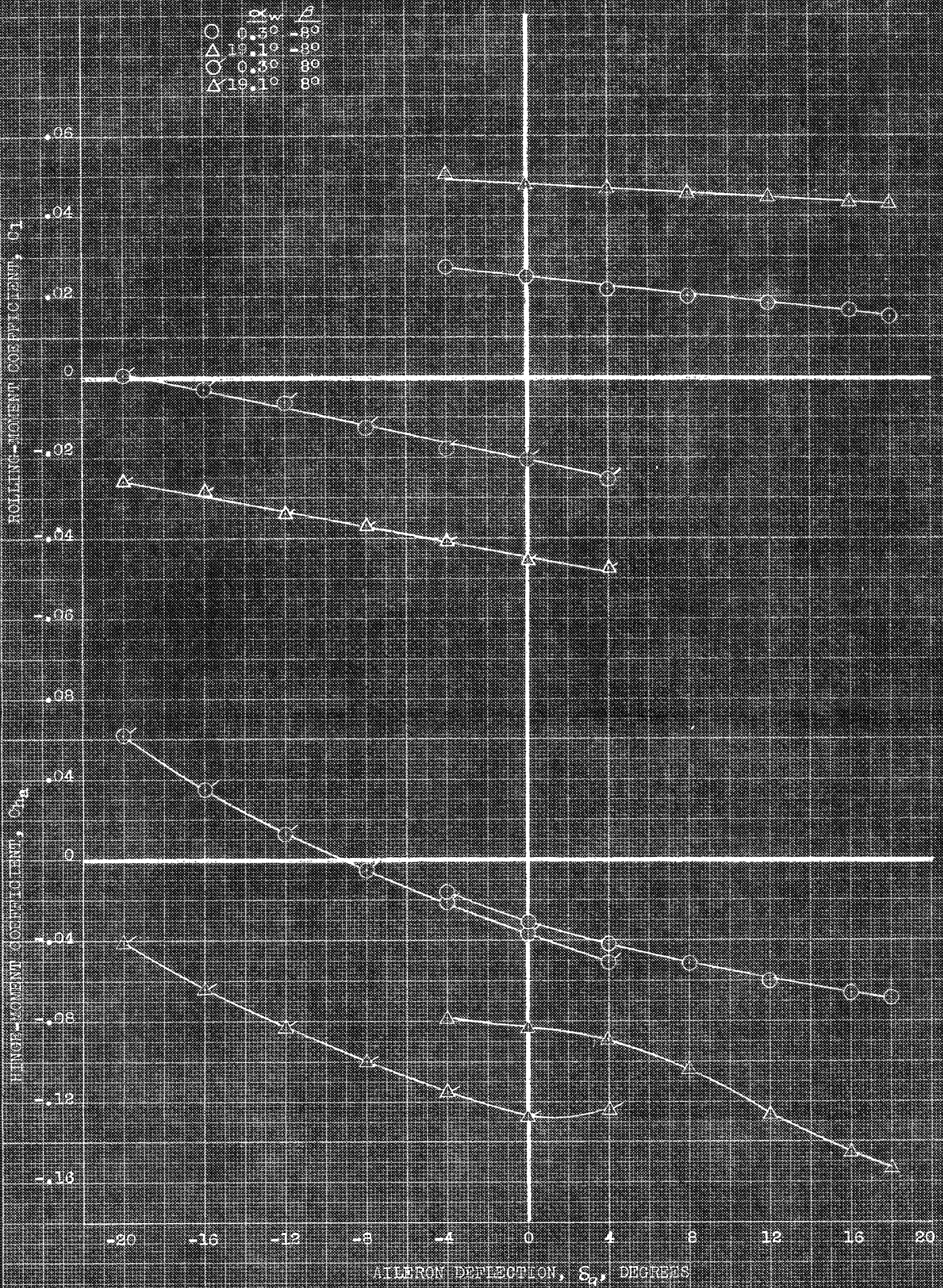
FIGURE 1.6. - CONCLUDED.

	α	β
\circ	0.5°	5°
Δ	19.1°	5°
\circ	0.5°	8°
Δ	19.1°	8°



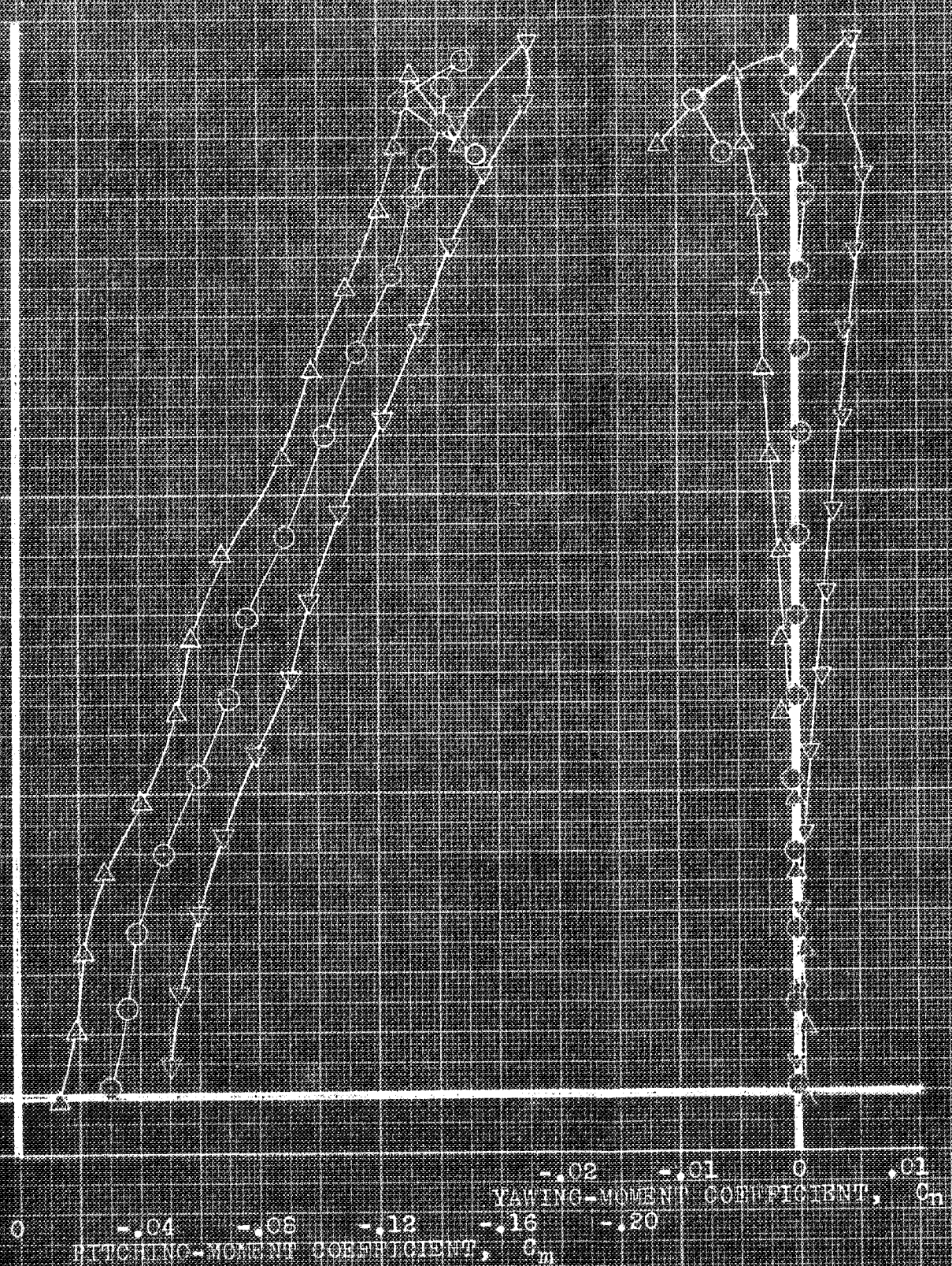
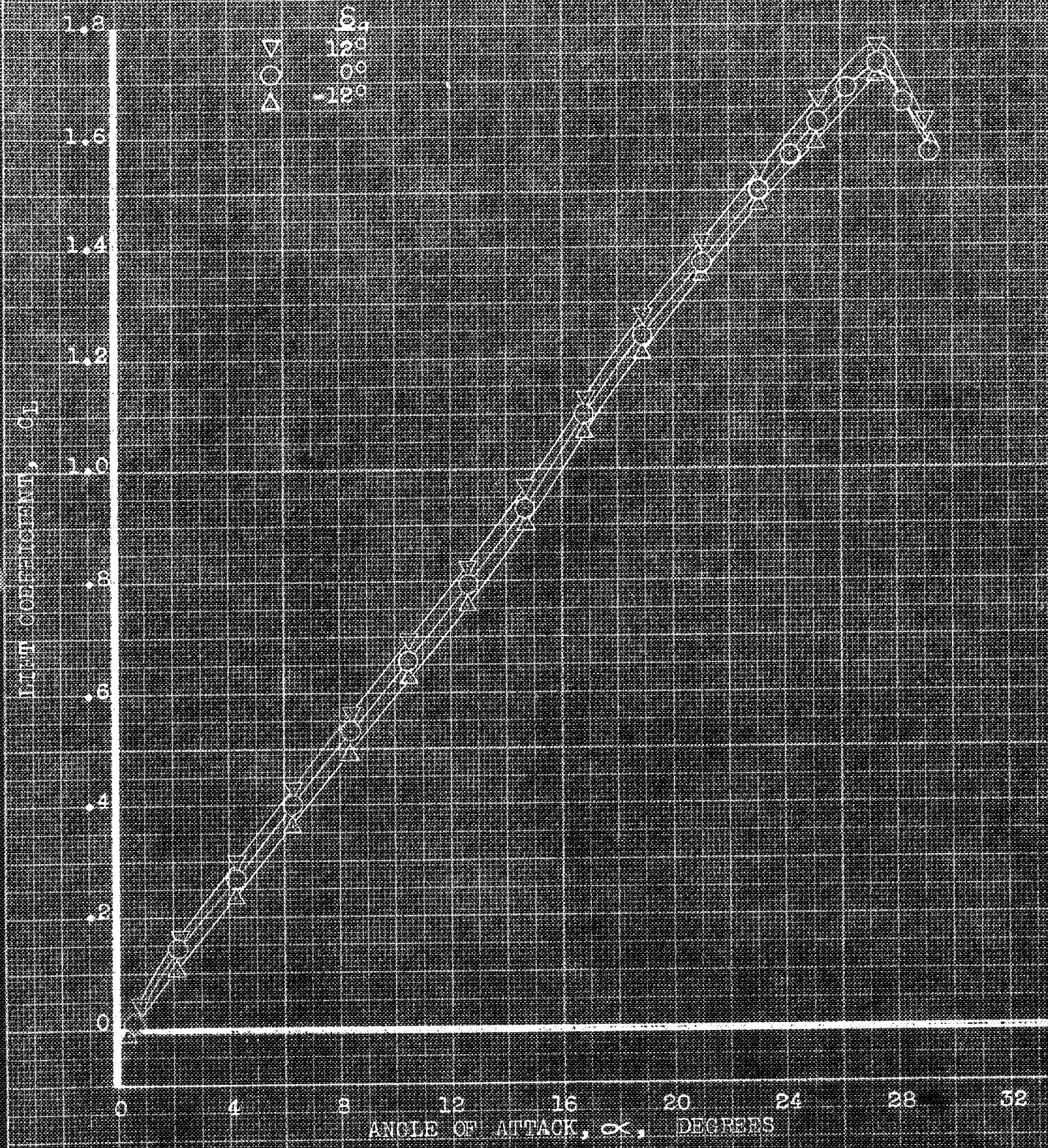
(a) C_m, C_n vs δ_a

FIGURE 17. VARIATION WITH RIGHT AILERON DEFLECTION OF THE AERODYNAMIC CHARACTERISTICS OF THE MODEL IN SIDESLIP AT SEVERAL ANGLES OF ATTACK. DROOPED SLATS; PLAIN FLAPS, $400\% i_w$, 6° .



(b) C_l, C_{ha} vs δ_a .

FIGURE 17.- CONCLUDED.

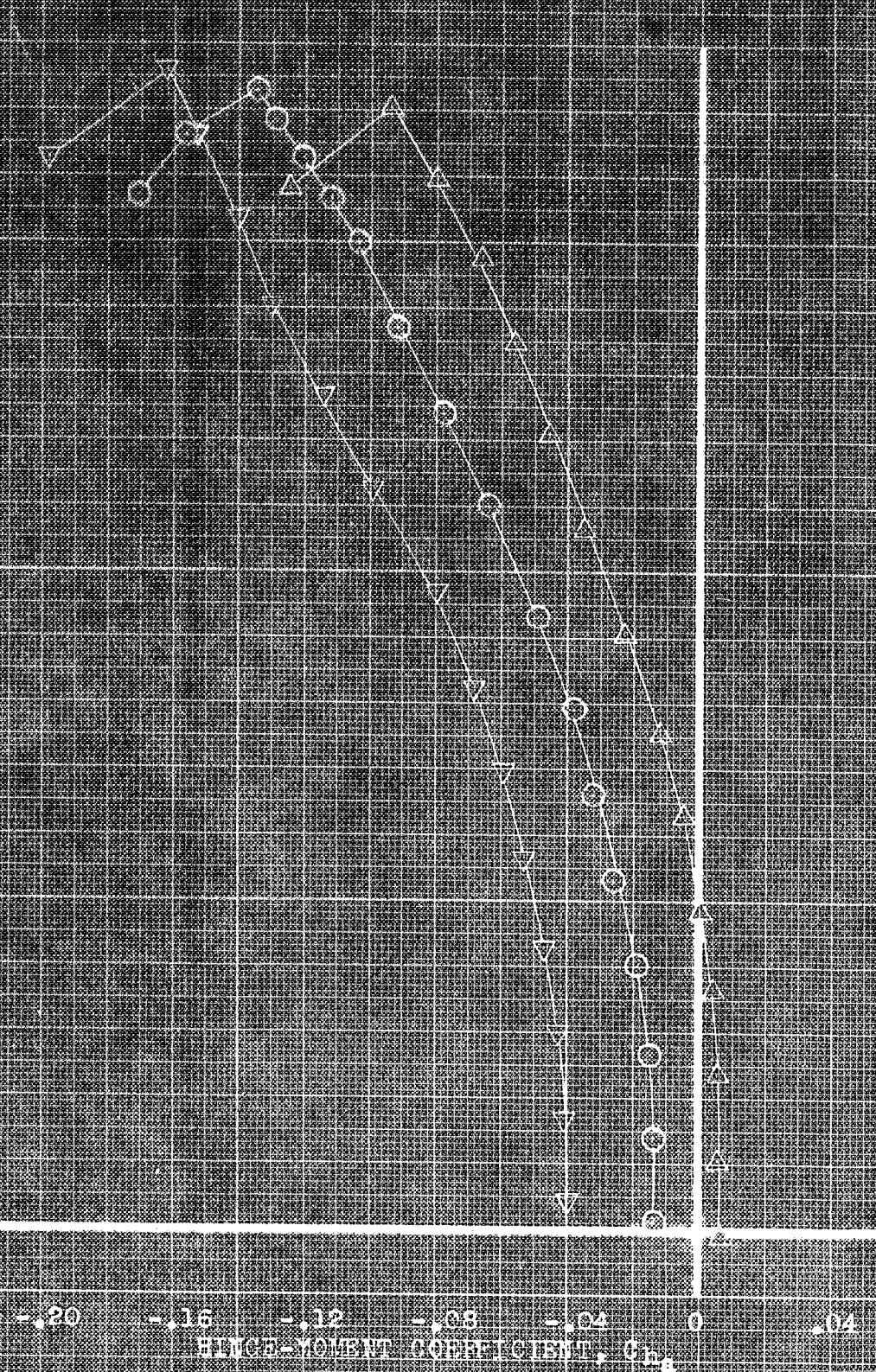
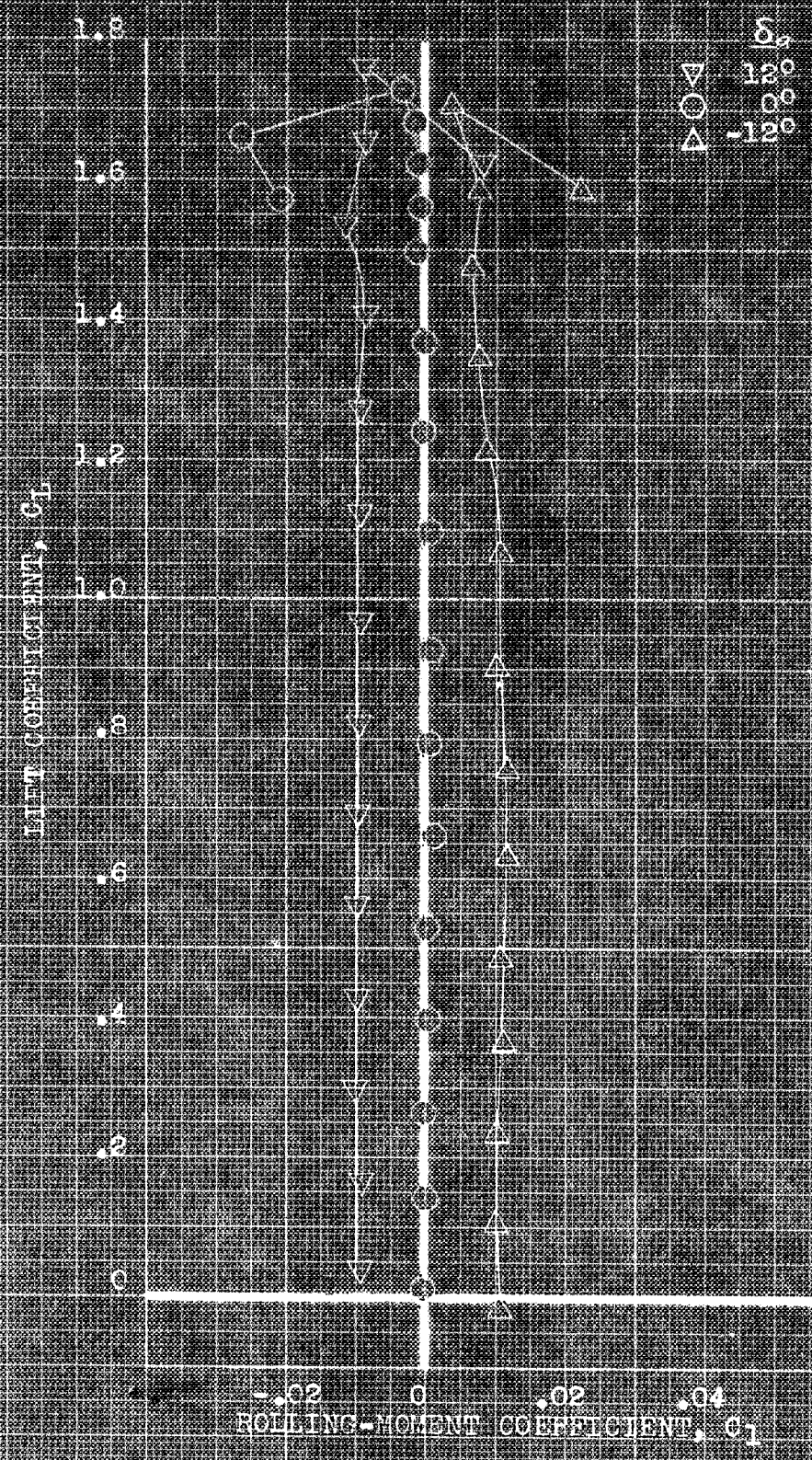


(a) α , c_m , c_n vs δ .

FIGURE 11. EFFECT OF FIXED DEFLECTIONS ON THE RIGHT ALLERON ON THE AERODYNAMIC CHARACTERISTICS OF THE MODEL IN FITCH, DROOPED SLATS, $\delta = 0^\circ$.

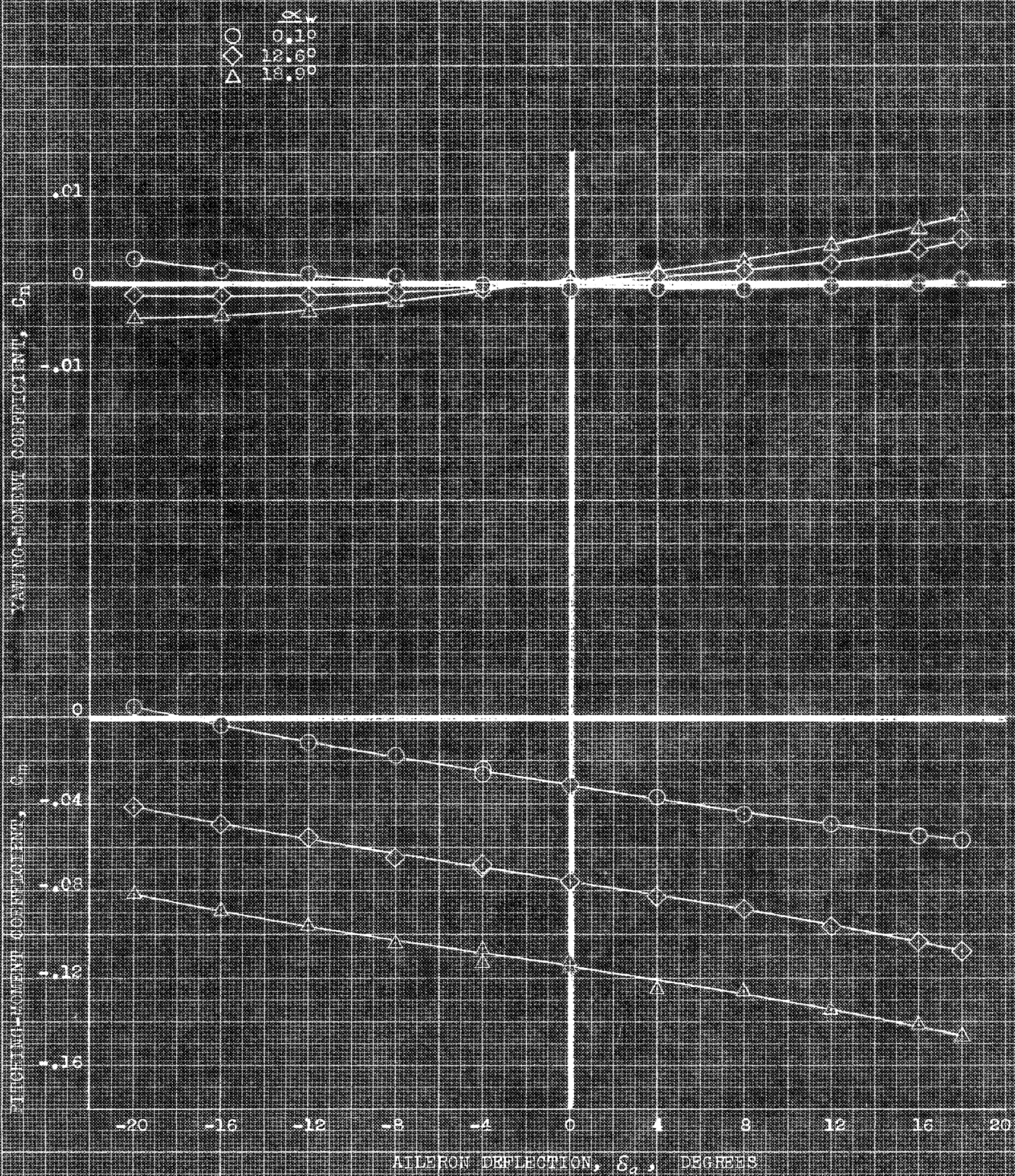
CONFIDENTIAL

Naval Air Station, Dayton, Ohio



(b) C_L , C_{Lr} , $\delta = 12^\circ$, 0° , -12° .
 FIGURE 11. CONCLUDED.

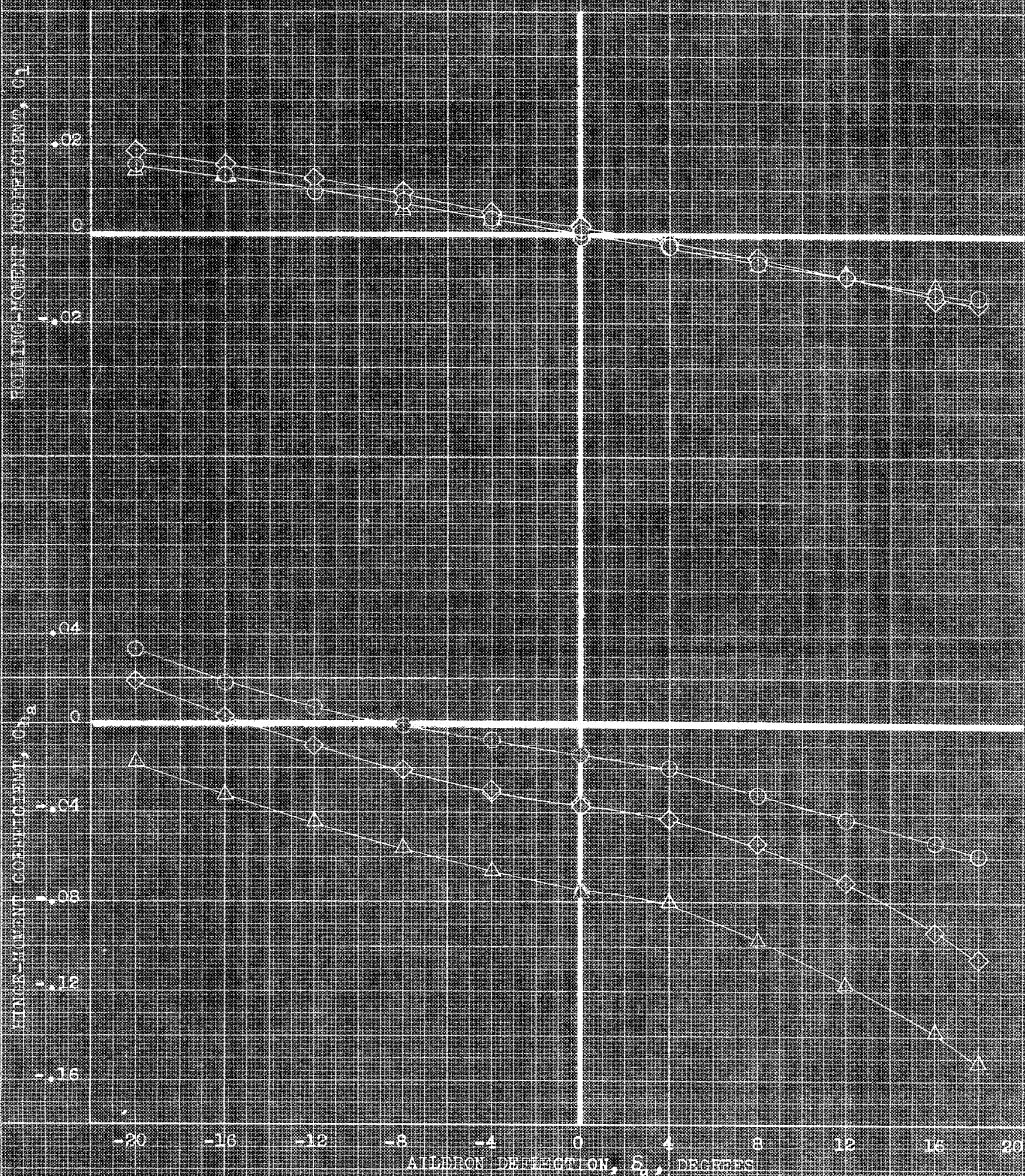
CONFIDENTIAL
 NATIONAL ADVISORY COMMITTEE FOR AERONAUTICS



(a) C_n, C_m vs δ_a

FIGURE 10. VARIATION WITH RIGHT AILERON DEFLECTION OF THE AERODYNAMIC CHARACTERISTICS OF THE MODEL AT SEVERAL ANGLES OF ATTACK. DROOPED SLATS; 14.0° .

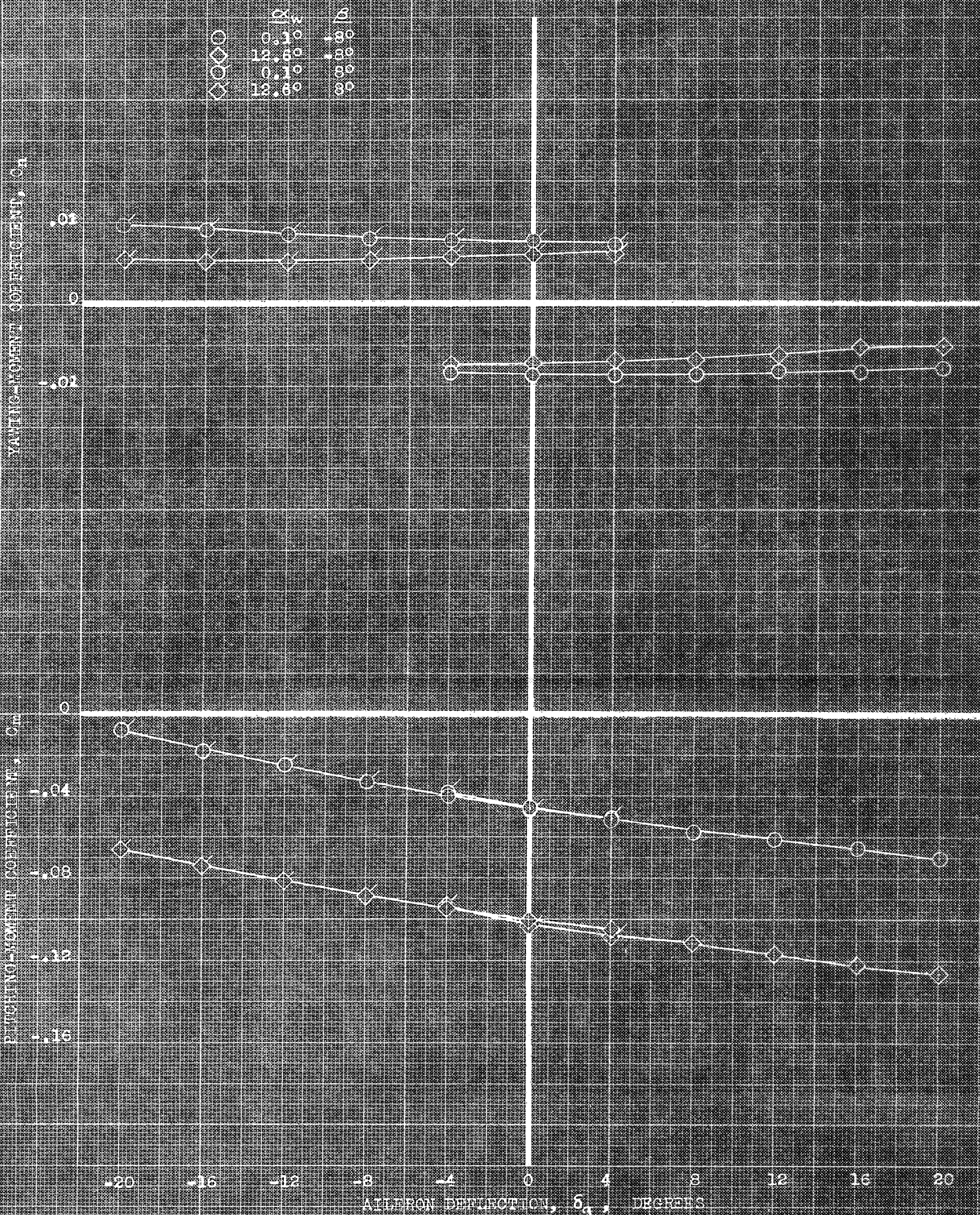
α
 \circ 6.10°
 \diamond 12.60°
 \triangle 18.90°



(b) C_l , C_{l_a} vs δ_a

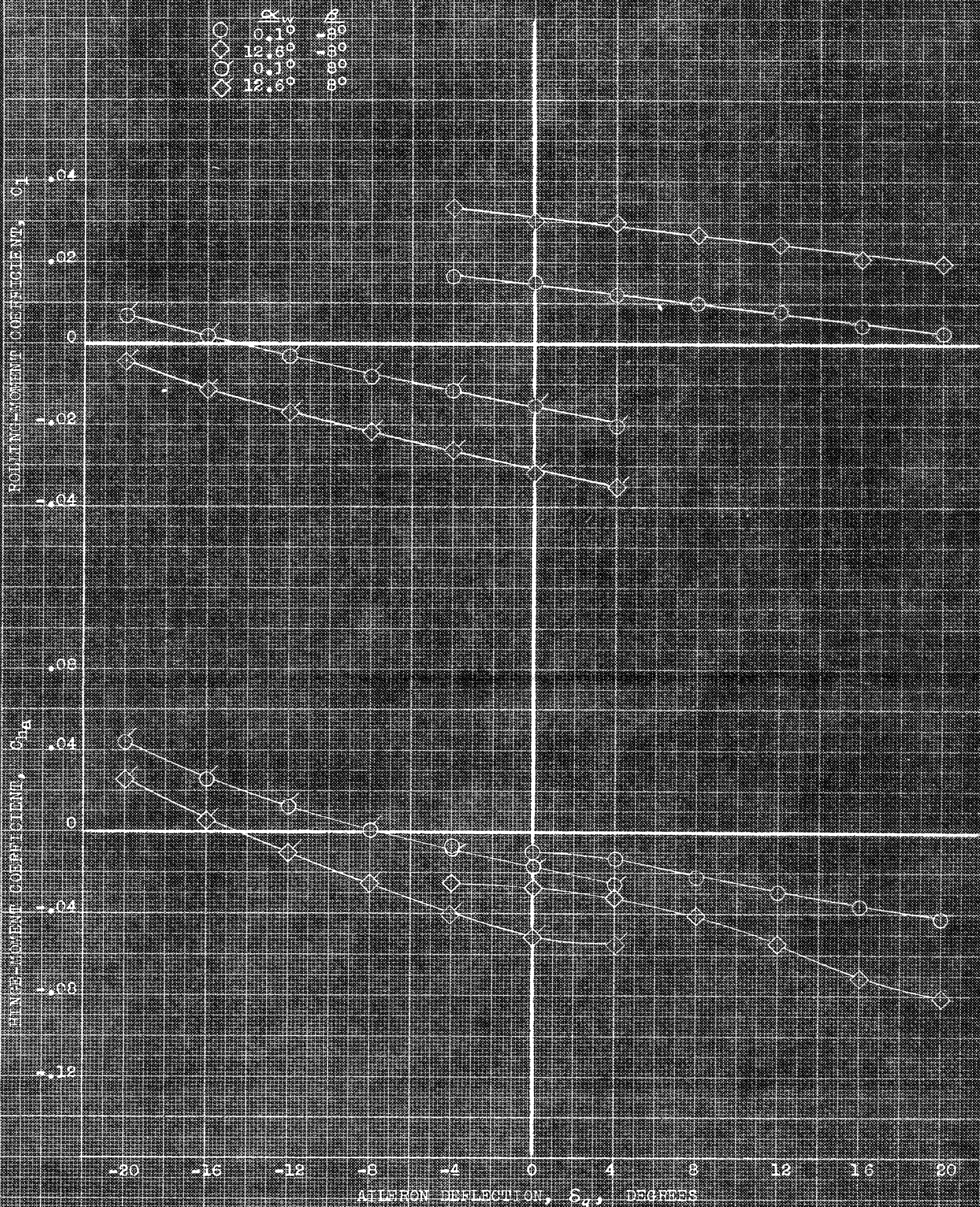
FIGURE 10. CONCLUDING.

CONFIDENTIAL
 NATIONAL ADVISORY COMMITTEE FOR AERONAUTICS



(a) C_y, C_m vs δ_a .

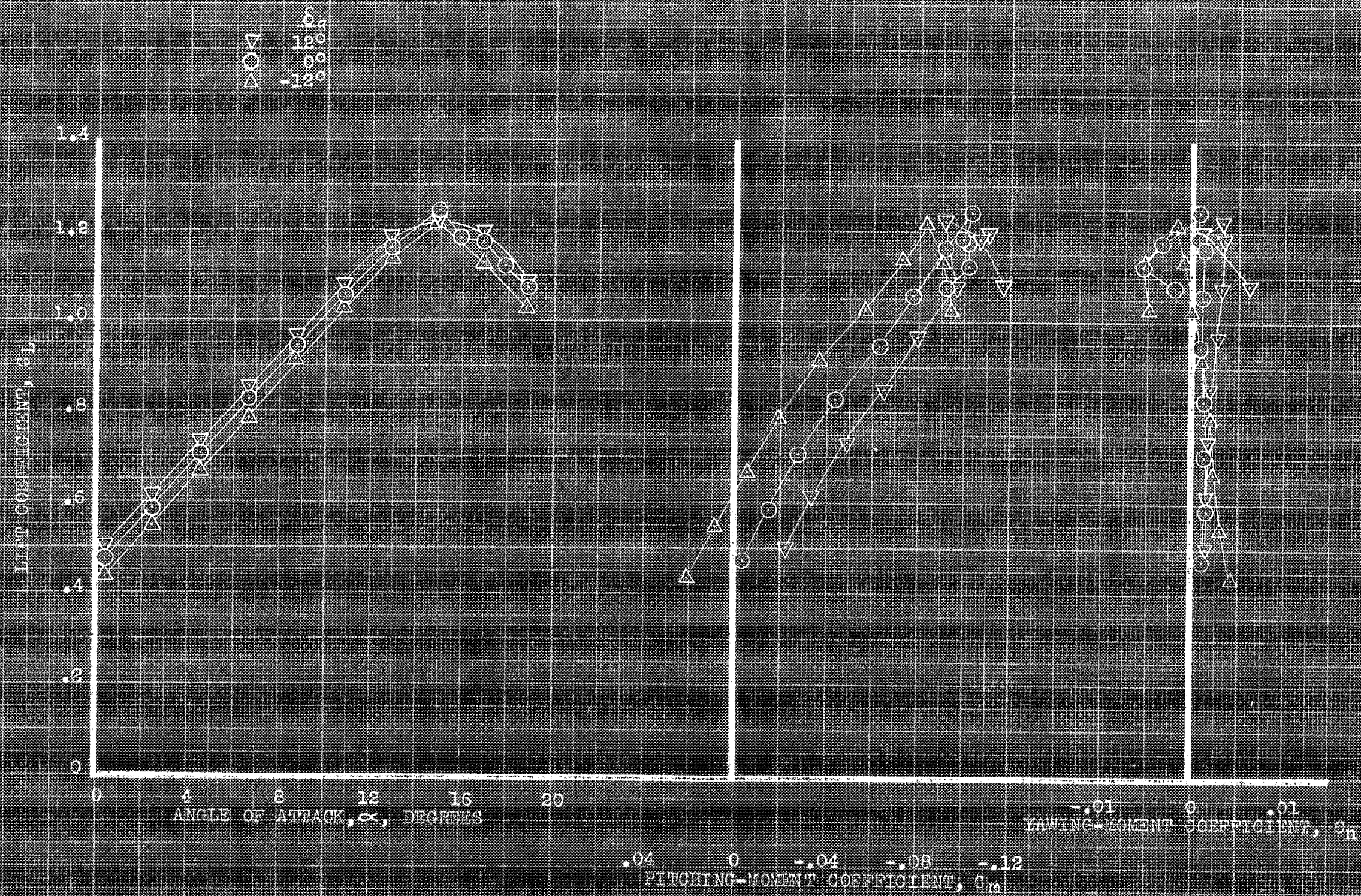
FIGURE 10. VARIATION WITH RIGHT AILERON DEFLECTION OF THE AERODYNAMIC CHARACTERISTICS OF THE MODEL IN SIDESLIP AT SEVERAL ANGLES OF ATTACK. DROOPED SLATS; $1_w, 0^\circ$.



(b) C_l, C_{ha} vs δ_a .

FIGURE 10. CONTINUED.

CONFIDENTIAL
NATIONAL ADVISORY COMMITTEE FOR AERONAUTICS

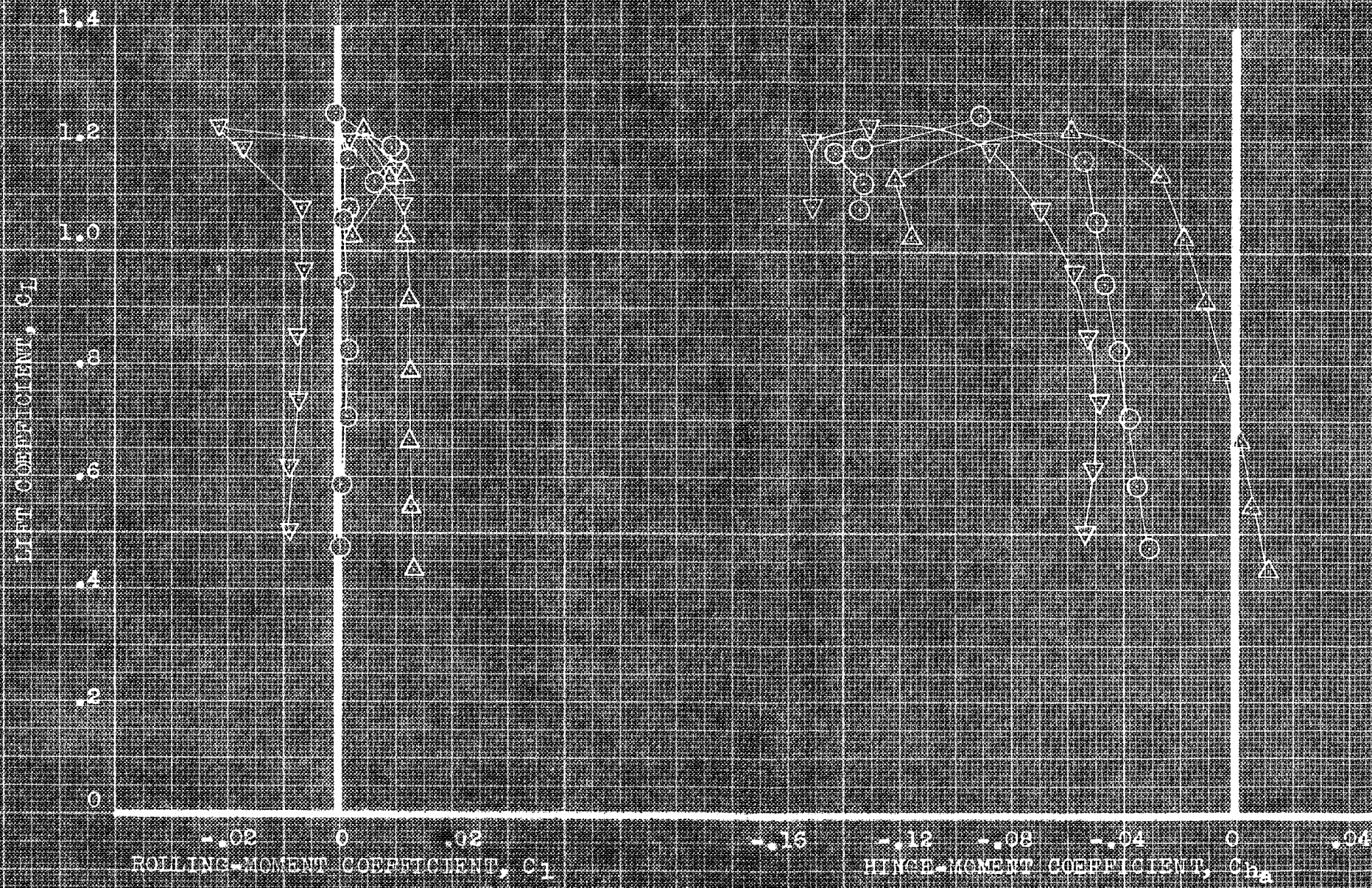


(a) α , C_L , C_m vs C_L .

FIGURE 11. - EFFECT OF FIXED DEFLECTIONS OF THE RIGHT ALLERON ON THE AERODYNAMIC CHARACTERISTICS OF THE MODEL IN PITCH. PLAIN FLAPS, 40° , $1,000$.

CONFIDENTIAL

NATIONAL ADVISORY COMMITTEE FOR AERONAUTICS

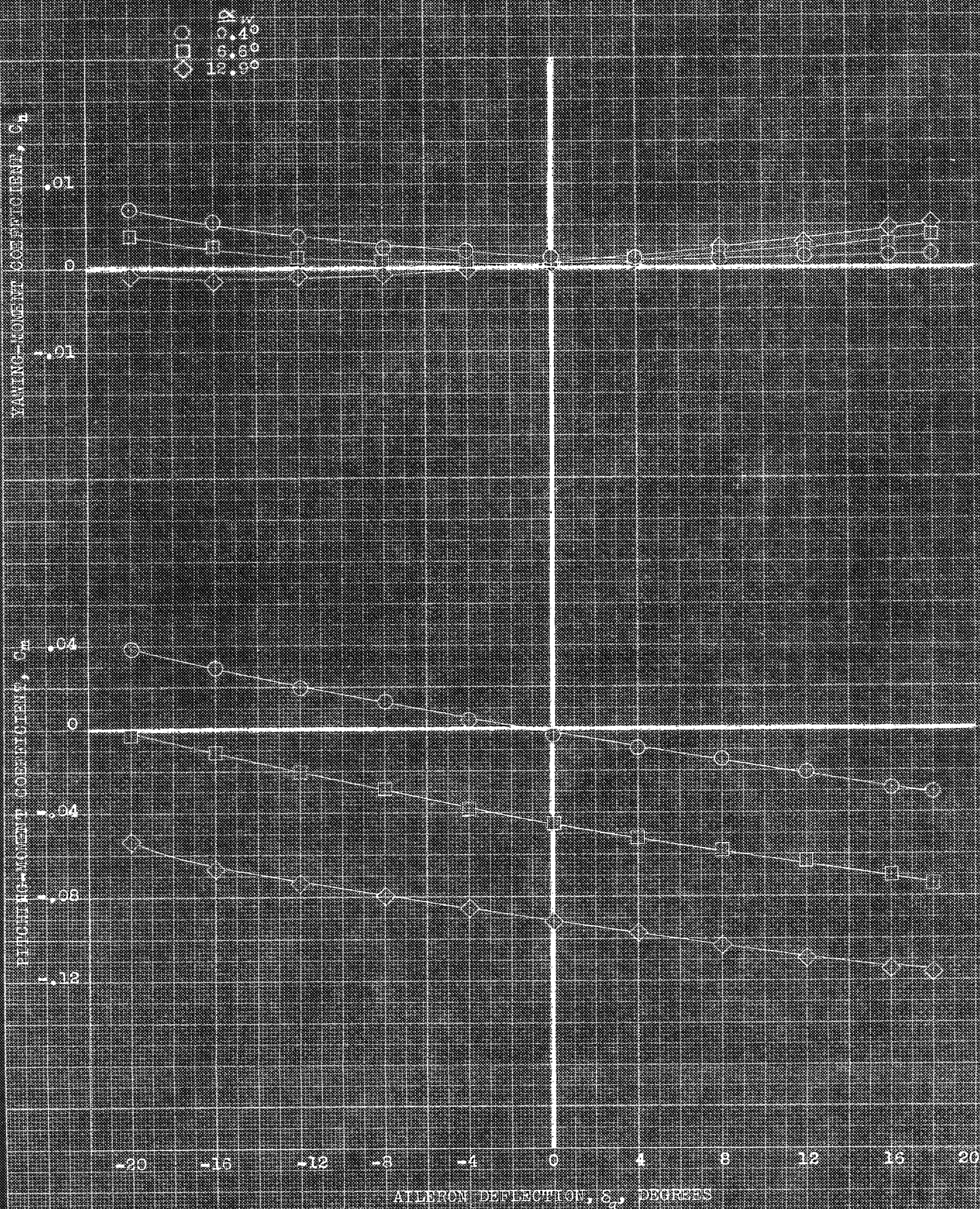


(b) C_L , C_{pa} vs C_1 .

FIGURE 1. - CONCLUDED.

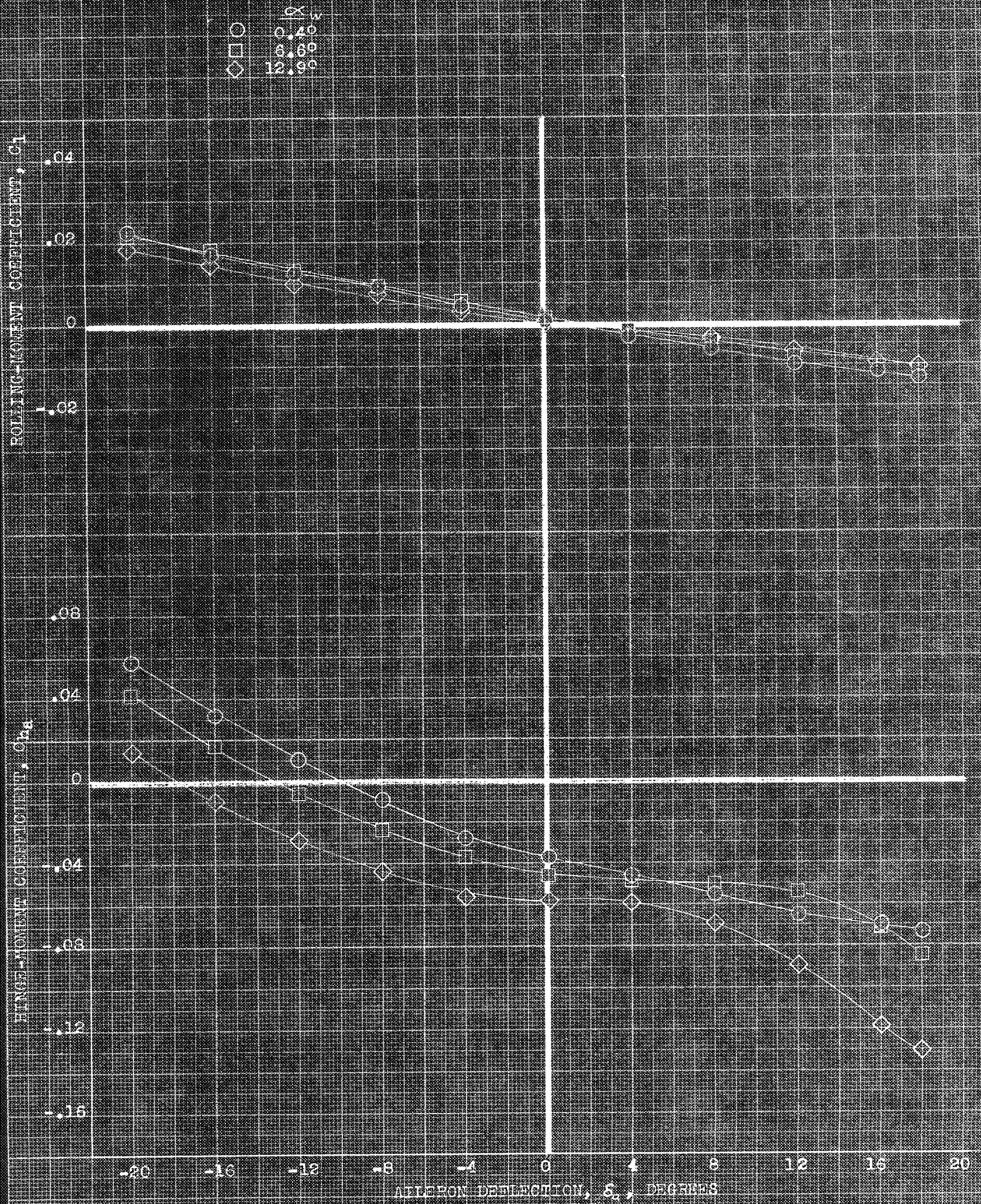
CONFIDENTIAL

NATIONAL BUREAU OF AERONAUTICS



(a) C_n, C_m vs δ_a .

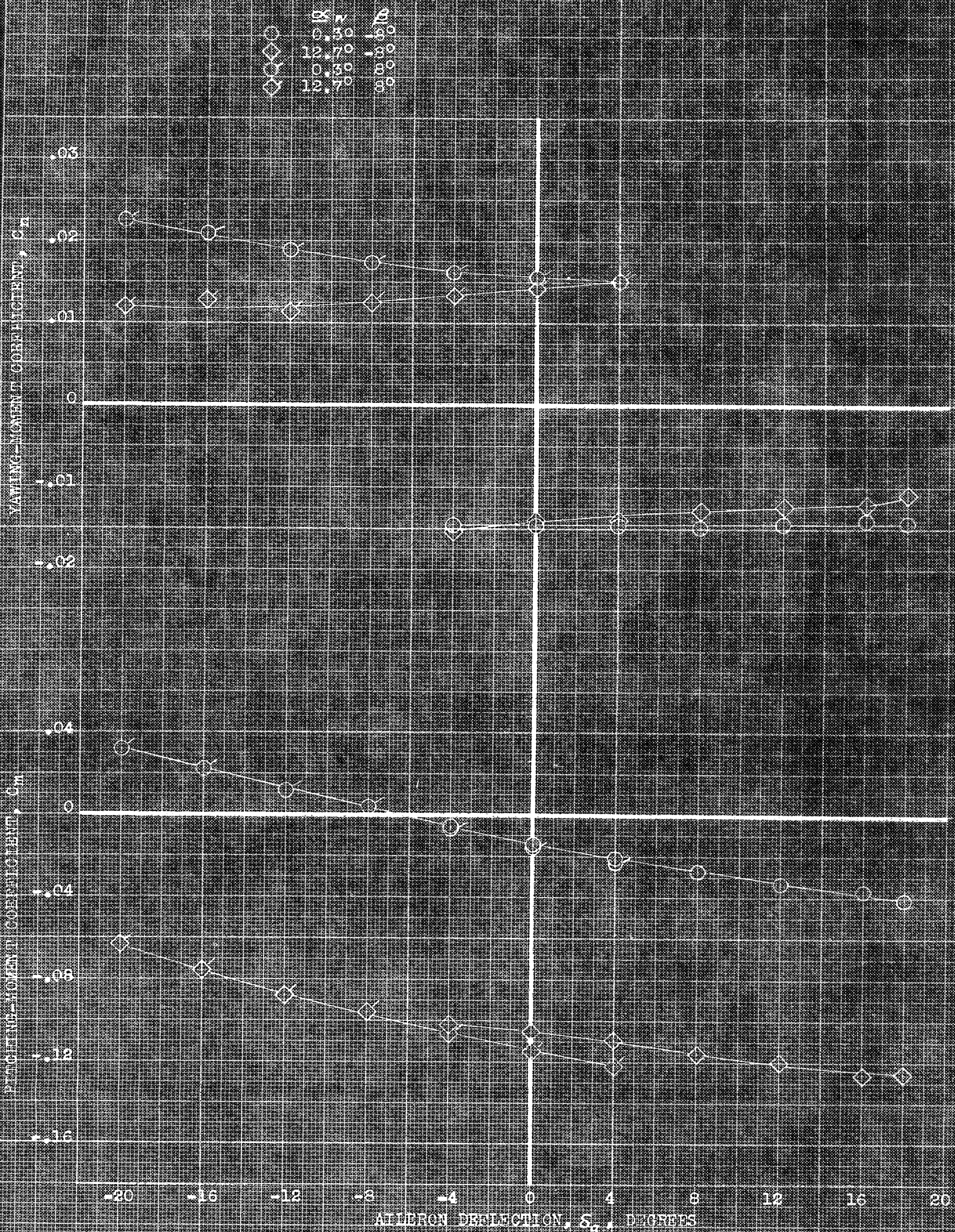
FIGURE 52. -- VARIATION WITH RIGHT AILERON DEFLECTION OF THE AERODYNAMIC CHARACTERISTICS OF THE MODEL AT SEVERAL ANGLES OF ATTACK. PLAIN FLAPS, 400; $i_w, 0^\circ$.



(b) C_l , C_{hg} vs δ_a .

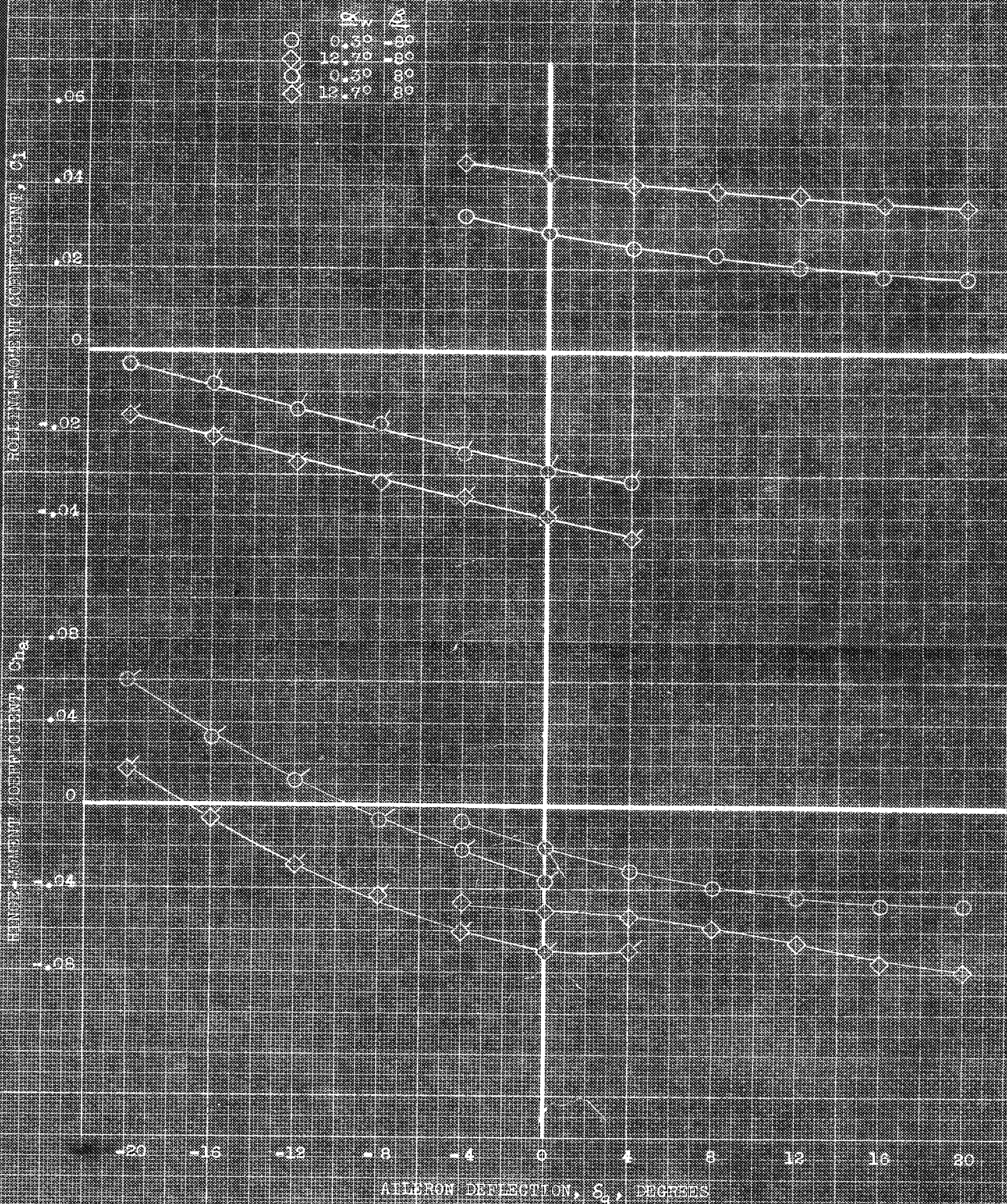
FIGURE 52. - CONCLUDED.

CONFIDENTIAL
NATIONAL RESEARCH COMMITTEE FOR AERONAUTICS



(a) C_y, C_m vs S_a

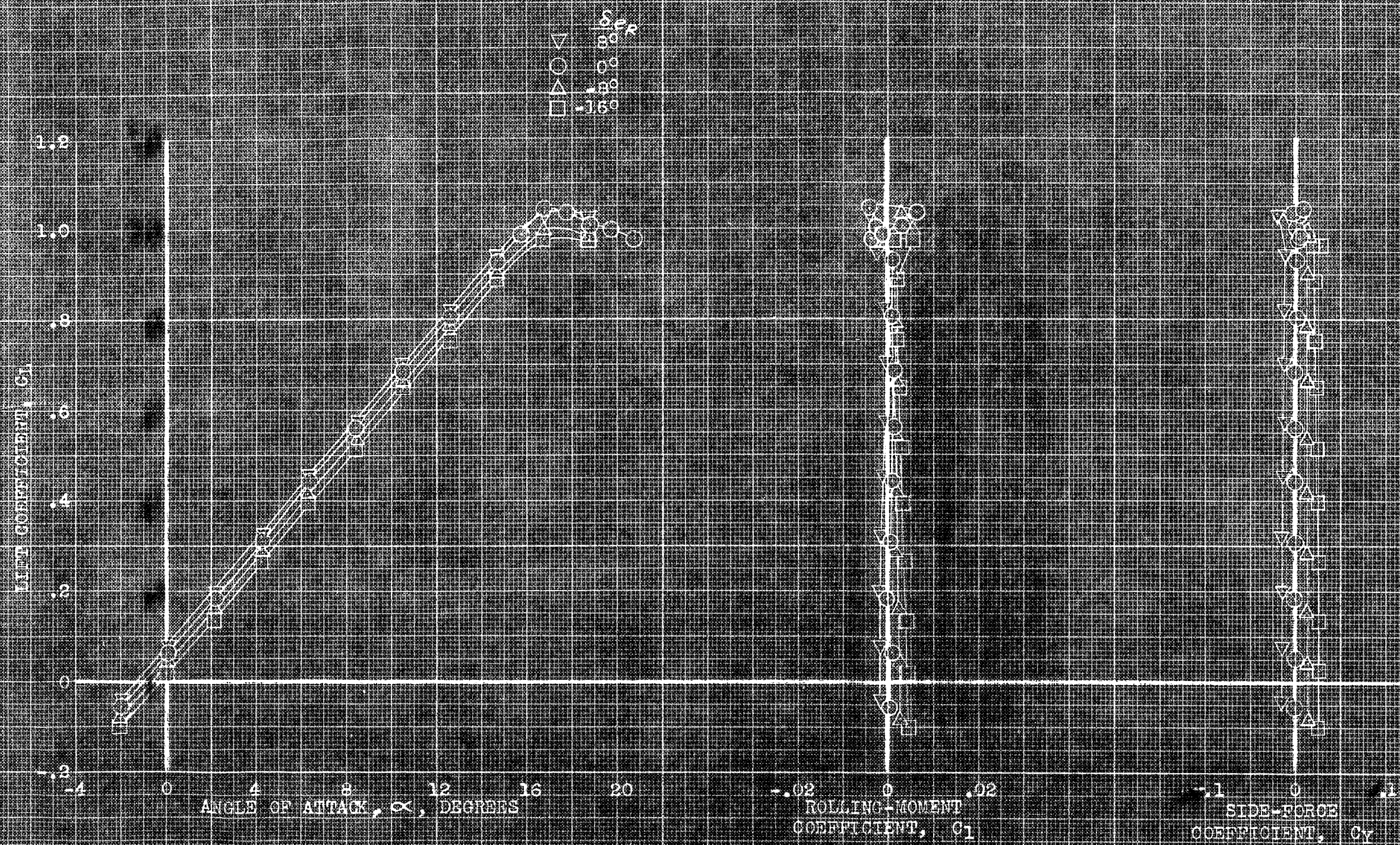
FIGURE 52. -- VARIATION WITH RIGHT AILERON DEFLECTION OF THE AERODYNAMIC CHARACTERISTICS OF THE MODEL IN SIDESLIP AT SEVERAL ANGLES OF ATTACK. PLAIN FLAPS, 40°; α_w 0°.



(b) C_l , C_h vs S_a .

FIGURE 3. -- CONCLUDED.

CONFIDENTIAL
NATIONAL ADVISORY COMMITTEE FOR AERONAUTICS

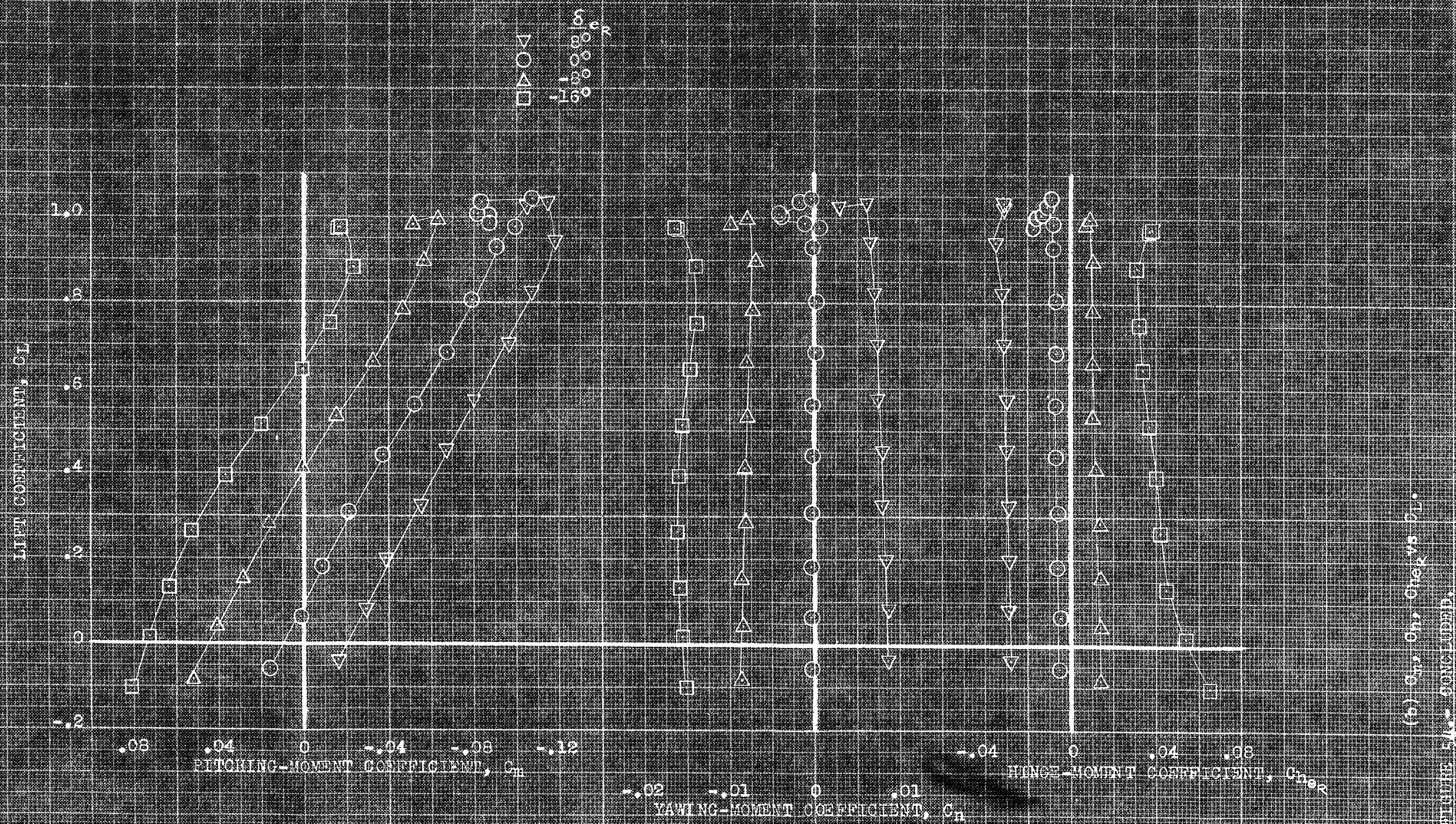


(a) α , C_l , C_Y vs C_L .

FIGURE 1. EFFECT OF FLIGHT CONDITIONS ON THE ROLLING-MOMENT ON THE AERODYNAMIC CHARACTERISTICS OF THE MODEL IN PITCH. PLAIN WING, 17° .

CONFIDENTIAL

UNCLASSIFIED//FOR OFFICIAL USE ONLY



(6) C_L vs C_m vs C_n

FIGURE 1.1. CONCLUDED.

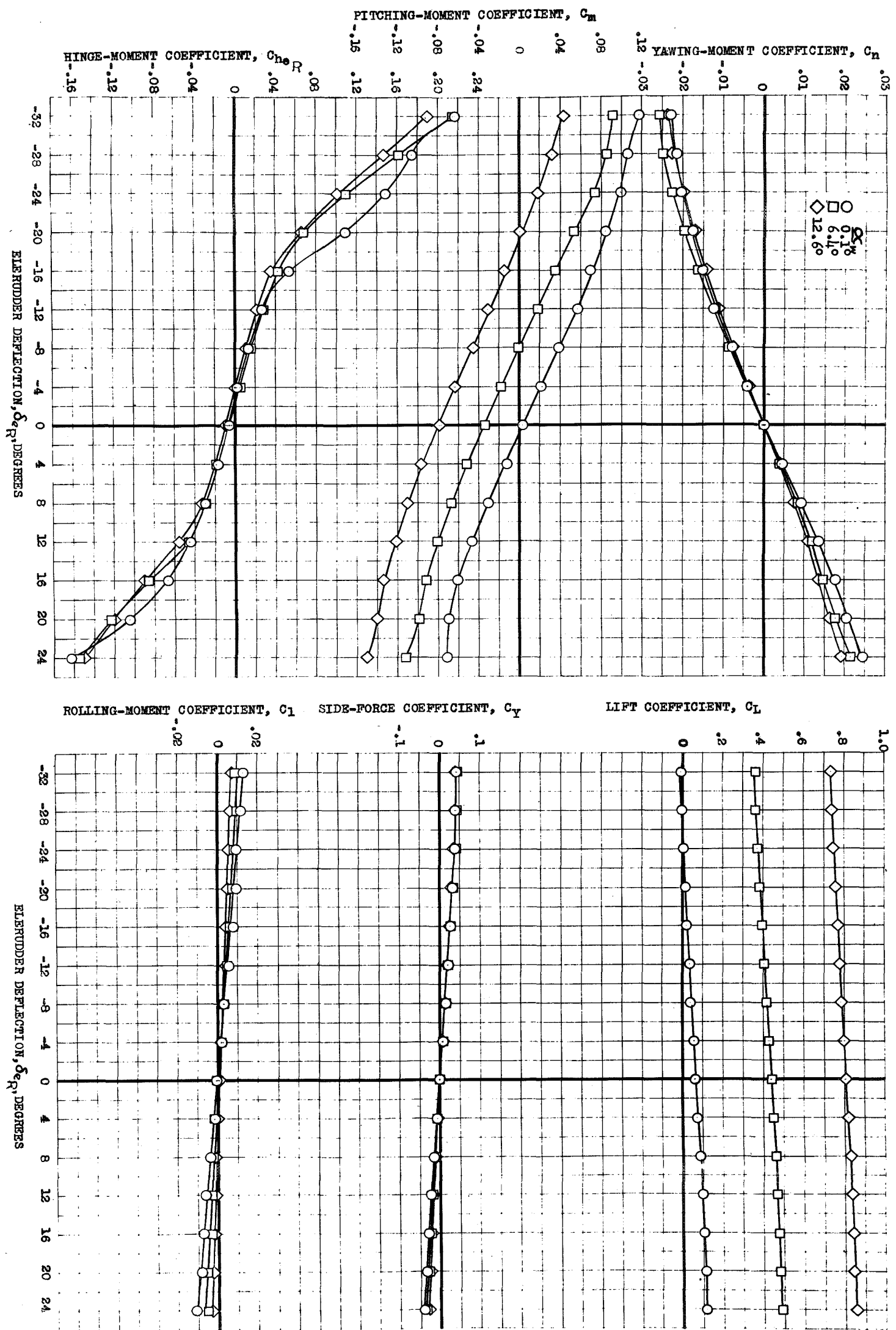


FIGURE 55.- VARIATION WITH ELERUDDER DEFLECTION OF THE AERO-DYNAMIC CHARACTERISTICS OF THE MODEL AT SEVERAL ANGLES OF ATTACK. PLAIN WING; $i_w, 0^\circ$

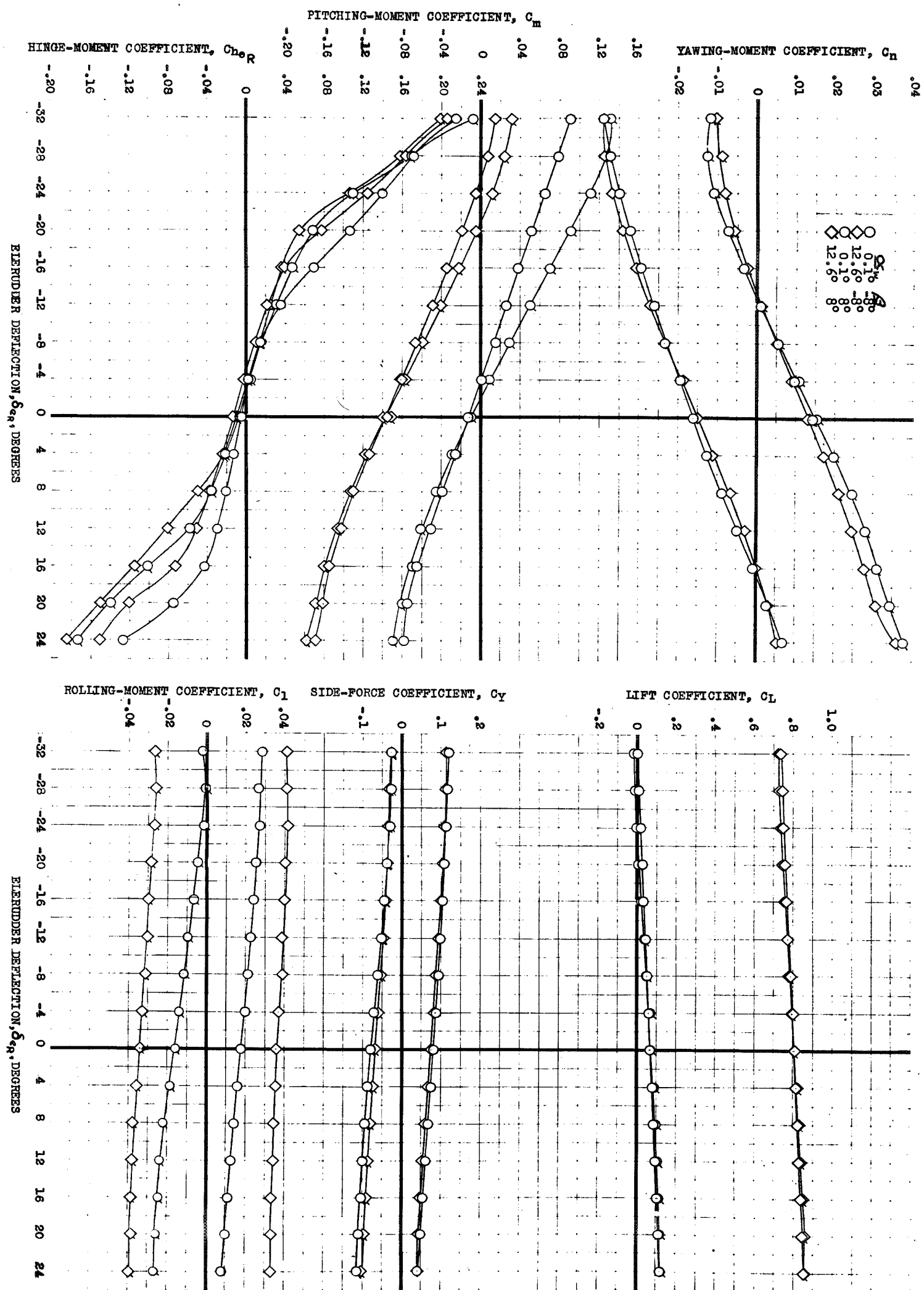
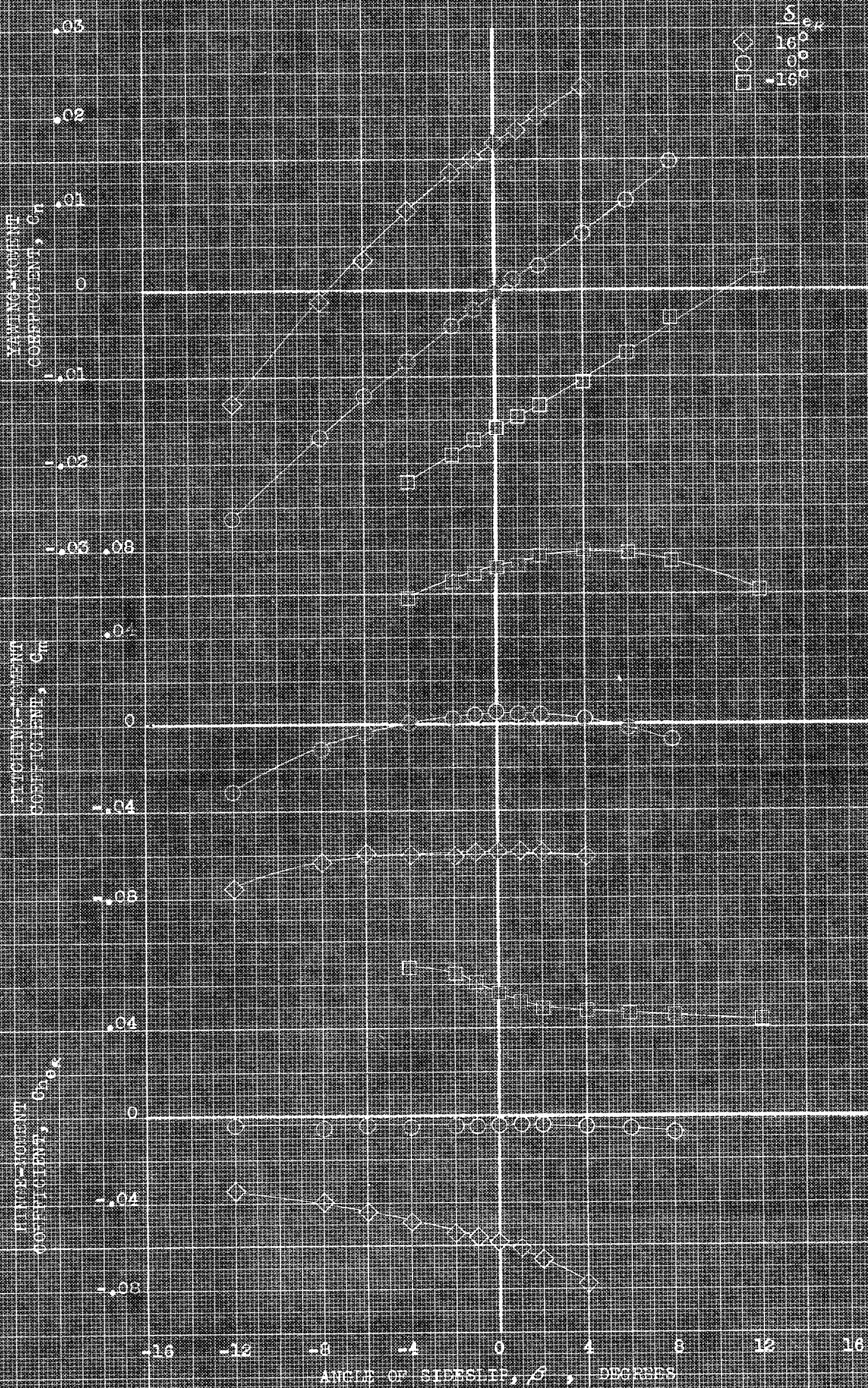


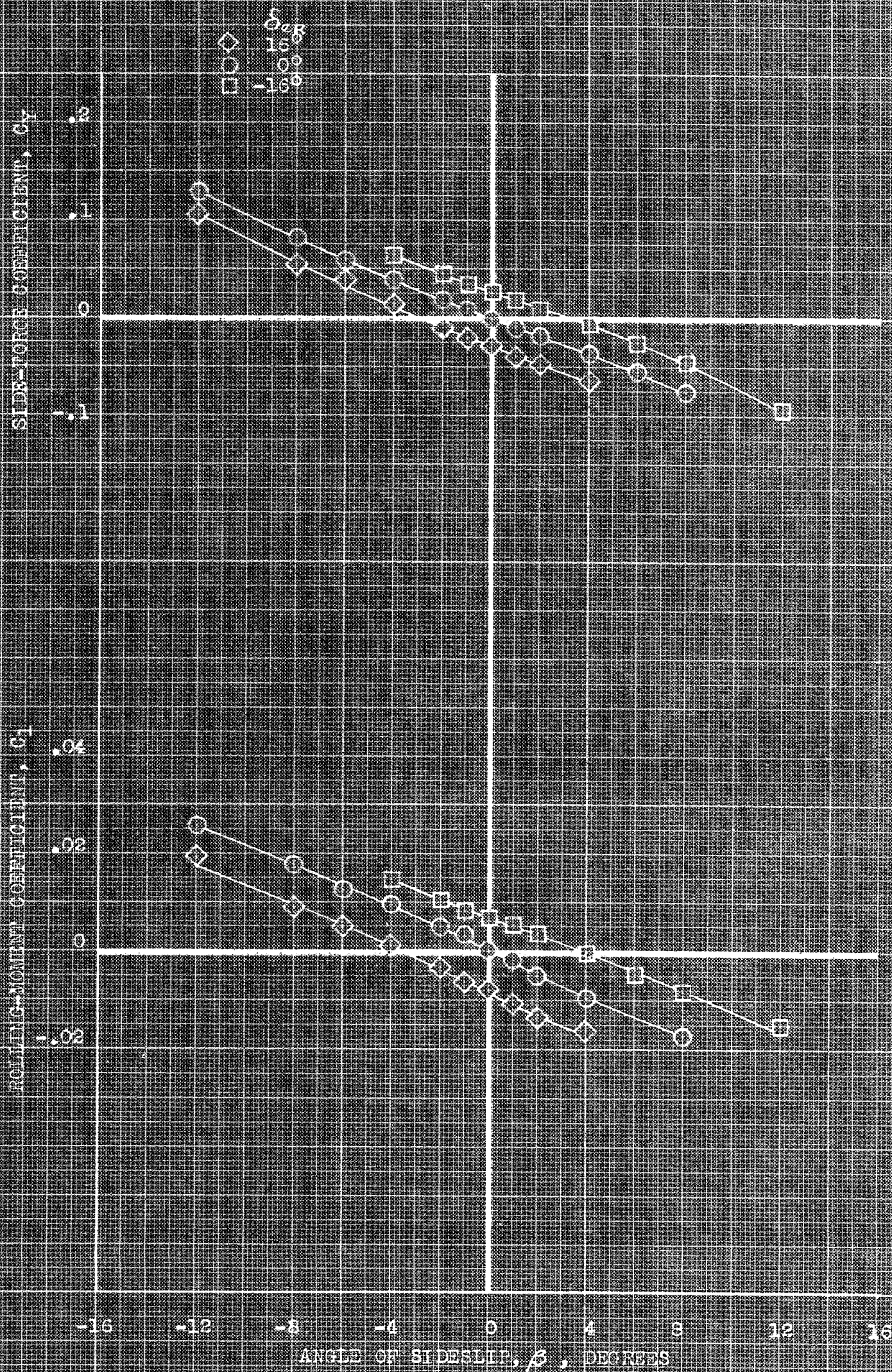
FIGURE 56.- VARIATION WITH ELERUDDER DEFLECTION OF THE AERO-DYNAMIC CHARACTERISTICS OF THE MODEL IN SIDESLIP AT SEVERAL ANGLES OF ATTACK. PLAIN WING; $i_w, 0^\circ$.



(a) $\alpha_{w,0} = 0.1^\circ$; $C_{Y,0}$, $C_{m,0}$, $C_{l,0}$ vs δ

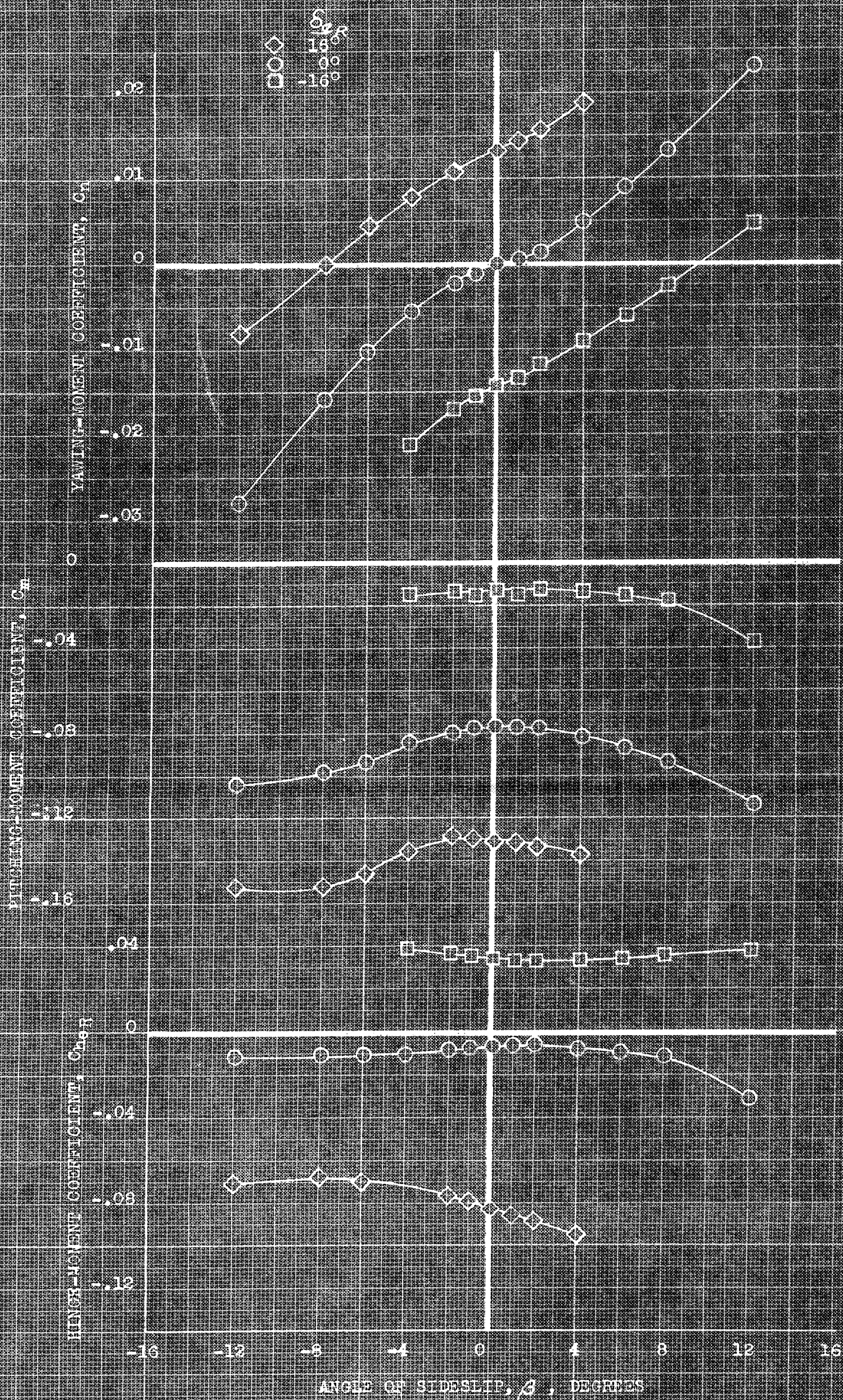
FIGURE 57. EFFECT OF FIN-LESS DEFLECTIONS ON THE DEFLECTION ON THE AEROBOMBYLIC CHARACTERISTICS OF THE MODEL IN SIDESLIP. PLAIN WING; $i_w, 0^\circ$.

CONFIDENTIAL
NATIONAL AERONAUTICS COMMITTEE FOR AERONAUTICS



(b) $\alpha_w, 0.1^\circ$; C_Y, C_L, C_R vs β .

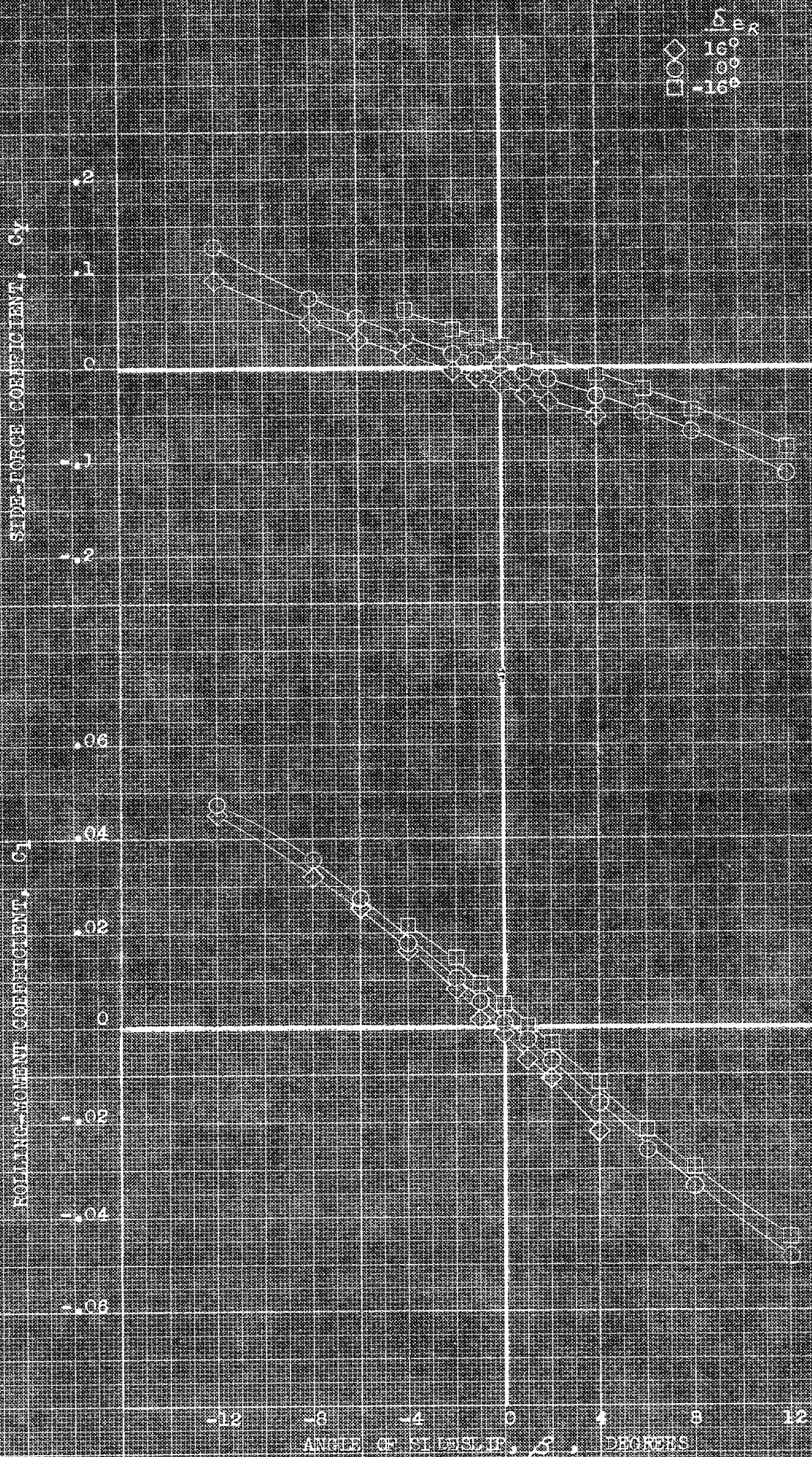
FIGURE 57. - CONTINUED.



(c) $\alpha_w = 12.6^\circ$; C_y , C_m , C_l vs β

FIGURE 57.- CONTINUED.

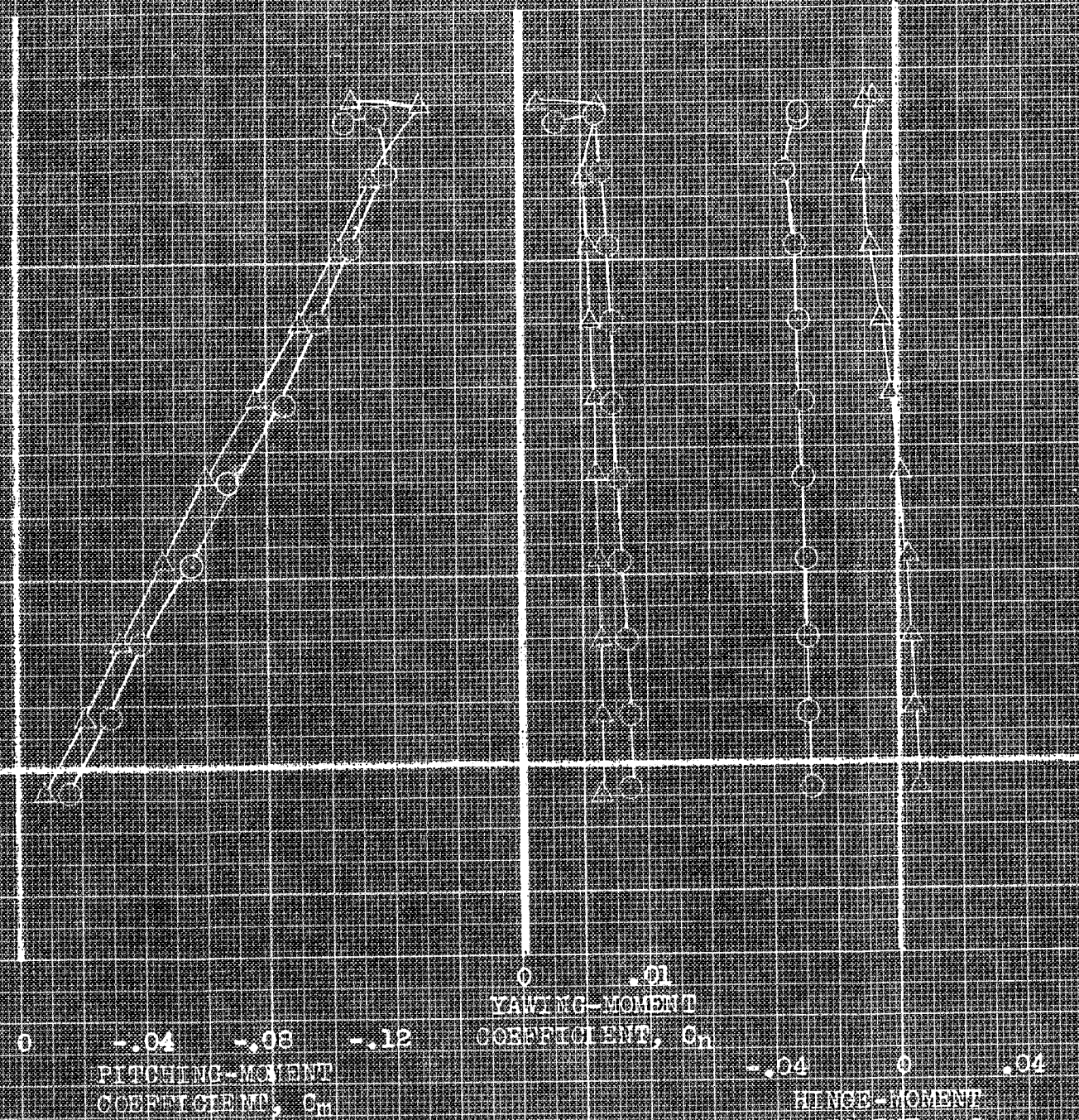
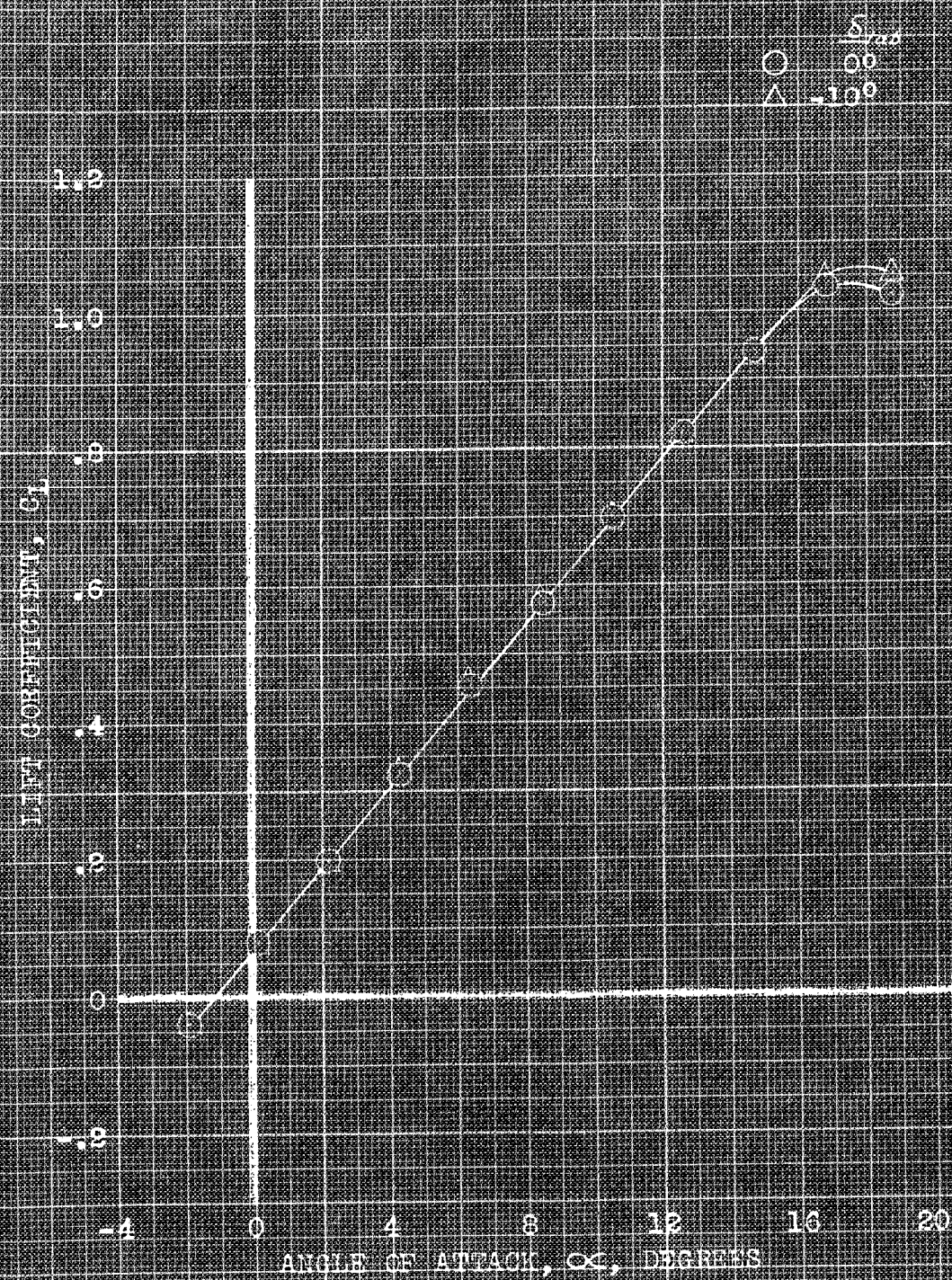
CONFIDENTIAL
 NATIONAL AERONAUTICS AND SPACE ADMINISTRATION



(a) $\delta_{\perp} = 12.6^\circ$; C_v , C_1 vs δ .

FIGURE 57.- CONCLUDED.

CONFIDENTIAL

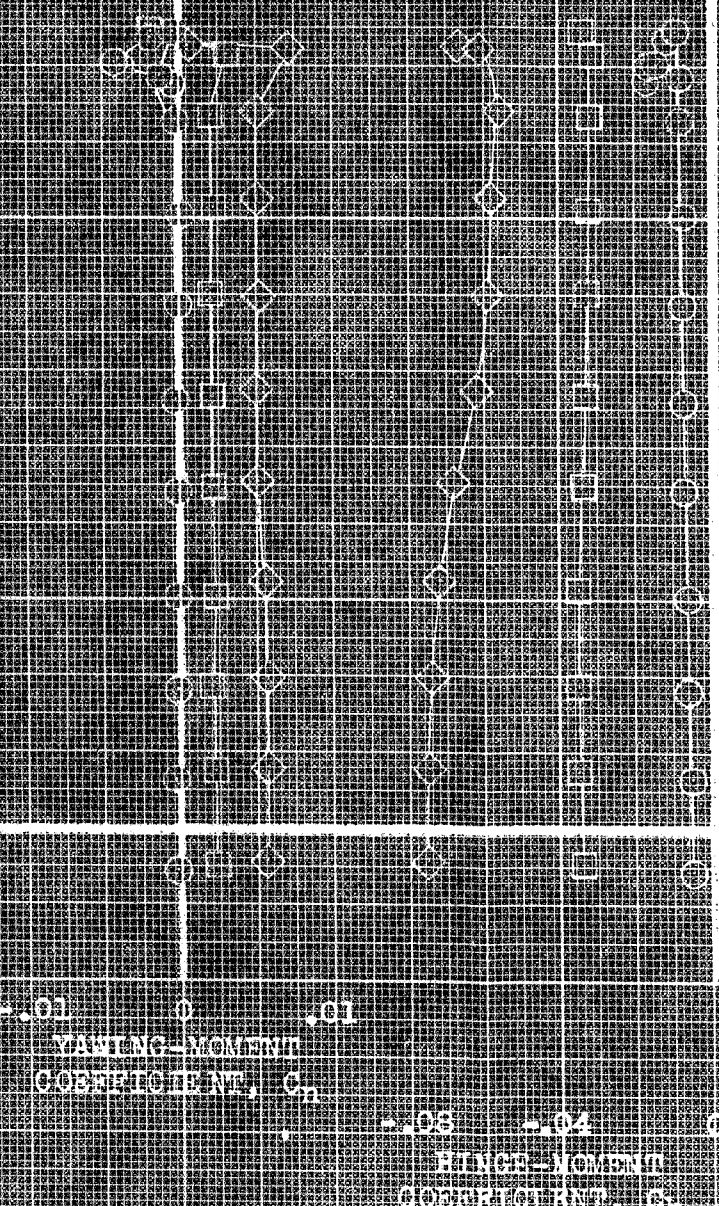
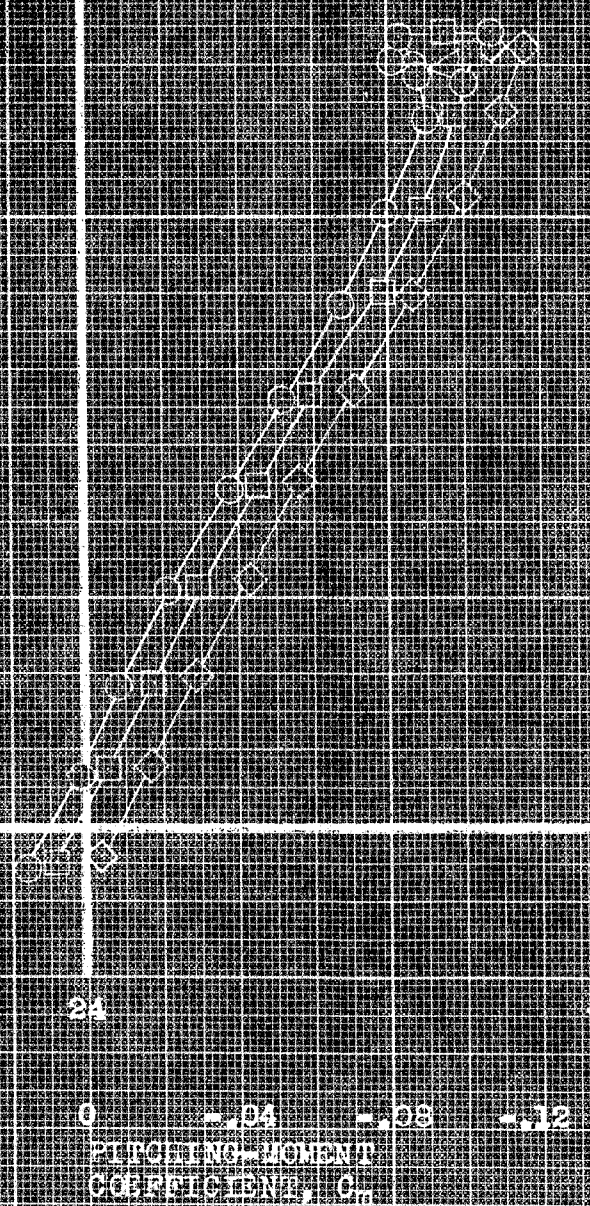
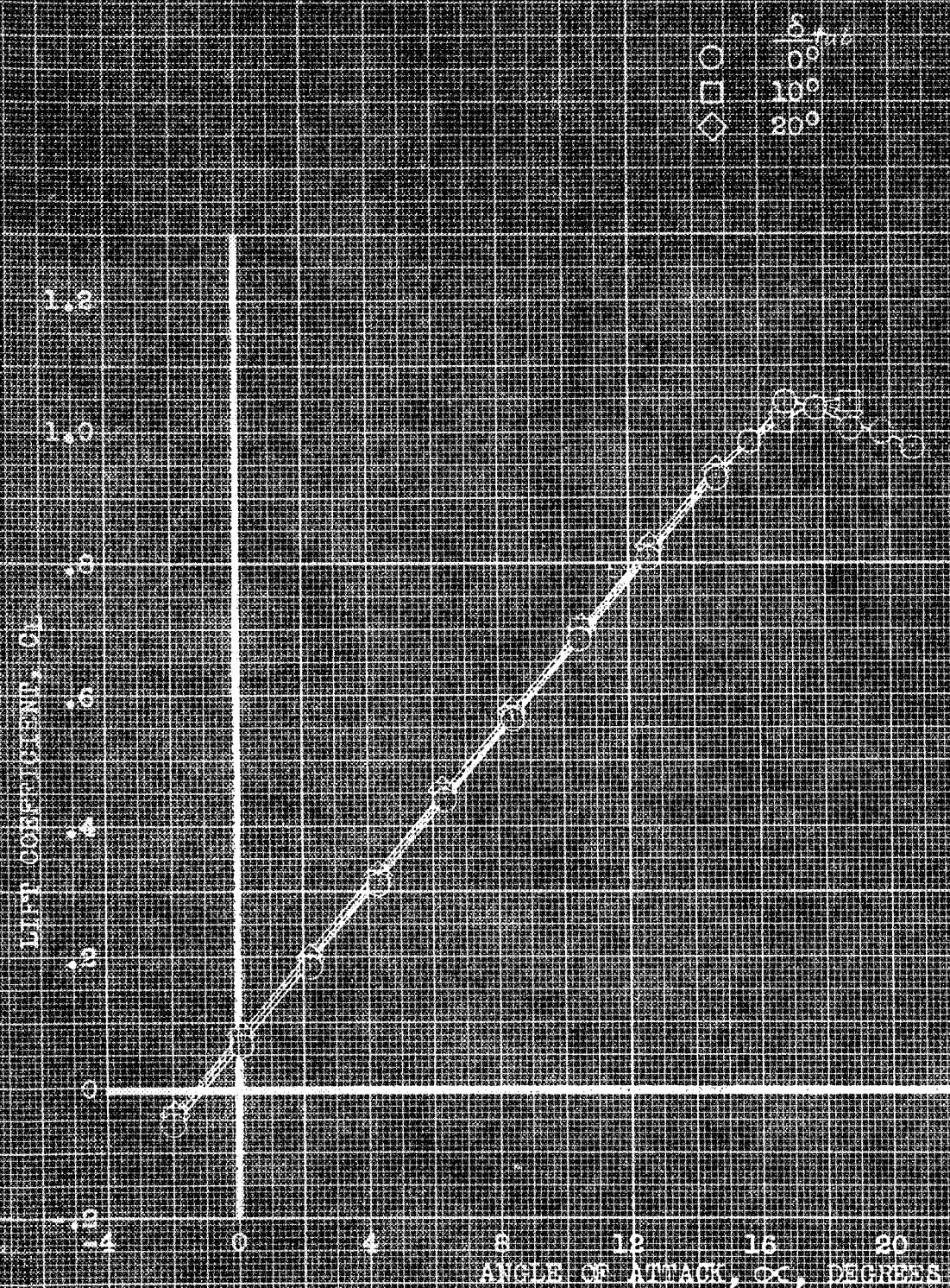


CONFIDENTIAL

Naval Air Station, Corpus Christi, Texas

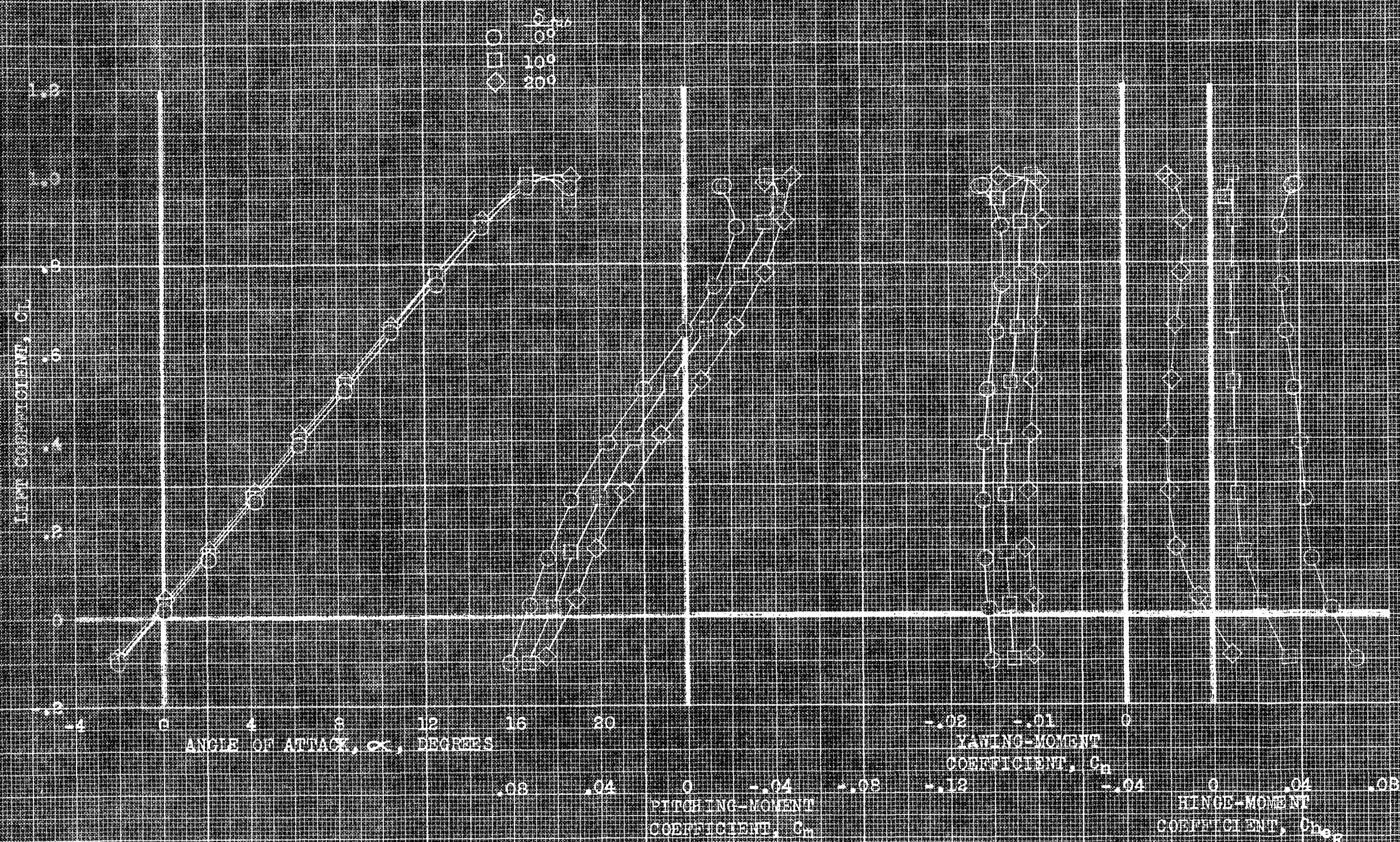
(a) $\delta_{wing} = 0^\circ$; α , C_L , C_m , C_n , C_{hR} vs C_L .

FIGURE 3. EFFECT OF FLIGHT SPEED ON THE DEFLECTION OF THE AERODYNAMIC CHARACTERISTICS OF THE MODEL IN PITCH AT SEVERAL ELEVATION ANGLES. FLAT WING; $1w, 0^\circ$.



(b) $\delta = 0^\circ, 10^\circ, 20^\circ$ for Curve C_L .

FIGURE 5. CONTINUED.



(a) δ_{deg} , α , C_L , C_m , C_n , C_{h_R} vs α
 FIGURE 10. - CONCLUDED.

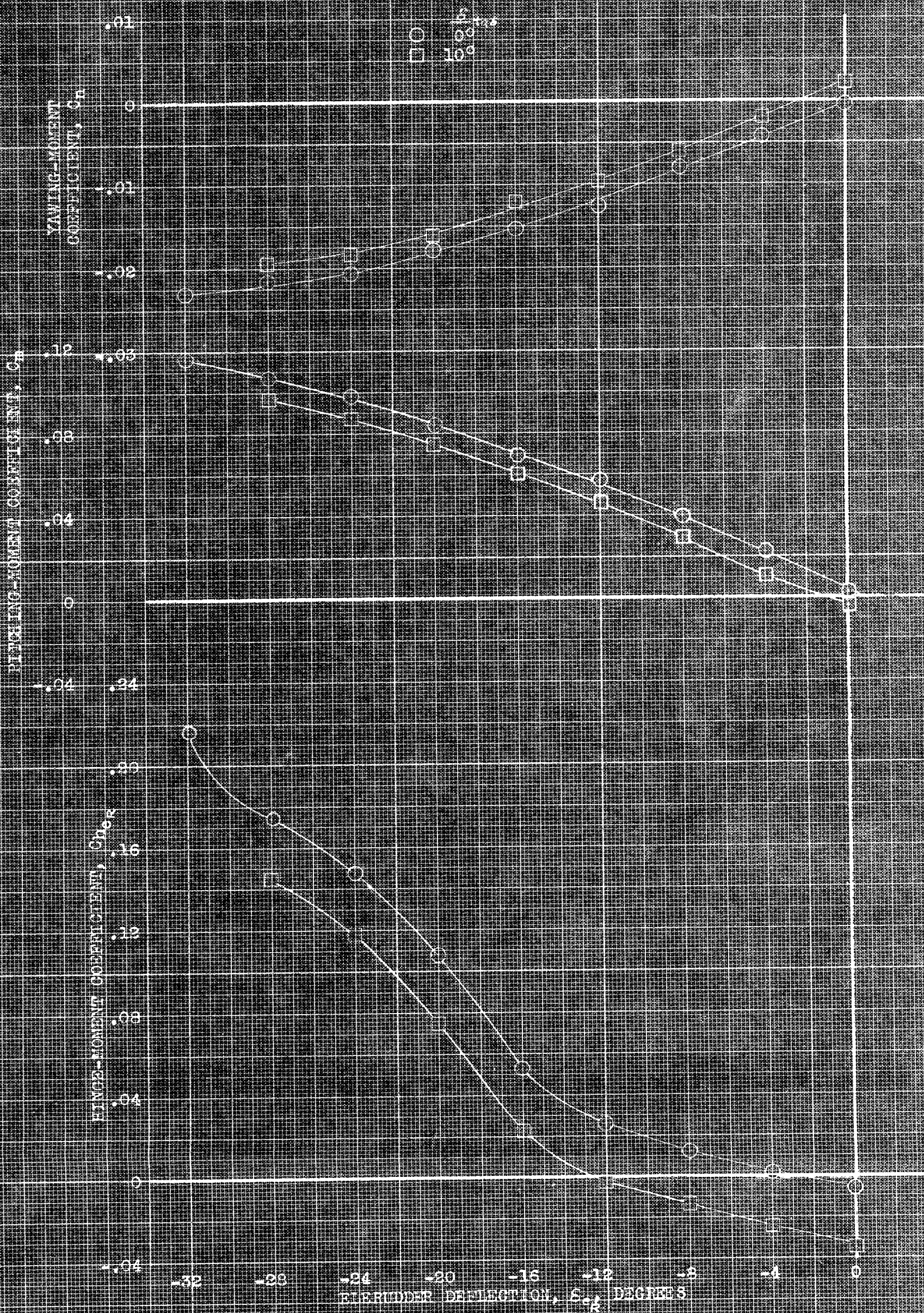
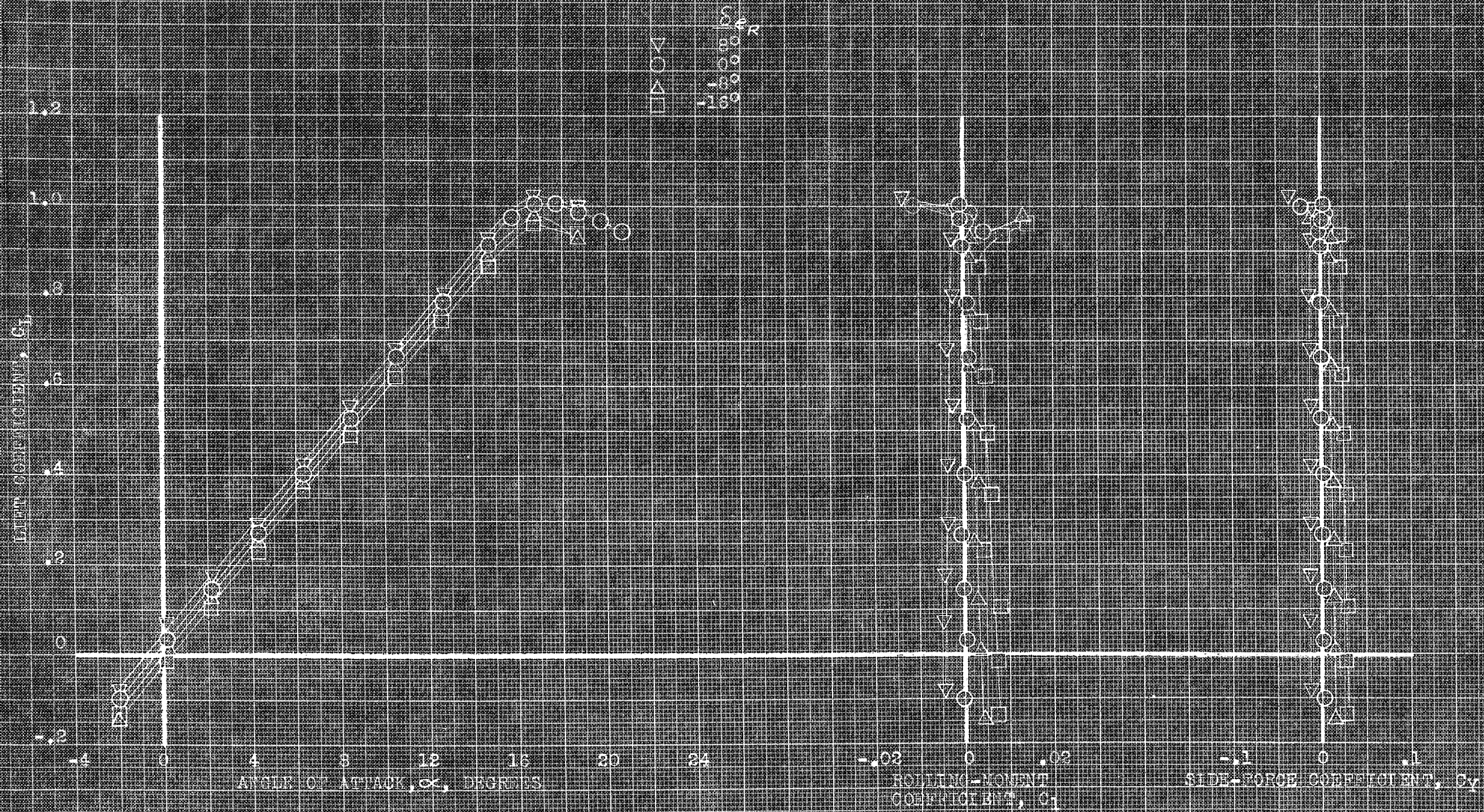


FIGURE 56.- VARIATION WITH ELEVATOR DEFLECTION OF THE AERODYNAMIC CHARACTERISTICS OF THE MODEL FOR SEVERAL TRIM TAB ANGLES. PLAIN WING; $1_w, 0^\circ$.



(a) α , C_L , C_M vs α .

FIGURE 10. EFFECT OF FIXED DEFLECTIONS OF THE FLAP ON THE AERODYNAMIC CHARACTERISTICS OF THE MODEL IN HIGH-EXTRUDER FLOW.

CONFIDENTIAL

NATIONAL ADVISORY COMMITTEE ON AERONAUTICS

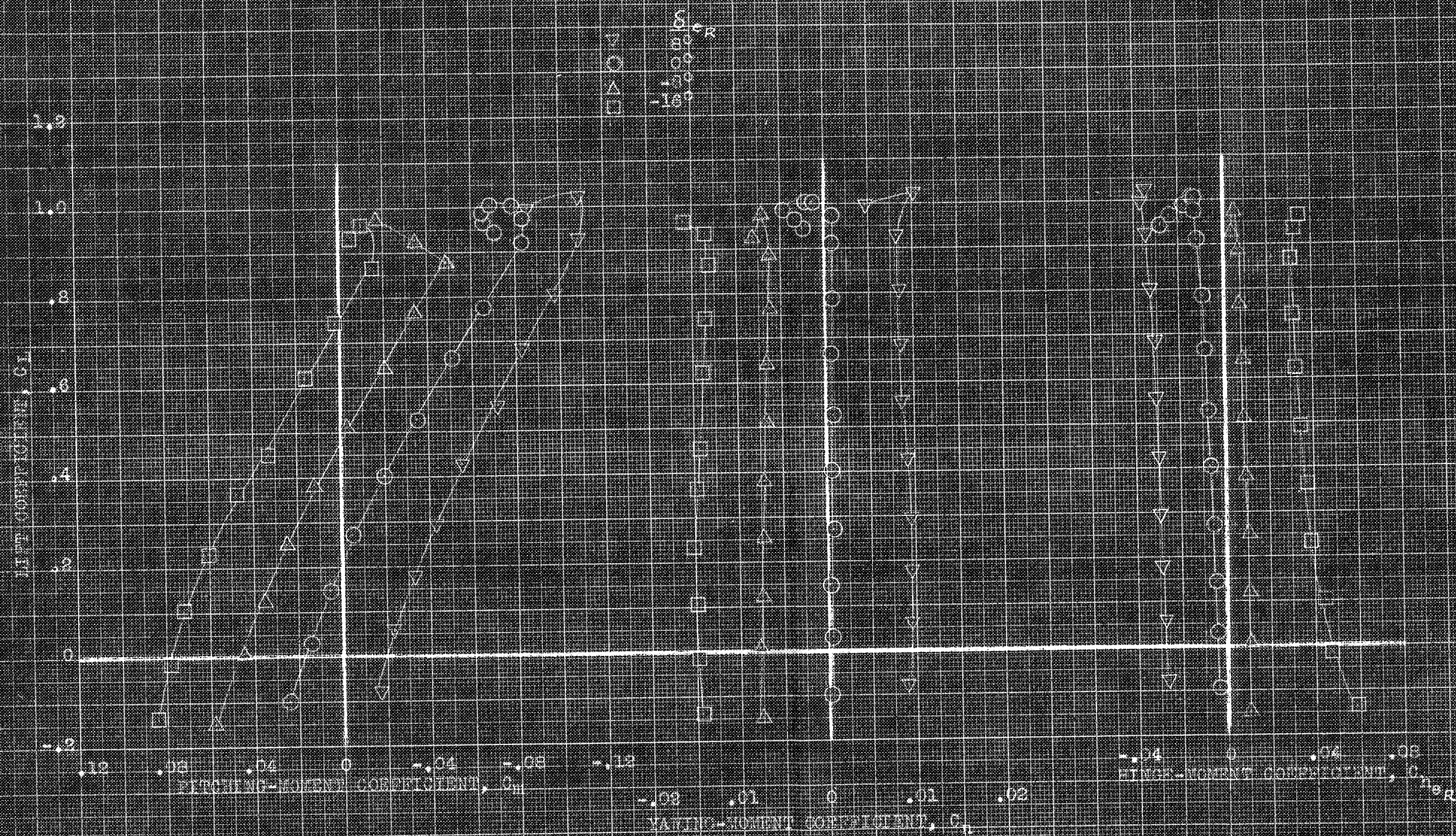


FIGURE 2. - CONTINUED.

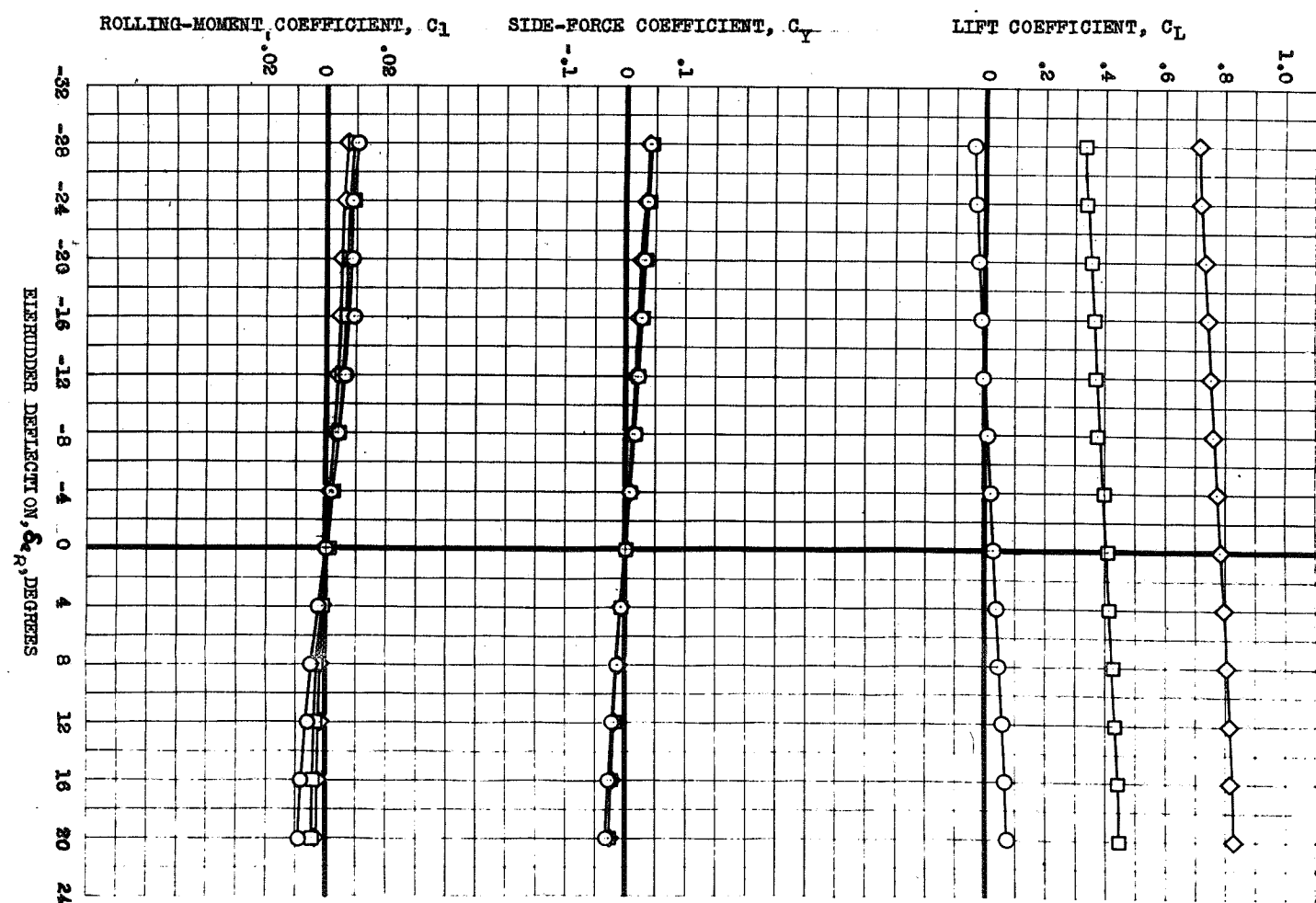
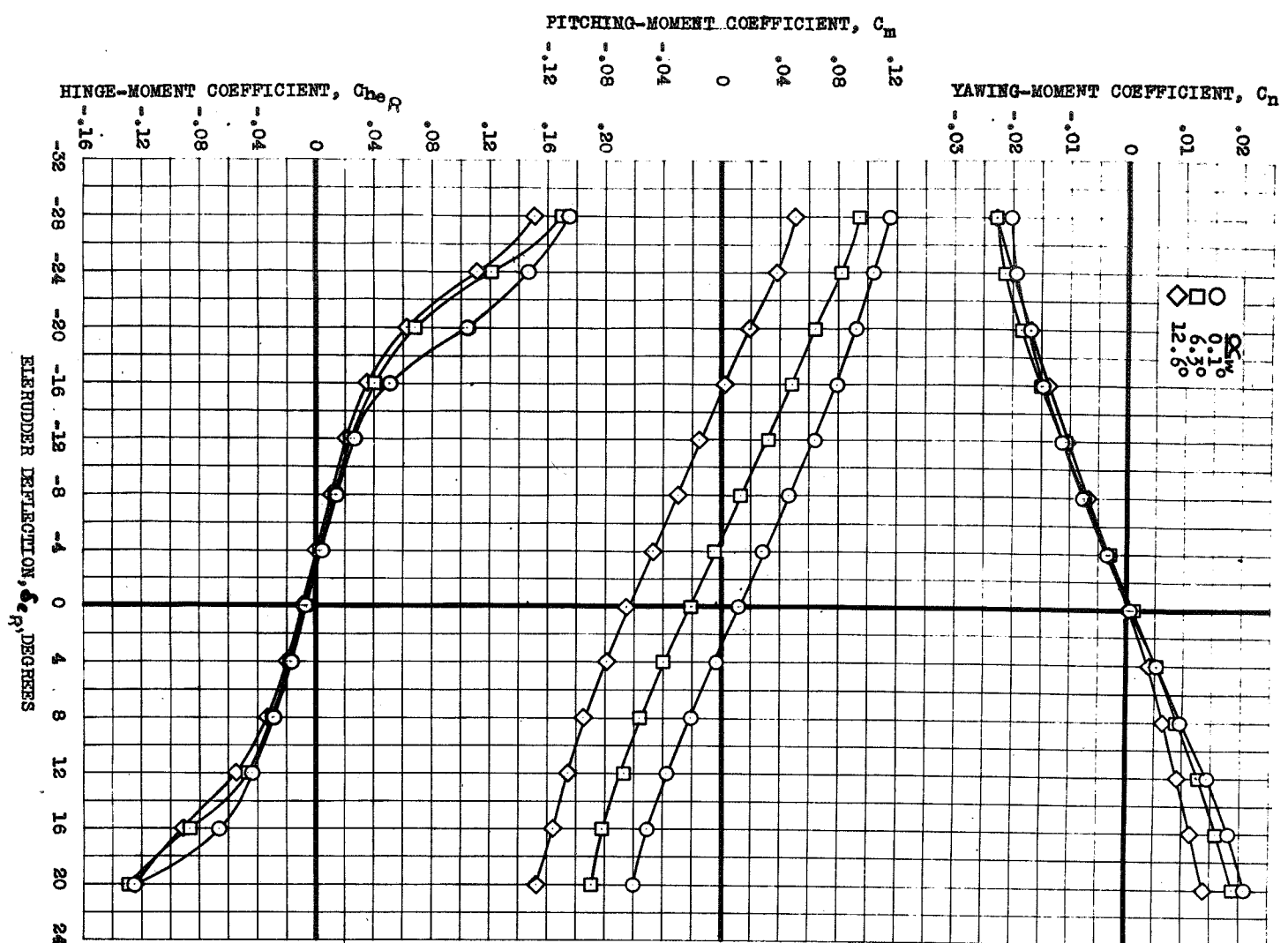


FIGURE 61.- VARIATION WITH ELERUDDER DEFLECTION OF THE AERO-DYNAMIC CHARACTERISTICS OF THE MODEL AT SEVERAL ANGLES OF ATTACK. EXTERNAL TANKS; i_w , 0° .

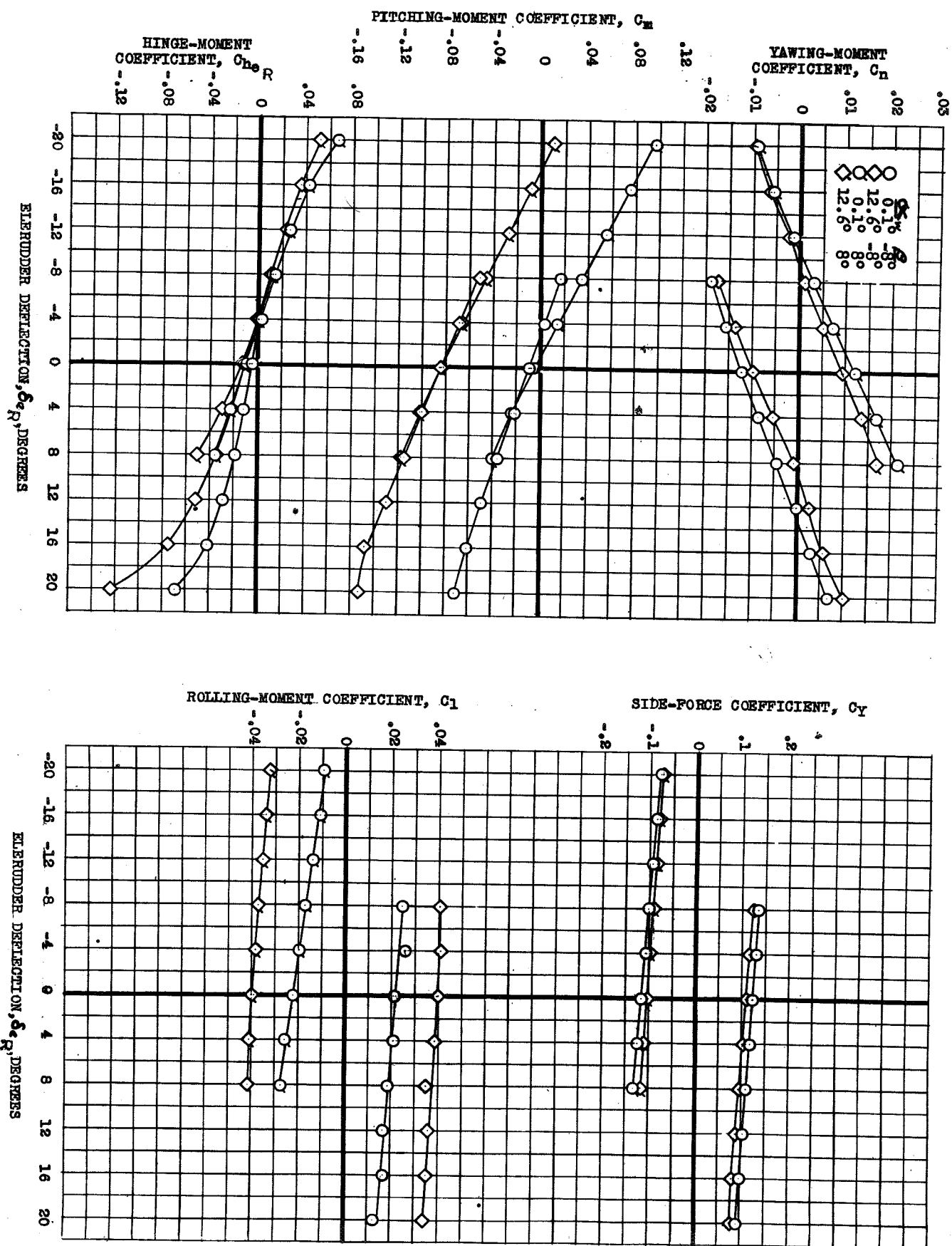
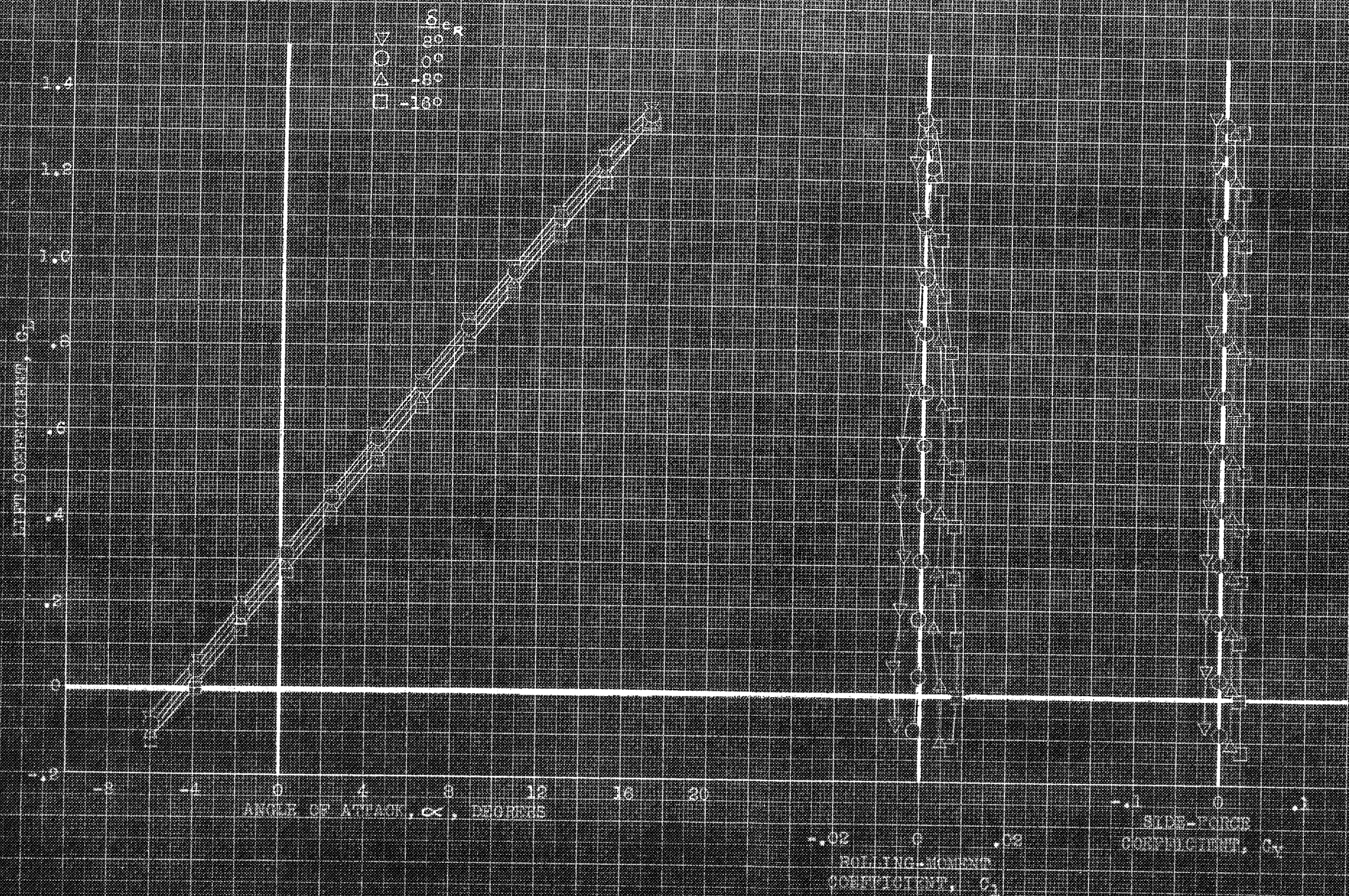
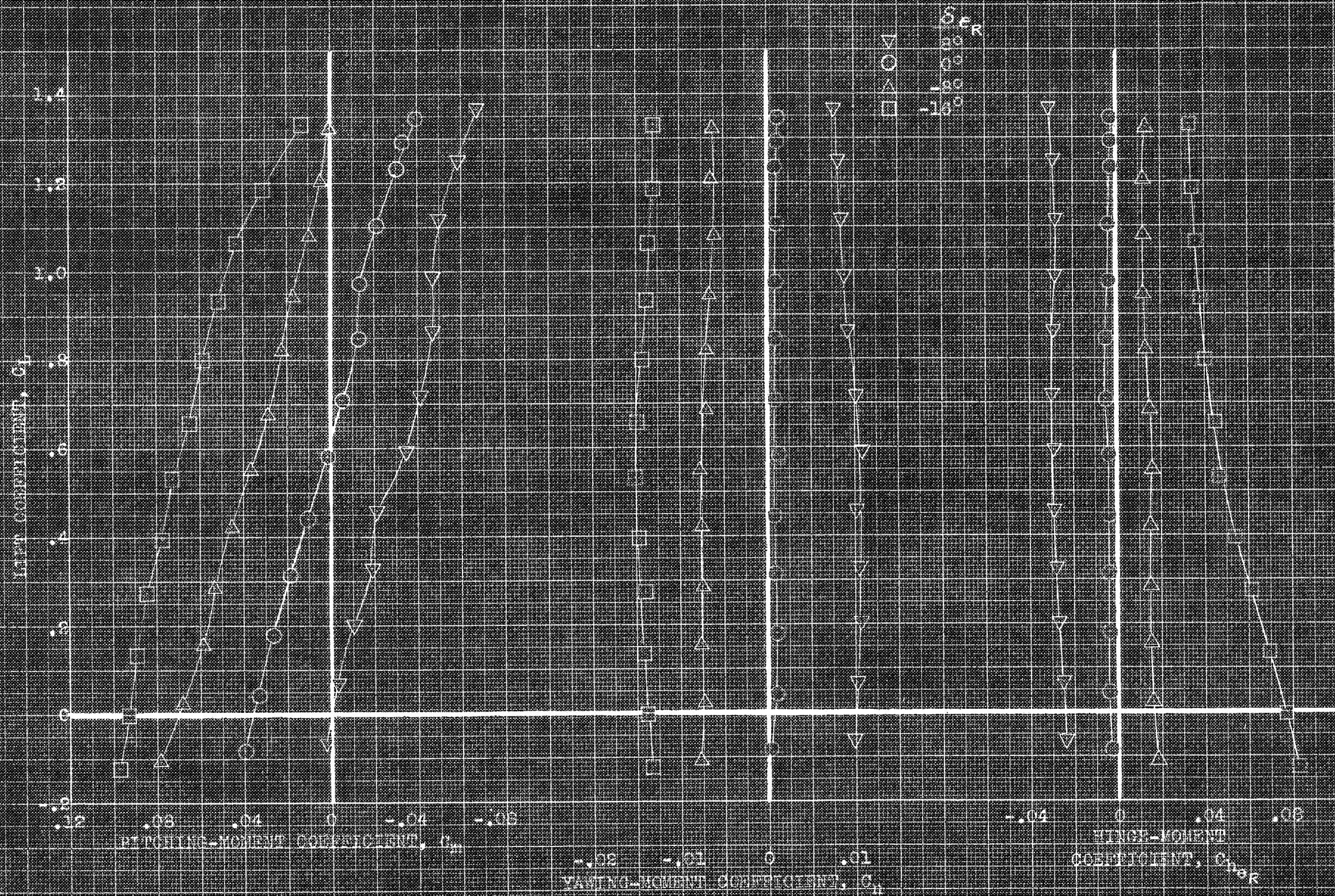


FIGURE 62.- VARIATION WITH ELERUDDER DEFLECTION OF THE AERO-DYNAMIC CHARACTERISTICS OF THE MODEL IN SIDESLIP AT SEVERAL ANGLES OF ATTACK. EXTERNAL TANKS; $1_w, 0^\circ$.



(a) α , C_L , C_Y vs α .

FIGURE 1. EFFECT OF THREE DEGREES OF FREEDOM ON THE AERODYNAMIC CHARACTERISTICS OF THE MODEL IN THREE DEGREES OF FREEDOM.



(a) C_L , C_M , C_{Y_0} vs C_{M_0}
 (b) C_L , C_M , C_{Y_0} vs C_{Y_0}

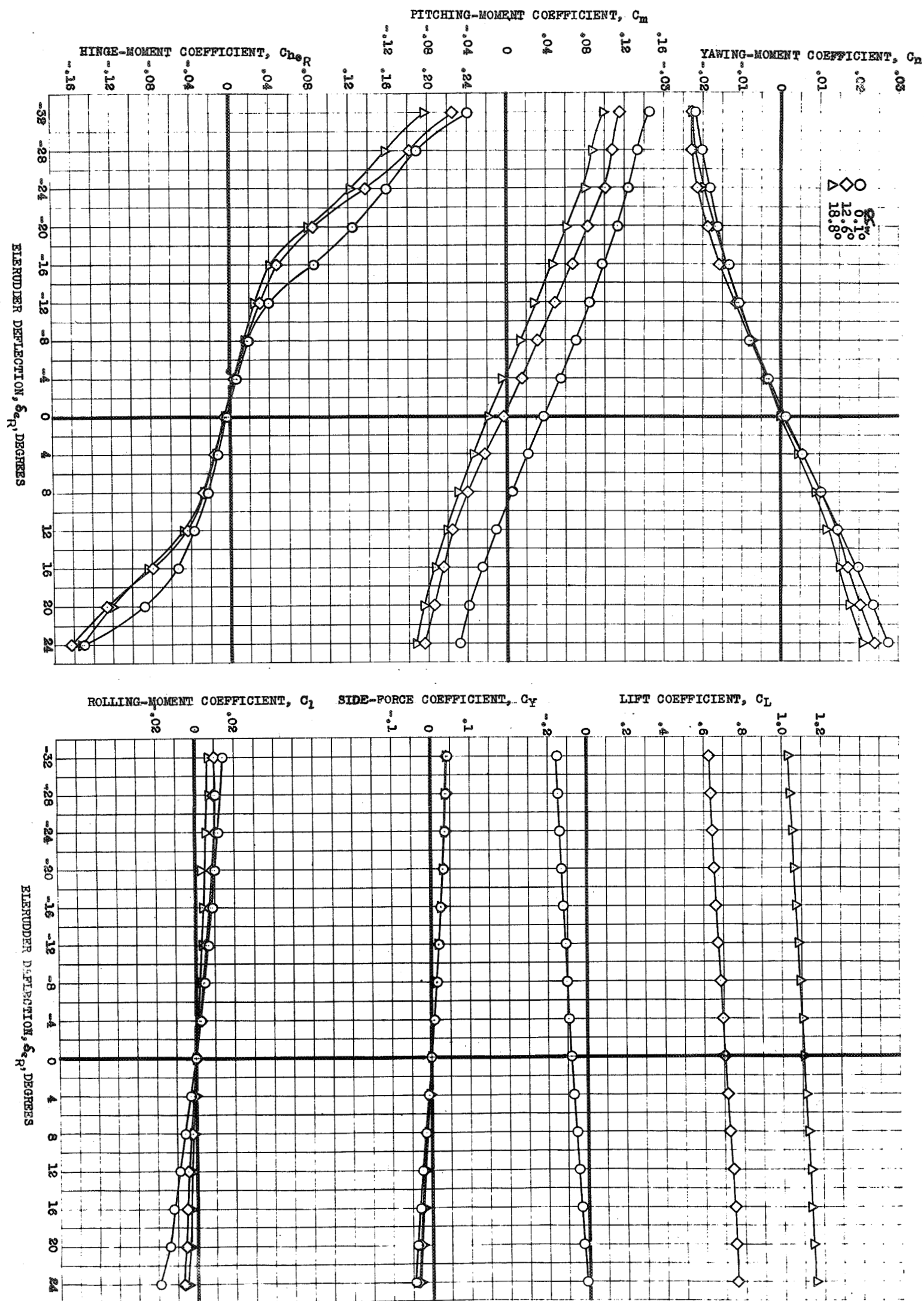


FIGURE 64.- VARIATION WITH ELERUDDER DEFLECTION OF THE AERO-
DYNAMIC CHARACTERISTICS OF THE MODEL AT SEVERAL ANGLES OF
ATTACK. EXTERNAL TANKS; DROOPED SLATS; GEAR; i_w , 6° .

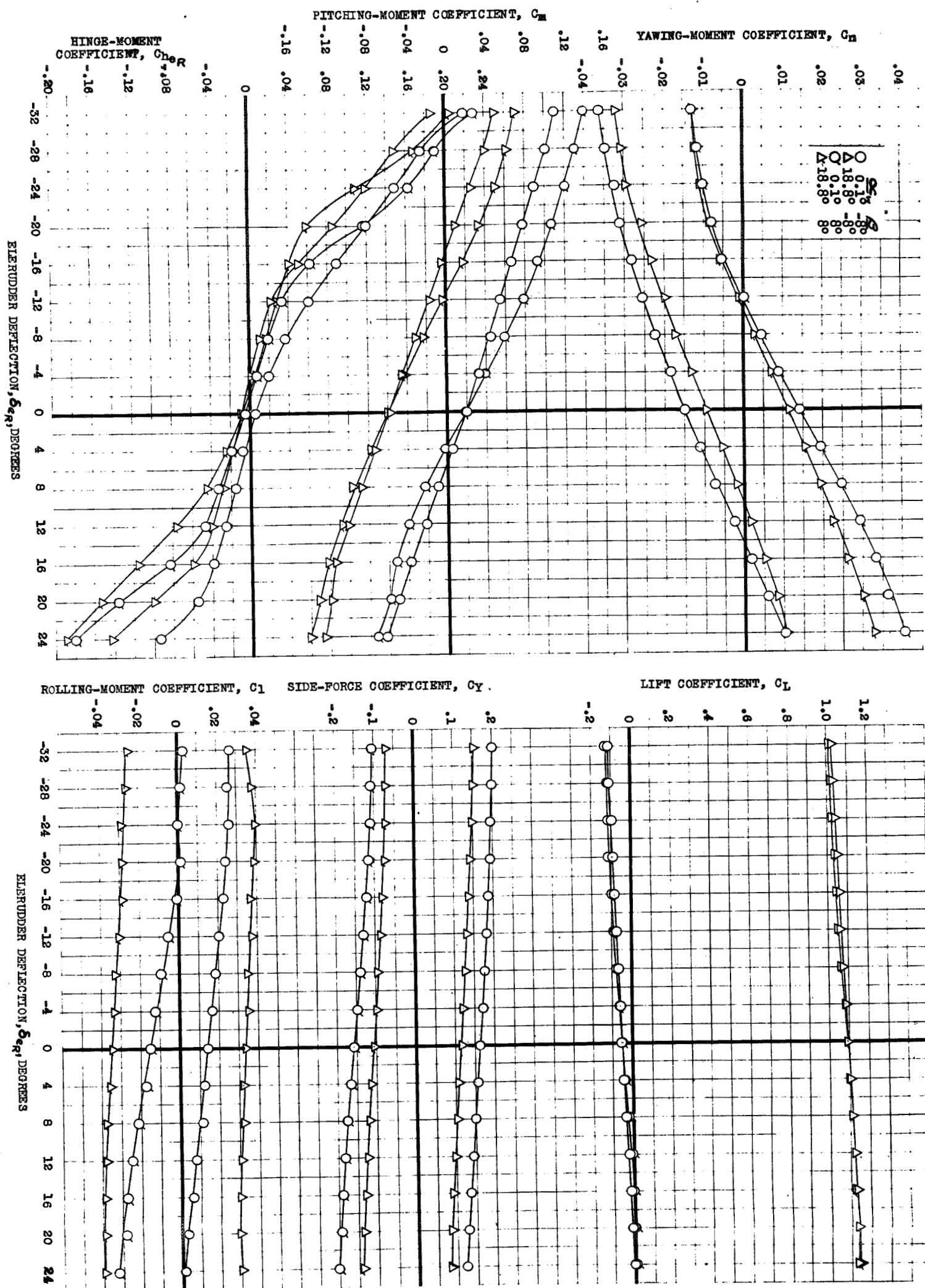
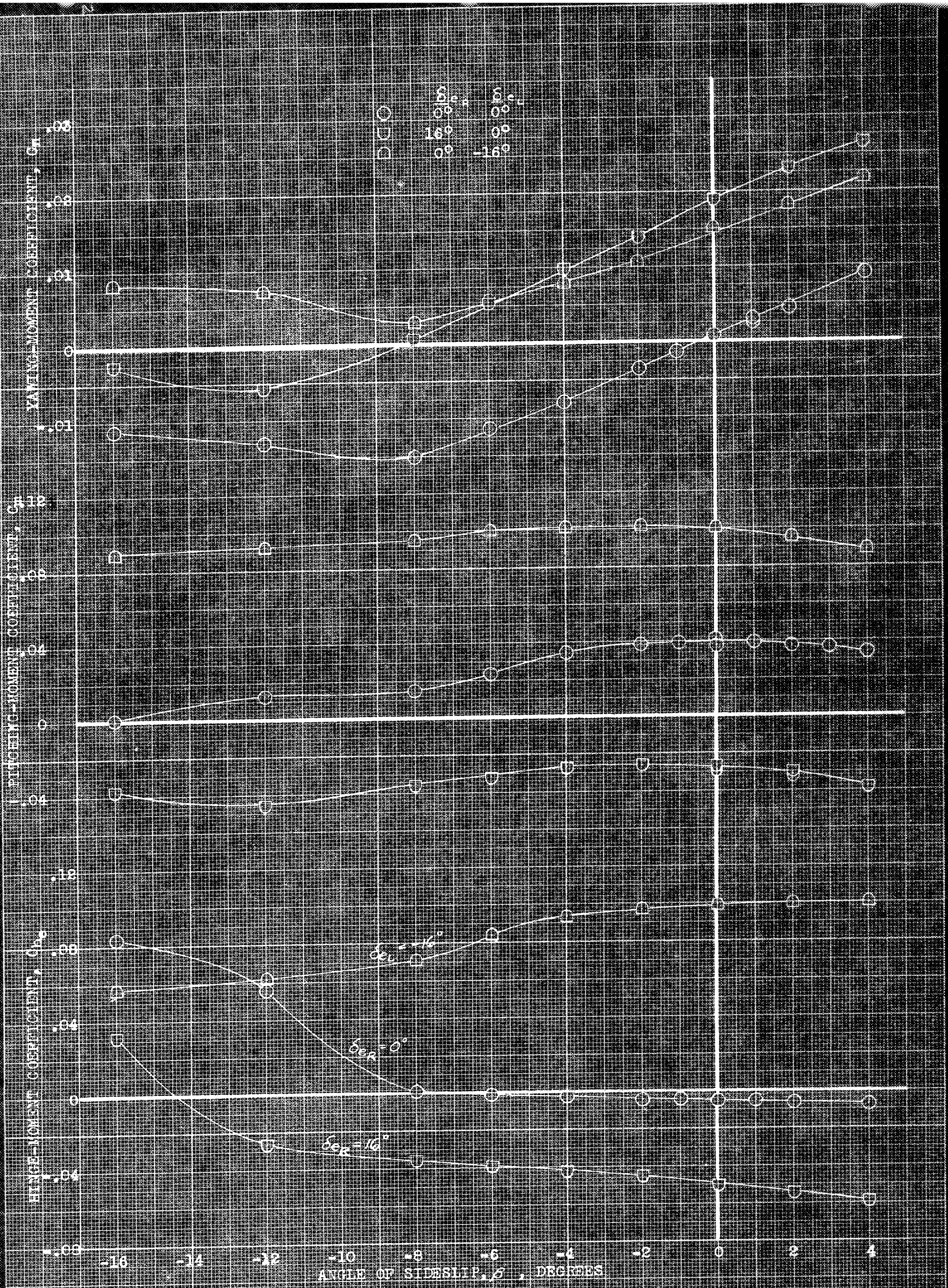
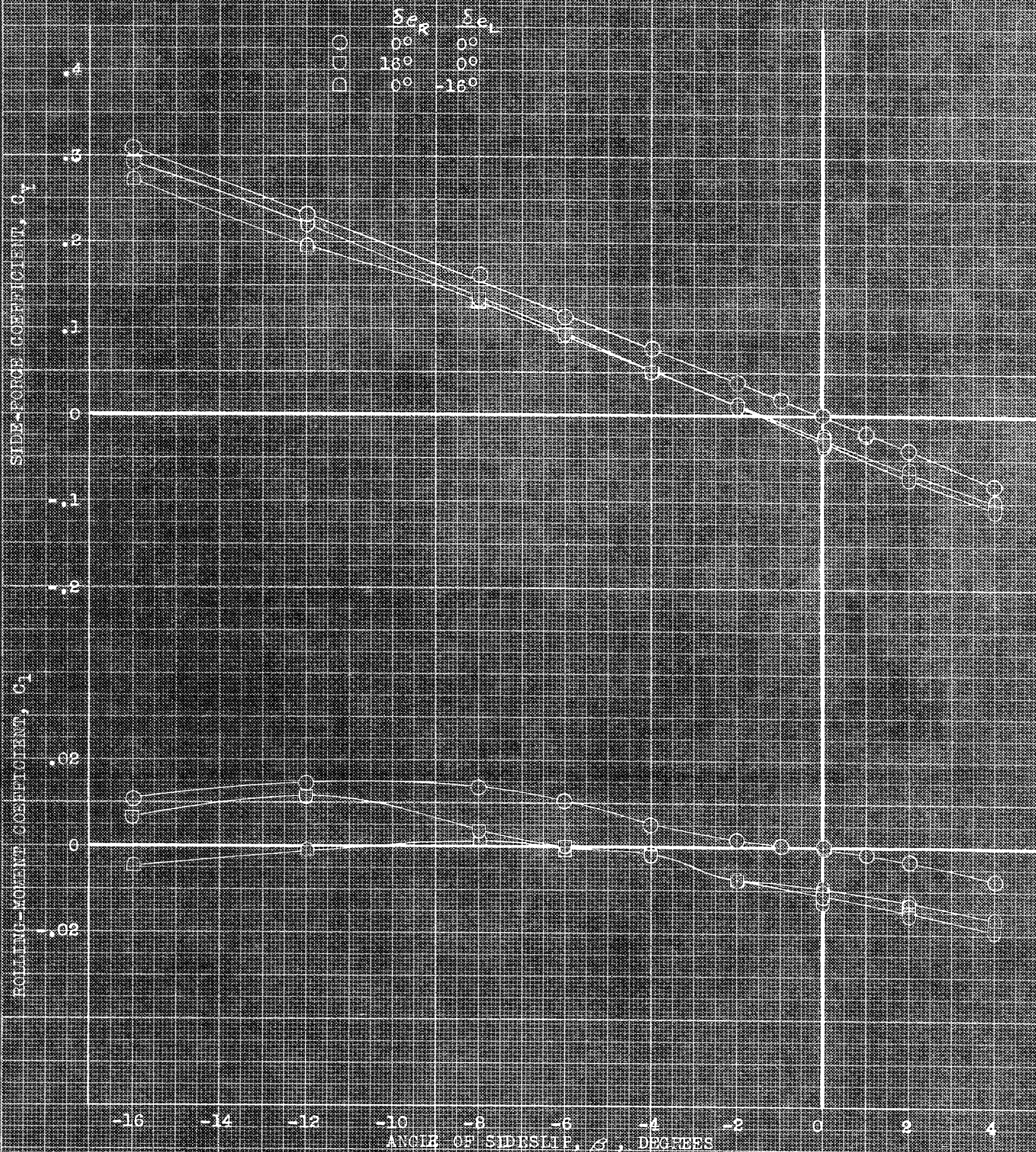


FIGURE 65.- VARIATION WITH ELERUDDER DEFLECTION OF THE AERO-DYNAMIC CHARACTERISTICS OF THE MODEL IN SIDESLIP AT SEVERAL ANGLES OF ATTACK. GEAR; EXTERNAL TANKS; DROPPED SLATS; i_w , 6°.



(a) $\alpha_w = 0^\circ$; C_{ny} , C_{nr} , C_{ye} vs δ .
 FIGURE 62. INFLUENCE OF FIXED CONFIGURATIONS OF THE SUPERBINDER ON THE AERODYNAMIC CHARACTERISTICS OF THE MODEL IN SIDESLIP. EXTERNAL TANKS, GEAR, DROOPED SLATS; $\alpha_w = 6^\circ$.



(b) $\alpha_n, 0^\circ$; C_Y, C_L vs β .
FIGURE 66.- CONTINUED.

	δ_{CR}	δ_{CL}
○	0°	0°
□	16°	0°
△	0°	-16°

ROLLING-MOMENT
COEFFICIENT, C_{Lr}

ROLLING-MOMENT
COEFFICIENT, C_{Lr}

ROLLING-MOMENT
COEFFICIENT, C_{Lr}

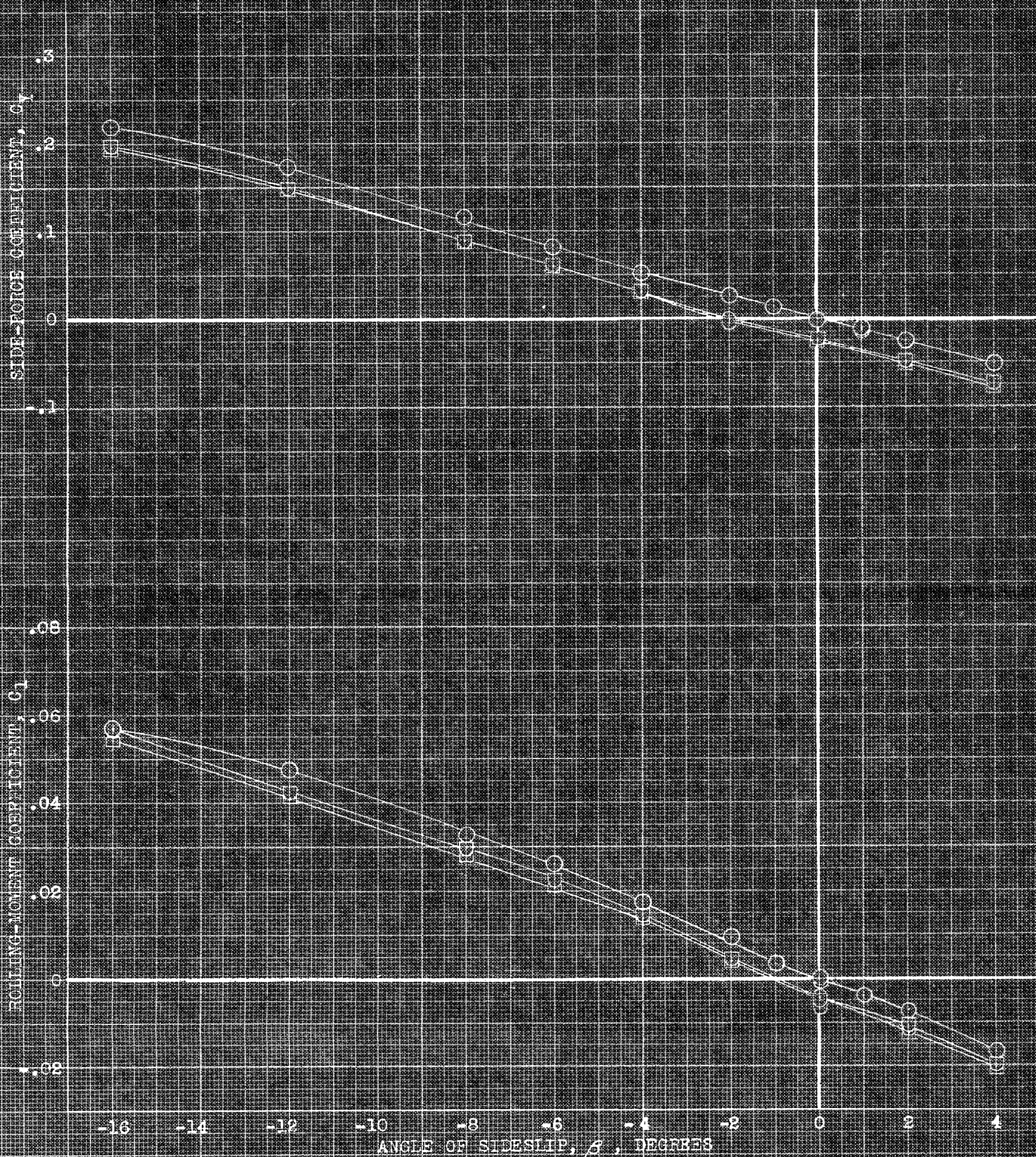
ANGLE OF SIDESLIP, β , DEGREES

(continued) $\delta_{CL} = 16.0^\circ$, C_{Lr} , C_{Lr} , C_{Lr} vs β

FIGURE 66 (continued)

CONFIDENTIAL
NATIONAL ADVISORY COMMITTEE FOR AERONAUTICS

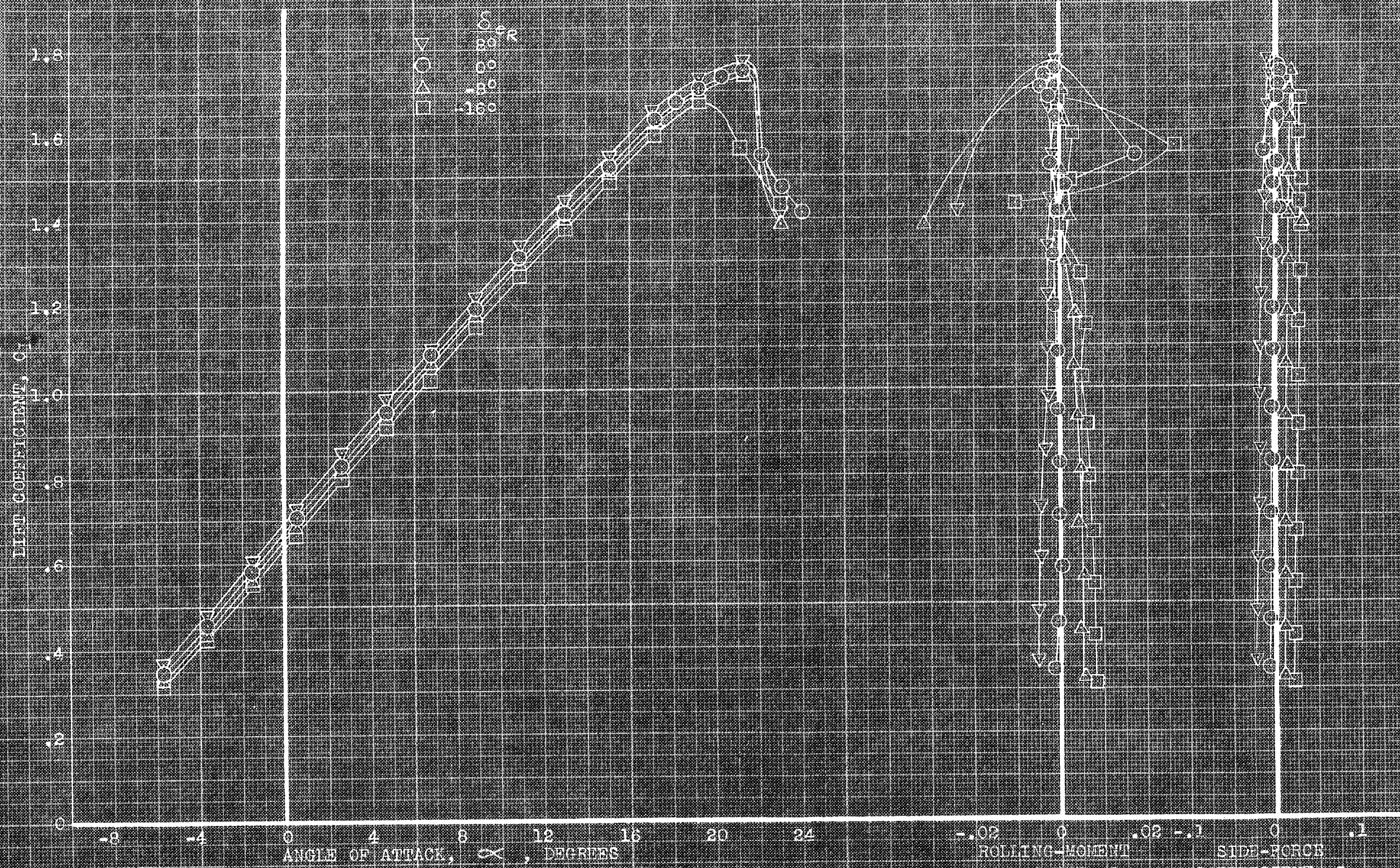
$\frac{\delta}{\alpha}$	$\frac{\delta}{\alpha} R$	$\frac{\delta}{\alpha} L$
0°	0°	0°
16°	0°	0°
0°	16°	-16°



(a) $\alpha_w, 18.8^\circ$; C_y, C_l vs β .

FIGURE 66. - CONCLUDED.

CONFIDENTIAL
NATIONAL ADVISORY COMMITTEE FOR AERONAUTICS

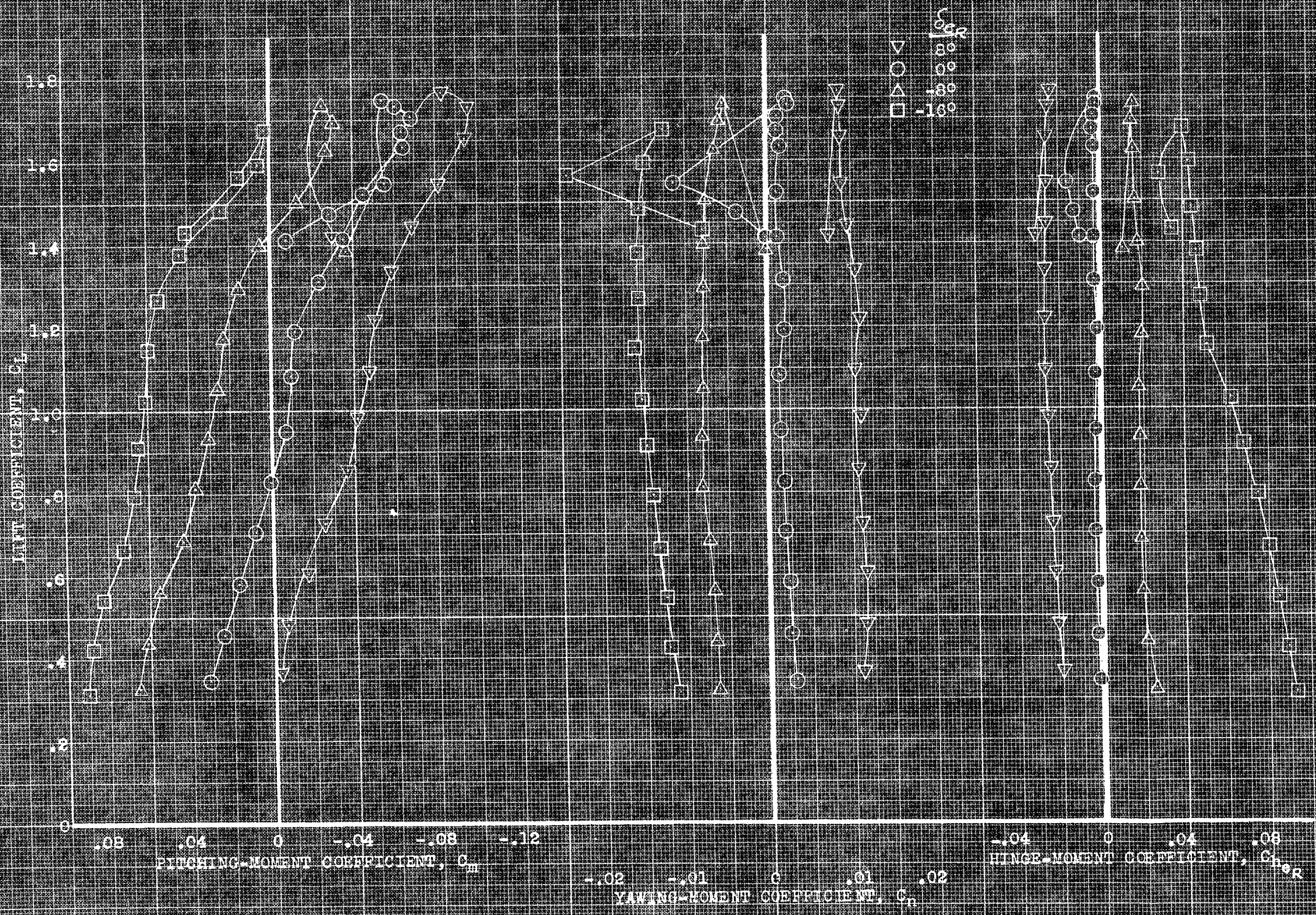


(a) α , C_L , C_l vs C_y .

FIGURE 67. EFFECT OF FIXED DEFLECTIONS OF THE PILERIDER ON THE AERODYNAMIC CHARACTERISTICS OF THE MODEL IN PITCH, GEAR, DROPPED FLAPS, 400, 1w, 60.

CONFIDENTIAL

NATIONAL ADVISORY COMMITTEE FOR AERONAUTICS



(b) C_m vs C_L vs C_n

FIGURE 17. - CONCLUDED.

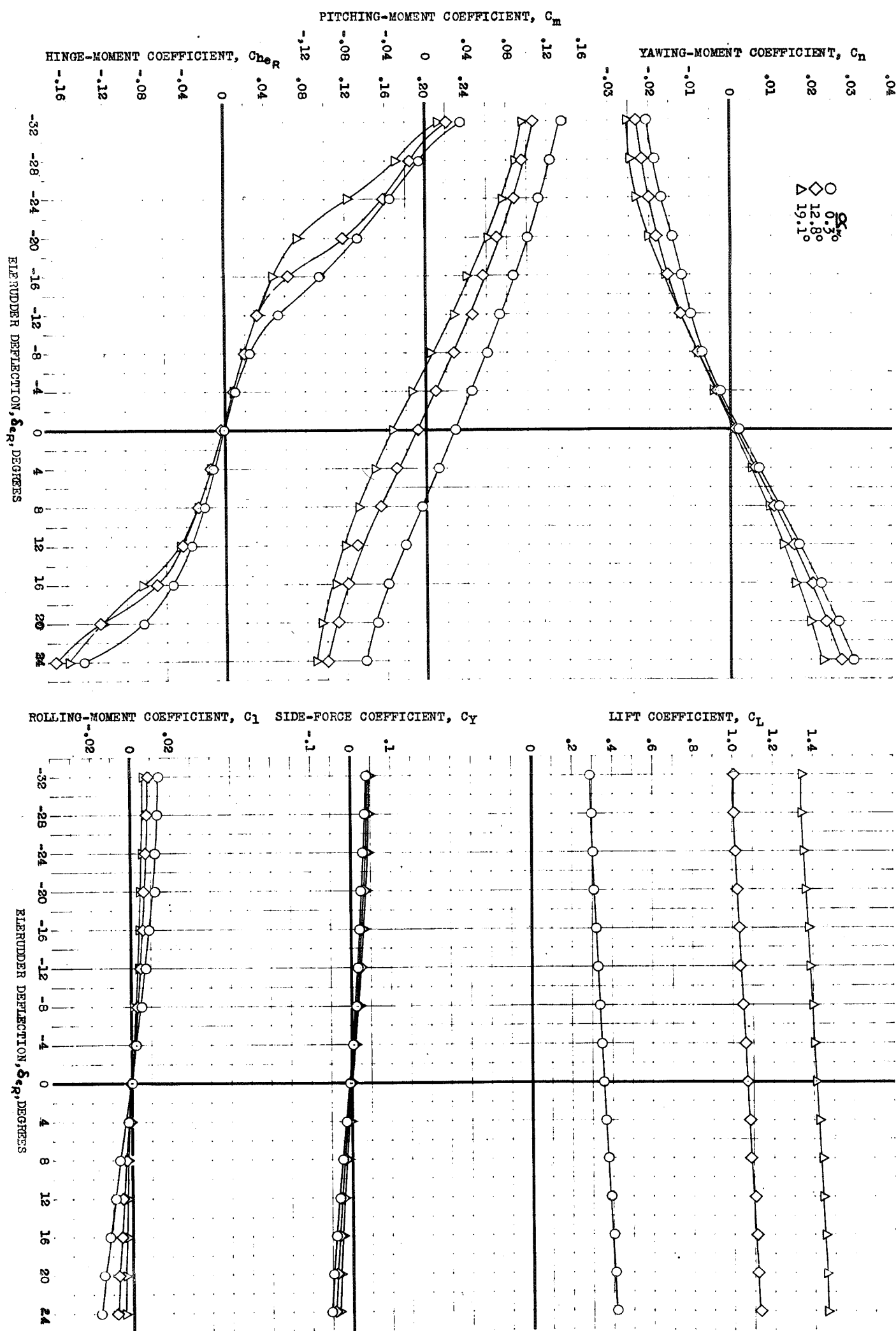


FIGURE 68.- VARIATION WITH ELERUDDER DEFLECTION OF THE AERO-DYNAMIC CHARACTERISTICS OF THE MODEL AT SEVERAL ANGLES OF ATTACK. GEAR; DROOPED SLATS; PLAIN FLAPS, 40° ; i_w , 6° .

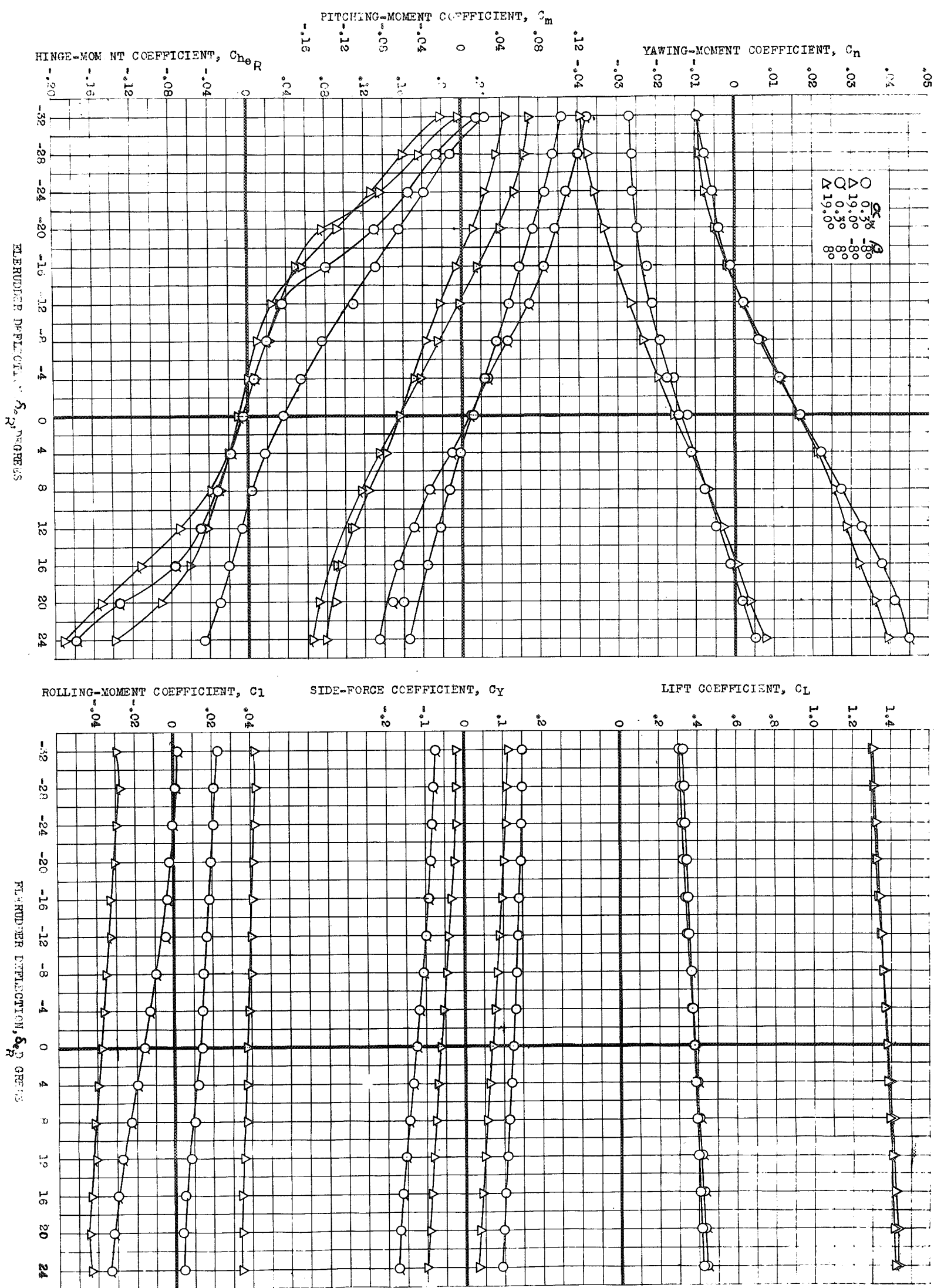
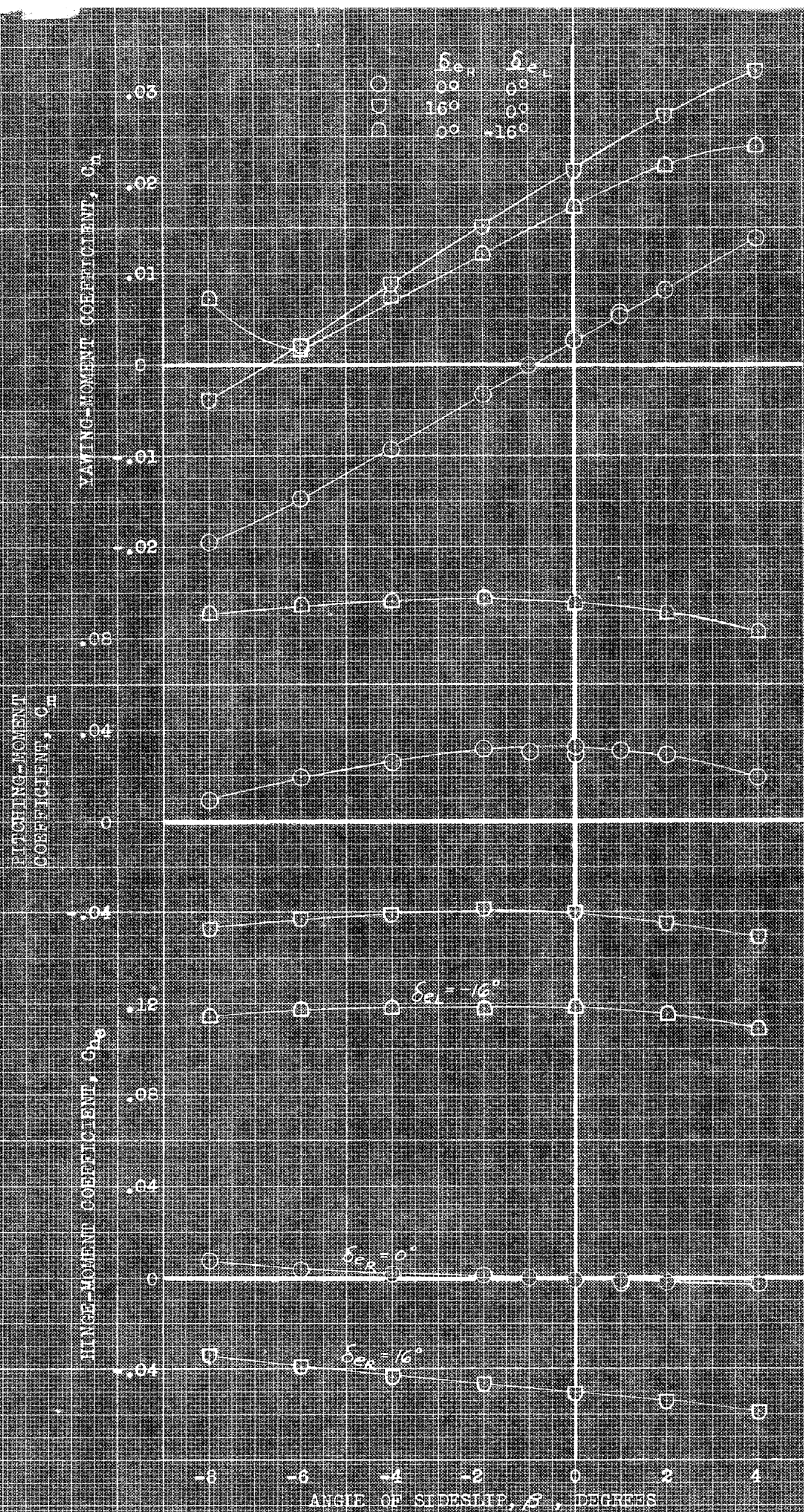


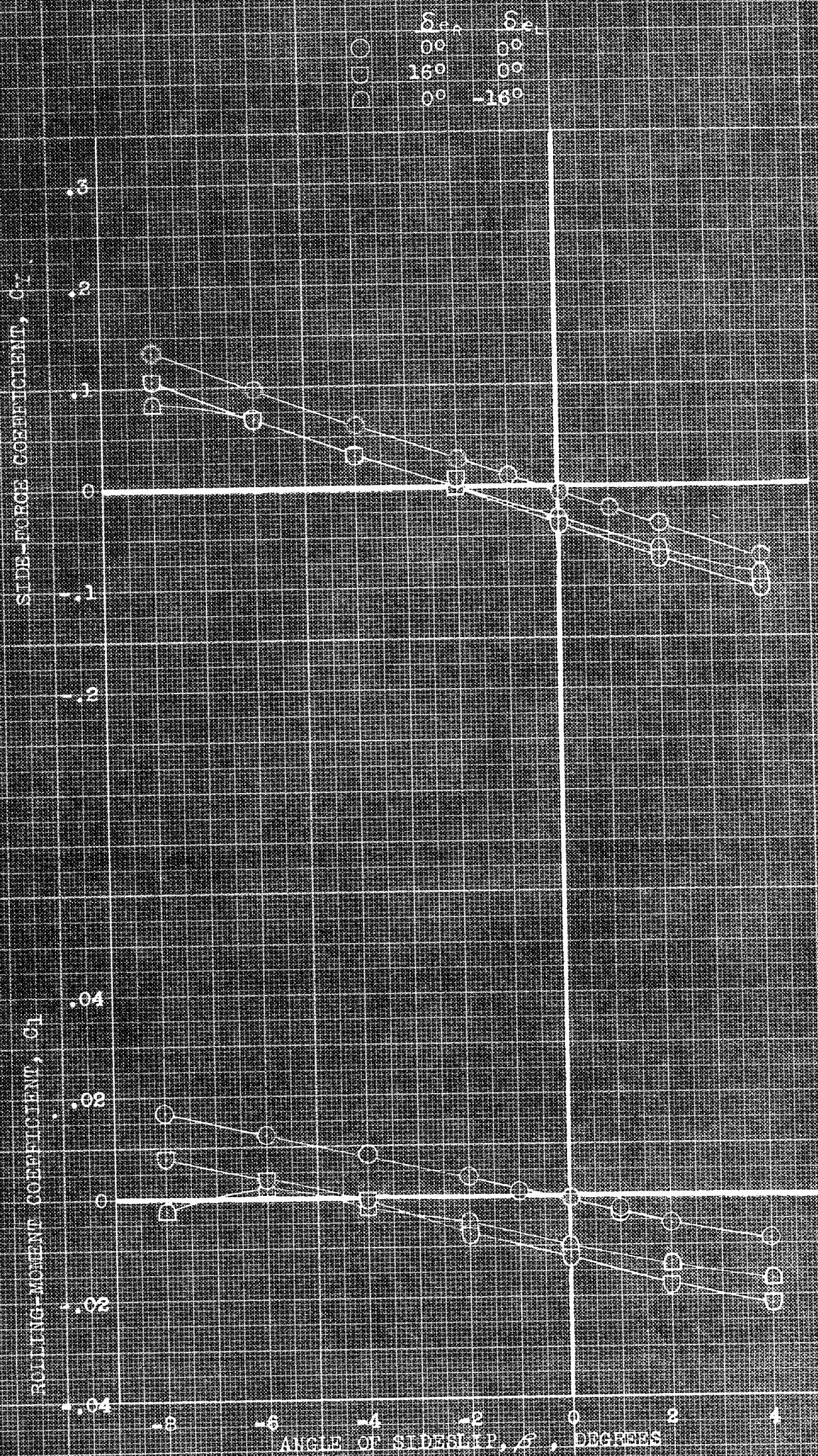
FIGURE 69.- VARIATION WITH ELERUDDER DEFLECTION OF THE AERO-DYNAMIC CHARACTERISTICS OF THE MODEL IN SIDESLIP AT SEVERAL ANGLES OF ATTACK. GEAR; DROOPED SLATS; PLAIN FLAPS, 40° ; i_w , 6° .



(a) $\alpha_w, 0.5^\circ$; $\delta_{eR}, \delta_{eL}, C_{h\delta}$ vs β .

FIGURE 76.- EFFECT OF FIXED DEFLECTIONS OF THE ELERIDDER ON THE AERODYNAMIC CHARACTERISTICS OF THE MODEL IN SIDESLIP. GEAR; DROOPED SLATS; PLAIN FLAPS, 40° ; $i_w, 6^\circ$.

CONFIDENTIAL
NATIONAL ADVISORY COMMITTEE FOR AERONAUTICS

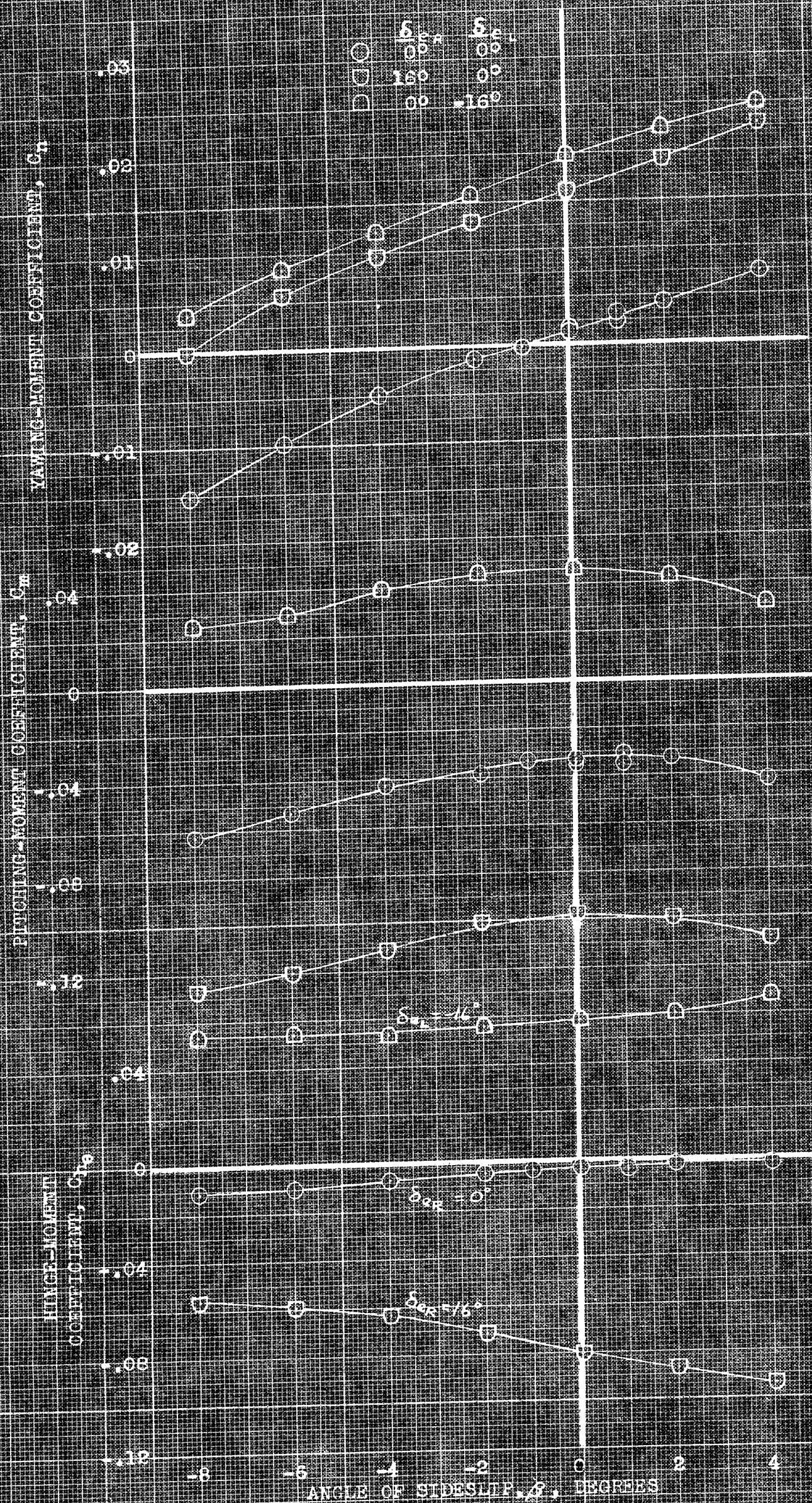


(b) $\alpha_w, 0.3^\circ$; C_Y, C_L vs β .

FIGURE 10. - CONTINUED.

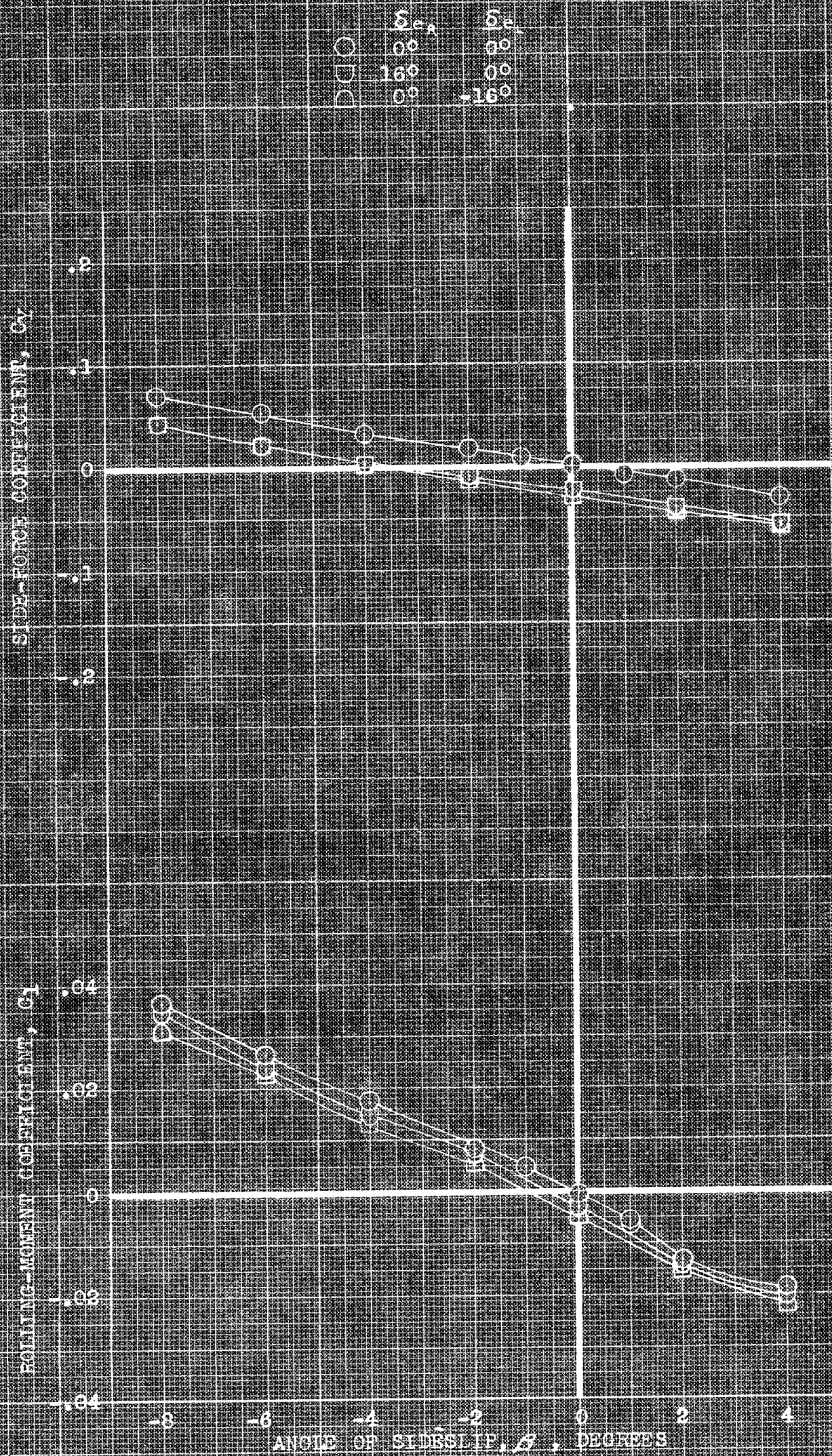
CONFIDENTIAL

NOT FOR DISTRIBUTION OUTSIDE OF AGENCY



(c) $\alpha_w = 18.6^\circ$; C_n , C_m , C_{mo} vs β .

FIGURE 70. - CONTINUED.



(d) $\alpha = 18.5^\circ$; C_y, C_l vs β

FIGURE 70 (Continued)

CONFIDENTIAL
NATIONAL ADVISORY COMMITTEE FOR AERONAUTICS

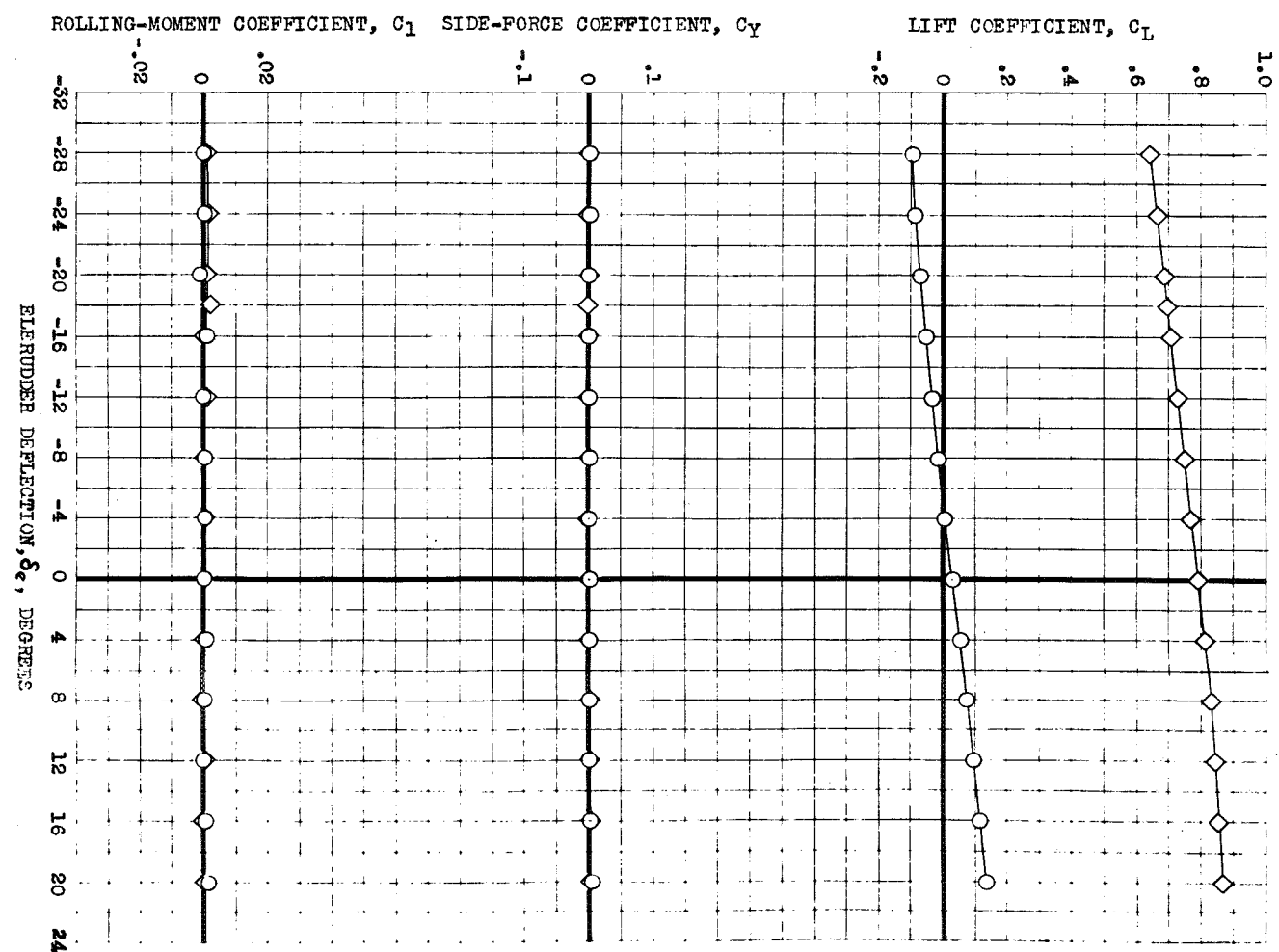
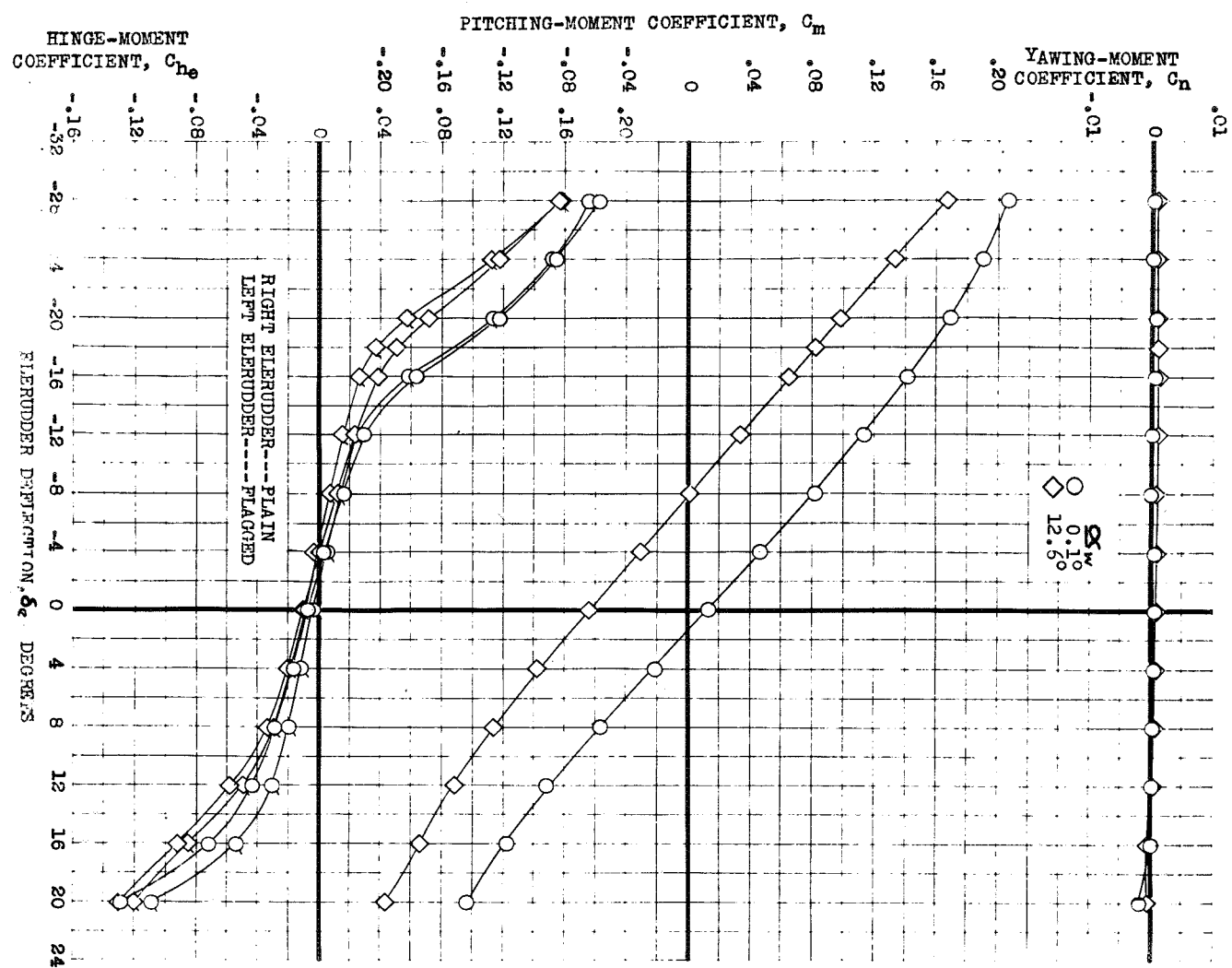


FIGURE 71.- EFFECTIVENESS OF THE COMPLETE ELERUDDER SYSTEM OPERATED FOR PURE ELEVATOR ACTION WITH THE MODEL AT SEVERAL ANGLES OF ATTACK. EXTERNAL TANKS; $i_w, 0^\circ$; $\epsilon, 0^\circ$.

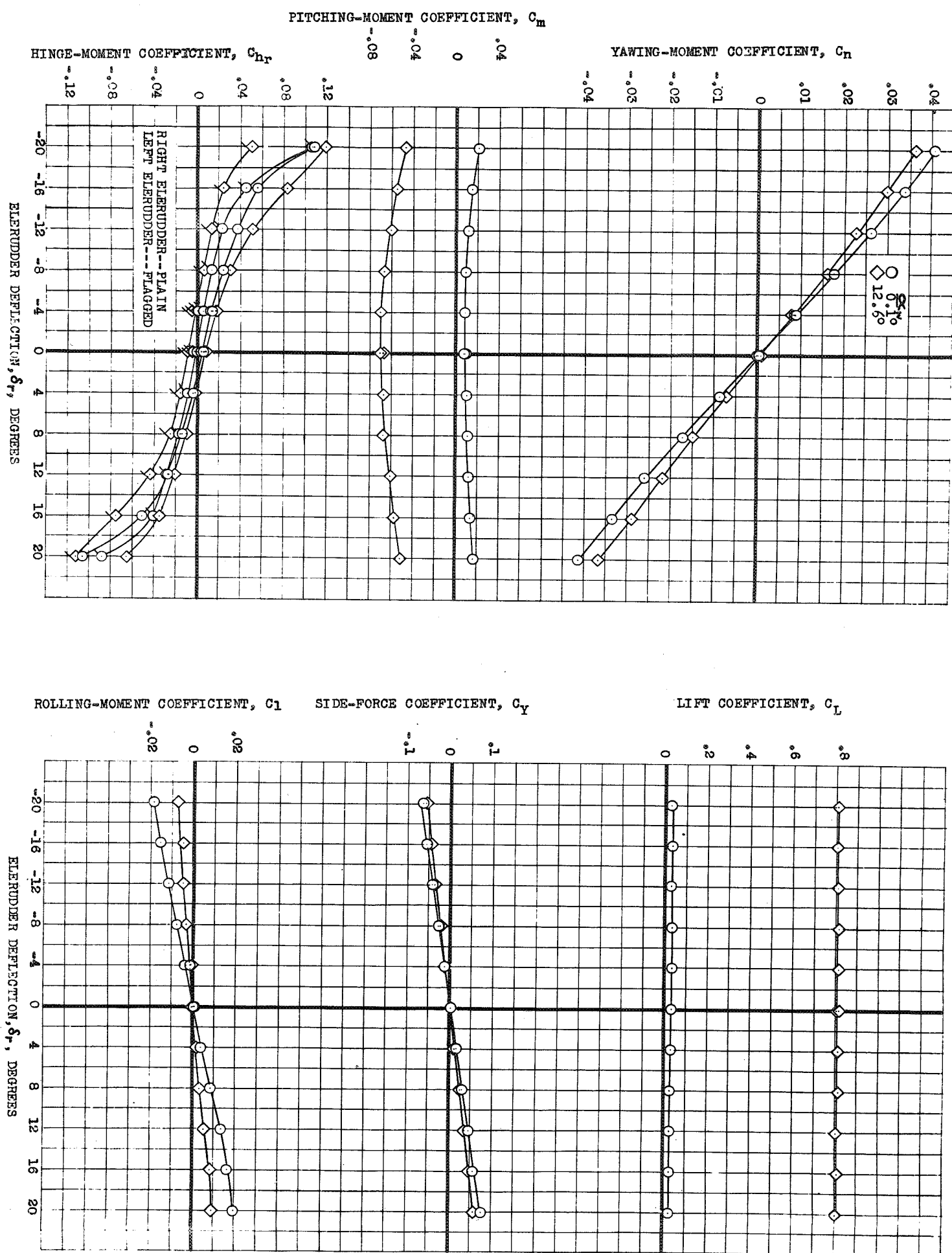
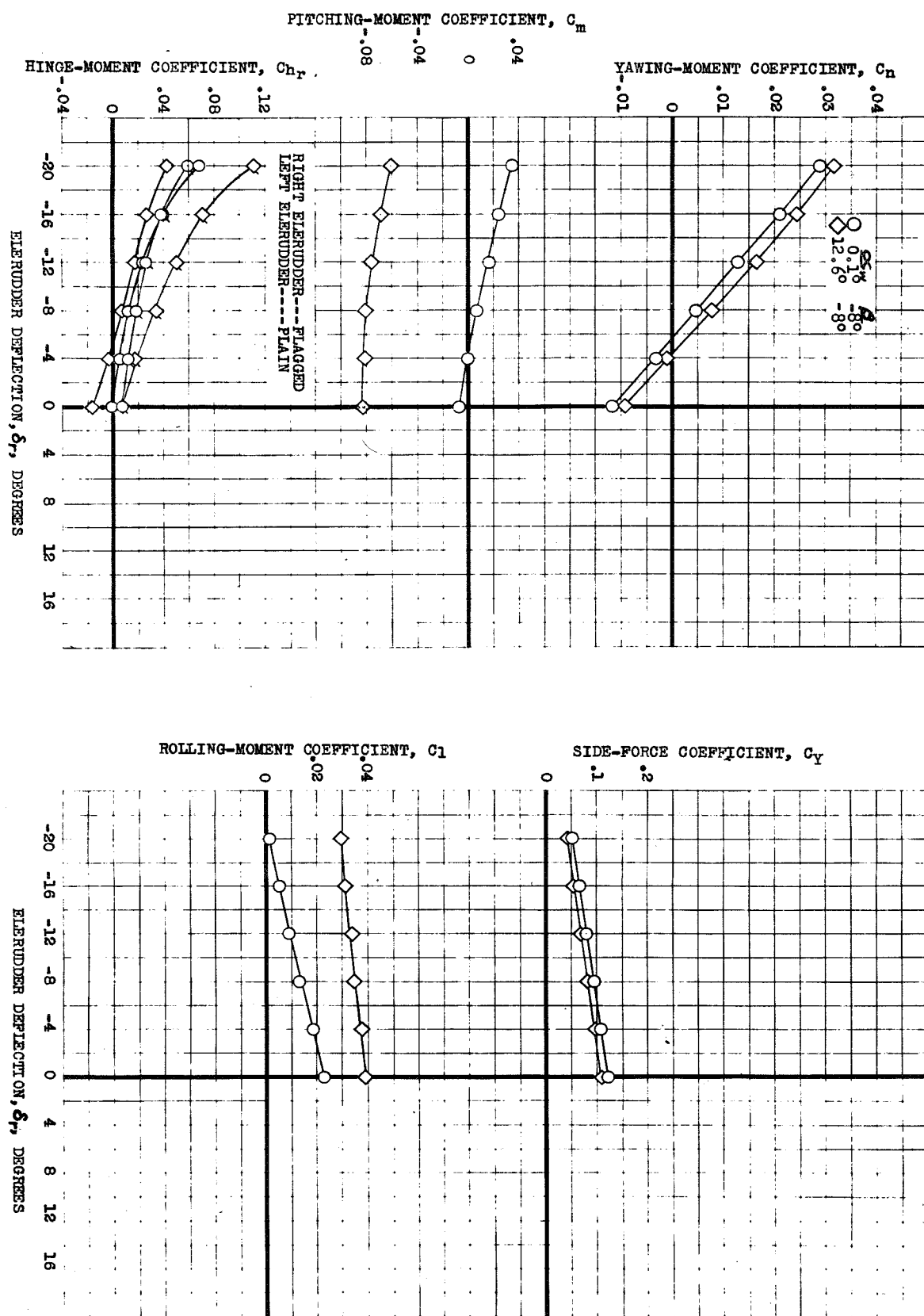
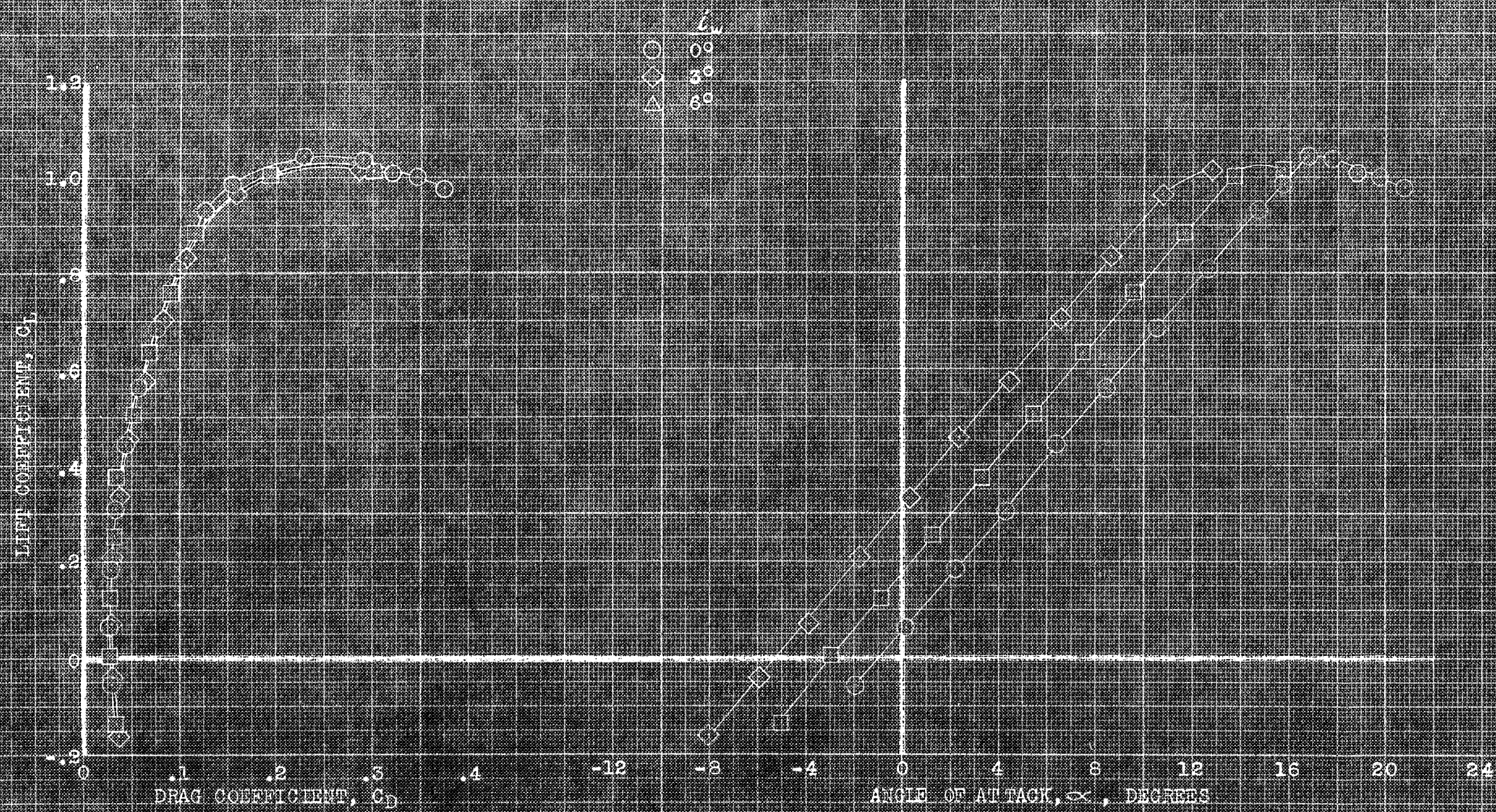


FIGURE 72.- EFFECTIVENESS OF THE COMPLETE ELERUDDER SYSTEM OPERATED FOR PURE RUDDER ACTION WITH THE MODEL AT SEVERAL ANGLES OF ATTACK. EXTERNAL TANKS; $i_w, 0^\circ$.



(b) $\beta, -8^\circ$.

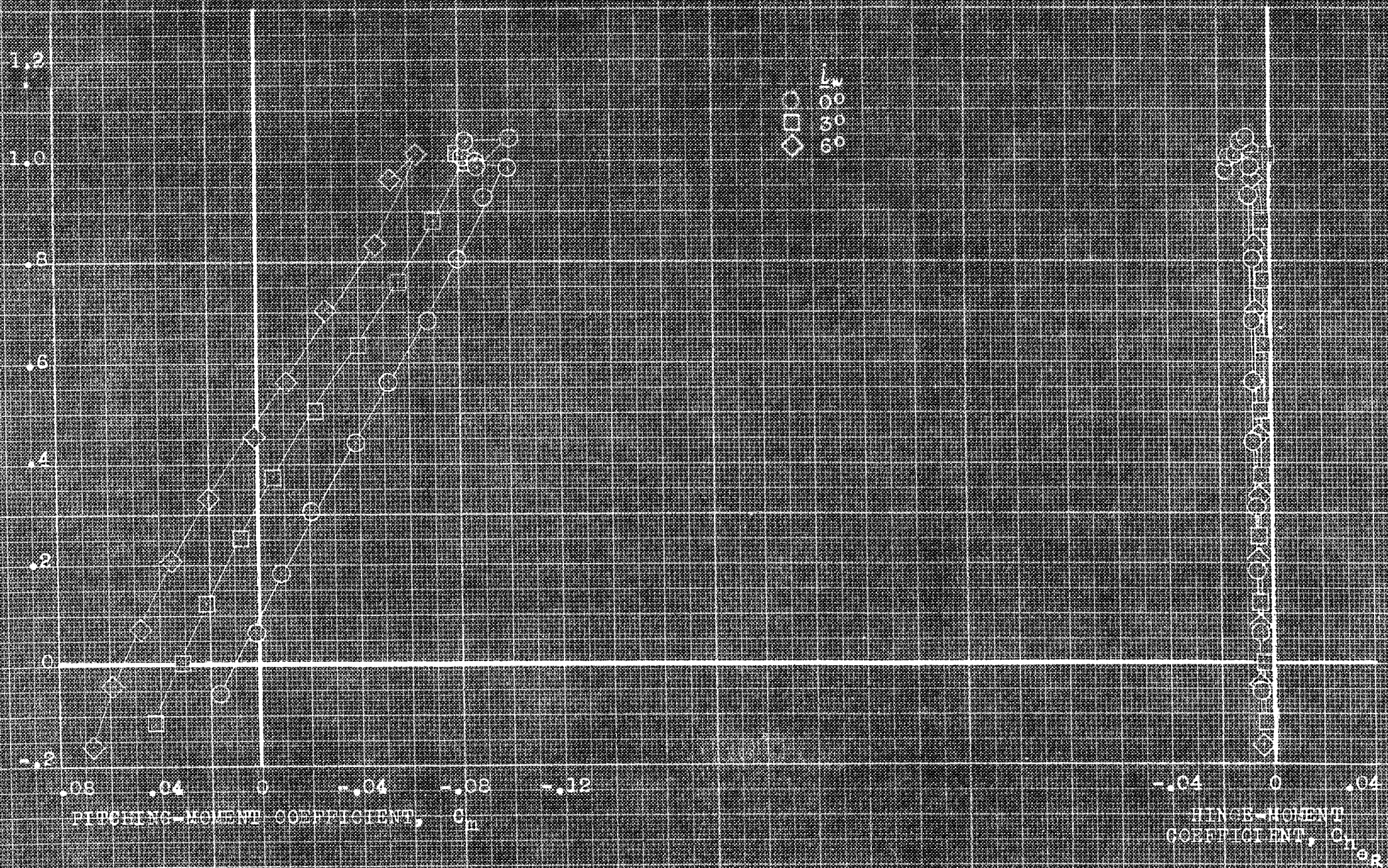
FIGURE 72.- CONCLUDED



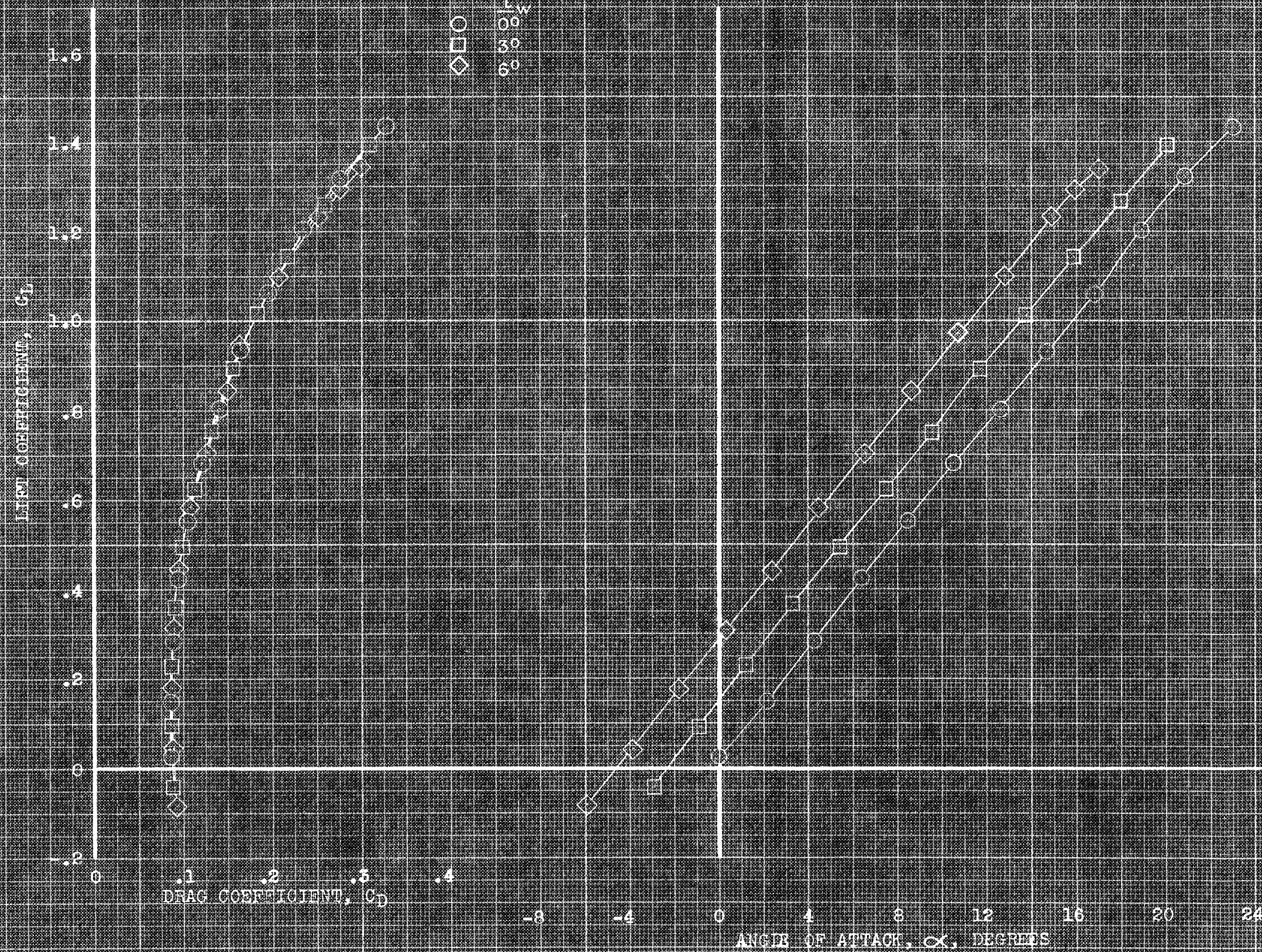
(9) $\phi_D, \alpha, \nu \in \mathbb{C}^*$,
 FIGURE 3. EFFECT OF FIELD ANGLES OF WAVE INCIDENCE ON THE ACOUSTIC CHARACTERISTICS OF THE MODEL IN FLUID PLAIN WAVE; ϕ_e, ϕ_i

1000
 900
 800
 700
 600
 500
 400
 300
 200
 100
 0

THE NATIONAL ARCHIVES



(a) C_{m_i} vs C_{h_i}
FIGURE 72. - CONTINUED

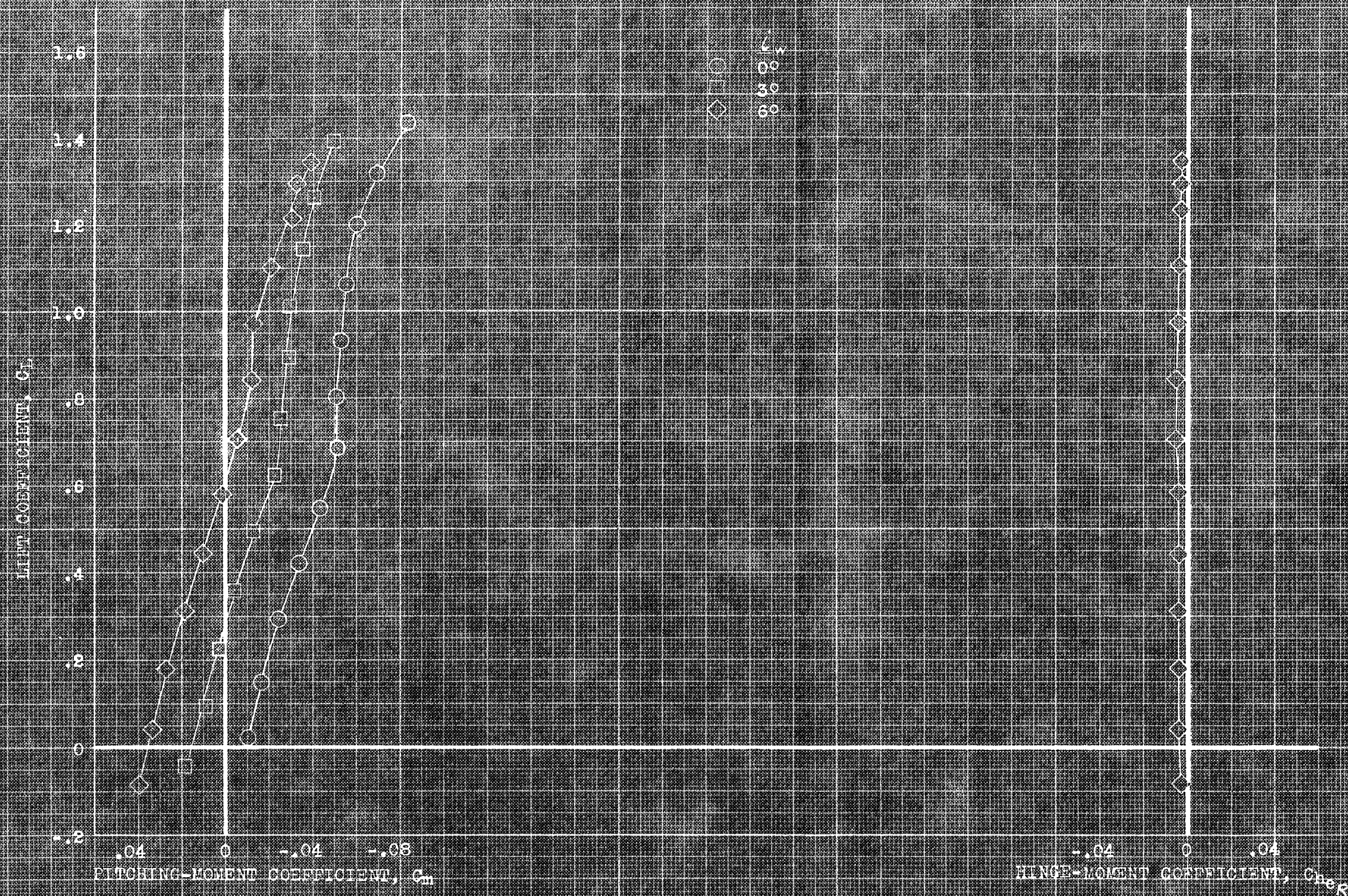


(a) C_D , α , vs C_L .

FIGURE 1.1. EFFECT OF FIXED ANGLES OF TANK INCIDENCE ON THE AERODYNAMIC CHARACTERISTICS OF THE MODEL IN PITCH. EXTERNAL TANKS; GEARY, DROPPED SLATS; $\delta_e, 0^\circ$.

CONFIDENTIAL

NATIONAL AERONAUTICS AND SPACE ADMINISTRATION



(b) C_m , Ch_R vs C_L .

FIGURE 7.1.- CONTINUED.

LIFT COEFFICIENT, C_L

1.6
1.4
1.2
1.0
.8
.6
.4
.2
0

DRAG COEFFICIENT, C_D

.1
.2
.3
.4
.5
.6

-8
-4
0

ANGLE OF ATTACK, α , DEGREES

4
8
12
16
20
24
28

40°
30°
20°

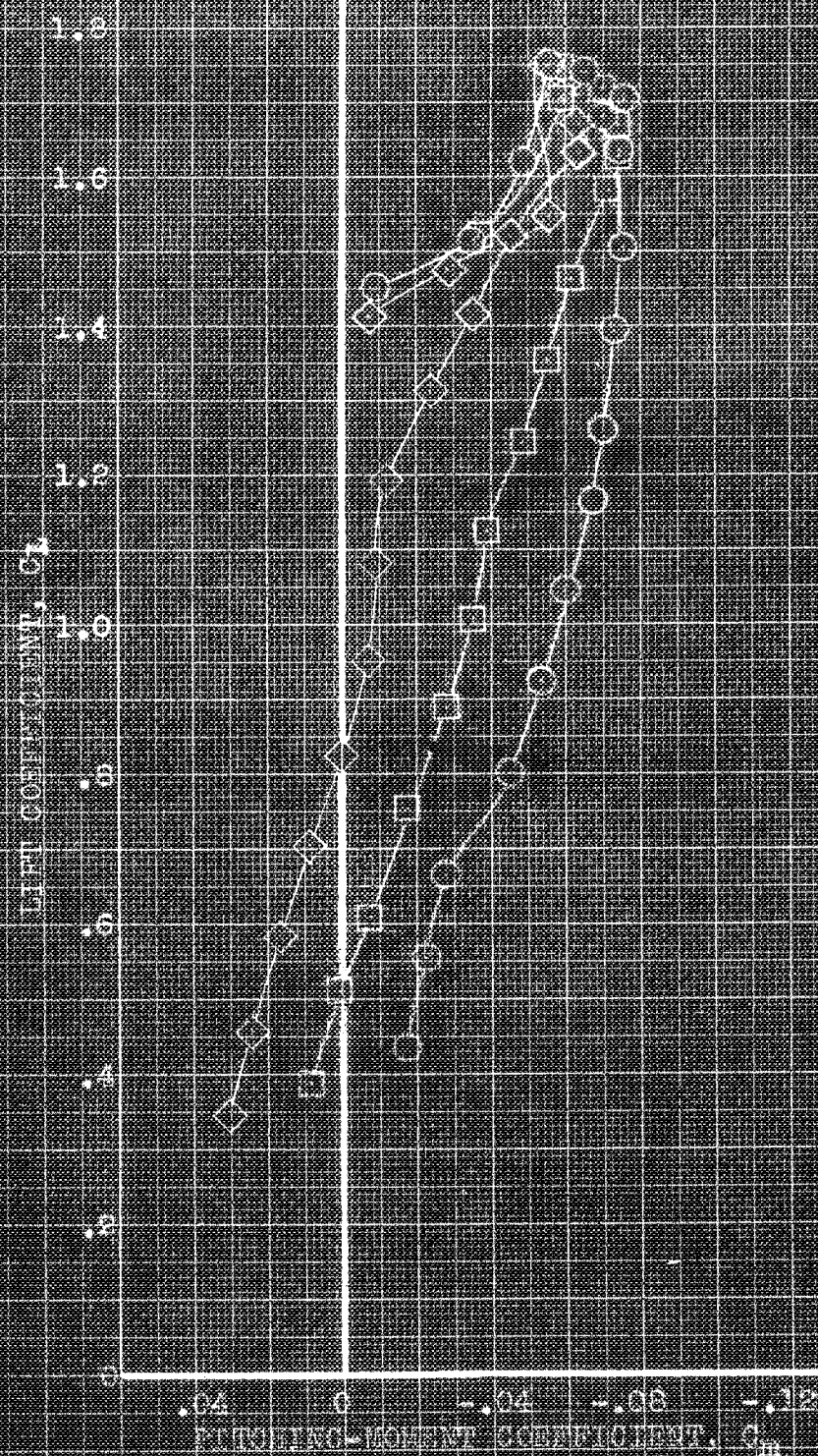
(B) C_D , α , VS C_L

FIGURE 15. - EFFECT OF FLIGHT INVERTER POSITION ON THE AERODYNAMIC CHARACTERISTICS OF THE AIRCRAFT. DATA: DRAG COEFFICIENT, C_D ; LIFT COEFFICIENT, C_L ; ANGLE OF ATTACK, α ; PLAIN FLARE, 40°.

40°

CONFIDENTIAL

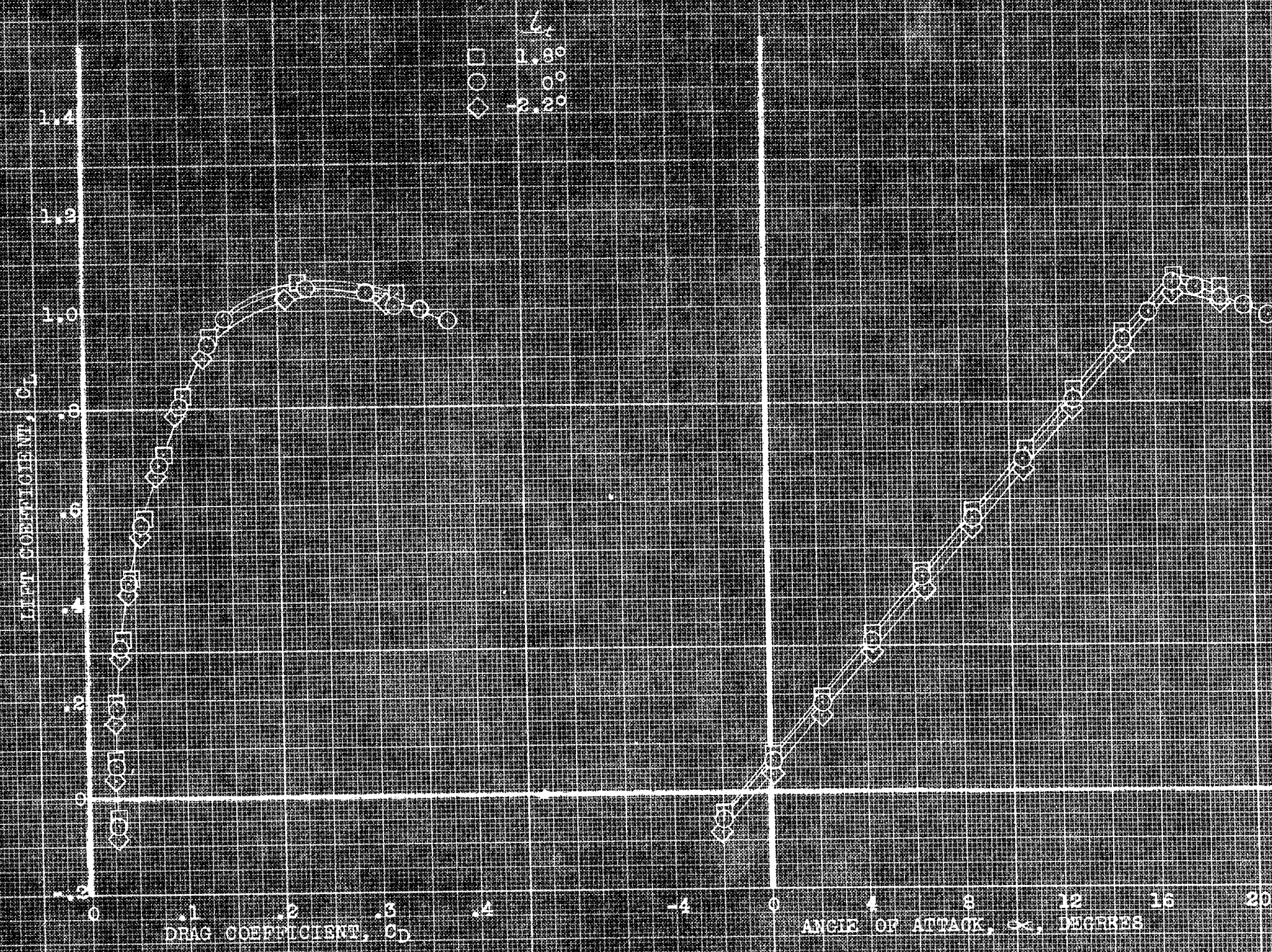
NATIONAL ADVISORY COMMITTEE ON AERONAUTICS



Rolling-Moment Coefficient, C_{LR}

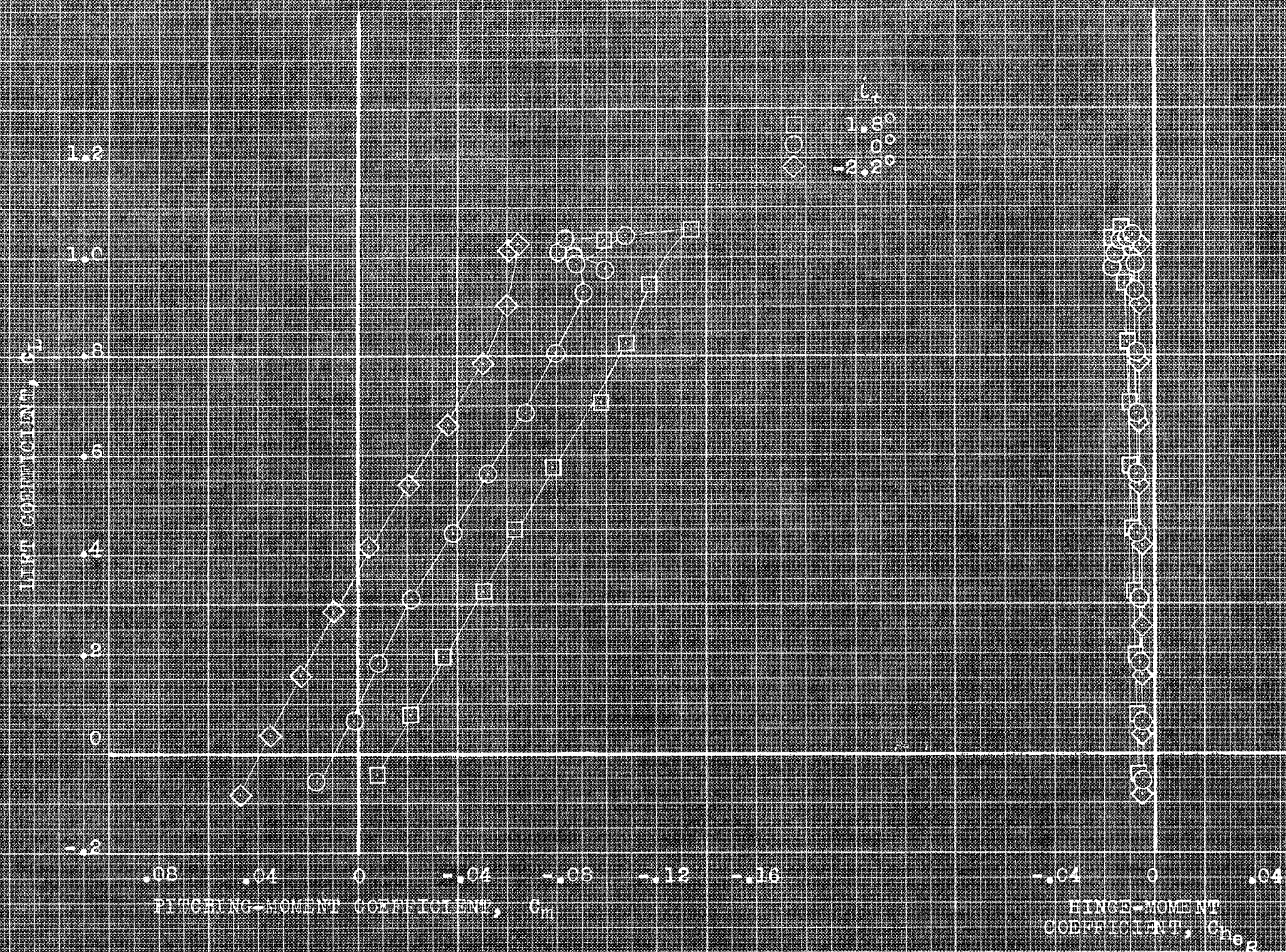
(b) C_L , C_{LR} vs C_M

FIGURE 1. - CONTINUED.



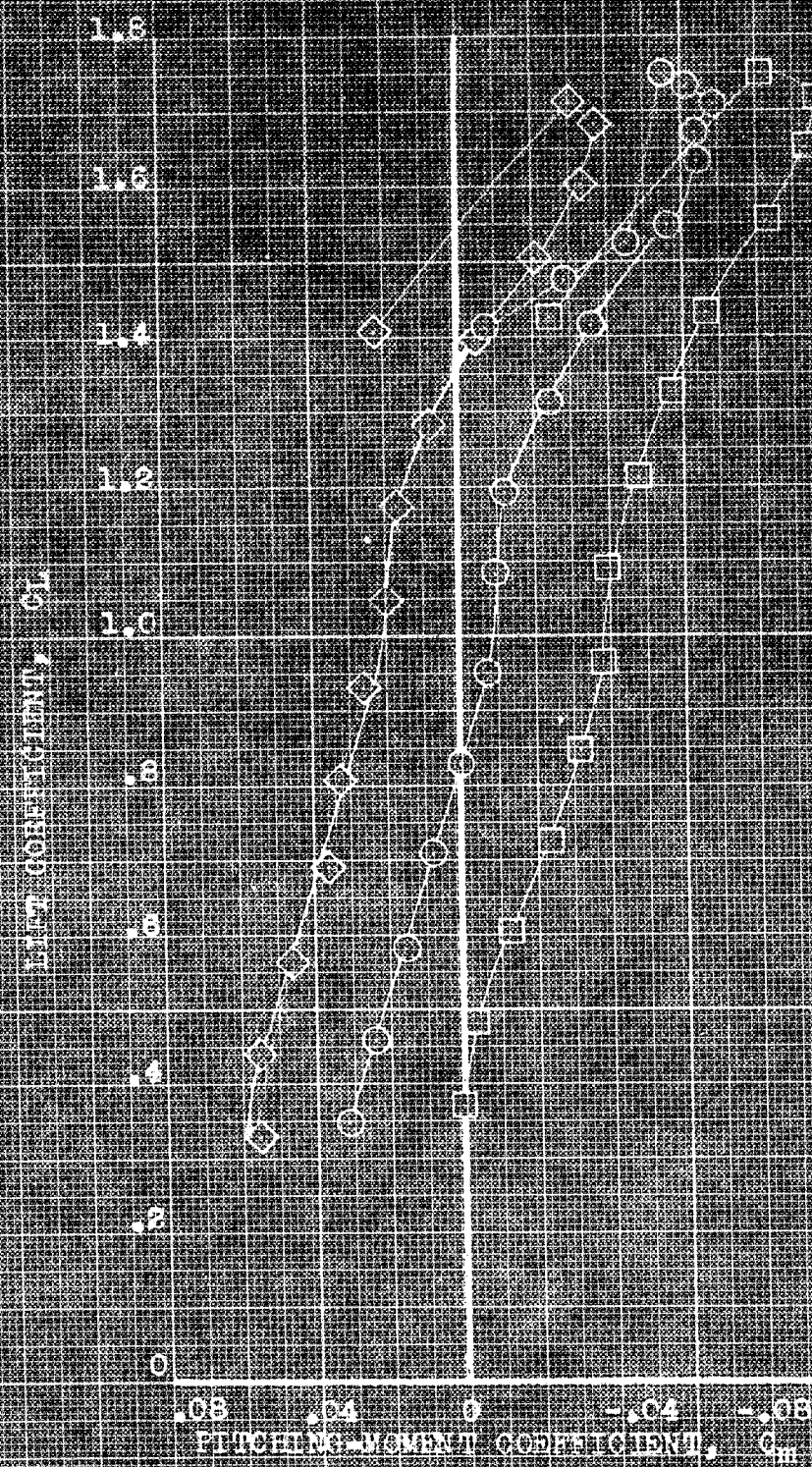
(a) C_D vs α vs C_L

FIGURE 76. EFFECT OF FLIGHT ANGLES OF TAIL INCIDENCE ON THE AERODYNAMIC CHARACTERISTICS OF THE MODERN FLIGHT PLAN WING; 1.8° , 0.0° , -2.2° .



(b) C_M , C_{H_R} vs C_L .

FIGURE 76.- CONCLUDED.



\diamond \square \circ \triangle
 $\frac{C_L}{C_m}$
 $\frac{1.80}{-2.20}$

HINGE-MOMENT COEFFICIENT, C_{mR}
 0.04 0 0.04

(a) C_{mR} vs C_L

FIGURE 17-1. CONTINUED.

Restriction/Classification Cancelled

UNCLASSIFIED
UNRESTRICTED FOR ALL PURPOSES